The impact of staged combustion on the operation of a precalciner cement kiln

Lars-André Tokheim

1999

Contents

List of Figures

List of Tables

Preface

This thesis, which is submitted in partial fulfillment of the requirements for the degree of Dr.Ing., is the result of about four and a half years of work.

From July 1994 to June 1998, I had the pleasure of receiving a four-year scholarship from Telemark College, Department of Technology, Institute of Environmental Technology. My current employer, Norcem AS, kindly provided funding for another six months, which is greatly acknowledged.

During these years, I have spent a considerable number of hours in the central control room of Norcem's cement plant in Brevik, Norway. Through this, I have learned a lot about cement manufacture. I have also learned that the cement production process is a very challenging one, in particular because there are so many subjects involved; including chemical engineering, fluid mechanics, thermodynamics, chemical reaction engineering, combustion physics and technology, control engineering, inorganic chemistry and powder technology — to mention some of the more important ones.

I want to thank:

- Professor Dag Bjerketvedt, my supervisor, for his guidance, encouragement and true interest in my work.

- Professor II Are Mjaavatten at the Institute of Environmental Technology, for his many suggestions and comments to several of the reports I have written as part of this work.

- Associate professor Tore Haug-Warberg at the Institute of Environmental Technology, for providing me with a MATLAB® subroutine for calculating thermodynamic equilibria. I also appreciate the many interesting discussions we have had on life in general.

- Associate professor Bernt Lie at the Institute of Process Automation, for answering my many questions regarding the use of *Scientific WorkPlace* and LaTeX.

- Dr.ing. student Ernst Petter Axelsen, for 'being in the same boat', and for kindly assisting me during three full-scale experiments at the Brevik plant.

- Miss Lene Hjertager, for running most of the thermogravimetric analyses.
- Øivind Høidalen, Director of the Technical Support Division of Scancem International, for reading and commenting on my manuscript.
- The staff at Norcem, for always being positive and helpful; we will certainly see more of each other in the future.
- My wife, Gitte, for her care and support throughout the years.

Porsgrunn, September 5, 1999

Lars-André Tokheim

Abstract

In this thesis, the impact of staged combustion on the operation of a precalciner cement kiln, is considered. Mathematical modelling and full-scale experiments at the Norcem cement works in Brevik, Norway, is the basis for the thesis.

The goal of the work was to characterize and explain operational disturbances related to the application of alternative solid fuels in staged combustion, and to take actions to avoid such disturbances.

A mass and energy balance of a precalciner cement kiln system, MEBCEM, was implemented in MATLAB®, and used as a tool for analysis of the kiln system, planning of experiments and interpretation of experimental data. The mass balance was calibrated and validated by means of process data collected during tests.

Full-scale experiments using plastic as reburning fuel in the kiln inlet proved a NO_x reduction potential of about 40 %. However, operational disturbances related to an alteration of the internal material cycles in the kiln system, were also experienced.

To be able to analyse the sulphur chemistry at the kiln inlet, a program for the calculation of thermodynamic equilibria, SEACEM, was implemented in MATLAB®. The thermodynamic analysis indicated that contact between fuel, precalcined meal and kiln gas caused the operational disturbances. This was supported by thermogravimetric analyses. Furthermore, CFD calculations conducted with FLUENT®, and laboratory experiments carried out to determine the entrainment velocity of various alternative fuels, demonstrated that, in the kiln system that was studied, such contact is hard to avoid. Based on these findings, a mechanism explaining the phenomena observed in the experiments was suggested, and a re-location of the feeding point for alternative fuels was prescribed.

In subsequent experiments with a new feeding point location — where precalcined meal, reburning fuel and kiln gas was not brought into simultaneous contact — operational impacts were avoided or strongly reduced. However, the NO_x reduction efficiency was at the same time reduced to about 20 %.

One trial with so-called lean reburning was conducted. Whole car tyres were fed to the rotary kiln, and a 25 % reduction in NO_x emissions was demonstrated by this technique.

As part of the experimental program, the distribution of sulphur, sodium, potassium and chlorine — all circulating elements — in the kiln system, was determined. This was achieved by analysing a large number of meal and gas samples from the process, in

combination with a program for the calculation of internal material cycles, CIRCCEM, implemented in MATLAB®. For S, K and Na, the balance errors were in the interval 5-7 %, while the chlorine imbalance was much larger. The very intense circulation of chlorine explains why it is difficult to obtain a material balance for chlorine in a cement kiln system.

A procedure for optimizing the degree of sulphatization of the alkalis in the clinker was also developed. By means of this procedure it is possible to control the internal material cycles of the kiln system, and hence have an improved basis for staged combustion.

Nomenclature

Notation conventions

Generally, $X_{y,z}$ means property X of y in substance z. For example, $w_{\mathrm{SO_3,cli}}$ is the weight fraction of SO_3 in clinker. In $X_{y,z,w}$, w is some additional information, either about y or about z. For example, $w_{\mathrm{SO_3,meal,1}}$ denotes the weight fraction of SO_3 in meal in string 1. To enhance readability of the mathematical formulas, (hopefully) meaningful abbreviations are used for the many substances involved.[1]

[1] In cases where the meaning of the index is self-explaining, the index is not included in the nomenclature list.

Latin letters

Symbol	Unit	Description
A	$\mathrm{m^3\,mol^{-1}\,s^{-1}}$	Pre-exponential factor in Arrhenius expression
A	$\mathrm{kg\,s^{-1}}$	Mass flow of uncalcined meal [see Figure 10.1]
A_{calc}	$\mathrm{kg\,s^{-1}}$	Mass flow of uncalcined meal to be calcined in the calciner [see Figure 10.1]
B	$\mathrm{kg\,s^{-1}}$	Mass flow of calcined meal [see Figure 10.1]
B_{calc}	$\mathrm{kg\,s^{-1}}$	Mass flow of meal calcined in the calciner [see Figure 10.1]
C_k	$\mathrm{kg\,kg^{-1}}$	Circulation factor of component k
$c_{p,i}$	$\mathrm{J\,kg^{-1}\,K^{-1}}$	Specific heat of component i
$c^0_{p,i}$	$\mathrm{J\,mol^{-1}\,K^{-1}}$	Specific heat of component i at p^0
E	$\mathrm{J\,mol^{-1}}$	Activation energy
E_{imb}	–	Relative energy imbalance
$E^{\max}_{imb}$	–	Maximum relative energy imbalance
E_k	$\mathrm{kg\,kg^{-1}}$	Evaporation factor of component k
G	J	Gibbs energy
$\dot{H}$	$\mathrm{J\,s^{-1}}$	Energy flow
$\hat{H}_b$	$\mathrm{J\,kg^{-1}}$	Lower heating value
H_p	J	Total enthalpy of products
H_r	J	Total enthalpy of reactants
M	$\mathrm{kg\,mol^{-1}}$	Formula mass

m	kg	Mass
$\dot{m}$	$\mathrm{kg\,s^{-1}}$	Mass flow
n_i	mol	Mole number of component i
$\dot{n}$	$\mathrm{mol\,s^{-1}}$	Mole flow
$\mathbf{n}$	mol	Mole vector
p	bar	Pressure
p^0	bar	Standard pressure (=1)
$p_{\varepsilon,k}$	%	Percentage mass imbalance of component k
Q	J	Heat loss
R	$\mathrm{J\,mol^{-1}\,K^{-1}}$	Universal gas constant (=8,314)
R_k	$\mathrm{kg\,kg^{-1}}$	Residual factor of component k
SD_{out}	%	Degree of sulphatization, based on clinker composition
SD_{in}	%	Degree of sulphatization, based on inlet flows
$s^0_{i,T_{ref}}$	$\mathrm{J\,K^{-1}}$	Entropy of component i at T_{ref} and p^0
SP^{new}_{PC}	%	New setpoint value for the petcoke supply
T	K	Temperature
T_{ref}	K	Reference temperature
t	s	Time
$\mathbf{t_M}$	h	Time vector used in MEBCEM
$\mathbf{t_S}$	h	Time vector for sample collection
$\mathbf{t_{S,new}}$	h	Extrapolated time vector for sample collection
$V_{i,k}$	$\mathrm{kg\,kg^{-1}}$	Cyclone valve factor of cyclone i and component k
w	$\mathrm{kg\,kg^{-1}}$	Mass fraction
$\mathbf{x_M}$	-	Variable vector corresponding to the MEBCEM time vector $\mathbf{t_M}$
$\mathbf{x_S}$	-	Variable vector corresponding to the sample time vector $\mathbf{t_S}$
$\mathbf{x_{S,new}}$	-	Variable vector corresponding to the extrapolated sample time vector $\mathbf{t_{S,new}}$
$\mathbf{x_{S,inter}}$	-	Extrapolated and interpolated variable vector corresponding to the MEBCEM time vector $\mathbf{t_M}$
y_i	$\mathrm{mol\,mol^{-1}}$	Mole fraction of component i

Greek letters

Symbol	Unit	Description
$\Delta H^0_{f,i,T_{ref}}$	$\mathrm{J\,mol^{-1}}$	Standard enthalpy of formation of component i at T_{ref}
$\Delta \dot{m}_{k,rx}$	$\mathrm{kg\,s^{-1}}$	Total mass change of component k due to chemical reactions
ΔT	K	Temperature change
ε_H	$\mathrm{J\,s^{-1}}$	Energy flow error
$\varepsilon_H^{\max}$	$\mathrm{J\,s^{-1}}$	Maximum energy flow error
ε_k	$\mathrm{kg\,s^{-1}}$	Total mass imbalance of component k
η	%	Degree of calcination (real)
$\eta_\#$	-	Cyclone efficiency
η_{app}	%	Degree of calcination (apparent)
μ_i	$\mathrm{J\,mol^{-1}}$	Chemical potential of component i
μ_i^0	$\mathrm{J\,mol^{-1}}$	Standard chemical potential of component i
ϕ_{NO}	%	NO_x conversion ratio

Subscripts

Symbol	Description
0	Raw conditions (raw meal) [see Figure 10.1]
1-4	Cyclone stage 1-4 [see Figure 10.1]
3'	Precalciner [see Figure 10.1]
c#	Cyclone stage #; # = 1,2,3,4
cli	Clinker
CM	Coal mill(s)
D#	Dust out of cyclone stage # [see Figure 10.1]
D	Dust
eq	Equilibrium
G	Gas
G/D	Gas and dust
in	Inflow
K	Rotary kiln [see Figure 10.1]
s#	String #; # = 1,2

Abbreviations

AFM	Aerofall mill
AS	Air separate
AT	Air through
CFD	Computational fluid dynamics
CM	Coal mill
ESP	Electrostatic precipitator
ILC	In-line calciner
LHW	Liquid hazardous waste
LOI	Loss on ignition
PC	Petcoke
PEA	Partial equilibrium assumption
PET	Polyethylene-terephthalate
PP	Polypropylene
RDF	Refuse derived fuel
SFT	Statens Forurensningstilsyn (Norwegian State Pollution Control Authority)
SHW	Solid hazardous waste
SLC	Separate-line calciner
SLC-S	Semi SLC
SP	Suspension preheater
SSA	Steady-state approximation
TGA	Thermogravimetric analysis

Chapter 1

Introduction

1.1 Background

Mankind has benefited from combustion for more than half a million years [1]. Today our society totally depends on power, heat and transportation provided by combustion processes. Unfortunately, combustion processes generate a series of air pollutants, including particulate matter (e.g. soot and fly ash), partially oxidized hydrocarbons, greenhouse gases (especially CO_2), sulfur oxides (SO_2 and SO_3) and nitrogen oxides.

Nitric oxide (NO) and nitrogen dioxide (NO_2), jointly referred to as NO_x, are the principal nitrogen oxides present in the atmosphere.[1] Increased emissions of NO_x have become a problem because of the negative impact that these oxides have on the environment and on health. Examples of negative effects are contribution to the formation of acid rain and photochemical smog [2].[2]

A significant amount of the increased emissions of NO_x during the last 150 years can be attributed to human activities, in particular increased combustion of biomass and fossil fuels [2]. As a consequence of this, more stringent regulations on NO_x emissions have been and are being implemented in several industrialized countries.

In 1997, the Norwegian NO_x emissions amounted to 225,000 tons, measured as NO_2 [5]. No NO_x legislation is introduced in Norway yet, but the Norwegian State Pollution Control Authority[3] is working on the subject. All Norwegian plants emitting more than 100 tons of NO_x per year have been asked to work out a report on their potential for NO_x reduction and the appurtenant costs, and it is probably just a question of time before regulations will be implemented.

Cement kilns belong to the group of industrial processes that generate high emissions

[1] Nitrous oxide, N_2O, is usually not included in the NO_x term and is not addressed here.

[2] As far as the greenhouse effect is concerned, NO_x from aircraft has an indirect effect through the impact on the ozone concentration in the upper troposphere. For earth surface sources of NO_x, however, the impact on global warming is of the opposite sign [3, 4].

[3] Statens Forurensningstilsyn (SFT)

of NO_x. This is due to the special process conditions prevailing in cement kilns; high temperatures, high excess air and long residence times promote thermal NO_x formation, whereas the extensive use of nitrogen-containing fuels leads to fuel NO_x formation.

In 1997, the NO_x emissions from Norwegian cement plants summed up to 3172 tons (measured as NO_2), i.e. about 1.4 % of the total emissions of NO_x in Norway. This seems to be a typical level for industrialized countries; for instance, the corresponding number for Germany is 1.3 % [6]. In the European Union, the European Commission has recently [7] proposed a NO_x emission limit of 500 $\frac{mg}{Nm^3}$ (NO_2, dry, at 11 % O_2) by the year 2007 for cement kilns. This is identical to the current German legislation for new cement plants. The average NO_x concentration in the exhaust gas from Norwegian cement plants is about 800 $\frac{mg}{Nm^3}$ (NO_2, dry, at 11 % O_2).

The Norwegian cement industry has adopted staged combustion as the main measure for reducing NO_x emissions. Staged combustion is a primary NO_x reduction measure, i.e. a measure involving combustion modifications. From an economic as well as an environmental viewpoint it appears rational to utilize the potential of primary measures before secondary measures, i.e. flue-gas cleaning methods, are put to use.

In staged combustion, fuel is added in two (or more) stages. In the primary zone, combustion takes place with excess air, and NO_x is formed through one ore more formation mechanisms. In the second stage, which is often called the reburning zone, more fuel is injected in order to create reducing conditions, which promote the chemical reduction of NO_x to molecular nitrogen. Finally, in the burnout zone, air is added to ensure complete oxidation of the fuel. The potential reduction level of staged combustion in cement kilns is about 50 %. Furthermore, alternative fuels, such as used car tyres, plastic waste and refuse derived fuel (RDF), may be used as a replacement for fossil fuels in the precalciner. This is advantageous, both in an economic and environmental sense.

However, applying staged combustion in precalciner cement kilns without increasing the emissions of other pollutants, deteriorating the quality of the clinker or otherwise disturbing the kiln process has proved difficult: Increased emissions of carbon monoxide (CO), increased concentrations of free-lime in the clinker and increased tendencies of deposit formation in the cyclone tower of such kilns is a situation frequently encountered.

In order to be able to extensively employ staged combustion in precalciner cement kilns, the impact of this NO_x reduction measure on the kiln process needs to be investigated. That is the subject of this thesis.

1.2 Problem statement

The frequently experienced detrimental effects of staged combustion on the operation of precalciner cement kilns impede the application of this NO_x reduction technique. To be able to improve on the situation, the following questions need to be answered:

1. What characterizes the operational disturbances?

2. Why do the operational impacts occur?

3. How can the disturbances be minimized?

These are the questions of main concern in the current piece of work. In the process of finding appropriate answers, mathematical modelling, full-scale trials and laboratory-scale experiments were performed. Kiln 6 at the Norcem cement works in Brevik, Norway, was used as a case study.

1.3 Outline of the thesis

Chapter 2 gives an overview of the cement manufacturing process. The relations between different kiln systems are outlined, and the characteristics of the precalciner kiln, which is the kiln system in focus here, are discussed. A brief overview of emissions from cement plants is also included.

The basic theory underlying the work in this thesis, including a short overview of related work, is presented in Chapter 3.

The following chapters contain the theoretical parts of the work:

- In Chapter 4, a mathematical model of Kiln 6, based on mass and energy balances, is developed. The model is implemented in a computer program.

- In Chapter 6, a thermodynamic equilibrium analysis is performed. Another computer program is developed for this purpose.

- In Chapter 8, some fluid mechanical aspects of staged combustion are considered. A computational fluid dynamic (CFD) analysis of the flow in the kiln inlet zone is included.

- In Chapter 10, a computer program for calculating the circulation of various species in the kiln system is developed. In addition, a procedure for improved control of the internal material cycles is developed.

In Chapter 5, 7, 9 and 11 the experimental work is presented.[4]

Finally, Chapter 12 contains the conclusion and suggestions for further work.

[4]The order of the experimental and theoretical chapters is based on the logical and chronological relationship between them.

1.4 Previously reported results

From 1994–1997 Norcem participated in a NO_x reduction project funded by the European Commission[5]. The reporting of Norcem's work [8] includes some of the work presented in this thesis. A paper on some of the experimental work has also been written [9], and an article on relations between NO_x emissions and other operational parameters has been published [10]. Finally, some recent results were presented as a work-in-progress poster at the 27th International Symposium on Combustion [11].

It should also be mentioned that the work presented in this thesis rests heavily on reports that previously have been written primarily for internal use [12, 13, 14, 15, 16, 17, 18, 19].

The main results from previous papers and reports are included in this thesis.

[5]EC Environment Research Programme DG XXI-Science, Research and Development, Directorate D, Project Nr. EV5V-CT94-0551, "NO_x emissions from cement manufacture and evaluation of various possibilities for NOx reduction in the cement industry". This project was coordinated by the German research institute Forschungsinstitut der Zementindustrie, with Italcementi S.p.A. and Norcem AS as contractors.

Chapter 2

Cement manufacture

In 1997 the Norwegian cement production amounted to 1.7 million tonnes, and it was produced in three kilns at two plants. In comparison, the total world production of cement in 1995 was 1420 million tonnes, the major part being produced in Asia (60 %) [20]. Furthermore, in 1995 in the countries of the European Union there were 252 cement plants with a total of 437 cement kilns, producing 172 million tonnes of cement [20]. And in 1990 the corresponding figures of the United States were 109 plants, 213 kilns and 80.1 million tonnes of cement [21].

Cement production is an energy intensive process with energy costs typically accounting for 30–40 % of the production costs [20].

2.1 Overview of the process

In short, cement is made by heating a mixture of calcareous and argillaceous materials to a temperature of about 1450 °C. In the process, partial fusion occurs and nodules of so-called clinker are formed. The cooled clinker is mixed with a few percent of gypsum, and sometimes other additives, and ground into a fine meal — cement[1].

In the following, a brief overview of the cement manufacturing process is given. More comprehensive descriptions can be found elsewhere [22, 23, 24]. The manufacturing process is schematically represented in Figure 2.1.

[1] *Cement* is used here as a synonym to *Portland cement*. This designation was chosen by the British bricklayer Joseph Aspdin in 1824; when he burnt a mixture containing certain proportions of lime and clay, he considered that the 'artificial stone' he had produced, resembled Portland stone, a limestone found in southern Britain [22].

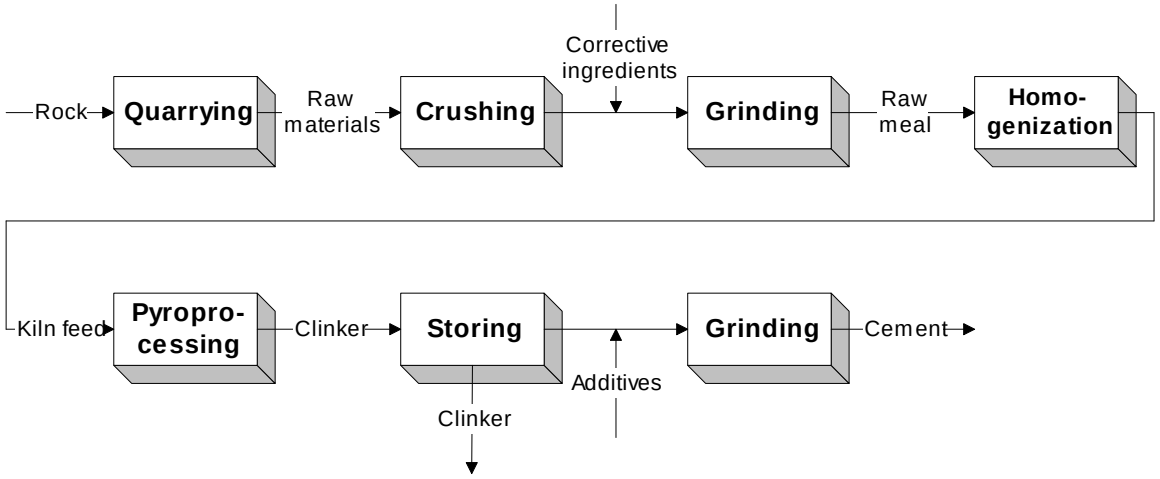

Figure 2.1: Principle drawing of the cement manufacturing process.

2.1.1 Quarrying of raw materials and kiln feed preparation

The main components of clinker are lime (CaO), silica (SiO_2), alumina (Al_2O_3) and iron oxide (Fe_2O_3). Varying amounts of these oxides are found in different mineral compounds, such as limestone, marl and clay, which can be found in nature as deposits of varying geological age. Accordingly, the first stage in the industrial process of cement manufacture is the quarrying of raw materials. This may take place in open works or in mines.

To obtain the proper composition of the raw mix, corrective ingredients normally have to be added to the quarried raw materials. Examples of corrective materials are sand, bauxite and iron ore; which compensate for deficiencies of silica, alumina and iron oxide, respectively. Fly ash, iron slag and other types of process residues can also be used as partial replacements for the natural raw materials [20].

The raw materials are ground in a mill into a fine powder[2] — raw meal or raw mix — that is suitable for burning in a cement kiln. Typical compositions of raw meal and various raw materials are given in Table 2.1.

2.1.2 Pyroprocessing

Based on the raw meal composition given in Table 2.1, the clinker would typically contain 66 % CaO, 21 % SiO_2, 5 % Al_2O_3, 3 % Fe_2O_3 and 5 % of other components. The four main oxides make up four major clinker phases, called alite, belite, aluminate and ferrite

[2]The fineness of the meal may be specified as the percentage residue on a 90 μm sieve. This percentage depends on the type of meal produced, but is typically 15 %.

Table 2.1: Typical composition (weight percent) of some raw materials [23] and raw meal.

Component	**Limestone**	**Marl**	**Clay**	**Sand**	**Bauxite**	**Iron ore**	**Raw meal**
LOI	40.38	24.68	7.19	0.2	15-20	5-12	35.8
SiO_2	3.76	27.98	67.29	99.2	16-22	20-25	13.2
Al_2O_3	1.10	10.87	8.97	–	44-58	3-9	3.3
Fe_2O_3	0.66	3.08	4.28	0.5	10-16	45-60	2.2
CaO	52.46	30.12	7.27	–	2-4	0.5-2.5	42.1
MgO	1.23	1.95	1.97	–	0.2-1-0	1.5-7	1.9
K_2O	0.18	0.20	1.20	–	–	0.3-0.6	0.6
Na_2O	0.22	0.33	1.51	–	–	–	0.3
SO_3	0.01	0.70	0.32	–	–	–	0.6
Sum	100.00	99.91	100.00	99.9	–	–	100.0

Table 2.2: Major phases in cement clinker.

Name	**Formula**	**Abbreviation**
Alite	$3CaO{\cdot}SiO_2$	C_3S
Belite	$2CaO{\cdot}SiO_2$	C_2S
Aluminate	$3CaO{\cdot}Al_2O_3$	C_3A
Ferrite	$4CaO{\cdot}Al_2O_3{\cdot}Fe_2O_3$	C_4AF

[25], see Table 2.2[3]. To produce these phases, and to obtain them in right proportions, the raw meal is pyroprocessed[4] ('burned').

The first stage in the thermal treatment of the meal [22] is the drying: Free water is driven out of the raw meal at temperatures ranging up to 200 °C; and from 100 to 400 °C, adsorbed water escapes:

$$H_2O(l) \longrightarrow H_2O(g) \tag{2.1}$$

Next, from 400 to 750 °C, clay minerals are dehydrated, i.e. chemically combined water is expelled. In this process, e.g., metakaolinite is formed through the dehydration of kaolinite:

$$Al_4[(OH)_8Si_4O_{10}] \longrightarrow 2(Al_2O_3{\cdot}2SiO_2)+4H_2O \tag{2.2}$$

Subsequently, decomposition of metakaolinite and other compounds takes place in the temperature interval from 600 to 900 °C, and a reactive mixture of oxides is formed, such

[3] In the cement industry, the following abbreviations are often used in order to simplify the rather complex formulas frequently occuring: $CaO \triangleq C$, $SiO_2 \triangleq S$, $Al_2O_3 \triangleq A$, $Fe_2O_3 \triangleq F$, $K_2O \triangleq K$, $Na_2O \triangleq N$, and $SO_3 \triangleq \overline{S}$.

[4] The term 'pyroprocessing' is used to designate any type of thermal treatment of the meal inside the kiln system. The term 'clinker burning' is used synonymously.

as:

$$Al_2O_3{\cdot}2SiO_2 \longrightarrow Al_2O_3{+}2SiO_2 \tag{2.3}$$

Any organic carbon present is oxidized; the global reaction is:

$$C + O_2 \longrightarrow CO_2 \tag{2.4}$$

In the range from 600 to 900 °C, calcium carbonate decomposes to calcium oxide and carbon dioxide:

$$CaCO_3 \longrightarrow CaO + CO_2 \tag{2.5}$$

Calcination of magnesium carbonate follows the same pattern, but takes place at lower temperatures:

$$MgCO_3 \longrightarrow MgO + CO_2 \tag{2.6}$$

From 600 °C onwards, several solid reactions occur in parallel with the calcination, for instance:

$$CaO + Al_2O_3 \longrightarrow CaO{\cdot}Al_2O_3 \tag{2.7}$$

$$CaO + SiO_2 \longrightarrow CaO{\cdot}SiO_2 \tag{2.8}$$

The following reactions begin at about 800 °C:

$$CaO{\cdot}Al_2O_3{+}2CaO \longrightarrow 3CaO{\cdot}Al_2O_3 \tag{2.9}$$

$$CaO{\cdot}Al_2O_3{+}3CaO + Fe_2O_3 \longrightarrow 4CaO{\cdot}Al_2O_3{\cdot}Fe_2O_3 \tag{2.10}$$

$$CaO{\cdot}SiO_2{+}CaO \longrightarrow 2CaO{\cdot}SiO_2 \tag{2.11}$$

Sintering (clinkering) takes place in the presence of liquid phase at temperatures above 1260 °C:

$$CaO + 2CaO \cdot SiO_2 \longrightarrow 3CaO{\cdot}SiO_2 \tag{2.12}$$

A clinker temperature of about 1450 °C is required in order to obtain a proper product quality.

The final stage in the thermal treatment process is the cooling of the clinker. This process has to be performed rapidly in order to keep the desired mineralogical composition of the product; alite tends to decompose if the clinker is cooled too slowly.

The standard reaction enthalpies for the most important reactions occuring are given in Table 2.3[5].

Figure 2.2 shows the phases occuring during the clinker formation.

[5]In table 2.3, the formation and the decomposition of metakaolinite, i.e. equation 2.2 and 2.3, are lumped together. Furthermore, the formation of the intermediate compound C_2F is specified separately; in the text it is included in equation 2.10.

Table 2.3: Reactions and reaction enthalpies [26].

Reaction	**Reaction equation**	**Standard reaction enthalpy** [kJ/kg]
I. Formation of oxides and decomposing reactions		
Evaporation of water	$H_2O(l) \longrightarrow H_2O(g)$	2453
Decomposition of kaolinite	$Al_2O_3{\cdot}2SiO_2{\cdot}2H_2O \longrightarrow$ $Al_2O_3{+}2SiO_2{+}2H_2O$	780
Oxidation of carbon	$C + O_2 \longrightarrow CO_2$	-33913
Dissociation of $MgCO_3$	$MgCO_3 \longrightarrow MgO + CO_2$	1395
Dissociation of $CaCO_3$	$CaCO_3 \longrightarrow CaO + CO_2$	1780
II. Formation of intermediates		
Formation of CA	$CaO + Al_2O_3 \longrightarrow CaO{\cdot}Al_2O_3$	-100
Formation of C_2F	$2CaO + Fe_2O_3 \longrightarrow 2CaO{\cdot}Fe_2O_3$	-114
Formation of β-C_2S	$2CaO + SiO_2 \longrightarrow 2CaO{\cdot}SiO_2$	-732
III. Sintering reactions		
Formation of C_4AF	$CA + C_2F + CaO \longrightarrow C_4AF$	25
Formation of C_3A	$CA + 2CaO \longrightarrow C_3A$	25
Formation of C_3S	β-$C_2S + CaO \longrightarrow C_3S$	59

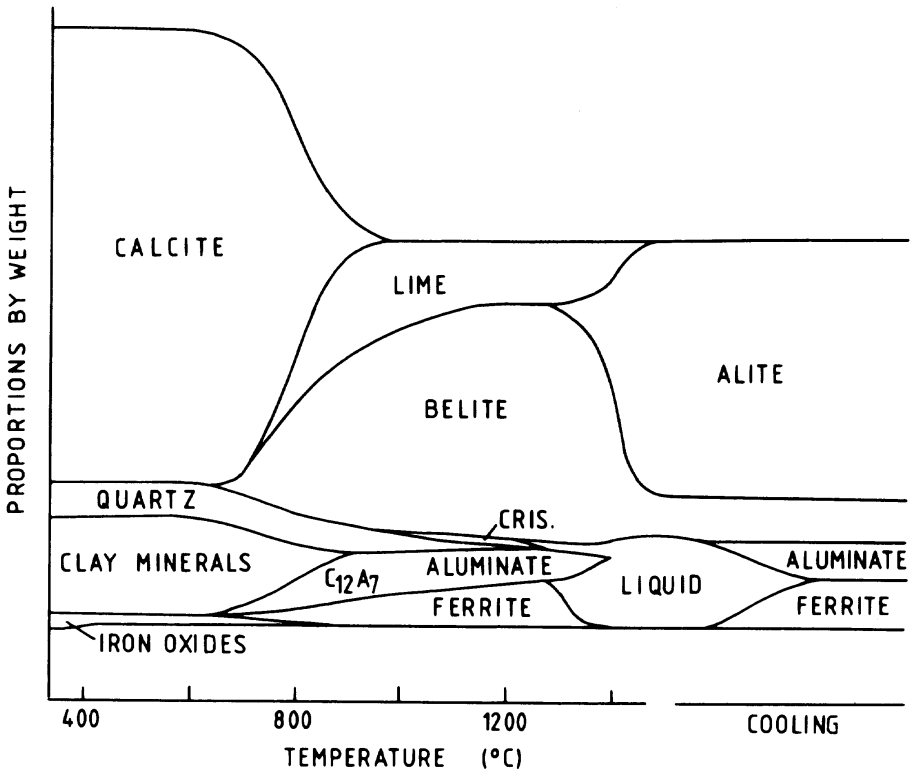

Figure 2.2: Variations in typical contents of phases during the clinker formation [25].

2.1.3 Cement

The cooled clinker is mixed with additives such as gypsum, iron sulphate and flyash. Different clinker types and different types of additives are used, depending on what type of cement that is to be produced. The mix is then ground in cement mills and intermediately stored in cement silos. Finally the cement is packed in bags and sold, or it is sold in bulk.

2.2 Classification of kiln processes

Today, virtually all clinker burning processes take place in rotary kilns. (It should be mentioned that Japanese researchers are currently working on clinker burning in fludized beds [27]. But so far, this technology appears to be on the research level.) However, different types of processes and different types of rotary kilns are used. Hence, some classification may be useful.

Cement kiln processes may be classified as wet or dry — depending on the state of the raw material [24, 25]:

- *Wet process:* The feed is a slurry with 30–40 % of water.
- *Semi-wet process:* Part of the water in the slurry is removed, and a cake containing about 20 % of water is produced. This cake is fed to the kiln either directly or via a preheater.
- *Semi-dry process:* A pulverized dry kiln feed is pelletized into small nodules by adding 10–15 % of water; the nodules are then fed onto a traveling grate where the particles are dried and partly calcined before they enter the rotary kiln. (This process is often called the Lepol[6] process, the grate preheater being known as the Lepol grate [22].)
- *Dry process:* The feed is a dry powder.

Rotary kilns are alternatively classified on the basis of the kiln length [22]:

- *Long kiln:* This kiln may operate with a wet or dry process. The meal is (generally) not thermally treated before it enters the kiln, which has a length of typically 32–35 times the shell diameter.
- *Short kiln:* This kiln uses a dry or semi-dry process, and has a length typically 15–17 times the shell diameter. The shorter kiln is obtained by pyroprocessing the meal before it enters the kiln.

[6] Lepol is a trademark of Polysius.

The above groupings may even be combined in order to produce a somewhat more detailed classification of kiln processes, see Duda [23].

Based on the degree of preprocessing of the meal before it enters the rotary kiln, dry process kilns may be further classified:

- *Long dry kiln:* The meal is not thermally pretreated, but enters the kiln directly, i.e. drying and calcination takes place inside the kiln. The fuel is supplied through a burner positioned axially in the kiln outlet[7], i.e. at the solids discharge end. Heat exchanging between gas and solids is usually promoted by means of internal heat exchanging devices, for instance chains. The specific heat requirement of the long dry kiln is about 4.8 MJ/(kg clinker) [21].

- *Preheater kiln:* In dry processes with preheaters, the raw mix is heated and partly calcined by the hot kiln-gases before it enters the kiln. In the so-called suspension preheater (SP)[8], this process takes place in a series of cyclones placed on top of each other. Typically, there are two parallel strings, each consisting of four cyclones. There is close contact between the meal flowing downwards and the gas flowing upwards, resulting in an improved heat economy of SP kilns compared to long kilns; the heat input requirement is about 4.0 MJ/(kg clinker) [21]. Also, since the meal is dried and partly calcined, the rotary kiln can be made shorter. Most SP kilns only have combustion taking place at the kiln outlet — in the main burner — but SP kilns equipped with a riser duct between the kiln and the preheater may apply riser-duct firing. Several types of suspension preheaters are available, see for instance Duda [23] for an overview.

- *Precalciner kiln:* The most modern suspension preheaters are equipped with a precalciner (also called calciner), see Figure 2.3. The precalciner is a separate furnace, usually positioned after the penultimate cyclone stage. Normally more than half of the total fuel energy input is supplied to the calciner, and the meal is typically 90 % calcined when it enters the rotary kiln, where the rest of the fuel is supplied in the main burner. The high degree of precalcination means that the length of the calcining zone in the rotary kiln is reduced to a minimum; hence, the rotary kiln can be considerably shortened. In addition, compared to an SP kiln, the production capacity is higher and the heat input requirement is lower, about 3.5 MJ/(kg clinker) [21]. Kiln systems with five cyclone stages and precalciner are considered standard technology for new plants [20].

[7] The term *kiln outlet* is used here with respect to the solids, not the gas phase. Accordingly, the *kiln inlet* is where the solids enter the rotary kiln. Frequently used synonyms are the kiln's front-end and back-end, respectively.

[8] The SP was patented in 1932 by Mr. M. Vogel-Jörgensen, an employe of the Danish firm of F.L.Smidth. The concept was first applied in the cement industry by the Humboldt Company in 1951 [23].

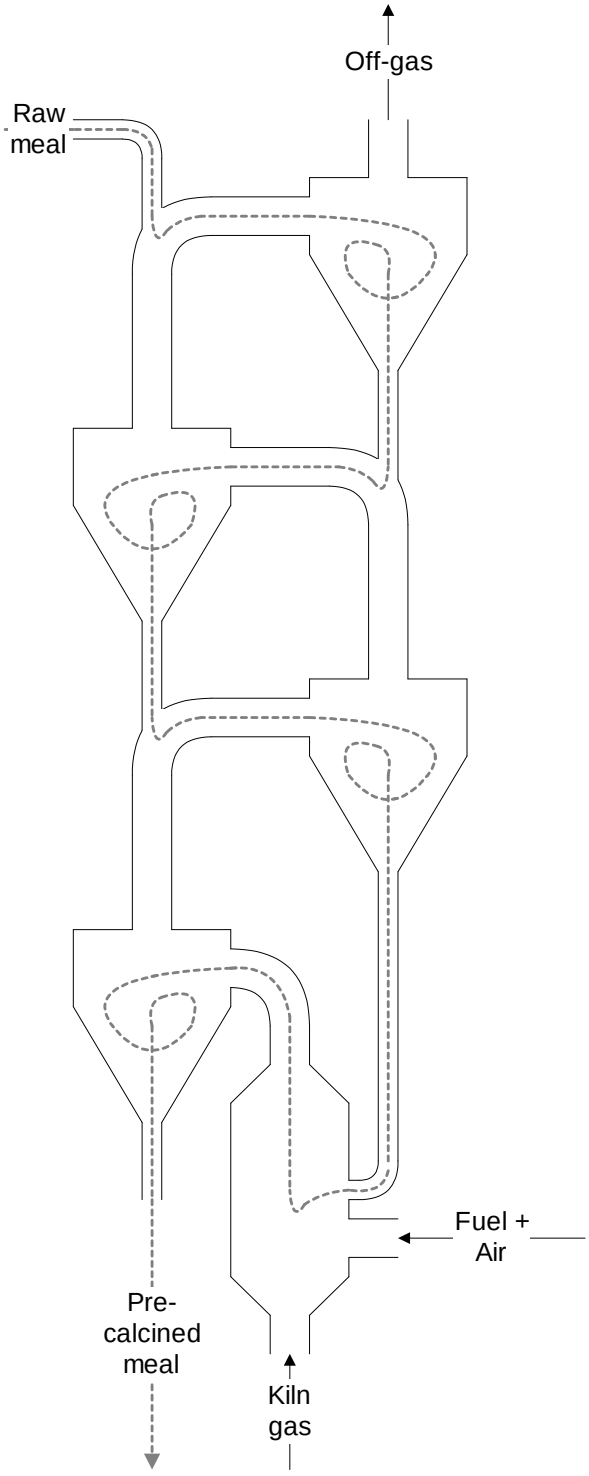

Figure 2.3: Suspension preheater with precalciner.

In the next section, the process in a precalciner kiln, which is in focus in this thesis, is described in somewhat more detail.

2.3 The precalciner cement kiln process

A principle drawing of a precalciner cement kiln system is shown in Figure 2.4.

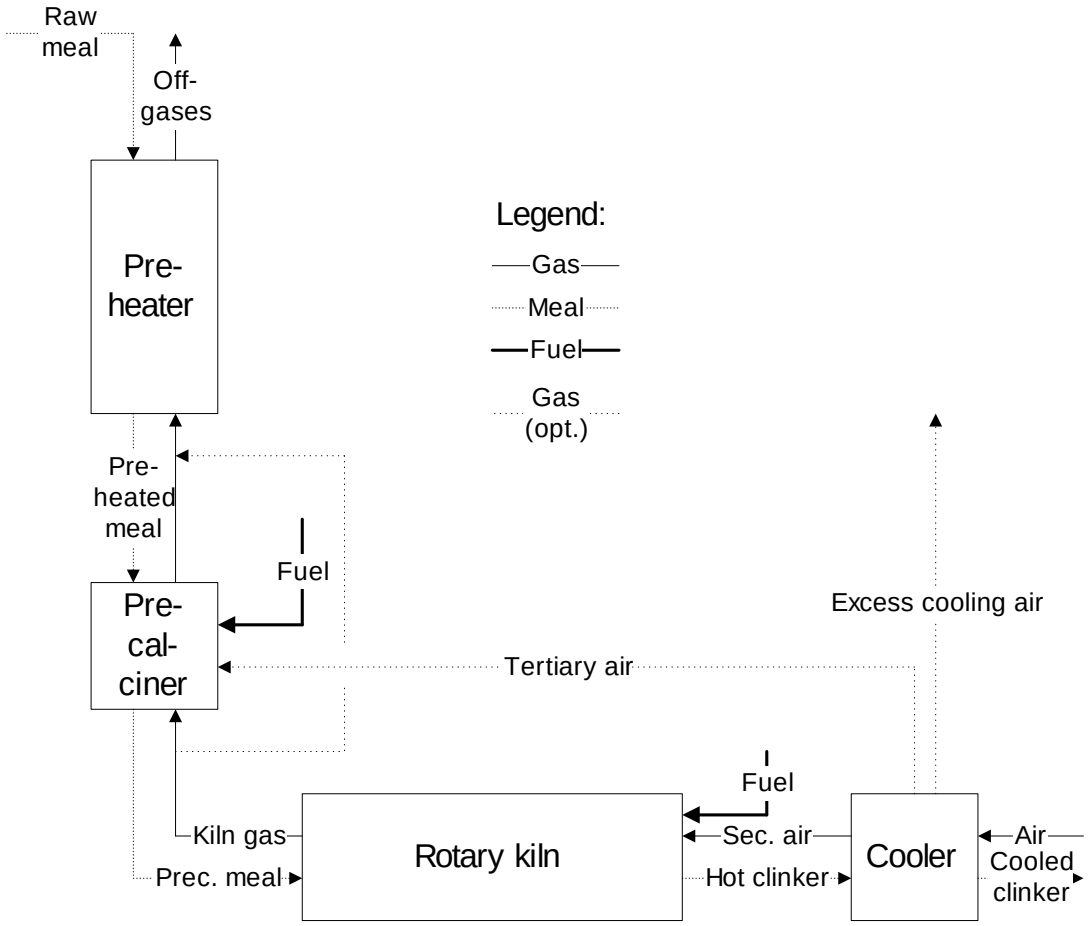

Figure 2.4: Principle drawing of a rotary cement kiln with suspension preheater, precalciner and clinker cooler.

The cold raw meal is injected into the gas flow between the upper two cyclone stages of the preheater. Flowing down the cyclone tower, the meal is dried and the clay minerals dehydrate and decompose. Also, any organic compounds present in the raw meal are oxidized, and magnesium carbonate is calcined. In this preheating process, the meal

temperature is typically increased to about 700 °C, while the temperature of the counterflowing gas is reduced from about 900 °C to about 350 °C, depending on the SP type. (There may be four, five or six cyclone stages, resulting in different thermal efficiencies.)

In the precalciner, the meal is calcined at a temperature of about 900 °C. The solids residence time in the preheater and precalciner is about 2 minutes.

After precipitation in the lower cyclone stage (which is sometimes regarded as being part of the precalciner), the precalcined meal enters the rotary kiln. In the kiln, the meal is first completely calcined, whereafter the clinker formation reactions take place. The combination of the slight inclination (typically 3°) and the revolution of the kiln causes the solid material to be transported slowly through it. Typically, the residence time in the rotary kiln is 30 minutes.

After reaching the maximum temperature of approximately 1450 °C, the clinker is discharged from the kiln and cooled in the clinker cooler[9], the residence time in the cooler being about 15 minutes. The purpose of the cooler is both to recover heat from the hot clinker and to cool the clinker to a temperature level suitable for the downstream equipment.

The cooling air is generally divided into three: One part, the secondary air, is used as combustion air in the primary burning zone, in the rotary kiln. Another part, called the tertiary air, is drawn from the cooler to the precalciner through a separate duct — the tertiary air duct — and used as combustion air in the secondary burning zone, in the precalciner. The last part of the cooling air, which may be called excess cooling air, is drawn out of the cooler and released to the surroundings. The temperature of the excess cooling air discharged from the cooler is typically 200-300 °C.

The energy required for the process in the rotary kiln is supplied by burning various types of fuel (primary fuel) in the main burner (primary burner). Today, pulverized coal and petroleum coke (petcoke) are the fuels most commonly used. However, oil and gas as well as liquid and solid waste fuels are also employed. The air supplied through the main burner is called primary air. With indirect firing[10], it contributes about 10 % to the total combustion air required in the primary burning zone. The secondary air, which is preheated in the cooler to about 900 °C, constitutes the major part of the combustion air.

The energy required for the precalcining process is mainly provided by combustion in the precalciner; typically 50-60 % of the total fuel input is fed to the calciner. In kiln

[9] There are four main types of clinker coolers [23]: 1) *the rotary cooler*, which is a cooling drum located underneath the rotary kiln, 2) *the satellite cooler*, which consists of several cooling drums attached to the circumference of the discharge end of the rotary kiln, 3) *the grate cooler*, in which the clinker is transported by moving grates while being cooled by cross- and counter-flowing air, and 4) *the shaft cooler*, where the clinker is cooled while being fluidized by counter-flowing air.

[10] Indirect firing means that the pulverized coal is intermediatly stored in silos after being ground in the coal mill. In direct firing, which is less common, the ground coal goes directly from the mill to the kiln.

systems with a separate tertiary air duct, i.e. 'air separate' (AS) systems, tertiary air preheated to about 800 °C in the cooler is used for the precalciner combustion process. However, in systems without a tertiary air duct, i.e. 'air through' (AT) systems, the precalciner combustion air is drawn through the kiln[11].

In AT systems, the off-gas from the kiln is led through the calciner. This is usually also the case in AS systems. The term 'in-line calciner' (ILC) can be used to designate this process. However, in some AS systems the kiln gas bypasses the calciner, and the tertiary air is the only gas entering the calciner. Then, if the off-gas from the precalciner is not subsequently mixed with the kiln gases, the term 'separate-line calciner' (SLC) is used. If mixing occurs, the term semi-SLC (SLC-S) is used[12].

In the cyclone tower, the meal is conveyed by the gas from one cyclone to another. In the cyclones, typically 80 % of the solid phase is separated from the gas and is supplied to the cyclone stage beneath. The gas phase, containing the remaining solids, flows directly to the cyclone stage above. Usually, smaller double-cyclones are used in the uppermost cyclone stage on each string, giving a higher cyclone efficiency, typically 95 %.

2.3.1 Precalciner design

Different manufacturers, such as F.L.Smidth, KHD Humboldt-Wedag and Krupp-Polysius, provide kilns with different precalciner designs. As indicated in Appendix A, the most common precalciner kiln system used today is probably the AS-ILC system.

Apart from differences with regard to the tertiary air duct (AS vs. AT) and the flow of the off-gas from the kiln (ILC vs. SLC), the precalciners provided by the various manufacturers are different in many respects, such as:

- Geometrical design
- Feeding of tertiary air:
  - Cross-current or co-current inlet(s) relative to the kiln gas
  - Tangential or radial inlet(s)
  - Staggered or non-staggered inlets
  - Swirl degree
  - Feeding above, below or vis-à-vis the fuel inlet(s)
  - Feeding above, below or vis-à-vis the meal inlet(s)
  - Number of inlets
  - Inlet velocity

[11] AT and AS are terms originally used by the kiln manufacturer Polysius.
[12] ILC, SLC and SLS-S are terms originally used by the kiln manufacturer F.L.Smidth.

  - Premixing with the kiln gas before entering the calciner?

- Feeding of fuel:
  - Downfired or horizontal (or slightly inclined) burner(s)
  - Tangential or radial inlet(s)
  - Feeding above, below, vis-à-vis or inside the tertiary air duct
  - Feeding above, below or vis-à-vis the meal inlet(s)
  - Number of inlets
  - No fuel staging, two-staged combustion or multi-staged combustion
  - Fuel type flexibility

- Feeding of preheated meal:
  - Lateral feeding or feeding from the top
  - Feeding above, below, vis-à-vis or inside the tertiary air inlet(s)
  - Feeding above, below or vis-à-vis the fuel inlet(s)
  - Number of inlets

- Fluidization regime: pneumatic transport, circulating fluidized bed or spouted bed

A description of the precalciner cement kiln system that has been studied in this work is given in Section 4.1.

2.4 Pollutant emissions from precalciner cement kilns

Carbon dioxide, nitrogen oxides and sulphur oxides are the main gaseous pollutants from cement plants.

About 60 % of the CO_2 emissions originate from the calcination of carbonates; the remaining 40 % comes from the oxidation of carbon in the fuels. Typically, 1 kg of CO_2 is emitted for each kg of clinker produced. In the US, some states are imposing a tax on CO_2 emissions [38]. This has been discussed also in Norway, but so far it has not been implemented. In 1997, the CO_2 emissions from Norwegian precalciner cement plants amounted to 830 grams per kg clinker produced. CO_2 reduction measures are very expensive, and apparently no plant in the world has implemented such.

NO_x emissions from cement kilns mainly arise from oxidation of fuel-bound nitrogen and nitrogen in the combustion air. For precalciner kilns, emissions range from 0.4 to 3.2 grams per kg clinker produced, see Table 2.4. The NO_x emissions from Norwegian

Table 2.4: Specific NOx (as NO2) emission rates for different kiln types [21].

Kiln type	**Typical heat input requirement [MJ/kg clinker]**	**Range of NO_x emissions [g/kg clinker]**
Long wet kiln	6.3	1.6 – 8.8
Long dry kiln	4.7	2.8 – 4.8
Preheater kiln	4.0	1.1 – 5.3
Precalciner kiln	3.5	0.4 – 3.2

cement kilns are of the order 1.7 g per kg of clinker. In some countries there are taxes on NO_x emissions. A number of techniques can be applied in order to reduce the NO_x emissions. Staged combustion and selective non-catalytic reduction (SNCR) are examples of measures that have been implemented in cement plants.

99 % of the sulphur oxides emitted via the stack of cement kilns is in the form of SO_2 [39]. SO_2 mainly originates from sulphides and organically bound sulphur in the raw materials. In 1982, the average SO_2 emissions from precalciner kilns was 1.1 g per kg clinker, with a standard deviation of 2.2 g per kg clinker. In 1997, the Norwegian cement plants emitted on average 0.5 g per kg clinker. Many countries have regulations on sulphur emissions, and plants with high SO_2 levels may have to clean the off-gases, for instance by installing a wet scrubber, in order to meet the emission requirements.

In addition to species mentioned above, several minor gaseous components are emitted. In Norway, there are regulations on the emissions of chlorine compounds, total organic carbon, dioxins, fluorine compounds, mercury and several other metals (see Table 4.2).

Dust emitted from cement plants is mainly a local problem. Most cement plants have dedusting equipment installed, such as electrostatic precipitators and bag filters, that effectively reduce the dust emissions.

Chapter 3

Basic theory and related work

There seems to be few publications specifically dealing with the relationship between staged combustion and the internal material cycles in precalciner cement kilns. However, there is a substantial amount of material on NO_x formation and reduction, internal material circulation and modelling of cement kilns — all of which are topics that play a role in this thesis. Below, a brief overview of these topics is given. Simultaneously, the basic theory underlying the present work, is given.

3.1 NO_x in precalciner cement kilns

3.1.1 NO_x formation in general

In combustion processes, more than 90 % of the NO_x formed is nitrogen monoxide [2]. In general, NO may be formed through the following mechanisms:

- The thermal NO mechanism
- Several prompt NO mechanisms
- The fuel NO mechanism

In addition to the NO formation mechanisms, NO_2 may contribute somewhat to the total NO_x content in the off-gases.

Thermal NO formation

Thermal NO is formed in the post-flame gases by fixation of molecular nitrogen in the combustion air. The NO formation increases exponentially with temperature, which is why the mechanism is called the thermal mechanism. The thermal NO formation is also strongly dependent on oxygen concentration.

Table 3.1: Rate constants for the extended Zeldovich mechanism [41].

Rate constant, $k = AT^n e^{\frac{E}{RT}}$	$A\ \left[\frac{\mathrm{m}^3}{\mathrm{mol}\cdot\mathrm{s}}\right]$	n **in** T^n	$E/R\ [K]$
$k_{1,\mathrm{f}}$	$1.8 \cdot 10^8$	0	-38370
$k_{1,\mathrm{b}}$	$3.8 \cdot 10^7$	0	-425
$k_{2,\mathrm{f}}$	$1.8 \cdot 10^4$	1	-4680
$k_{2,\mathrm{b}}$	$3.8 \cdot 10^3$	1	-20820
$k_{3,\mathrm{f}}$	$7.1 \cdot 10^7$	0	-450
$k_{3,\mathrm{b}}$	$1.7 \cdot 10^8$	0	-24560

A chemical mechanism consisting of two chain reactions was first proposed by Zeldovich [40], hence it is often called the Zeldovich mechanism:

$$\mathrm{O} + \mathrm{N_2} \underset{k_{1,\mathrm{b}}}{\overset{k_{1,\mathrm{f}}}{\rightleftharpoons}} \mathrm{NO} + \mathrm{N} \tag{3.1}$$

$$\mathrm{N} + \mathrm{O_2} \underset{k_{2,\mathrm{b}}}{\overset{k_{2,\mathrm{f}}}{\rightleftharpoons}} \mathrm{NO} + \mathrm{O} \tag{3.2}$$

Sometimes, the following reaction, involving only radical reactants, is also included:

$$\mathrm{N} + \mathrm{OH} \underset{k_{3,\mathrm{b}}}{\overset{k_{3,\mathrm{f}}}{\rightleftharpoons}} \mathrm{NO} + \mathrm{H} \tag{3.3}$$

Equations 3.1, 3.2 and 3.3 are referred to as the extended Zeldovich mechanism. The Arrhenius rate constants are given in Table 3.1. The strong triple bond in the nitrogen molecule makes the first reaction the rate limiting step of the mechanism. It also explains the strong temperature dependence of the Zeldovich mechanism.

By invoking a steady-state approximation (SSA) for the N-atom and a partial equilibrium assumption (PEA) for the O-, OH- and H-radicals, it is possible to estimate the maximum thermal NO formation when the temperature and the concentration of the major gas components are known, see for instance Flagan and Seinfeld [41]. However, often the spatial distribution of temperature and concentration of the chemical species in the reactor is not known. Turbulence, which usually occurs in practical combustion devices, makes the situation even more complex. Then this SSA-PEA approach is not adequate for calculating the thermal NO formation, and it becomes difficult to predict the NO concentration in the off-gas from the combustor.

Prompt NO formation

Fenimore [42] investigated $\mathrm{NO_x}$ formation in hydrocarbon flames. He found that the thermal mechanism could predict the growth of NO in the post-flame gas, after hydrocarbon

consumption. However, the thermal mechanism could not describe a faster, transient formation of NO in the primary reaction zone — a prompt NO formation. Since this transient formation did not occur in CO or H_2 flames, Fenimore deduced that hydrocarbon radicals probably were involved in an attack on nitrogen molecules. Today, this mechanism, which is dominant in fuel-rich premixed hydrocarbon combustion and in hydrocarbon diffusion flames [2], is often referred to as *the Fenimore mechanism*, or simply the prompt NO mechanism. The initial steps in the mechanism are:

$$CH + N_2 \rightleftharpoons HCN + N \tag{3.4}$$

$$C + N_2 \rightleftharpoons CN + N \tag{3.5}$$

Thereafter, for (fuel) equivalence ratios[1] less than about 1.2, the following chain sequence is followed [43] (see Figure 3.1):

$$HCN + O \rightleftharpoons NCO + H \tag{3.6}$$

$$NCO + H \rightleftharpoons NH + CO \tag{3.7}$$

$$NH + H \rightleftharpoons N + H_2 \tag{3.8}$$

$$N + OH \rightleftharpoons NO + H \tag{3.9}$$

Two other mechanisms also take place at a faster rate than the thermal mechanism, and these are included in the prompt NO term by some researchers, for instance Bowman [2]. The first one involves super-equilibrium concentrations of O and OH in the reaction zone, leading to an acceleration of the thermal NO mechanism. It may be called *the super-equilbrium mechanism*.

The last prompt NO mechanism, which may prevail when the total NO formation is low, is *the N_2O mechanism*. This mechanism, which is particularly important in lean low-temperature combustion processes, e.g. in gas-turbines, involves N_2O as an intermediate [2]:

$$O + N_2 + M \rightleftharpoons N_2O + M \tag{3.10}$$

[1] The fuel equivalence ratio, or simply equivalence ratio, ϕ, is frequently employed within the field of combustion; it is defined as the ratio of actual to stoichiometric air/fuel ratios:

$$\phi \triangleq \frac{\left(\frac{m_{air}}{m_{fuel}}\right)_{actual}}{\left(\frac{m_{air}}{m_{fuel}}\right)_{stoichiometric}}$$

The air equivalence ratio, λ, which is also in frequent use, is the inverse of ϕ:

$$\lambda \triangleq \frac{1}{\phi}$$

The air equivalence ratio is also called stoichiometric ratio, *SR*.

In American literature ϕ prevails, whereas λ is preferred in German literature. In this thesis, both of them are used.

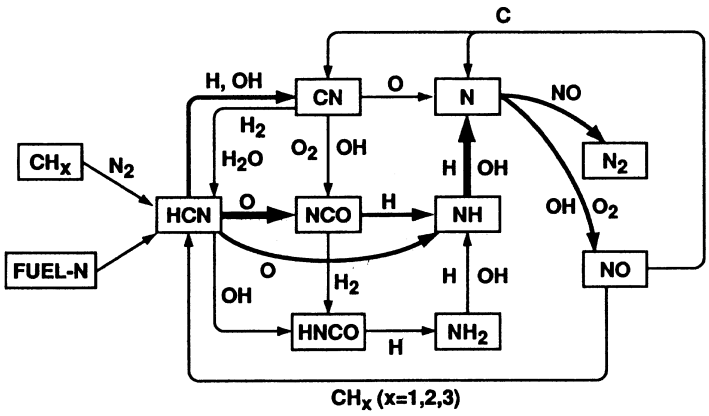

Figure 3.1: Reaction path diagram showing the major steps in fuel NO formation, Fenimore prompt NO formation and reburning [2].

$$N_2O + O \rightleftharpoons 2NO \tag{3.11}$$

Fuel NO formation

Many fuels contain small amounts of chemically bound organic nitrogen. Coal, for instance, typically contains 1-2 % nitrogen. During the combustion process, part of this nitrogen reacts with oxygen to form NO, the rest mainly forms N_2. The reaction path goes via several intermediate products, of which HCN plays an important role, see Figure 3.1. The conversion of fuel-N to NO is enhanced in a fuel lean environment. The heating rate is also an important parameter in this context.

NO_2 formation

The mechanisms outlined above are usually the most important NO_x formation mechanisms. However, production of NO_2 also contributes to a certain extent, at rather low temperatures. The main formation reaction is [2]:

$$NO + HO_2 + M \rightleftharpoons NO_2 + OH \tag{3.12}$$

3.1.2 NO_x formation in precalciner cement kilns

Rotary cement kilns operate with maximum flame temperatures of more than 2000 °C and an oxidizing atmosphere. Moreover, the gas residence time in the rotary kiln is several seconds. Accordingly, the Zeldovich mechanism should be an important NO formation mechanism in the primary combustion zone in cement kilns.

Precalciner kilns are burning 50-60 % of the fuel at a lower temperature (usually <1200 °C), leading to negligible thermal NO in the precalciner. Hence, the thermal NO formation is often suppressed in such kilns compared to other types of cement kilns [21].

Because prompt NO tends to dominate when the total NO concentration in the system is low, this mechanism is presumably not important in cement kilns, in which NO_x concentrations are relatively high.

In a precalciner cement kiln fired by nitrogen-containing fuels, such as pulverized coal, fuel NO is the main source of NO_x in the precalciner. In the primary burning zone, thermal NO_x formation is claimed to be the main mechanism [44], due to the high flame temperature. However, fuel NO should not be neglected; the contribution of fuel NO will probably depend on the total NO_x level in the rotary kiln, which in turn is a function of the kiln temperature. This question will be further addressed in Chapter 9.

In cement kilns the temperature is so high that NO_2 formation is likely to be negligible relative to thermal NO and fuel NO formation.

Gardeik *et al.* [45, 46] performed full-scale experiments in several kilns with secondary firing to determine the relationships of the formation and destruction of NO_x in such kilns. Their work indicated that thermal NO_x formation is of major importance in the primary burner — coals with different nitrogen content did not affect the NO_x formation significantly — whereas fuel NO_x formation dominates in the secondary combustion process. In the kilns that were examined, an average of 20 % of the NO_x was formed in the secondary combustion zone.

Scheuer and Gardeik [47] performed model calculations and compared them to measurements. They found that in the primary burning zone, a short flame gives a high NO_x formation due to an increased temperature, and that the fuel-NO_x formation is low in the primary burner because of the prevailing fuel-rich conditions. It was also found [48] that the N-content of the fuel as well as the tendency of the fuel to form hydrocarbon radicals are important as far as NO_x formation in the secondary firing is concerned. Large variations in NO_x emissions were calculated, ranging from 0.5 to 2.4 kg NO per ton of clinker.

Feed NO formation

In cement kilns, one more NO formation mechanism has to be taken into account: Feed NO is formed by reactions between oxygen and nitrogen in the feed, i.e. in the raw meal. The conversion of feed nitrogen to NO mainly occurs in the temperature range of 300 to 800 °C. At slow heating rates, up to 50 % of the nitrogen can be converted to NO_x. The conversion rate is lower for fast heating rates. The contribution of feed NO to the total NO_x concentration depends on the feed nitrogen content, which may vary from 7 to 1000 ppm [21]. But the feed NO mechanism is probably less important than thermal and fuel NO_x formation in most cases [21].

Gartner and Wilk [49] performed laboratory studies on the influence of raw meal

nitrogen on the NO_x emissions. They placed a meal sample in an electric tube furnace under a flowing atmosphere, and found that NO_x formation was promoted by slow heating rates and by high gas-solids ratios. However, on the basis of the investigations, they concluded that in precalciner cement kilns, in which the heating rates are high, feed nitrogen contributes little to the total NO_x formation.

Jøns and Rabia [50] investigated two different raw meals, containing 0.021 and 0.031 % nitrogen, respectively, in a laboratory experiment. They found that the NO release started at about 600 °C, that approximately 50 % of the feed nitrogen was converted to NO_x, and that this corresponded to a preheater emission of 150–200 ppm. However, they pointed out that a lower net feed NO_x formation is to be expected in practice because experiments with a carrier gas doped with NO showed that NO_x reduction also occurs, giving lower net NO_x emissions.

3.1.3 NO_x reduction in precalciner cement kilns

In general, approaches for controlling the NO_x emissions can be divided into primary and secondary measures. *Primary measures* focus on combustion modifications in order to avoid or reduce the formation of NO_x. In *secondary measures* the purpose is to convert NO_x in the post-combustion zone.

Several techniques are available for the reduction of NO_x in precalciner cement kilns [6, 51, 20]. A broad discussion of these measures is beyond the scope of this work, but some of the more important measures should be mentioned:

- *Use of low-NO_x burners:* Reduced gas temperature, low excess air and reduced residence time in the high-temperature zone are strategies for reducing the formation of thermal NO in the primary burning zone. These measures are utilized in low-NO_x burners, which are frequently used in the main burning zone of cement kilns [52, 53, 54, 55]. NO_x reductions up to 30 % are achievable [20].

- *Flame cooling:* The flame in the primary burning zone can be cooled for instance by injecting water or recirculating flue-gas. This will suppress the formation of thermal NO_x by 0–50 % [51, 20].

- *Staged combustion:* As pointed out in Chapter 1, in staged combustion — or fuel staging — the point is to add fuel in two or more stages in order to create a zone where NO_x can be chemically reduced to molecular nitrogen. In a cement kiln, this technique appears to lie somewhere between primary and secondary measures, but it is usually categorized as a primary measure. This technique is discussed more thoroughly in the next subsection.

- *Selective non-catalytic reduction (SNCR):* Reagents that contain NH_x (e.g. ammonia, urea, cyanamide) are supplied to the post-combustion gases in a temperature

range of 900–1100 °C. The overall chemical reaction is [56]:

$$4NO + 4NH_3 + O_2 \rightarrow 4N_2 + 6H_2O \quad (3.13)$$

80 % reduction has been demonstrated through the use of urea ($NO_xOUT^{®}$) [57], and in a Swedish cement plant, more than 80 % reduction on a continuous basis has been demonstrated by using ammonia water ($DeNO_x^{®}$) [58]. Recently, a modified $NO_xOUT^{®}$ process was reported, using solid urea prills instead of aqueous urea solution. This modifed process was found to give NO_x reduction rates equivalent to those possible with ammonia water [59]. A disadvantage of SNCR is that generally a little excess of the reagent is used to ensure the desired NO_x reduction. This may result in increased ammonia emissions, often referred to as 'ammonia slip' [21]. Besides, capital and operational costs are relatively high, compared to the costs of primary measures. At present there are 18 full-scale SNCR installation in the EU and EFTA countries [20].

3.1.4 Staged combustion in precalciner cement kilns

The fuel staging principle is illustrated in Figure **??**. NO_x formation occurs in the primary zone, i.e. in the rotary kiln, under oxidizing conditions. Fuel is then added to the kiln exhaust gas, in the kiln inlet or in the kiln riser duct, so that a reducing zone, a reburning zone, is created. This promotes the reduction of NO_x to molecular nitrogen. Finally, in the upper part of the precalciner, the burnout zone, air is added to attain complete burnout.

It appears that reduction of NO_x in staged combustion may take place by three different mechanisms:

- Gaseous reburning reactions
- Heterogeneous reactions
- Heterogeneous-catalytic reactions

These are discussed in the following paragraphs.

Reburning

When fuel staging is applied in gaseous combustion, the reduction of NO_x is usually attributed to the so-called reburning reactions. The aim of reburning (also known as 'in-furnace NO_x reduction') is to convert the NO_x already formed during combustion in the primary zone, to N_2 [60, 61, 2, 62]. The reburning process can be divided into three zones; the primary zone (in this case: the rotary kiln), the reburning zone (the kiln inlet

and/or the kiln riser duct) and the burnout zone (the last part of the precalciner). In the reburning zone, reburning fuel is added to the kiln exhaust gas to bring about an overall fuel-rich chemistry. This promotes the formation of a hydrocarbon radical pool:

$$\text{Fuel} + ... \rightarrow \text{CH}_i + ... \tag{3.14}$$

The NO_x in the exhaust gas from the rotary kiln is then partly reduced to NH_3, HCN or N_2 (X):

$$\text{CH}_i + \text{NO} \rightarrow \text{XN} + ... \tag{3.15}$$

$$\text{XN} + \text{NO} \rightarrow \text{N}_2 + ... \tag{3.16}$$

In the burnout zone, oxygen rich gas is supplied, and the total fixed nitrogen species will either be oxidized to nitric oxide or reduced to molecular nitrogen:

$$\text{XN} + ... \rightarrow \text{NO} + ... \tag{3.17}$$

$$\text{XN} + ... \rightarrow \text{N}_2 + ... \tag{3.18}$$

The reburning mechanism is also included in Figure 3.1.

NO_x reduction by heterogeneous reactions

When a solid fuel, such as coal, is used, heterogeneous reactions will add to the total chemistry. Char (formed during devolatilazation of coal) has been found to efficiently reduce NO [63, 64]. The reaction between char and NO is enhanced by CO [65]. The reaction mechanism is, however, not fully established yet [66, 67].

NO_x reduction by heterogeneous-catalytic reactions

In addition to the heterogeneous reduction, heterogeneous-catalytic reactions may occur.

Ono *et al.* [68] showed in laboratory experiments that the NO-CO reaction...

$$\text{NO} + \text{CO} \rightarrow \frac{1}{2}\text{N}_2 + \text{CO}_2 \tag{3.19}$$

...was catalyzed by cement raw meal in the temperature interval 700–1000 °C. They found that iron compounds, i.e. ferrous sulphates, in the meal were the most active catalysts compared with other constituents of the raw mix.

Tsujimura *et al.* [69] performed experiments over the temperature range 588–922 °C which showed that CaO had a catalytic effect on Reaction 3.19, and that this effect could be compared with catalytic activities of *in situ* formed char. Tsujimura *et al.* [70] also demonstrated a similar catalytic activity of CaO on the reduction of NO with hydrogen:

$$\text{NO} + \text{H}_2 \rightarrow \frac{1}{2}\text{N}_2 + \text{H}_2\text{O} \tag{3.20}$$

$$NO + \frac{5}{2}H_2 \rightarrow NH_3 + H_2O \quad (3.21)$$

Furusawa *et al.* [71] found that the reaction between NO and CO over calcined limestone could be enhanced when SO_2 was supplied under reducing conditions, an effect that was attributed to the formation of calcium sulphide.

The above mentioned results suggest that the CaO catalyzed reaction between NO and CO may be of major importance when applying fuel staging in cement kilns. On the other hand, Dam-Johansen *et al.* [72] demonstrated that CO_2 strongly inhibits the reduction and conclude that investigations on nitric oxide reduction by carbon monoxide over CaO should be carried out in the presence of carbon dioxide.

At present, it is not determined which of the mechanisms — reburning, heterogeneous reactions or heterogeneous-catalytic reactions — is more important for the NO_x reduction effect experienced in staged combustion in cement kilns.

Reported results applying staged combustion

Reduction of NO_x by means of staged combustion in cement kilns has been reported in several publications [73, 48, 74, 75, 29, 30, 76, 77, 33, 34, 35, 37, 36].

Scheuer [73] found that in kilns operating with tertiary air duct and two-stage secondary firing, under certain circumstances, it is possible to reduce the NO_x concentration in the exit gases by about 50 %. In his doctoral thesis [48], Scheuer discusses formation mechanisms and NO_x reduction measures in cement kilns. A model is used to try out different precalciner designs, and several operational actions for the purpose of reducing the NO_x are suggested, including staged combustion in the precalciner.

Rother and Kupper [74] found that by supplying fuel through a burner at the kiln inlet of an SP kiln of the Dopol[2] type they were able to reduce the NO_x emissions by about 45 %. However, the authors point out that fuel supply at the kiln inlet may cause disturbances in the internal circulation of sulphur.

Høidalen [75] and Syverud *et al.* [76] found that a NO_x reduction of about 30 % was attainable by supplying pulverized coal to the kiln riser duct of a Pyroclon® Low-NO_x calciner. This calciner is reported to work well also in other plants, giving NO_x reductions of about 35 % [33, 34, 35].

Syverud *et al.* [76, 77] also supplied shredded car tyres to the kiln inlet of a kiln with a Pyroclon® Low-NO_x calciner, reducing the NO_x emissions by up to 40 %.

Dusome [37] reported that a NO_x reduction of about 35 % could be achieved by means of a special design called RSP-MINOX®.

Recently, Thomsen *et al.* [32] measured NO_x emissions less than 400 mg/Nm^3 at 10 % O_2, corresponding to more than 40 % NO_x reduction, by using pulverized coal for staged combustion in a low-NO_x calciner of the FLS ILC type.

[2] Dopol is a trademark of Polysius.

Table 3.2: Fuels used by the European cement industry in 1995 [20].

Petcoke	39 %
Coal	36 %
Different types of waste	10 %
Fuel oil	7 %
Lignite	6 %
Gas	2 %

3.1.5 Alternative fuels in the cement industry

Today, coal and petcoke are the fuels most commonly used in the cement industry, but the utilization of secondary fuels, such as whole car tyres [78, 79], shredded car tyres [80, 76, 77, 79], RDF [81, 82], plastic waste [83] and paper slurry [84] is continuously increasing, see Table 3.2. Moreover, due to the favourable combustion conditions in a cement kiln — high temperature and long residence time — liquid hazardous wastes (LHW) and solid hazardous wastes (SHW) are efficiently destroyed.

The use of secondary fuels has so far primarily been implemented for economic reasons. However, investigations have shown that combustion of alternative fuels [80, 78, 81, 82] and hazardous wastes [85, 86] affects the emissions of pollutants only to a little degree. Furthermore, fuel ash is incorporated in the cement clinker, leaving no ash disposal problem. Besides, replacing coal by non-fossil fuels is equivalent to reducing the net emissions of carbon dioxide. Thus, the combustion of various types of waste is favourable not only economically, but also environmentally.

In general, alternative fuels are burnt in cement kilns under oxidizing conditions. Due to the potential process disturbances, secondary combustion under reducing conditions, i.e. staged combustion, is normally not applied. However, if the use of alternative fuels can be successfully combined with NO_x reduction through staged combustion, the utilization of such fuels becomes even more desirable.

3.1.6 Lean reburning; advanced reburning

In conventional reburning, overall fuel-rich conditions are applied in order to reduce NO_x. However, the unmixed environments often present in large full-scale units may in fact allow substantial reduction of NO_x under overall fuel-lean conditions in the reburning zone. This is due to the existence of local blobs of fuel in which combustion takes place in a diffusion flame environment. Recently, 40–50 % NO_x reduction was demonstrated by means of lean reburning in a pilot-scale boiler [87].

Different NO_x reduction processes may be combined synergistically in so-called CombiNO_x processes [88]. An example of such a process is advanced reburning, in which basic reburning is combined with urea injection. Zamansky *et al.* [89, 90] have demonstrated 90 %

NO_x reduction in a boiler simulator facility using advanced reburning. The mechanism is like this: After an initially rapid NO reduction by basic reburning, the subsequent NO reduction rate is normally slow, since the radical pool has been depleted. When an N-agent such as urea is injected, the reduction reactions are re-started, and the overall NO_x reduction level is increased beyond that of basic reburning. In the same experiments, biomass was found to reduce NO_x more effectively than natural gas. This can be attributed to the sodium content of the biomass; sodium promotes the effect of N-agents [91, 92, 93]. Heap *et al.* [94] showed that cyanuric acid and ammonium sulphate are interesting alternatives to urea in advanced reburning.

Apparently, neither lean reburning nor advanced reburning have been demonstrated in cement kilns. However, it should be of interest to the cement industry to explore the potential of lean and advanced reburning in cement kilns.

3.2 Modelling of cement kilns

Gardeik and Rosemann [95, 96, 26] developed a generic 0-D steady state model[3] (a balance model) of a precalciner cement kiln system, consisting of four units; preheater, precalciner, rotary kiln and cooler. Some crucial simplifications were made: The air equivalence ratios of the rotary kiln and the precalciner were set as input parameters, the cooling air was taken as proportional to the clinker production, the degree of calcination was taken as a temperature function, and the kiln gas temperature was calculated by assuming a constant temperature difference between the gas and the precalcined meal. The model was used to investigate the fuel energy consumption and the fuel energy apportionment in the precalcining process. Farag [97] constructed a similar model, but lumped together the preheater and the precalciner. The model was used to discuss possible thermal energy saving in precalciner kilns with complete bypass of kiln exit gases.

Jeschar *et al.* [98] developed a mathematical model of a precalciner. Different precalciner stages were modelled as ideal stirred vessels, and models for the formation and reduction of thermal and fuel NO_x were included. Various staging-configurations were investigated. A NO_x reduction of about 50 % was simulated by means of a three-stage variant, applying stepped supply of fuel, raw meal and air. A reasonable agreement with experimental data was found.

Several researchers have developed 1-D steady state models of rotary kilns: Gardeik and Jeschar [99, 100] investigated the heat transfer through the wall of a rotary tube by dividing the tube into a finite number of cross-sectional elements and solving the mass

[3] A given system can be represented by either physical or mathematical models. A mathematical model is either statistical (inductive) or deterministic (deductive). Here, only the latter is considered. Deterministic models (which are also called classical models) may be classified as zero-, one-, two- or three-dimensional (0-, 1-, 2- or 3-D). Furthermore, a model is either a steady-state (time-independent) or a dynamic (time-dependent) model.

and energy balances of each element. Frisch and co-workers used a similar model to examine the impact of tertiary air on the energy flow in the system [101] and to optimize the burning process [102]. More recently, Ghoshdastidar and Unni [103] performed a parametric study of the heat-transfer in the drying and preheating zone of a wet process kiln.

Gardeik et al. [104] made a steady state 0-D model of a clinker cooler to investigate the thermal efficiency of such units. Steinbach [105] developed a steady state 1-D model of a rotary cooler. The temperature profile of the solid material and the rotary tube were found by dividing the cooler into a finite number of cross-sectional segments and solving the mass and energy balance by an iterative procedure.

Few dynamic models of cement kiln systems are found in the literature. However, Sælid developed a 1-D dynamic model to simulate the rotary cement kiln process and used it as a basis for designing a control system [106]. (Mordt [107] did a similar work on a rotary kiln used for production of expanded clay aggregates.)

Computational fluid dynamics (CFD) is a continuously expanding field, and it appears that CFD is a technique now being increasingly employed also in the modelling of cement kiln systems: Huttunen and Kjäldman [108] employed the commercial CFD code Fluent® to calculate the flow in the kiln riser duct. The simulations made possible a comparison of flow trajectories and residence time of various particles, providing guidelines on what particles to use in the firing of alternative fuels in the kiln riser duct. Kolyfetis and Markatos [109, 110] modelled the coal flame in the primary burning zone a cement kilns. Eike [111] used Fluent® to calculate the combustion of coal and plastic particles in the main burner. Recently, Mastorakos *et al.* [112] published a work on CFD modelling of rotary kiln that included chemical reactions of calcination and formation of the main clinker oxides (see Subection 2.1.2).

3.3 Circulation phenomena in the kiln system

Sulphur, potassium, sodium and chlorine are elements that circulate in the cement kiln system. The intensity of the cycles vary between different systems, and there are also considerable variations within one single kiln system, depending on the operating conditions. Contributions within this area have been published by for instance Goes [113], Sprung [114], Ritzmann [115], Hatano [116], Goldman *et al.* [117], Rosemann and Gardeik [118], Kreft [119, 120], Schütte and Kupper and co-workers [121, 122, 123, 124], Schulz *et al.* [125], Schmidt *et al.* [126], Farag and Camel [127] and Nielsen and Jepsen [39].

When fuel is added at the kiln inlet, where the circulating substances are present at relatively high concentrations, reducing conditions may occur. This may alter the material circulation considerably and lead to operational problems.

3.3.1 Sulphur

Sulphur comes into the system through the raw meal and through the fuels. The sulphur content of the raw meal and fuels varies a lot from plant to plant. In plants where petcoke is used as a fuel, a considerable amount of the sulphur is introduced through the fuel mix, since petcoke typically contains 5 % S (15 % measured as SO_3).

Raw meal contains sulphur as sulphates (e.g. $CaSO_4$), sulphites (e.g. $CaSO_3$), sulphides (e.g. CaS), disulphides (e.g. FeS_2) and organically bound sulphur, of which sulphates and disulphides are most common [122]. According to Goldmann *et al.* [117], gypsum ($CaSO_4 \cdot 2H_2O$), anhydrite ($CaSO_4$) and pyrite (FeS_2) are the major sulphur components.

Except for sulphates, all sulphur compounds undergo SO_2 releasing reactions at temperatures of 300–600 °C [122], i.e. in the upper part of the cyclone tower. For instance, pyrite (FeS_2) is oxidized according to the following exothermic net reaction:

$$4FeS_2 + 11O_2 \rightarrow 2Fe_2O_3 + 8SO_2 \tag{3.22}$$

The SO_2 released at low temperatures in the preheating tower is the main cause of sulphur emissions from cement kilns. However, if the off-gases are used for drying of the raw materials in the raw meal mill, the raw materials will capture a portion of the sulphur oxides, and hence lower the SO_2 emissions.

Sulphates are thermally more stable; they decompose in the hotter part of the rotary kiln. Calcium sulphate decomposes according to the following endothermic net reaction:

$$CaSO_4 \rightarrow CaO + SO_2 + \frac{1}{2}O_2 \tag{3.23}$$

The SO_2 is transported towards the feed end of the kiln and to the precalciner. In these colder zones, it may react with CaO under oxidizing conditions to re-form calcium sulphate:

$$CaO + SO_2 + \frac{1}{2}O_2 \rightarrow CaSO_4 \tag{3.24}$$

SO_2 capture by calcined limestone is at an optimum at a temperature of about 850 °C [128], which is close to the temperature prevailing in the precalciner. The calcium sulphate returns to the rotary kiln where it decomposes, and so on; thus an internal sulphur cycle is generated.

However, SO_2 will also react with alkalies to form alkali sulphates in the colder part of the kiln and in the precalciner. The alkali sulphates are less volatile than calcium sulphate, thus they do not decompose in the burning zone as readily as calcium sulphate. Consequently, sulphur is discharged from the kiln primarily as alkali sulphates in the clinker.

Pyrite is the dominant sulphurous inorganic compound in coal [129]. In the combustion of pulverized coal in the primary and secondary burner, the fuel sulphur will be oxidized to SO_2, that will follow the same pattern as the SO_2 generated from the raw meal.

3.3.2 Potassium and sodium

Alkalies enter the system primarily through the raw meal and the ash from the solid fuels. The alkalies in the raw meal are mainly present as oxides bound to various minerals [113]. After decomposition, the oxides will react with SO_2 in the kiln gases to form alkali sulphates:

$$K_2O + SO_2 + \frac{1}{2}O_2 \rightarrow K_2SO_4 \tag{3.25}$$

$$Na_2O + SO_2 + \frac{1}{2}O_2 \rightarrow Na_2SO_4 \tag{3.26}$$

The alkalies originating from the fuel ash will most likely form sulphates in a similar manner.

Some of the alkalies leave the preheater as a component of the dust. But in most plants, the off-gas is cleaned and the dust returned to the kiln system along with the raw meal. Hence, the alkalies that enter the system, leave almost entirely as part of the clinker, primarily as sulphates.

During production of specific clinker types high concentrations of alkalies in the clinker must be avoided to obtain the required quality. Therefore, in systems with a high content of alkalies in the raw meal it may be necessary to bypass some of the kiln gas to draw off a portion of the alkalies. In such instances it may be necessary to add chlorine to the system in order to increase the volatility of the alkalies.

3.3.3 Chlorine

Raw meal usually contains only small amounts of chlorine, typically less than 0.01 % [130]. Likewise, fossil fuels are almost chlorine free, but alternative fuels and hazardous wastes may contain considerable amounts of chlorine.

The chlorine reacts with alkalies and form alkali chlorides, that are very volatile. They tend to vaporize in the hot part of the kiln and condense in the colder part and in the precalciner. In a condensed state, they return to the hotter part of the kiln, where they again vaporize, and so on. Hence, an internal chlorine circulation exists in the kiln system. Chlorine compounds may give rise to coating problems. Accordingly, in processes with high intakes of chlorine, it may be necessary to bypass some of the kiln gas in order to reduce the intensity of the chlorine cycle. According to Duda [23], bypassing is required in processes with more than 0.015 % Cl in the raw meal.

3.3.4 The impact of reducing conditions

Under reducing conditions, which is induced during staged combustion, some additional chemical reactions have to be considered. The presence of solid carbon and carbon monox-

ide gives rise to the following global reactions:

$$CaSO_4 + C(s) \rightarrow CaO + SO_2 + CO \quad (3.27)$$

$$CaSO_4 + CO \rightarrow CaO + SO_2 + CO_2 \quad (3.28)$$

Similar reactions apply to the alkalies. Because SO_2 is released in these reactions, reducing conditions tend to increase the intensity of the sulphur cycle in the kiln system, i.e. the concentration of SO_3 in precalcined meal will probably increase when fuel is supplied in the kiln inlet zone. Lowes and Evans [131] found that the SO_3 concentration in the lower cyclone stage increased significantly with increasing CO (decreasing O_2) level at the kiln back-end (kiln inlet), and that an SO_3 level of less than 3.5 % was required to maintain a stable operation of the kiln.

Calcium sulphate, potassium chloride and sulphate spurrite ($C_2S \cdot CaSO_4$) are components typically found in incrustation build-ups [132, 133]. Bonn and Lang [132] claim that, to avoid operational disturbances, the concentration of SO_3, Na_2O-equivalents and Cl in the precalcined meal should be less than 2.5, 2.5 and 0.8 %, respectively.

Enestam and co-workers [134, 135, 136] modelled the influence of car tyres on the alkali and sulphur chemistry in a cement kiln. The rotary tube and the kiln shaft were modelled as nine equilibrium reactors with a known temperature profile, and with the gas phase moving in one direction and the solid phase in the opposite direction. The equilibrium composition was then calculated, taking into account 125 gas species and 36 condensed phases consisting of the elements Ca, K, Na, S, Cl, C, H, O, N, P, F and Mg. One of the effects of adding tyres, at oxidizing conditions, was that the amount of potassium sulphate at the kiln inlet was somewhat reduced, due to the low sulphur content of the tyres compared to the coal/petcoke mix. In one of the calculated cases, the air equivalence ratio was set to 0.8, i.e. overall reducing conditions were simulated. In this case, no sulphate phases were found to be stable at the kiln inlet, meaning that all sulphur existed as gaseous compounds.

Later in this thesis it will be demonstrated that a reducing atmosphere in the kiln also leads to an increased transfer of energy from the rotary kiln to the precalciner.

In order to reduce the intensity of the material cycles, and hence reduce the risk of operational problems, it is necessary to balance the intakes of sulphur, alkalies and chlorine. This is particularly important during reducing conditions. This topic is highlighted in Chapter 10.

3.3.5 Dust cycles

Besides the elements S, K, Na and Cl, dust circulates in the kiln system. The secondary air carries dust from the cooler to the kiln, the kiln gas brings dust from the kiln to the precalciner, and the gas in the preheater of course carries dust from one cyclone to another. Because the dust contains circulating elements, and in general in other concentrations than

the gas and the solid phase, these dust cycles are coupled to the S, K, Na and Cl cycles. Moreover, the dust cycles transfer energy between the various pyroprocessing units.

Chapter 4

Mass and energy balance

In this chapter, the development of a mass and energy balance of Kiln 6 at the Norcem plant in Brevik is outlined. Both the pyroprocessing units (preheater, precalciner, rotary kiln and cooler) and the gas cleaning equipment downstream[1] of the preheater is included in the model. The purpose of the model was to facilitate the planning of experiments and the interpretation of experimental data as well as to enhance the general understanding of the process.

First, a description of the kiln system to be modelled is given, then the model is presented and, finally, calibration and validation of the model is demonstrated.

4.1 Norcem Kiln 6

In 1989, the plant in Brevik was modernized by introduction of the precalcination technology. In this modernization project [75], Kiln 6 was equipped with a new cyclone preheater string, with four cyclone stages, and a Pyroclon® Low-NO_x calciner, supplied by KHD. In addition, a tertiary air duct was installed, the reciprocating grate cooler was enlarged, the kiln drive was upgraded and a new conditioning tower as well as a new electrostatic precipitator (ESP 3) was installed on the new string (string 2).

Recently, two ESP's on string 1 (ESP 1 and ESP 2) were replaced by a new ESP (ESP 4) and a bag filter for additional cleaning of the off-gases from this string. A new bag filter was also installed on string 2.

A schematic drawing of the kiln process is presented in Figure 4.1, and some characteristics of the kiln system are given in Table 4.1 and 4.2.

[1] with regard to the gas phase

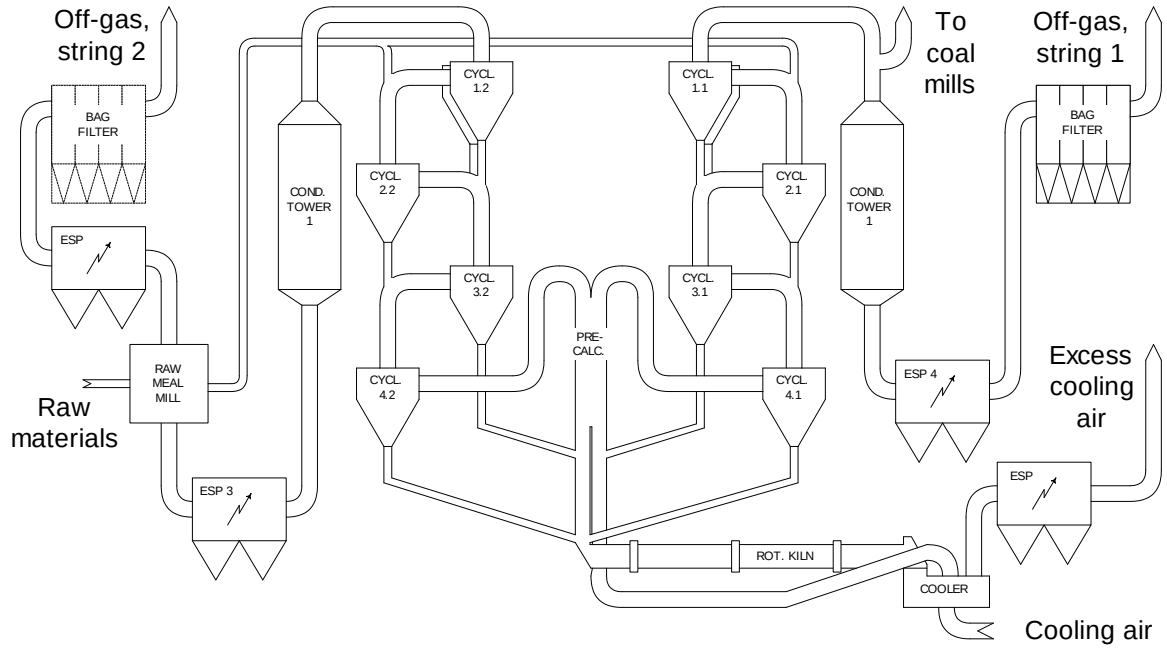

Figure 4.1: Schematic drawing showing the kiln system, including gas-cleaning equipment.

Table 4.1: Characteristics and production data (1997) of Kiln 6.

Kiln length	68	m
Outer kiln diameter	4.4	m
Nominal production capacity	3300	t/d
Typical specific fuel consumption	3300	kJ/(kg clinker)
Approximate static pressure loss in the preheater	7000	Pa
Grate area of the double grate cooler	48	$t/(m^2d)$
Clinker production	1,054,610	t/y
Fuel consumption [137]:		t/y
Coal and petcoke	107,477	t/y
Liquid hazardous waste (LHW)	7,510	t/y
Solid hazardous waste (SHW)	5,398	t/y
Waste oil	1106	t/y
Plastic, biomass and car tyres	2,037	t/y
Fuel oil (diesel oil)	235	t/y

Table 4.2: Mean concentration of pollutants in the off-gas from Kiln 6, 1997 [137].

Component $\left[\frac{mg}{Nm^3}\ @\ 11\ \%\ O_2\right]$	**String 1**	**String 2**	**SFT limit 1999**
NO_x, as NO_2	779	-	-
SO_x, as SO_2	407	75	300
Dust	47	43	50
Chlorine compounds, as HCl	22.7	2.1	10
Total organic carbon (TOC)	0.2	0.3	10
Dioxins	0.055	0.135	0.1
Sum Sb, As, Pb,Cr, Co, Mn, Ni, V and Sn	0.036	0.040	1.0
Mercury	0.016	0.008	0.1
Fluorine compounds, as HF	0.009	0.01	1
Sum Cd and Tl	0.007	0.008	0.1

4.1.1 Process description

The process taking place in the preheater, precalciner, rotary kiln and clinker cooler is essentially as described in subsection 2.1.2, and is not repeated here.

Downstream of the preheater, a small fraction (about 10 %) of the off-gas from string 1 is used for the purpose of drying coal in the coal mills (CM 1 and 2). In the coal mills, the gas flow is increased by about 50 % due to false air[2]. Then the gas is cleaned in a bag filter and released at a temperature of about 75 °C. (This is not shown in Figure 4.1.) The main part of the gas flow from preheater string 1 is, however, flowing through a conditioning tower, where water is evaporated in order to reduce the temperature of the gas to about 160 °C. The conditioning tower is followed by an ESP (ESP 4), where most of the dust is removed from the gas. Some false air in ESP 4 adds to the total gas flow. The cleaned gas is then released to the surroundings through the main stack of string 1 at a temperature of about 140 °C.

The off-gas from string 2 of the preheater is cooled in another conditioning tower. The outlet temperature is normally in the range 230–270 °C. As in string 1, the conditioning tower is followed by an ESP (ESP 3), where most of the dust is removed from the gas. Some false air adds to the total gas flow in this stage. Downstream of ESP 3 most of the gas is used for drying the raw materials in the raw meal mill, but a fraction may bypass the mill (this is not shown in Figure 4.1). Before the gas is released to the surroundings, most of the dust coming from the mill is removed in another ESP. The temperature of the off-gas is usually about 100 °C.

[2] A high oxygen content in the gas in the coal mills is a safety risk; fires and explosions may occur. Besides, false air reduces the grinding capacity of the mills. Hence, it is important to keep the false air portion as low as possible.

4.1.2 Fuels

A mixture of pulverized coal and petcoke (PC) is the main fuel used, both in the primary burner and in the calciner (on the tertiary air side).

Following permission from SFT, the Brevik Cement works is allowed to burn solid and liquid hazardous wastes in compliance with a special permit. LHW is regularly burnt at rates of 1-2 t/h in the main burner of the kiln, and SHW is normally fed at 2-3 t/h at the tertiary air side of the precalciner, as indicated in Figure 5.1.

Waste oil is also frequently used as an additional fuel in the main burner, whereas fuel oil is only used during startups.

Finally, a system for feeding solid wastes, such as RDF, at the kiln inlet and in the riser duct (on the kiln side of the precalciner) is operative.[3]

4.1.3 Control system and measuring equipment

A Honeywell control system is implemented, and the process is run from a central control room. One operator runs the kiln, and another one runs the raw meal mill and the cement mills. Automatic control of the secondary coal supply, based on the calciner outlet temperature (cascade control / loop control), is applied.[4]

The process is extensively monitored, and equipment for measuring the concentration of various gas components, such as O_2,CO and NO_x, is installed.

4.1.4 The precalciner

The Pyroclon® Low-NO_x calciner is shown in Figure 4.2 (see also Figure 4.1). The design of this calciner can be compared to the list of design characteristica given in Subsection 2.3.1:

- *Geometry / feeding of tertiary air:* A special feature of the Pyroclon® Low-NO_x calciner, which is a tube reactor, is the way in which tertiary air enters the calciner. In most calciners, the tertiary air is introduced cross-currently in the calciner; here, it flows co-currently with the kiln gases. This is achieved by extending the tertiary air duct by a vertical, rectangular duct. In the lowest part of the calciner, the tertiary air channel is physically separated from the kiln gas, which flows in parallel with the tertiary air in a similar rectangular duct. Above the separating wall, the

[3] A more extensive utilization of alternate fuels is on the agenda. Very recently, a system for feeding RDF and other types of solid wastes to the primary burning zone was built, but this system has not come into regular use yet. The goal is to replace at least 50 % of the fossil fuel energy with energy from alternative fuels.

[4] Automatic control of the primary coal supply (often termed 'kiln pilot') seems to be more and more common in cement plants, but is not yet implemented in the Brevik plant.

tertiary air gas mixes with the kiln gas. However, since swirl generation is avoided, the mixing occurs rather slowly.

- *Feeding of fuel:* Secondary coal is supplied by pneumatic conveying to the tertiary air side of the calciner through two lateral inlets. In addition, coal may be fed on the kiln side, for the purpose of reducing NO_x through the reburning principle[5]. In this context, the slow mixing of the kiln gas with the tertiary air gas is crucial for retaining reducing conditions for a sufficiently long time to convert NO_x to molecular nitrogen. However, this kiln side burner is not in regular use.

- *Feeding of meal:* The meal from string 1 is fed to the kiln side of the precalciner, vis-à-vis the optional coal inlet. The kiln gas, with a typical velocity of 25 m/s and a typical temperature of 1200 °C entrains the preheated meal. The meal from string 2 enters the tertiary air side of the precalciner vis-à-vis the secondary coal inlets. Distribution of the cross-currently fed meal over the entire cross section of the respective gas channels, is achieved by means of specially designed spreading boxes. By adjusting the meal flow in string 1, relative to string 2, it is possible to influence the temperature in the reducing atmosphere, which is important as far as NO_x reduction is concerned.

- *Fluidization regime:* The fluidization regime is pneumatic conveying[6], as in most other precalciner designs.

The description above is the original features of Pyroclon® Low-NO_x calciner. However, the calciner has been modified to make possible the feeding of alternative fuels: On the tertiary air side, perpendicular to the coal and meal inlets, an additional inlet is implemented for the supply of SHW. This inlet is in the same height level as the coal inlets, but it is sharply inclined (downwards) to ensure trouble-free conveying of the fuel. During the course of the this work, a similar inlet for other types of solid alternative fuels has been built on the kiln side of the precalciner, perpendicular to the meal inlet and the kiln-side burner.

4.2 Conceptual model

Conceptually, the pyroprocessing may be divided into four, corresponding to the preheater, the precalciner, the rotary kiln and the cooler. However, since focus of the experiments will be on staged combustion in the precalciner, it seems appropriate to split

[5] This fuel inlet is sometimes called a low-NO_x burner because of the intended NO_x reduction effect. This is somewhat misleading, because the term low-NO_x burner usually applies to burners with internal fuel staging. Such burners are often used in the primary burning zone of a cement kiln.

[6] See for instance Kunii and Levenspiel [139] for a description of different contacting modes in gas-solids flow systems.

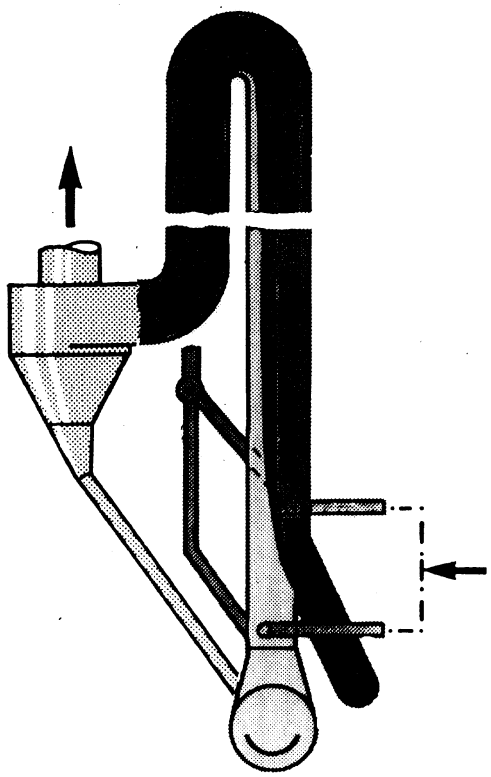

Figure 4.2: The Pyroclon Low-NO_x Calciner [138]. Fuel is supplied in the tertiary air channel and (optionally) in the kiln riser duct (see arrow).

the precalciner into three parts; henceforth called the reburning chamber, the tertiary air chamber and the burnout chamber. The reburning chamber and the tertiary air chamber correspond to the kiln side and the tertiary air side, respectively, of the lower part of the calciner. The burnout chamber corresponds to the upper part of the calciner, after mixing has occured. Conceptually, there are now six reactors, all with particle-gas-flow.[7] Each of these six reactors may be divided into two new reactors; one reactor for the gas phase, and the other for the solid phase, i.e. the meal/clinker. Heat and mass may be transferred between two such reactors in order to account for heating of meal, calcination, sintering and cooling of clinker. Accordingly, the pyroprocessing part of the system consists of 12 steady state reactors.[8]

However, the process units downstream (now with regard to the gas phase) of the preheater, i.e. conditioning towers, ESP's and mills, also must be included in the model. The whole system, consisting of all pyroprocessing units and all gas cleaning units, is shown in Figure 4.3.

4.2.1 Simplifications, approximations and assumptions

For the pyroprocessing units the following assumptions, approximations and simplifications are made:

1. *Steady state process:* In order to obtain a tractable model, the process is taken as a steady state process, i.e. $\frac{\partial()}{\partial t} = 0$ for all variables in the system. As far as the gas phase is concerned, this simplification is rather well justified, since the residence time for the gas phase is of the order of seconds. However, there is mass and heat exchange between the gas phase and the solid phase, the latter having a residence time of the order of one hour in the kiln system. This means that large fluctutations in the flow of solids will render the model useless. However, during normal operation of the kiln, the solids flow is fairly constant. But it is evident that during run-ups and shutdowns the model is not applicable.

2. *Solids reactions:* Endothermic dehydration of clay will occur in the preheater. Exothermic clay crystallization takes place in the precalciner. Calcination, which is strongly endothermic, takes place in the precalciner and in the rotary kiln. Finally, endothermic melting and exothermic sintering takes place in the rotary kiln. This distribution of the reactions is in agreement with the temperature regimes pertaining to the different chemical reactions, as described in Subsection 2.1.2. Evaporation of water is neglected, since the raw meal is dried before it enters the preheater. Also

[7] The flow is co-current in the precalciner, counter-current in the cooler and in the rotary kiln, and a combination of the two in the preheater.

[8] Alternatively, the six reactors can be regarded as heat exchangers, some of which are operating in co-current, others in counter-current, mode.

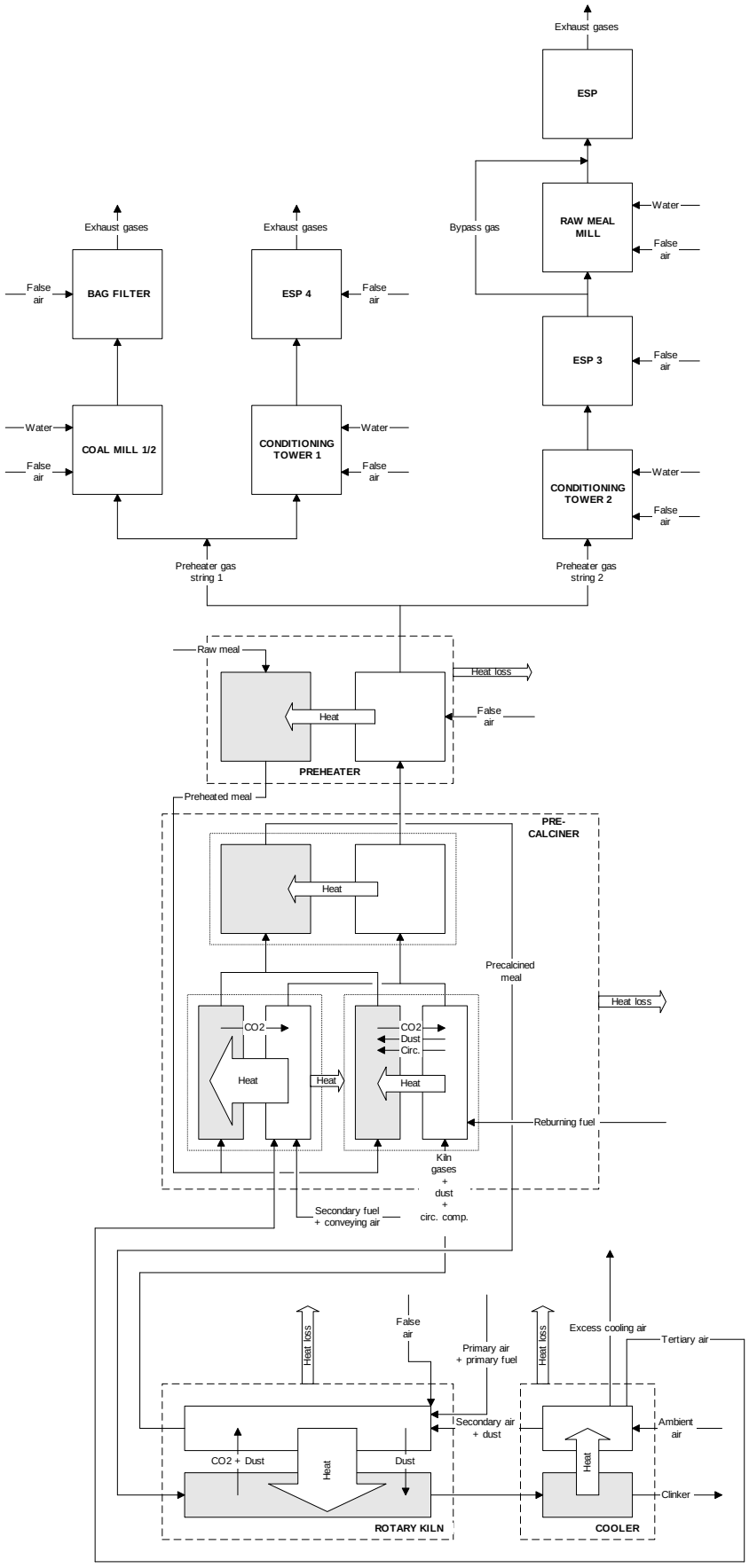

Figure 4.3: Reactor model of the precalciner cement kiln system.

combustion of organically bound carbon and dissociation of magnesium carbonate are neglected in the model.

3. *Constant solids composition in the preheater:* The mass loss from the raw meal in the preheater is relatively small; thus it is neglected.

4. *Calcination reactions:* The precalcination is regarded as completed on exiting the tertiary air chamber and the reburning chamber. For the tertiary air chamber this is probably a good approximation since the secondary fuel is supplied in this part of the precalciner, thus providing the required calcination energy. For the reburning chamber, the approximation is more questionable, since normally no fuel is supplied at this side of the precalciner. However, 'excess' energy in the form of radiation and convective heat is transferred from the tertiary air chamber to the reburning chamber. Also, chemically bound energy is released through condensation of circulating compounds. This makes the approximation more justifiable.

5. *Degree of calcination:* The real degree of calcination is set equal to the apparent degree of calcination (see discussion in Subsection 4.3.1). This is done as a first, simple approximation.

6. *Perfect mixing in both the tertiary air chamber and the reburning chamber:* This means that the outlet temperature of the solid phase equals the gas phase temperature. The approximation is justified by the fact that the raw meal which enters the two chambers is believed to distribute well in the flow and the residence time is of the order 1 second, i.e. rather long residence times; see for instance Hundebøl and Kumar [140].

7. *Ash transfer:* The secondary fuel ash and the reburning fuel ash is transferred to the meal. The primary fuel ash is transferred to the clinker.

8. *Sulphur absorption:* The fuel sulphur is assumed to initially react with oxygen to sulphur dioxide:

$$\mathrm{S} + \mathrm{O_2} \rightarrow \mathrm{SO_2} \tag{4.1}$$

However, most of the SO_2 will be absorbed by the meal, through reaction with CaO and O_2:

$$\mathrm{SO_2} + \mathrm{CaO} + \frac{1}{2}\mathrm{O_2} \rightarrow \mathrm{CaSO_4} \tag{4.2}$$

Accordingly, all the fuel sulphur and the stoichiometric amount of oxygen is transferred from the gas reactor to the solids reactor. This applies to both the tertiary air chamber, the reburning chamber and the rotary kiln. This simplification is in good agreement with the fact that most of the SO_2 that leaves the preheater originate from pyrrite and organic bound sulphur in the raw meal.

9. *False air:* In the preheater and in the kiln inlet/outlet, air will infiltrate the kiln system. Some false air is also believed to leak into the cooler, mainly through the clinker exit channel. The false air flows are taken into consideration through false air parameters, which express the amount of false air as a function of the clinker production. False air in the precalciner is neglected.

10. *Circulation of dust:* Dust will be entrained by the kiln gas and transferred to the meal in the reburning chamber of the precalciner. Likewise, dust is entrained by the secondary air and transferred to the solids in the rotary kiln. These dust cycles imply a transfer of energy from the kiln to the precalciner and the cooler, respectively. The dust flows are described by clinker specific parameters.

11. *No dust in the tertiary air:* For simplicity the dust content of the tertiary air is neglected.

12. *No solids in the exhaust gas:* The exit gas from the preheater is taken as clean, i.e. containing no solids, implicating a 100 % efficiency of the upper cyclone stage. This is however not realistic, since the efficiency of this stage is typically 95 %. To take this into account, the effective raw meal flow is set to 95 % of the raw meal setpoint value.

13. *Circulating species:* Considerable amounts of sulphur, alkali and chlorine compounds circulate between the kiln and the precalciner (internal cycles), see Section 3.3. KCl is an example of an important circulating compound [118], which repeatedly evaporates in the rotary kiln and condences in the precalciner. The heat of vaporization of KCl is about 3.13 MJ/kg, and the KCl level in the precalcined meal may be typically 3 %. This means that there is a considerable energy transfer from the kiln to the reburning chamber of the precalciner. All circulating compounds are represented by KCl, because in this context the energy transfer (rather than the different species) is the more important to model.

14. *Global combustion mechanisms:* The elements determined in an ultimate fuel analysis, i.e. C, H, O, N, S, ash and moisture, are taken into consideration in the combustion reactions. A global mechanism is assumed for all elements: S is oxidized to SO_2, N produces N_2, O produces O_2, H is oxidized to H_2O, and C is oxidized to CO. Finally, if there is enough oxygen, CO is oxidized to CO_2. Moisture and ash are taken as inert components. This model should be adequate for the major components N_2, CO_2, O_2 and H_2O. For CO and SO_2 the model is not very good. More complex mechanisms must be applied in order to predict the concentration of these components. In this work, however, the modelled CO and SO_2 concentration in the kiln system is not of major importance. Nevertheless, the inclusion of these species in the total model satisfy the mass balances.

15. *Irreversible combustion reactions:* All combustion reactions are taken as irreversible. Thermodynamic considerations suggest that in most cases this is a good approximation.

16. *Fast combustion reactions:* The kinetics of the fuel combustion reactions is disregarded, i.e. the rate of the combustion reactions are assumed to be fast compared to the residence time in the reactors, meaning that complete combustion is reached in all reactors with stoichiometric or excess air supply. For the rotary kiln, this assumption is justified by the high temperature and the long residence time. 100 % burnout of the coal particles can not be expected in the atmosphere prevailing in the precalciner, however; the coal char particles being difficult to oxidize completely. 95–99 % is a more typical burnout percentage interval for the coal in the precalciner. (The char residue mixes with the precalcined meal and is burned completely in the rotary kiln.) The assumption of complete burnout tends to give a too high estimate for the outlet temperature for these reactors.

17. *Constant heat loss:* The heat loss from the various process units will depend on the respective surface temperatures, among other factors. In lack of relevant data, constant estimated heat loss values are used in the model.

For the process units downstream of the preheater, the following assumptions, approximations and simplifications are made:

1. *Heat loss:* The heat loss from the various process units and gas ducts is neglected.

2. *Dust flow:* It follows from Paragraph 12 on Page 44 that the dust content of the gas cannot be included in the energy balances. Since the mass flow ratio of dust to gas is typically 1:20, this simplification is rather well justified.

3. *Temperature of the false air:* The temperature of the false air in all units is assumed to be equal to the ambient temperature. This is a good assumption.

4. *Off-gas from the coal mill:* From measurements the mean value of the off-gas flow from the coal mill has been calculated to about 14,400 Nm^3/h when CM 1 is operating and about 24,500 Nm^3/h when CM 2 is operating . These numbers are taken as constant values in the calculations. Realizing that the off-gas from the coal mills accounts for only about 10 % of the total gas flow out of the system, and taking into account the low standard deviation of the gas flow values, this simplification should be justified.

5. *False air in the coal mill:* From measurements of volume flow and O_2 concentration the false air in the coal mill is assumed to be 50 % of the total outflow from the mill.

6. *Temperature of the off-gas from the coal mill:* From measurements the mean value of the off-gas temperature is known to be about 75 °C. This value is taken as constant and is used in the calculations. The variation of this number is rather small , hence the approximation is good.

7. *Coal mill work:* The work done by the machinery in the coal mills is neglected. This results in an overprediction of the inlet gas flow because this flow is calculated by means of an energy balance.

8. *Sensible heat of water transferred in the mills:* The sensible heat of the water transferred from the solids (i.e. coal or raw meal) to the gas in the mills is neglected. This simplification introduces little error, since in these cases the sensible heat terms are negligible compared to the heat of vaporization.

9. *Temperature of the cooling water:* The temperature of the cooling water is set equal to the ambient temperature. This is a good approximation because the cooling water is stored at ambient conditions.

10. *Temperature of the off-gas from ESP 4 (line 1):* From measurements the mean value of the off-gas temperature is known to be about 140 °C. This value is taken as constant and is used in the calculations. The variation of this number is very small , hence it is a good approximation.

11. *Inlet temperature of raw materials:* The temperature of the raw materials entering the mill is set equal to the ambient temperature. This is a good approximation.

12. *Raw meal mill work:* The work done by the aerofall mill (AFM) is transferred to the raw materials as heat. The rest of the machinery in the raw meal mill is, however, not in contact with the gas phase, and can be disregarded in this context.

13. *Water transfer:* The amount of water transferred from the raw meal to the gas phase is set as a parameter.

The simplifications described above will affect the ability of the model to predict various properties of the kiln system. The choice of a steady state model is probably the most crucial point in this context. This is particularly important in the prediction of temperatures, because the thermal buffering capacity of the system cannot be taken into account in a steady state model.

4.3 Mathematical model

4.3.1 Mass balances for the pyroprocessing units

In general, for a given reactor, the total steady state mass balance is found by equalizing the sum of the inflows i to the sum of the outflows j:

$$\sum_i \dot{m}_i = \sum_j \dot{m}_j \tag{4.3}$$

The steady state mass balance for species k is found in a similar manner, however chemical reactions have to be accounted for:

$$\sum_i \dot{m}_{k,i} = \sum_j \dot{m}_{k,j} + \Delta\dot{m}_{k,rx} \tag{4.4}$$

The reaction term in Equation 4.4 is calculated from stoichiometric relations; all reactions are taken as irreversible.

The ash formed in a given reactor is the sum of the ash from the fuels i and SO_3 originating from the fuel sulphur:

$$\dot{m}_{ash} = \sum_i \dot{m}_i \left(w_{ash} + w_S \left[1 + 3\frac{M_O}{M_S} \right] \right)_i \tag{4.5}$$

The *real degree of calcination*, η, of a meal sample can be defined as:

$$\eta \triangleq \frac{m_{CO_2,rawmeal,lost}}{m_{CO_2,rawmeal}} 100\ \% \tag{4.6}$$

However, because of the circulation of solids in the kiln system, as well as the mixing of meal with fuel ash, the real degree of calcination is not easily measured. Instead, the *apparent degree of calcination*, η_{app}, is measured. This is often estimated as[9]:

$$\eta_{app} \triangleq \frac{LOI_{raw\ meal} - LOI_{sample}}{LOI_{raw\ meal}} 100\ \% \tag{4.7}$$

Here, LOI is the loss on ignition of the sample, i.e. the mass loss recorded after heating of the sample to a specified temperature for a certain period of time:

$$LOI = \frac{m_{inital} - m_{final}}{m_{initial}} 100\ \% \tag{4.8}$$

[9]The formula is somewhat odd, because the denominators in the LOI expressions (see Equation 4.8) are not the same. Nevertheless, the formula given in Equation 4.7 is frequently used in the cement industry [38].

The real degree of calcination is always lower than the apparent degree of calcination, but some functional relationship between the two measures exists:

$$\eta = f\left(\eta_{app}\right) \tag{4.9}$$

In the present model, η is used as an input parameter. According to the approximation given in Paragraph 5 on Page 43, $f\left(\eta_{app}\right)$ is set equal to η_{app}.

Applying mass balances to the four pyroprocessing units results in 12 total mass balance equations and eight other functional relations. The 20 equations have 29 unknowns. Applying component balances for H_2O, CO_2, N_2 and O_2 in the rotary kiln, four more equations are generated. Furthermore, models for the flow of tertiary air, primary air, coal conveying air, false air in the kiln and false air in the preheater can be developed, giving five more equations. By that, there are 29 equations in 29 unknowns, and the system can be solved. Component balances for N_2, CO_2, O_2, H_2O, CO and SO_2 in each of the six reactors are solved subsequently. On the basis of this information, also (wet and dry) mole and mass fractions of the various components in the entire kiln system can be calculated.

In addition, the mass flow of various pollutants, such as NO_x and SO_2, in different parts of the system, may calculated. This is done by considering the pollutants as minor species, and combining measured concentration values of the pollutants with calculated mass (or mole) flows. Such information is essential when NO_x reduction experiment results are to be interpreted.

Details of the mass balances for each of the pyroprocessing units are not given here, but can be found elsewhere [13].

4.3.2 Energy balances for the pyroprocessing units

The total steady state energy balance of a given system, i.e. a reactor, can be written as:

$$\sum_i m_i \left(\Delta H^0_{f,T_{ref}} + \int_{T_{ref}}^{T_{in}} c_p \mathrm{dT}\right)_i = \sum_j m_j \left(\Delta H^0_{f,T_{ref}} + \int_{T_{ref}}^{T_{out}} c_p \mathrm{dT}\right)_j + Q - W \tag{4.10}$$

Here, $\Delta H^0_{f,T_{ref}}$ is the enthalpy of formation, Q is the net heat loss from the system and W is the net work done on the system. Index i denotes inflow, and j denotes outflow.

The specific heat c_p of a given component can be calculated as:

$$c_p = a + bT + cT^2 + dT^3 \tag{4.11}$$

The coefficients a, b, c, and d for various substances can be found in the literature [141, 22].

Applying energy balances to the four pyroprocessing units results in six unknowns[10] and six equations. Hence, the equations can be solved. Details of the energy balances for each of the pyroprocessing units can be found elsewhere [13].

[10] The required mass flows in the energy equations are known from the solution of the mass balances.

4.3.3 Mass and energy balance for the gas cleaning equipment

Applying mass and energy balances to the system downstream of the preheater, i.e. the conditioning towers, the ESP's and the mills, results in 27 equations in 27 unknowns. Hence, the system is closed, and in can be solved. Details of the equations pertaining to this part of the kiln can be found elsewhere [14, 15].

4.3.4 Program implementation

The models presented in the preceding section are implemented in MATLAB® in a program called MEBCEM[11]. Details of the program structure and the source code of MEBCEM are not given here, but can be found elsewhere [15]. A brief description is, however, given in Appendix B.

4.3.5 The role of the model

First of all, the model can be used to calculate properties that are not easily measured in the process. Secondly, the model constitutes a necessary basis for quantifying NO_x reduction measures. Thirdly, as will be shown in Chapter 10, MEBCEM will be used in the calculation of the internal material cycles in the system. Furthermore, the model can be used to analyse the process, for instance by means of equivalence ratios and thermal efficiencies. Accordingly, corrective actions can be prescribed.

However it should be pointed out that — since several process outputs are used as model inputs — MEBCEM is not a predictive model. Hence, it can not be used for instance to directly predict the effects of operational changes.

4.4 Calibration and validation

In March 1998, three full-scale trials were conducted at the cement works in Brevik. The following data, collected in these trials, are used for calibration and validation of MEBCEM:

- Off-gas flow rate, string 1
- Off-gas flow rate, string 2
- Excess cooling air flow rate
- O_2 concentration in the off-gas, string 1
- CO_2 concentration in the off-gas, string 1

[11] MEBCEM is an acronym for Mass and Energy Balance of a CEMent kiln system.

- O_2 concentration in the off-gas, string 2
- CO_2 concentration in the off-gas, string 2

It should be noted that the temperature predictions of the model are not calibrated nor validated by this. In this work, however, the mass balances are the more important to verify, since these are the basis for data analysis to be performed. Besides, keeping in mind that the model is a steady state model, dynamic phenomena will probably influence the energy balances more than the mass balances. Hence, perfectly balancing the energy will be very difficult.

4.4.1 Calibration

The total inflow of cooling air is a measured process variable. This flow is divided in three: secondary air, tertiary air and excess cooling air. In MEBCEM, the secondary air is calculated by means of an oxygen balance, and the tertiary air is estimated by means of a flow model (see Subsection 4.3.1). The excess cooling air is calculated by difference. By adjusting an unknown valve constant in the tertiary air flow model, the distribution between tertiary air and excess cooling air can be manipulated. This affects the off-gas from the kiln system, since an increase in the tertiary air flow will lead to an increase in the off-gas from string 1 and 2. The concentration of gas components is also influenced.

Calibration of MEBCEM is done by adjusting the tertiary air gate valve constant until a best possible fit between measured and modelled data is achieved. Calibration by means of data from the first trial is shown in Figure 4.4–4.6.

Figure 4.4 shows that the values of measured gas flows out of the kiln system are somewhat higher than the calculated values. This discrepancy is difficult to explain. However, the calculated concentrations of O_2 and CO_2 in the off-gas from string 1 (Figure 4.5) and string 2 (Figure 4.6) are in very good agreement with the measured data.

4.4.2 Validation

Validation is done by testing the model on data measured and recorded during the two other full-scale trials, see Figure 4.7–4.9 and Figure 4.10–4.12 for the two trials, respectively. These data are independent of the data used for calibration.

In Figure 4.7 and 4.10 one can observe a relatively good agreement between measured and modelled flow data. Furthermore, there is an acceptable agreement for the O_2 and CO_2 (Figure 4.8 and 4.11) data on string 1. As far as string 2 is concerned, the accordance is not so good (see Figure 4.9 and 4.12). However, for the last trial (Figure 4.12) this is due to a temporary reduction in the raw material supply. Such heavy load changes, which are dynamic by nature, are not possible to reproduce in a steady state model, since during the transient period an accumulation (negative or positive) occurs within

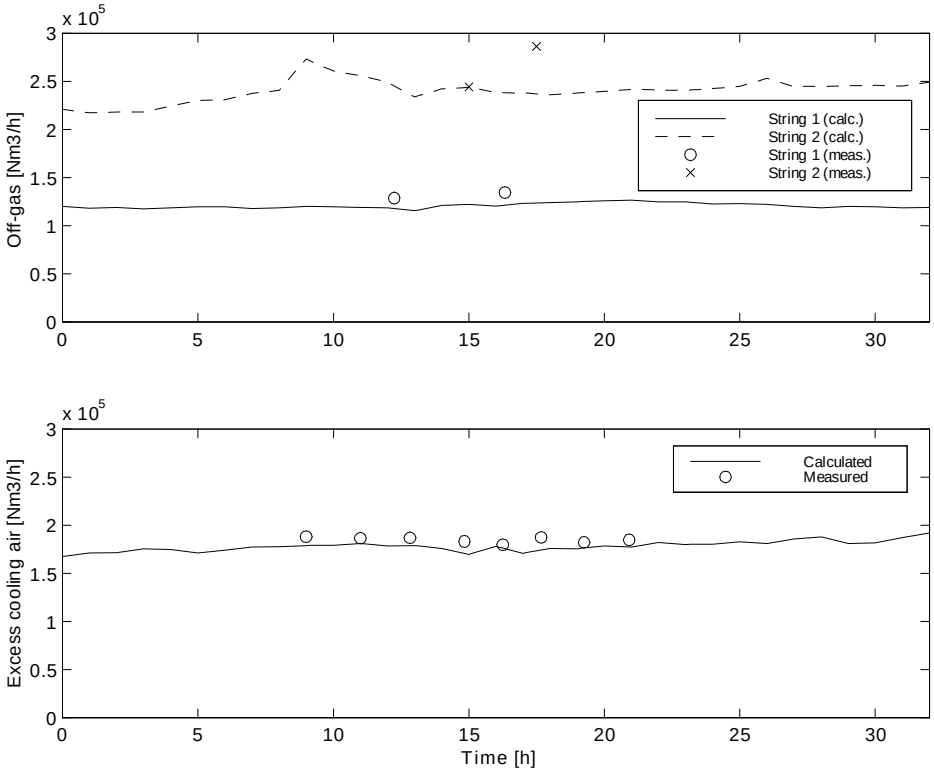

Figure 4.4: Calibration of MEBCEM with gas flow data from trial 1.

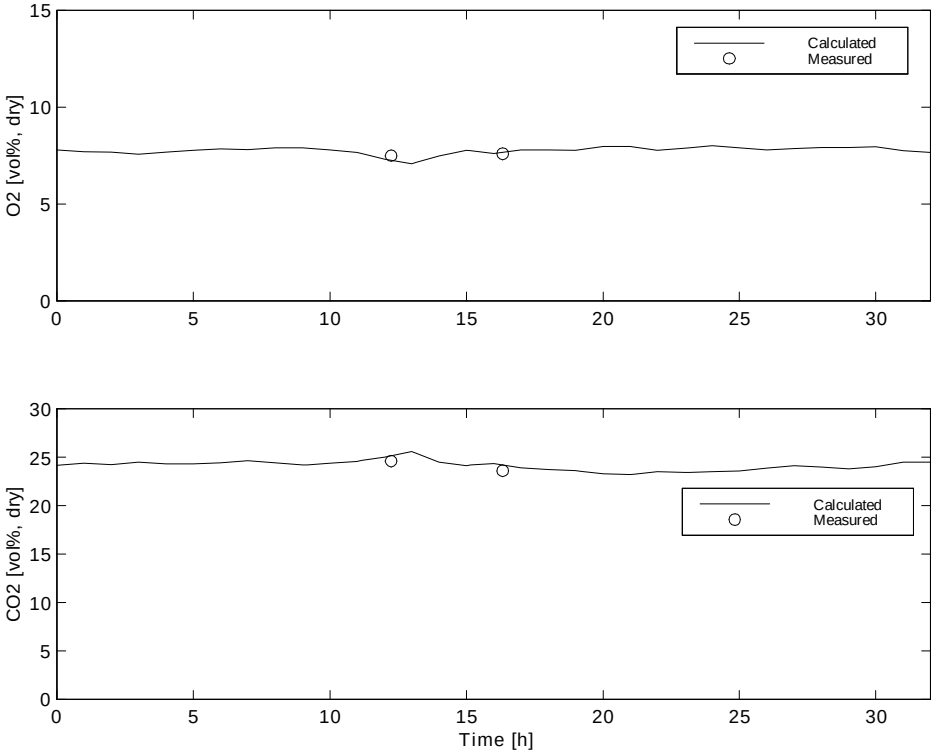

Figure 4.5: Calibration of MEBCEM with gas concentration data from string 1, trial 1.

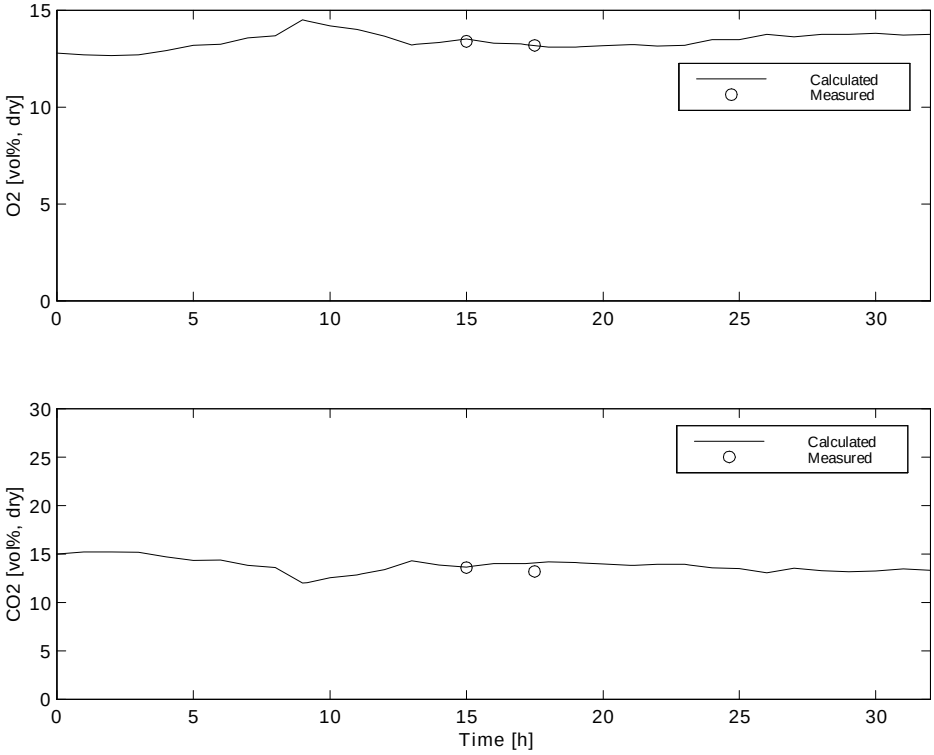

Figure 4.6: Calibration of MEBCEM with gas concentration data from string 2, trial 1.

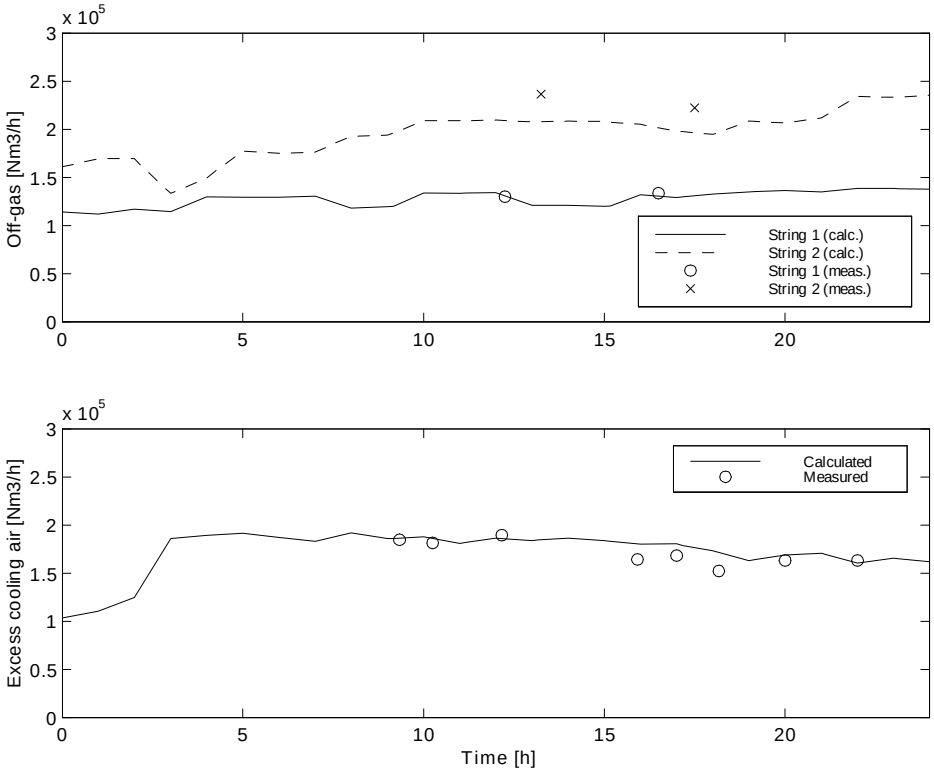

Figure 4.7: Validation of MEBCEM with gas flow data from trial 2.

the reactor. (This illustrates the weakness of a steady state model.) On the other hand, Figure 4.12 reveals that if the setpoint change had not occurred, there would probably be a reasonable agreement between measured and modelled data.

On the basis of the validation, the prediction abilities of MEBCEM can be regarded as satisfactory provided the process is at steady state.

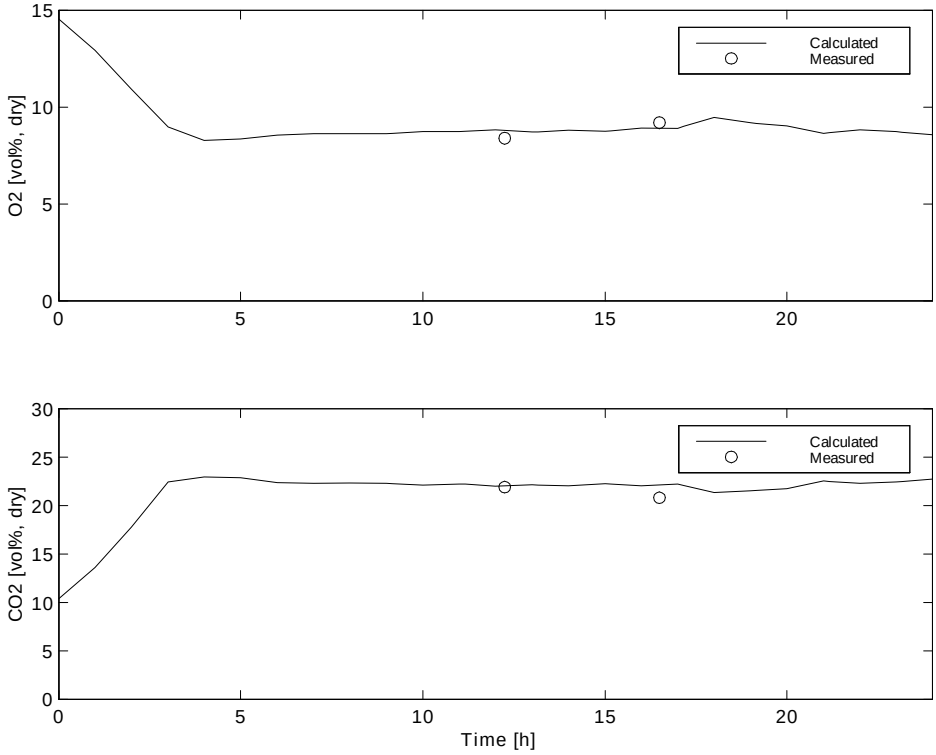

Figure 4.8: Validation of MEBCEM with gas concentration data from string 1, trial 2.

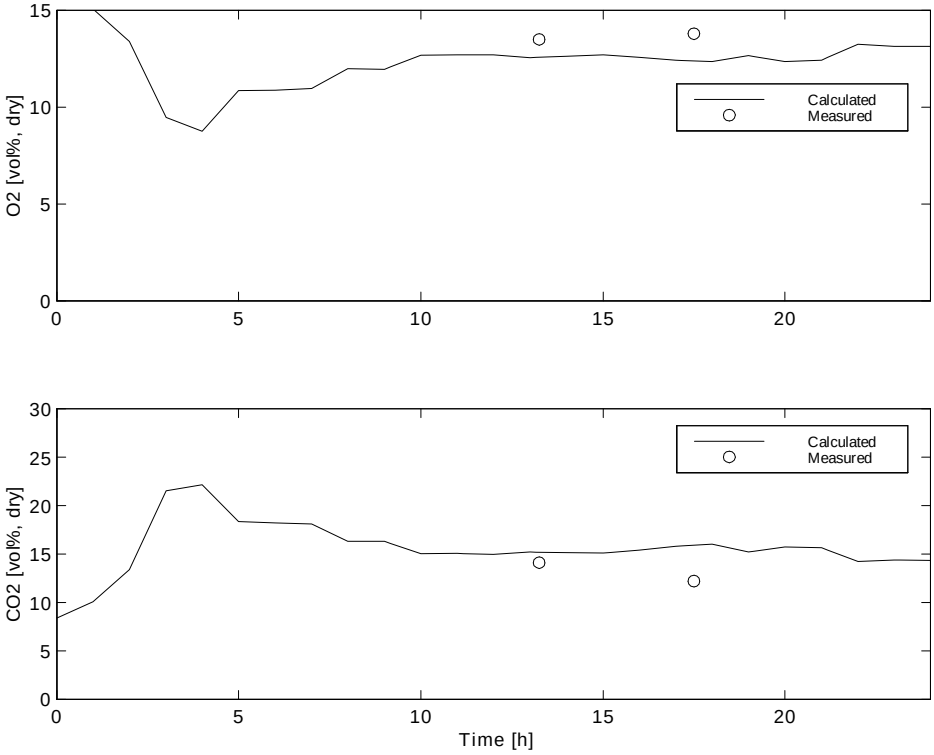

Figure 4.9: Validation of MEBCEM with gas concentration data from string 2, trial 2.

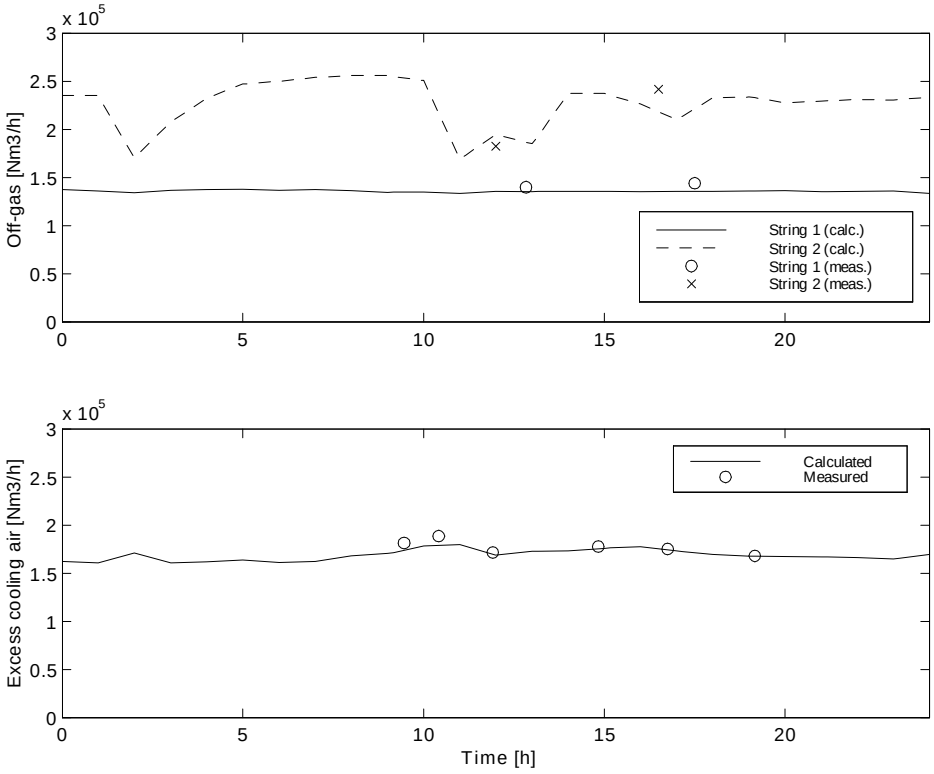

Figure 4.10: Validation of MEBCEM with gas flow data from trial 3.

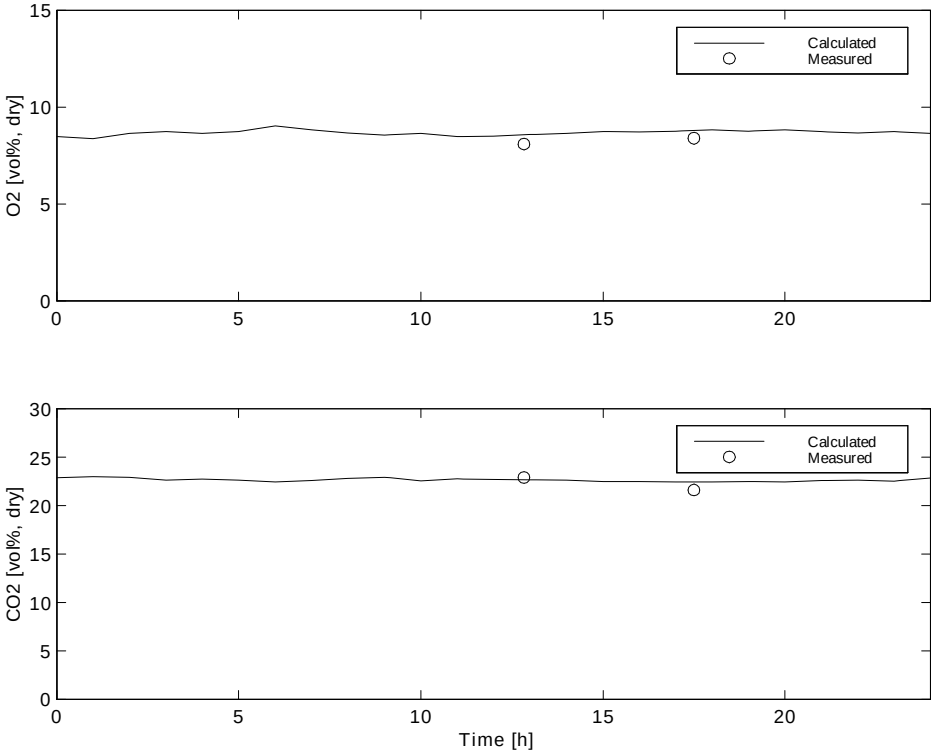

Figure 4.11: Validation of MEBCEM with gas concentration data from string 1, trial 3.

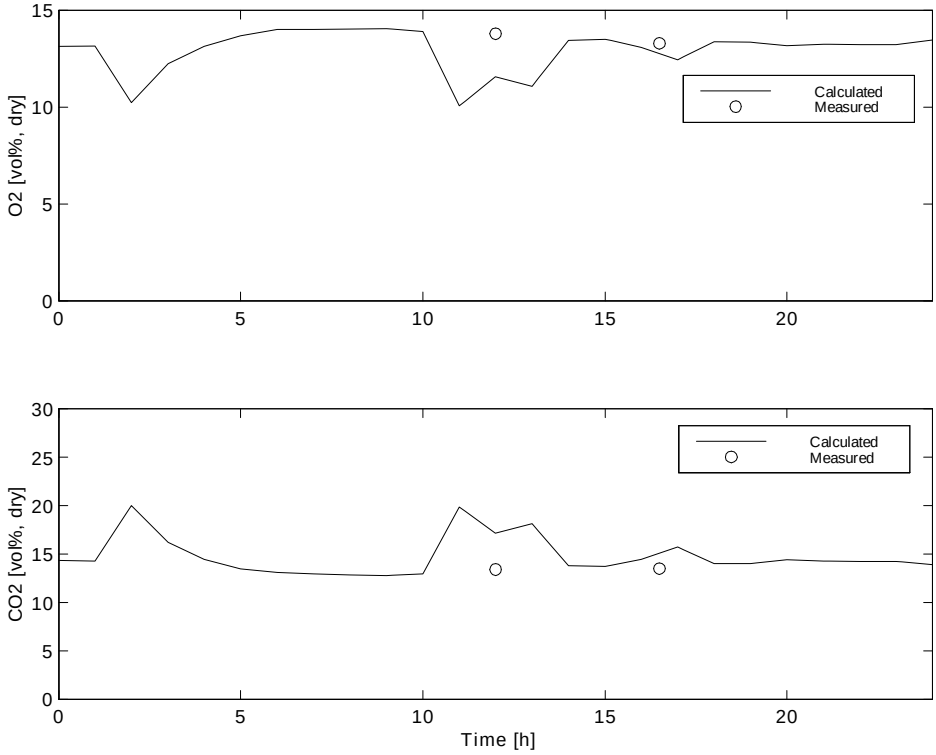

Figure 4.12: Validation of MEBCEM with gas concentration data from string 2, trial 3.

Chapter 5

Full-scale experiments I

Several trials employing the principle of staged combustion have been performed on Kiln 6. Results from trials with chipped car tyres have been published previously [76, 77, 8]. In this chapter, two full-scale trials supplying waste plastic at the back-end of Kiln 6 are discussed.

The purpose of the experiments was to reduce the NO_x formed in the rotary kiln by utilizing the principle of staged combustion, as described in Section 3.1.4.

Some results from these experiments have been published previously [9], and the experimental data from the trials have also been utilized in a statistical analysis of relations between NO_x emissions and other operational parameters [10].

The first trial was performed in October 1996 (Test A), the second in January 1997 (Test B); both during normal operation of the kiln, see Table 5.1.

5.1 Experimental details

5.1.1 Experimental procedure

The waste plastic was fed from a push-floor discharger to a belt conveyor, then through a chute with a double flap valve (to avoid false air) and into the dust settling chamber at

Table 5.1: Experimental conditions (average values) for Test A and B.

Parameter	**Unit**	**Test A**	**Test B**
Clinker production	t/d	3407	3502
Total specific fuel consumption	MJ/(kg clinker)	3.1	3.1
Degree of calcination in the precalciner	%	93	92
Fuel fraction in the precalciner	MJ/MJ	0.50	0.51
Nominal feed rate of plastic	t/h	2.0	2.0

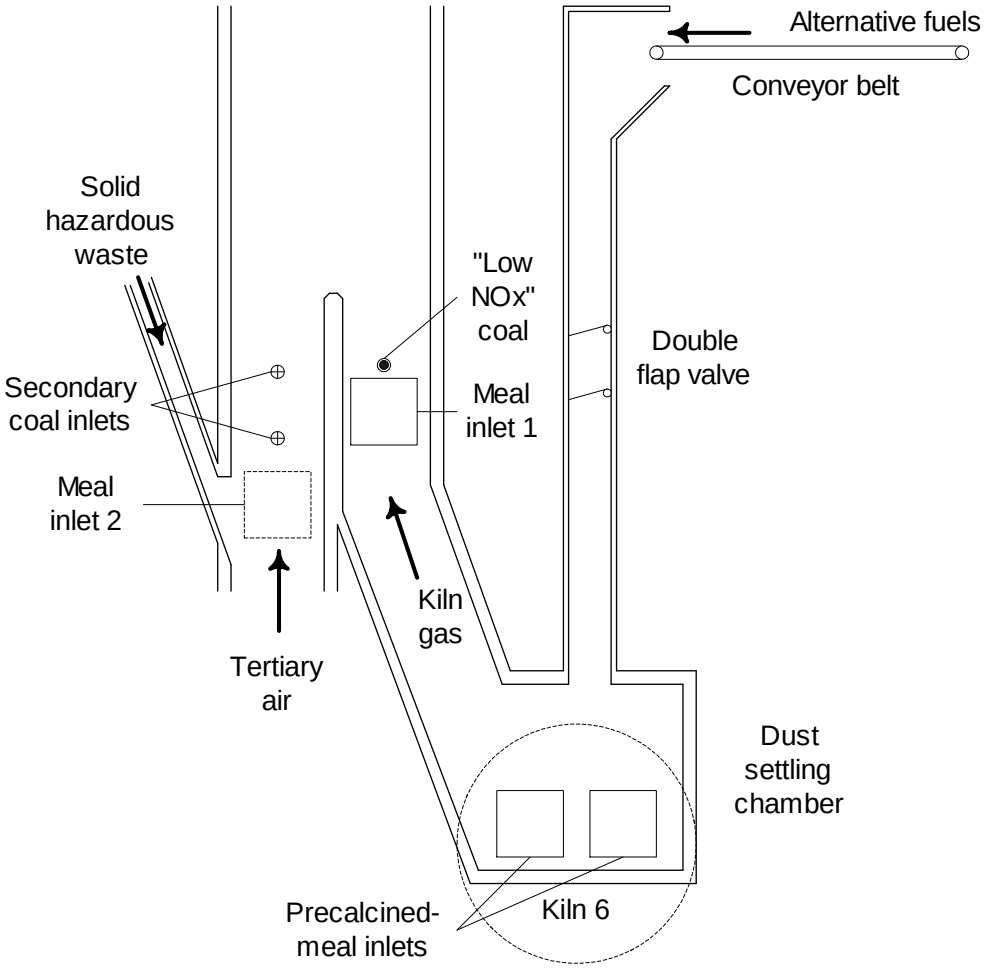

Figure 5.1: Principle drawing of system for feeding alternative fuels into the kiln inlet.

the back-end of the kiln. The feeding system is shown in Figure 5.1.

In each trial, process data were collected for about 20 hours, and a nominal plastic supply of 2 t/h was maintained for about eight hours. The continuous emission monitoring system provided NO_x and O_2 concentration data. Samples of precalcined meal on both strings were taken every two hours, and the SO_3 content was analyzed by means of a Leco SC-132 Sulfur Deteriminator.

5.1.2 Fuel analyses

The plastic fuel, see Table 5.2, was a mix of screw caps from soft drink bottles (made of polypropylene; PP) and shredded plastic bottles (made of polyethylene-terephthalate;

Table 5.2: Proximate analysis and heating value of the plastic wastes and the pulverized-coal mix used in the experiments.

Parameter	**Unit**	**PP**	**PET**	**Coal A**	**Coal B**
Moisture	%	0.01	0.08	3.07	2.04
Volatile matter	%	99.01	88.18	35.90	30.22
Fixed carbon	%	0.01	11.26	52.29	57.54
Ash	%	0.97	0.48	8.78	10.21
Sum	%	100.00	100.00	100.04	100.01
Lower heating value	MJ/kg	43.18	21.97	27.79	28.77

PET), about 2 mm thick. In Test A, the PET fraction was the smallest one (roughly 15 % by weight), consisting of rather small pieces (typically 1 by 1 cm), whereas in Test B, the PET fraction was the largest one (roughly 85 % by weight), and it was made up of considerably larger pieces (typically 2 by 10 cm). The exact fraction values were however not available.

Characteristics of the coal used in the primary and secondary burners in the two tests are also given in Table 5.2. The nitrogen content of the coal was approximately 1.5 % in both trials. The proximate analyses[1] were performed by means of a Leco MAC 400 Proximate Analysis Detector, and the heating values were determined by a Leco AC 300 Bomb Calorimeter.

5.2 Results and discussion

Figure 5.2 and 5.3 show the NO_x concentration at the rotary kiln inlet and in the stack gas as well as the fuel feed rates during the two experiments.[2]

In the first case, i.e. in Test A, the secondary coal feed rate drops by about 37 % when the plastic fuel is supplied at a feed rate of 2 t/h, see Table 5.3. (As mentioned in subsection 4.1.3, the secondary coal is automatically controlled by the calciner temperature: When the temperature rises due to plastic supply, the secondary coal supply is reduced.) This corresponds rather well to the difference in heating value between coal and plastic. The NO_x concentration at the kiln inlet increases by about 2 %, whereas the NO_x level after the precalciner drops by about 20 %. The NO_x concentration in the stack gas also drops after the plastic burning is finished, but this is due to a reduction in the NO_x level at the rotary kiln inlet, see Figure 5.2.

In Test B the coal feed rate drops by approximately 46 % (see Table 5.3) during plastic

[1] In a proximate analysis, which is a standard analysis for solid fuel characterization, the content of moisture, volatiles, fixed carbon and ash in the fuel is determined.

[2] Since the kiln inlet data contained some noise (originating from the continuous cleaning of the probes), the data were filtered by means of a FIR filter implemented in MATLAB®.

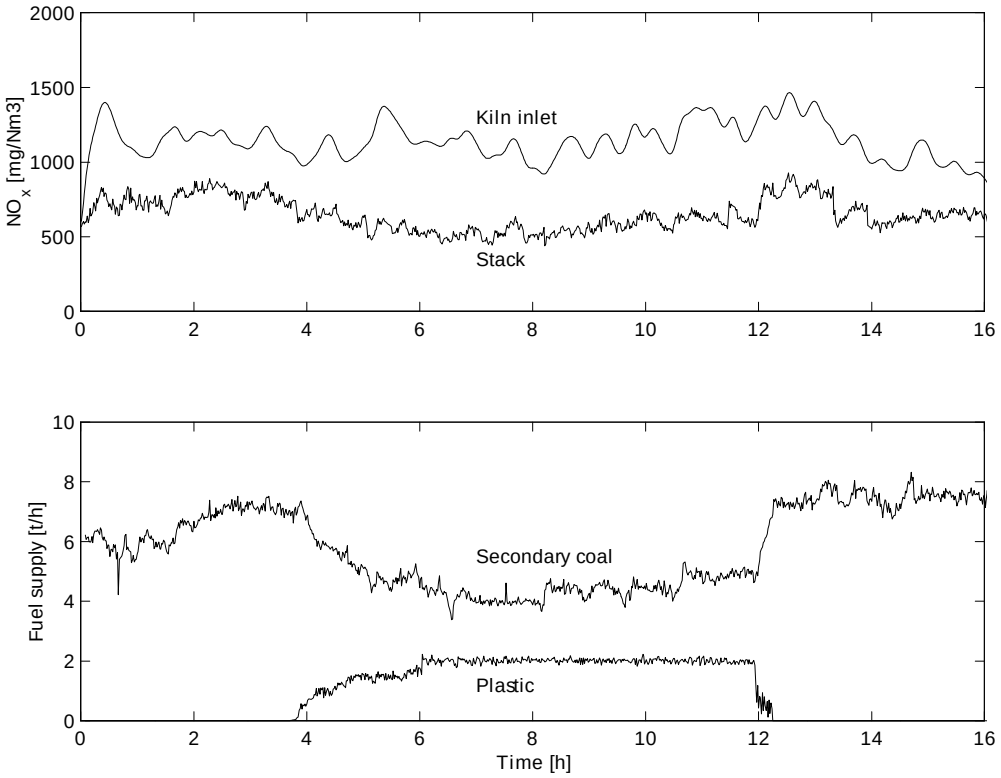

Figure 5.2: NO_x concentration in the kiln inlet and in the stack during supply of secondary coal and plastic in Test A.

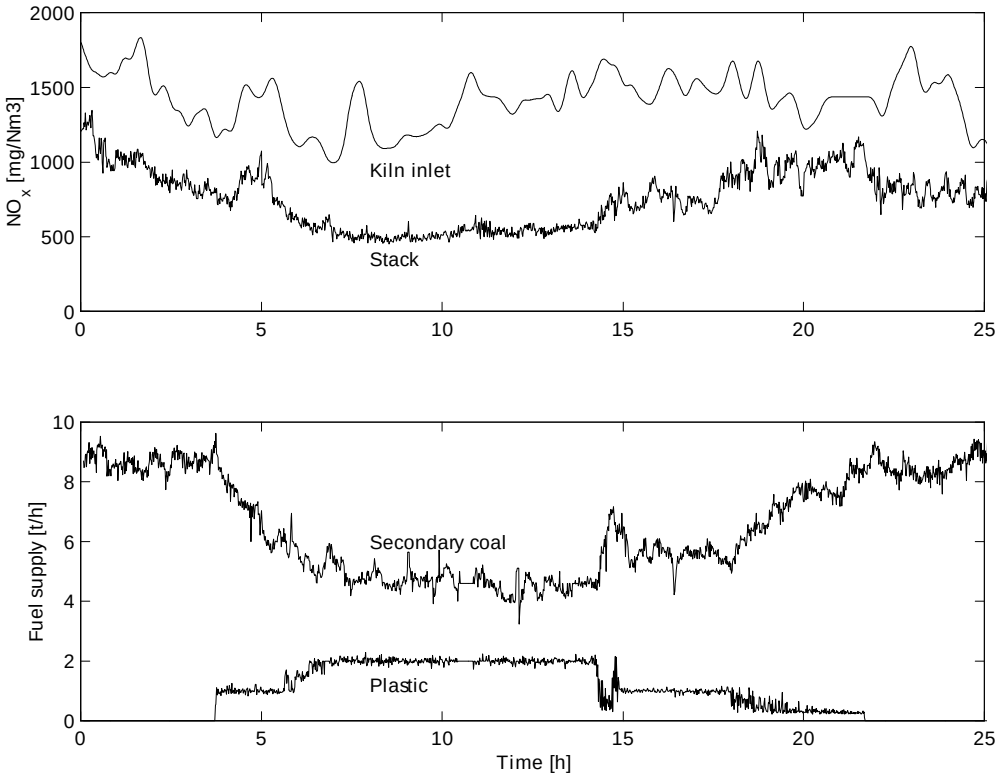

Figure 5.3: NO_x concentration in the kiln inlet and in the stack during supply of secondary coal and plastic in Test B.

Table 5.3: Experimental results (average values).

	Unit	**Test A**		**Test B**	
Plastic feed rate	t/h	0.0	2.0	0.0	2.0
Secondary coal feed rate	t/h	7.0	4.4	8.6	4.7
Clinker production	t/d	3460	3368	3577	3527
Total specific fuel consumption	MJ/(kg cli)	3.1	3.1	3.1	3.0
Fuel fraction in the precalciner	MJ/MJ	0.49	0.53	0.51	0.50
NO_x content in the kiln inlet	mg/Nm^3	1123	1141	1421	1295
NO_x content in the stack gas	mg/Nm^3	717	572	883	526
NO_x reduction, kiln inlet	%	–2		+9	
NO_x reduction, stack	%	+20		+40	

combustion, but simultaneously the supply of solid hazardous waste is increased, resulting in a reduction in total specific fuel consumption of about 3 %. The NO_x reduction is larger than in the first case. This may be due partly to a higher NO_x level at the kiln inlet in Test B; the NO_x reduction efficiency is known to increase with increasing NO_x concentration [142].

The mean NO_x level (measured as NO_2 at 10 % O_2, dry) in the stack gas during the tests were 572 and 526 mg/Nm^3, respectively, whereas the corresponding minimum values were as low as 439 and 452 mg/Nm^3.

In Figure 5.4 and 5.5, the NO_x in the stack gas is plotted versus clinker production. The NO_x reduction effect is seen to be independent of production. This is particularly clear in Test B. The rather low NO_x level at the highest production rates in Test A is due to particularly low NO_x concentrations at the kiln inlet, corresponding to an unstable state of production, see Figure 5.2. In Test A, the clinker specific NO_x emissions are reduced by an average of 22 % during plastic combustion; for Test B the equivalent number is 39 %.

Previous measurements have shown that the introduction of solid hazardous wastes in the precalciner has no significant effect on the NO_x emissions. The introduction of liquid hazardous wastes in the main burner, however, reduces the NO_x levels at the kiln inlet somewhat, due to the water content (25-30 %) of the wastes. The impact of liquid/solid wastes on the test results are regarded as being negligible.

5.2.1 The NO_x conversion ratio

The reburning effect can be visualized more clearly by means of the NO_x conversion ratio in the precalciner, ϕ_{NO}. This may be defined as:

$$\phi_{NO} \triangleq \frac{\dot{m}_{NO,\text{kiln inlet}} - \dot{m}_{NO,\text{stack}}}{\dot{m}_{NO,\text{kiln inlet}}} 100\ \% \tag{5.1}$$

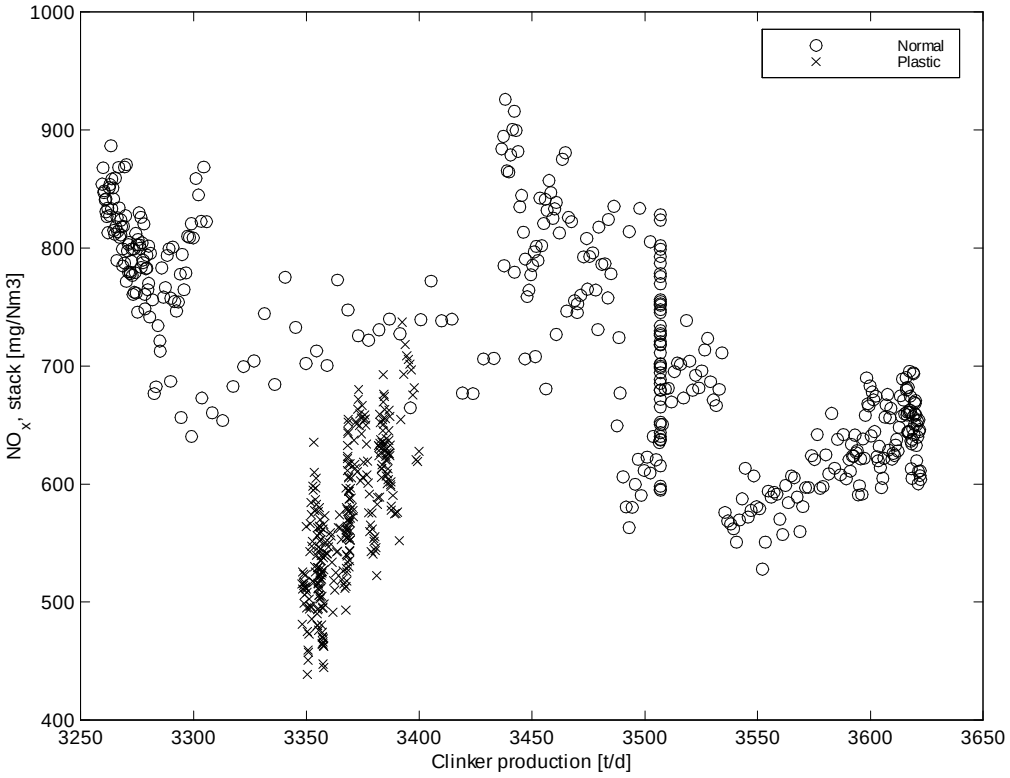

Figure 5.4: NO_x concentration in the stack gas versus clinker production, Test A.

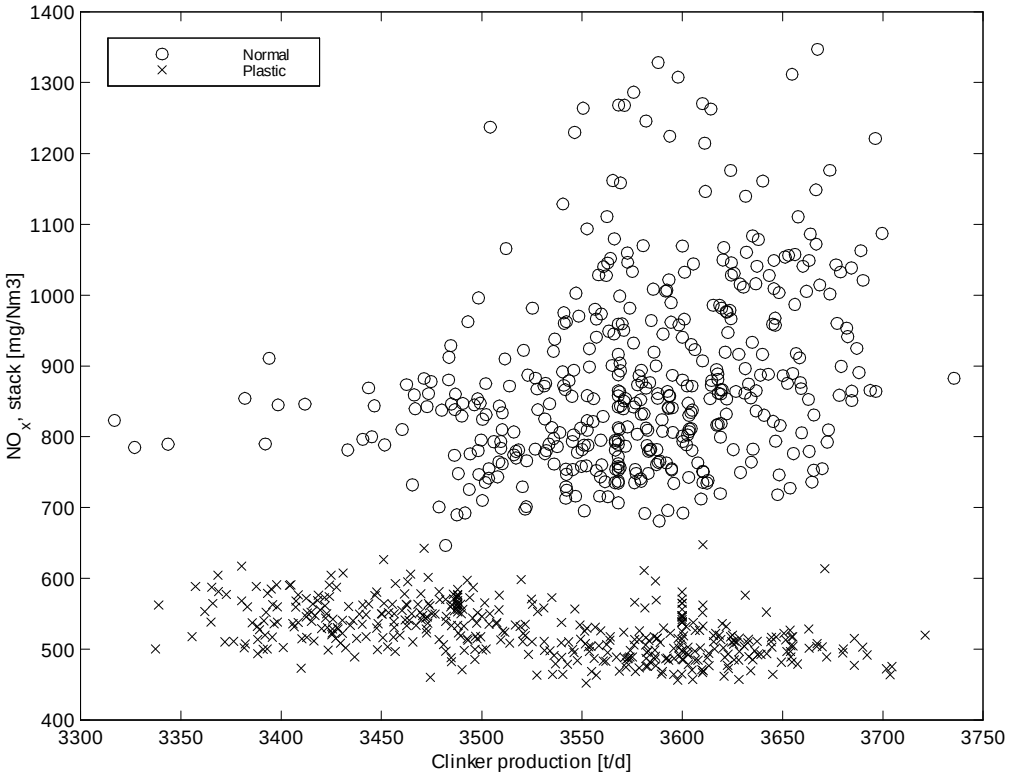

Figure 5.5: NO_x concentration in the stack gas versus clinker production, Test B.

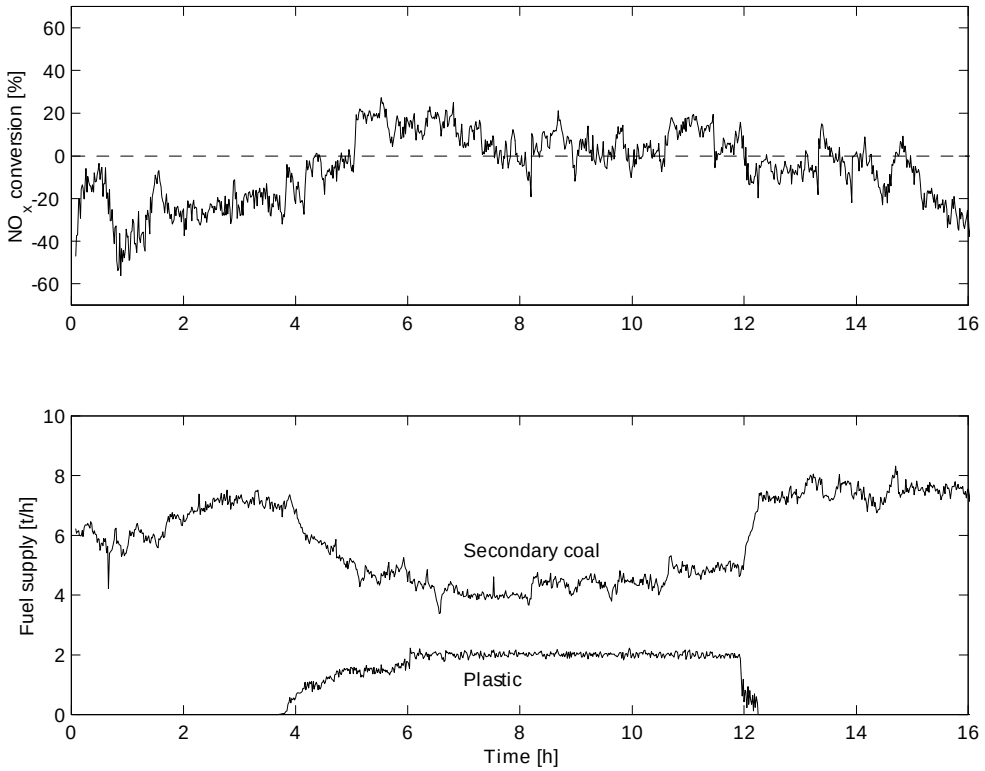

Figure 5.6: Calculated NO_x conversion in the precalciner, Test A.

$\phi_{NO} < 0$ is equivalent to a net increase of NO_x from the kiln inlet to the stack. This is to be expected during normal operation of the kiln, since fuel NO_x is formed in the precalciner. $\phi_{NO} > 0$ implies a net decrease of NO_x from the kiln inlet to the stack. Such a decrease must be due to reburning or some other NO_x reduction mechanism.

Use of Equation 5.1 is based on the assumption that the NO_x level at the kiln inlet is unaffected by the reburning fuel. This may not always be fully correct, since part of the reburning fuel may be transported into the kiln inlet zone and contribute to NO_x reduction before the kiln gas reaches the gas probe. This effect is, however, likely to be rather small. The fact that no significant changes in the O_2 concentration at the kiln inlet during the reburning trials have been observed, supports this assumption.

Calculation of ϕ_{NO} requires knowledge of the mass flows of NO_x and thus of the total gas flow rates at the kiln inlet and in the stack. Since direct measurement of the gas flow rates in the system is not possible, the flow rates have to be calculated. This is done by using MEBCEM (see Chapter 4). The resulting NO_x conversions are shown in Figure 5.6 and 5.7.

In Test A, the NO_x conversion ratio in the precalciner is on average –18 % when

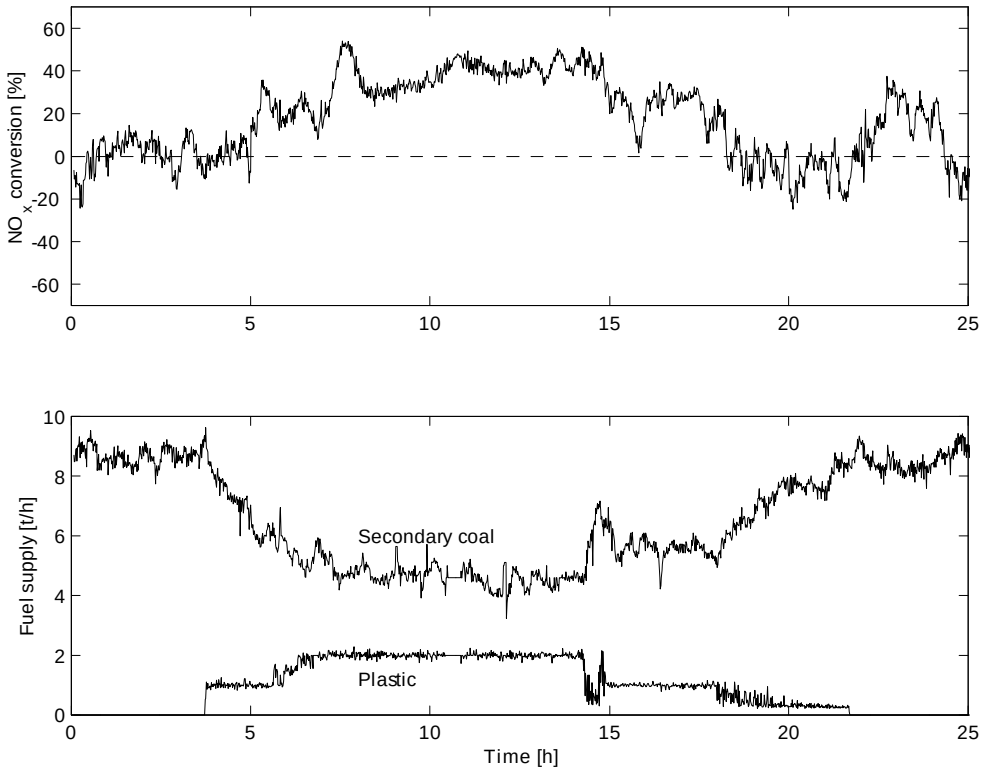

Figure 5.7: Calculated NO_x conversion in the precalciner, Test B.

reburning is not applied, i.e. there is a net increase in NO_x mass flow. This is likely to be due to fuel NO_x formation in the precalciner. (The fact that the NO_x concentration in the stack is lower than in the kiln inlet, is due to the mixing of kiln gas with off-gas from the tertiary air chamber, with false air, and with water.) During supply of plastic, the NO_x conversion ratio increases to an average of +5 %, i.e. there is a net decrease in the NO_x mass flow through the precalciner. This increase in ϕ_{NO} is probably partly due to the reduced supply of secondary coal, resulting in lower fuel NO_x formation. Partly it may be attributed to the (homogeneous) reburning effect, although heterogeneous and/or heterogeneous-catalytic effects may be effective, too.

In Test B, the average NO_x conversion ratio is 0 % and +36 % without and with reburning, respectively; giving a significantly higher NO_x reduction than in the first experiment.

However, operational difficulties related to an accumulation of sulphur compounds in the precalciner were experienced during the latest trial: The SO_3 content of the calcined meal increased from about 2 % to a maximum of about 6 % during the plastic burning, see Figure 5.8; the specific current for the kiln rotation (i.e. the kiln current divided by raw meal supply[3]) was reduced by about 20 % when plastic was supplied at a rate of 2 t/h, see Figure 5.9; and the concentration of free lime in the clinker product increased from about 0.7 % to a maximum of about 2.3 %, see Figure 5.10. Such operational disturbances were not experienced during Test A, or at least to a very little degree, see Figure 5.11.

The high average NO_x conversion ratio during maximum reburning fuel supply in Test B may be partly, but not fully, explained by the larger reduction in secondary coal supply. Accordingly, there must be additional NO_x reduction mechanisms present. There are two main differences between the two reburning fuels used in the experiments: the heating value and the size of the fuel particles. For a constant flow rate of the reburning fuel, the NO_x reduction is expected to increase with increasing heating value of the reburning fuel — because of reduced fuel NO_x formation and increased reburning. In this case, however, the reverse is true; the fuel with the lowest heating value gives the highest NO_x reduction (Test A). This suggests that the transportation and mixing of the reburning fuel in the gas phase may be a crucial factor: In Test A, a large portion of the plastic feed may have been entrained by the kiln gas; whereas in Test B, a major part of the plastic pieces — being considerably larger than in Test A — may have been transported into the kiln along with the calcined meal. This promotes the creation of a reducing atmosphere in the kiln inlet area. In this way, the internal circulation of sulphur and alkalies is altered, which in turn may influence the kiln temperature and

[3]The kiln current is proportional to the kiln horsepower, HP. The HP has two terms: the friction-HP, caused by the rotational friction, and the load-HP, caused by the the solid materials in the kiln. Whereas the friction-HP is more or less constant, the value of load-HP depends on the degree of filling as well as the material type. At standard operation, load-HP (85–90 %) is much larger than friction-HP (10–15 %) [23]. Changes in the raw meal supply will change the load-HP and hence kiln current. That is why the kiln current is here 'normalized' by the raw meal supply when different test results are compared.

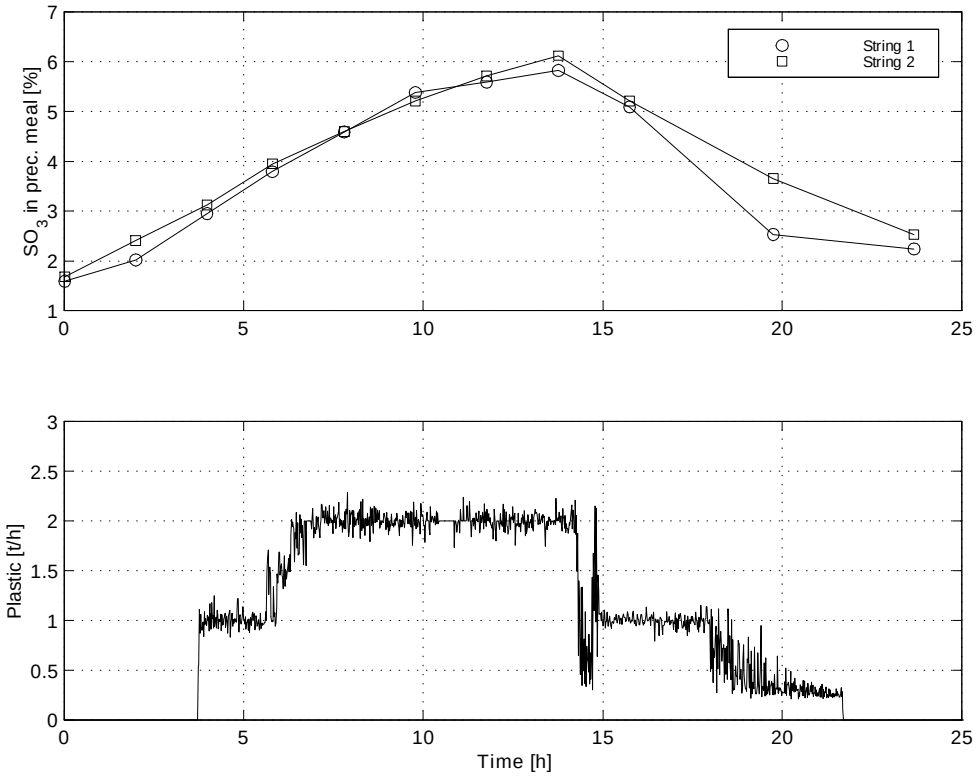

Figure 5.8: Accumulation of sulphur in precalcined meal, Test B.

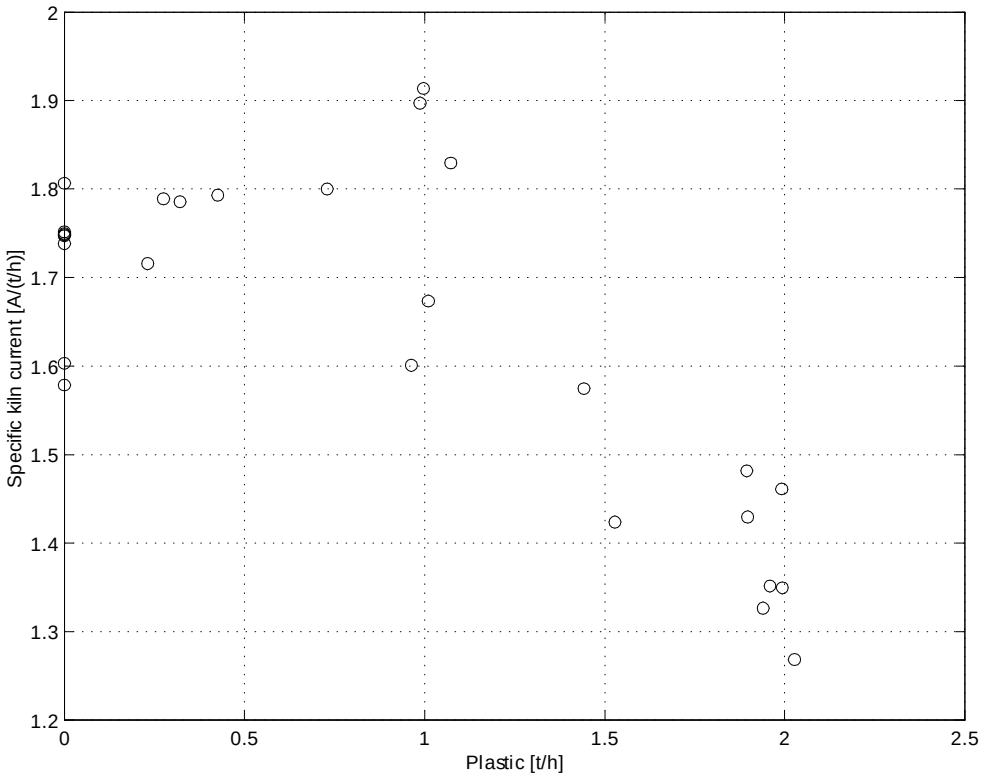

Figure 5.9: Specific kiln current consumption, Test B.

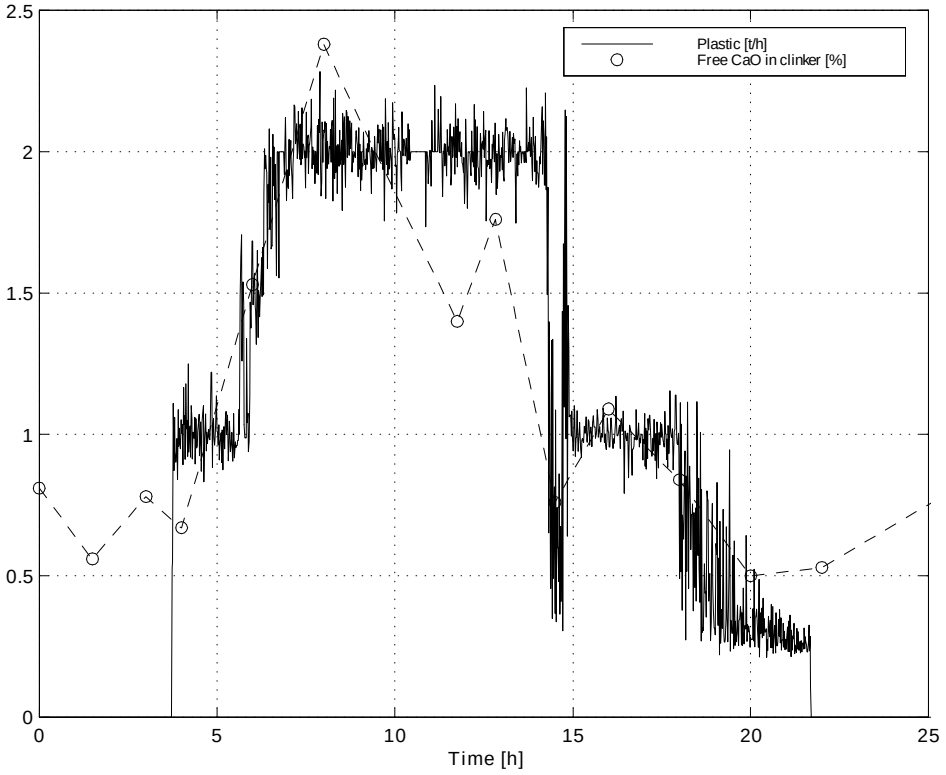

Figure 5.10: Free CaO in the clinker during plastic supply, Test B.

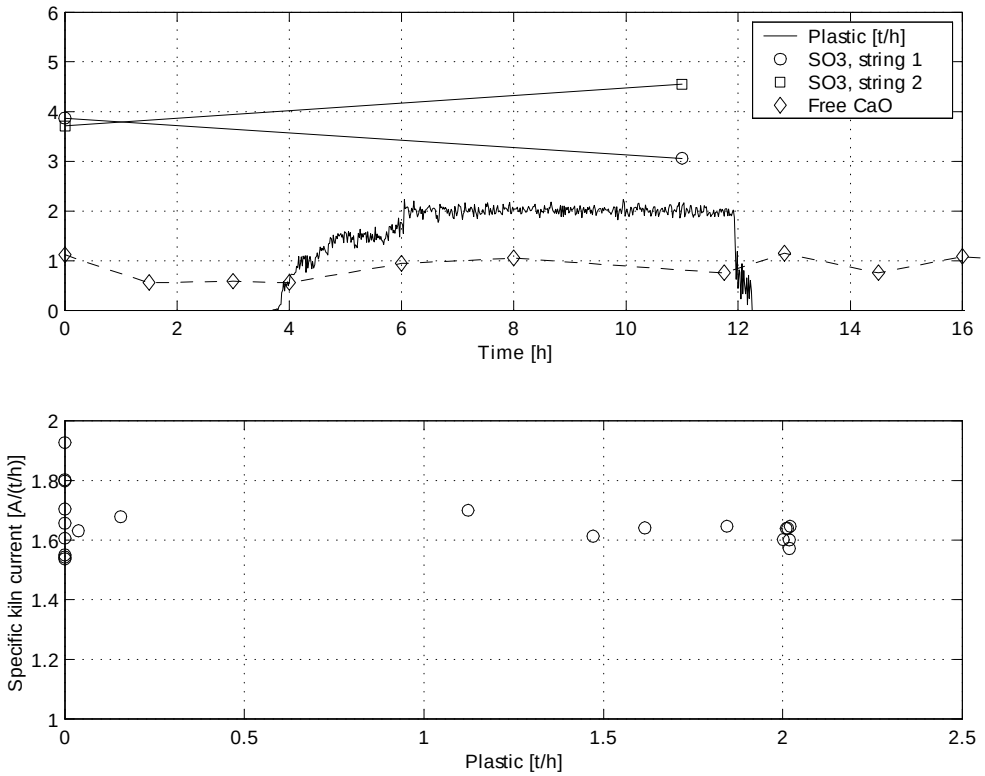

Figure 5.11: Free CaO in clinker, sulphur in precalcined meal and specific kiln current consumption, Test A.

thereby the clinker burning. The increased sulphur level in the precalciner may have contributed slightly to the reduction of NO [143], thus explaining partly the higher NO_x reduction in Test B. However, more important is probably an extension of the reburning zone due to reburning fuel being transported into the kiln inlet area: If the reburning fuel is entrained by the gas flow, no reducing zone is formed upstream of the feeding point, i.e. in the rotary kiln. But if the reburning fuel falls down into the kiln inlet zone and devolatilizes there, local reducing zones may form. Thus, the reburning zone is enlarged, both longitudinally and crosswise, resulting in a larger NO_x reduction. Besides, when there is close contact between reburning fuel and precalcined meal, the importance of the CaO catalyzed reduction of NO by CO, see Equation 3.19, will increase.

The importance of the alteration of the internal material cycles is highlighted in the next chapter.

Chapter 6

Thermodynamic equilibrium calculations

The experiments presented in Chapter 5 demonstrated an impact of staged combustion on the intensity of the material cycles. The chemistry related to the internal material circulation in the kiln system was discussed in Section 3.3. In this chapter, the process occuring in the kiln inlet zone during reducing conditions is investigated by means of a thermodynamic equilibrium analysis.

The global rate of the process taking place is a function of not only the kinetics of the pertinent chemical reactions, but also the rate of the diffusion of mass and heat in the solid phase, as well as the flow pattern (mixing) of the solid material and the gas phase. It is not easy to simulate such a process, and to a large extent there is a lack of relevant physical data. Hence, correct quantitative information is difficult to obtain. However, a thermodynamic equilibrium analysis can generate interesting qualitative results, giving important information about the direction in which the system is running[1]. On this basis, the qualitative effect of reducing conditions in the kiln inlet zone, caused by fuel staging, is investigated.

6.1 Development of procedure and program

6.1.1 Thermodynamic equilibrium

The equilibrium state of a closed system is that state for which the total Gibbs energy of the system is a minimum with respect to all possible changes at the given temperature

[1] Applying a thermodynamic equilbrium analysis can alternatively be regarded as being equivalent to assuming infinitely fast chemistry as well as perfect mixing of reactants and products. Hence, for a given reactor, if the chemistry is known to be fast relative to the residence time, and there is good mixing, a thermodynamic equilibrium analysis will also produce reasonable quantitative results.

and pressure [144].

The total gibbs energy, G, of a system of N components n_i, each with a chemical potential μ_i, can be written as [145]:

$$G = \sum_{i=1}^{N} n_i \mu_i \tag{6.1}$$

The chemical potential of an ideal gas at the temperature T is given as [145]:

$$\mu_i = \mu_i^0 + RT \ln \left(\frac{y_i p}{p^0} \right) \tag{6.2}$$

Here, μ_i^0 is the standard chemical potential, R is the universal gas constant, p is the pressure, y_i is the mole fraction of the component and p^0 is the standard pressure (=1 bar).

For a pure solid the chemical potential can be simplified to [146]:

$$\mu_i \approx \mu_i^0 \tag{6.3}$$

The standard chemical potential of a substance is given at the standard pressure $p^0 = 1\,\mathrm{bar}$ and the standard composition $y_i = 1$, and it is a function of the temperature T. It may be calculated by the following relation [145]:

$$\mu_{i,T}^0 = H_{i,T}^0 - T s_{i,T}^0 \tag{6.4}$$

The enthalpy, $H_{i,T}^0$, and the entropy, $s_{i,T}^0$, of the component i at the temperature T, at the standard pressure, are respectively given as [147]:

$$H_{i,T}^0 = \Delta H_{f,i,T_{ref}}^0 + \int_{T_{ref}}^{T} c_{p,i}^0 \mathrm{dT} \tag{6.5}$$

$$s_{i,T}^0 = s_{i,T_{ref}}^0 + \int_{T_{ref}}^{T} \frac{c_{p,i}^0}{T} \mathrm{dT} \tag{6.6}$$

Here, T_{ref} is the reference temperature (usually 298.15 K), $\Delta H_{f,i,T_{ref}}^0$ is the standard enthalpy of formation of component i at T_{ref}, $c_{p,i}^0$ is the specific heat of component i at p^0 and $s_{i,T_{ref}}^0$ is the entropy of component i at T_{ref} and p^0. Combining Equation 6.4, 6.5 and 6.6 gives:

$$\mu_{i,T}^0 = \Delta H_{f,i,T_{ref}}^0 + \int_{T_{ref}}^{T} c_{p,i}^0 \mathrm{dT} - T \left(s_{i,T_{ref}}^0 + \int_{T_{ref}}^{T} \frac{c_{p,i}^0}{T} \mathrm{dT} \right) \tag{6.7}$$

The enhalpy and entropy properties and the specific heat values can be found in the literature, for instance in the JANAF tables [147] or in the tables of Barin [146].

Using the relations given in Equation 6.1–6.7, for a specified pressure, temperature and molar composition of reactant phases, the minimum gibbs energy of the system can be calculated by an iterative procedure, and the equilibrium composition is found. Various algorithms may be used for this purpose. Here, a Gibbs energy minimization routine[2] written by Haug-Warberg [148] is used. Details of the mathematics underlying this routine is beyond the scope of this thesis, but may be found elsewhere [148]. The routine only treats gaseous and solid phases, not liquids.

If the equilibrium calculation program is implemented in for instance MATLAB®, an automated procedure may be constructed, permitting a range of initial conditions to be calculated in one single run. This will save a lot of time and also provide a flexible system.

The equilibrium calculations should be coupled with an energy balance of the pertinent system. The energy balance is discussed in the next subsection.

6.1.2 Energy balance

The equilibrium calculation procedure outlined in the preceding section is based on a given equilibrium pressure and temperature. If the equilibrium temperature is unknown, it has to be calculated. This requires an energy balance of the system. Such a balance can be formulated, by considering the reactants i, the products j, the heat loss from the system Q, and neglecting the work term (compare Equation 4.10), as follows:

$$\sum_i n_i \left(\Delta H^0_{f,T_{ref}} + \int_{T_{ref}}^{T_{equil}} c_p^0 \mathrm{dT} \right)_i = \sum_j n_j \left(\Delta H^0_{f,T_{ref}} + \int_{T_{ref}}^{T_{equil}} c_p^0 \mathrm{dT} \right)_j + Q \qquad (6.8)$$

...or in short:

$$H_r = H_p + Q \qquad (6.9)$$

The term on the left hand side is the enthalpy of the reactants, H_r, whereas the first term on the right hand side is the enthalpy of the products, H_p. (Combining Equation 6.9 with Equation 6.5 gives Equation 6.8.)

6.1.3 Calculation procedure

An algorithm can now be constructed:

1. Define the mole numbers of all reactants.
2. Calculate the reactant enthalpy, H_r, by using Equation 6.5.
3. Guess an equilbrium temperature, T_{eq1}, for instance by averaging the temperatures of the reactants.

[2] `GIBBMIN.M`

4. Calculate the equilibrium composition, $\mathbf{n}_1$, at T_{eq1}(and a given pressure), using Equations 6.1–6.7.

5. Calculate the product enthalpy, H_{p1}, and the heat loss , Q_1, at T_{eq1}.

6. Calculate the energy balance, using Equation 6.8 (6.9).

7. Estimate a new equilibrium temperature, T_{eq2}:

$$T_{eq2} = T_{eq1} + \Delta T \qquad \text{if } H_p + Q < H_r \tag{6.10}$$
$$T_{eq2} = T_{eq1} - \Delta T \qquad \text{if } H_p + Q > H_r \tag{6.11}$$

   Here ΔT is some small temperature difference. (The initial value of ΔT can be set to for instance 100 K.)

8. Calculate a new equilibrium composition, $\mathbf{n}_2$, at T_{eq2}, using Equations 6.1–6.7.

9. Calculate the new product enthalpy, H_{p2}, and the new heat loss, Q_2, at T_{eq2}.

10. Estimate a new equilibrium temperature, T_{eq3}:

$$T_{eq3} = T_{eq1} + \frac{T_{eq2} - T_{eq1}}{H_{p2} + Q_2 - H_{p1}} \left(H_r - H_{p1} - Q_1\right) \tag{6.12}$$

11. Calculate a new equilibrium composition, $\mathbf{n}_3$, at T_{eq3}, using Equations 6.1–6.7.

12. Calculate the new product enthalpy, H_{p3}, and the new heat loss, Q_3, at T_{eq3}.

13. Calculate the energy imbalance percentage, E_{imb}:

$$E_{imb} = \left| \frac{H_{p3} + Q_3 - H_r}{H_r} \right| \tag{6.13}$$

14. Update values:

$$\Delta T = \left| \frac{T_{eq1} - T_{eq3}}{2} \right| \tag{6.14}$$
$$H_{p1} = H_{p3} \tag{6.15}$$
$$Q_1 = Q_3 \tag{6.16}$$
$$\mathbf{n}_1 = \mathbf{n}_3 \tag{6.17}$$
$$T_{eq1} = T_{eq3} \tag{6.18}$$

15. If $E_{imb} > E_{imb}^{\max}$, where $E_{imb}^{\max}$ is a small tolerance value, then return to 6 and repeat. If $E_{imb} < E_{imb}^{\max}$, the equilibrium composition and temperature is found.

This calculation procedure is implemented in a MATLAB® program called SEACEM.[3] Details of the program structure and the source code of SEACEM are not given here, but can be found elsewhere [16]. However, a brief description of SEACEM is given in Appendix C.

SEACEM has been validated by comparing its performance to isothermal calculations published by Hayhurst and Tucker [149] and to a series of calculations executed with STANJAN [150]. SEACEM was found to calculate correctly; the verification can be found elsewhere [16].

6.2 The effect of reducing conditions on the sulphur cycle

In this section, a calculation example roughly corresponding to the conditions at the kiln inlet is given.

Precalcined meal, kiln gas and an alternative fuel, here taken as ethylene[4] (C_2H_4), are the reactants, entering a well-mixed reactor at different temperatures, and exiting at the equilibrium temperature and composition.

The values of precalcined meal and kiln gas given in Table 6.1 are typical of a normal operation of the kiln. A typical feed rate of the alternative fuel in a real situation is 2 t/h; the rather wide range of the fuel feed rates given in Table 6.1 is chosen in order to cover local zones with highly reducing conditions.

The following species are considered in the equilibrium calculation:

- Gases: N_2, CO_2, O_2, H_2O, CO, SO_2, H_2, H_2S, SO_3, OH, O and C_2H_4
- Solids: $CaCO_3$(s), CaO(s), $CaSO_4$(s) and CaS(s)

The thermodynamic data used are the same as those used by Hayhurst and Tucker [149]. The results from the calculation are shown in Figure 6.1 and 6.2, which reveal the following:

- Under oxidizing conditions (fuel supply < 2.09 t/h), the fuel is completely oxidized, forming carbon dioxide and water:

$$C_2H_4 + 3O_2 \rightarrow 2CO_2 + 2H_2O \tag{6.19}$$

  The sulphate in the precalcined meal will pass through the kiln inlet zone. Initially, the major part of the SO_2 in the kiln gas is absorbed according to Equation 3.24,

[3] SEACEM is an acronym for Sulphur Equilibrium Analysis of a CEMent kiln unit.

[4] Ethylene is selected because polyethylene, which is a possible reburning fuel, has the same elemental composition and is supposed to 'behave' approximately like ethylene.

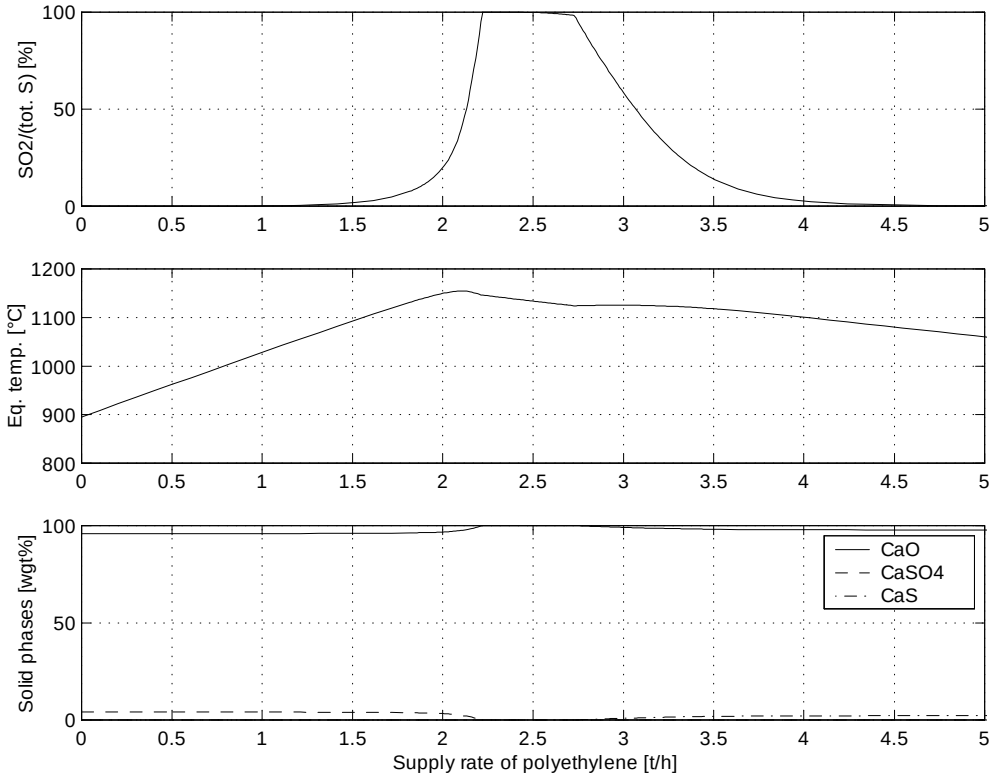

Figure 6.1: The effect of reducing conditions in the kiln inlet zone on the distribution of sulphur. (The abbreviation 'tot. S' means the sum of S in gas and meal.)

Table 6.1: Initial conditions for the thermodynamic equilibrium calculation.

Reactant specification		**Unit**	**Value**
Kiln gas	Flow rate	Nm^3/h	100,000
	Temperature	°C	1100
	N_2 conc.	mol%	73
	CO_2 conc.	mol%	18
	O_2 conc.	mol%	5
	H_2O conc.	mol%	4
Alt. fuel (100 % C_2H_4)	Flow rate	t/h	0–5
	Temperature	°C	25
Precalcined meal	Flow rate	t/h	162
	Temperature	°C	850
	$CaCO_3$ conc.	wgt%	14.1
	CaO conc.	wgt%	70.9
	$CaSO_4$ conc.	wgt%	3.2
	Inerts conc.	wgt%	11.8

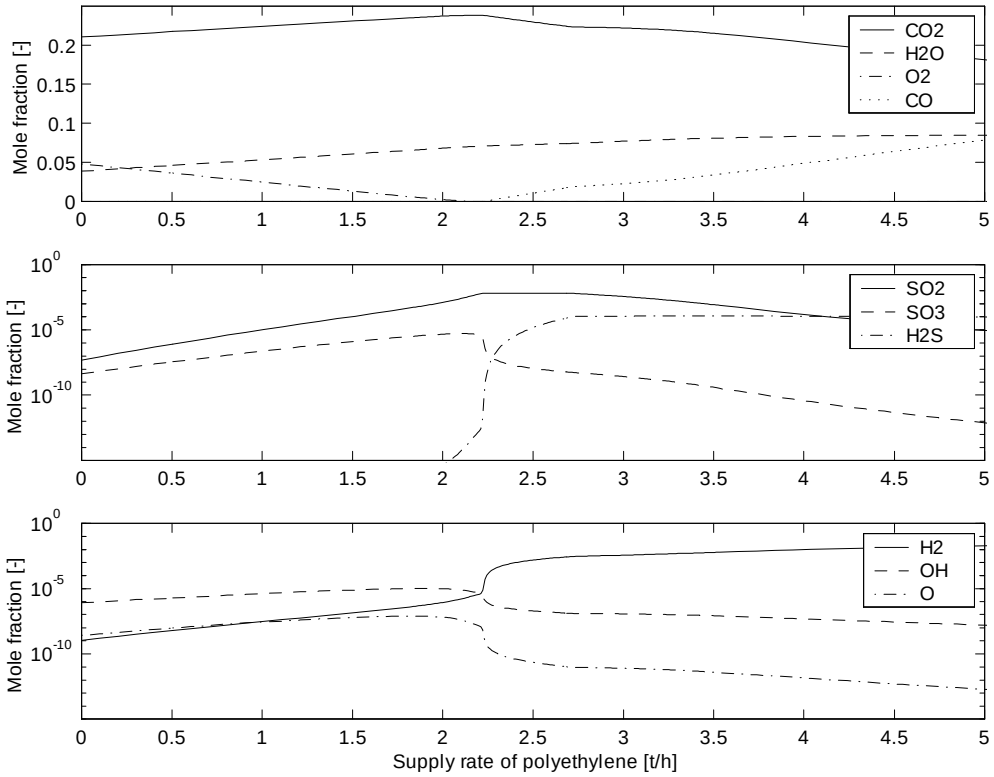

Figure 6.2: The effect of reducing conditions in the kiln inlet zone on the gas composition.

but as the fuel supply increases, an increasing portion of the SO_2 is not converted to sulphate. Hence, the SO_2 concentration slowly rises. At a fuel supply rate of 1.62 t/h, no SO_2 in the kiln gas is absorbed; and at higher fuel supply rates, the sulphate in the precalcined meal decomposes.

- At a fuel supply rate of 2.09 t/h, the air equivalence ratio has reached the value of 1, i.e. the oxygen is totally consumed, and the maximum equilibrium temperature (1154 °C) is reached.

- In the fuel supply rate interval 1.62 – 2.23 t/h, the sulphate decomposes according to Equation 3.23. Realizing that the oxygen released in the sulphate decomposition is consumed in the fuel oxidation, the net reaction can be written as:

$$C_2H_4 + 6CaSO_4 \rightarrow 6CaO + 6SO_2 + 2CO_2 + 2H_2O \tag{6.20}$$

- At a fuel supply of 2.23 t/h, all calcium sulphate is decomposed, and all sulphur exists as SO_2. The temperature has now decreased to about 1145 °C because the decomposition reaction is endothermic.

- In the fuel supply rate interval 2.23 – 2.72 t/h, the SO_2 concentration decreases slowly, and H_2S is formed to some extent. The formation of H_2S occurs through the following reaction:

$$SO_2 + H_2O \rightarrow H_2S + \frac{3}{2}O_2 \tag{6.21}$$

The net reaction is now:

$$C_2H_4 + 2SO_2 \rightarrow 2CO_2 + 2H_2S \tag{6.22}$$

Simultaneously, H_2O starts to dissociate into hydrogen and oxygen (which is consumed in fuel oxidation reactions):

$$H_2O \rightarrow H_2 + \frac{1}{2}O_2 \tag{6.23}$$

- H_2S never reaches high concentrations. Instead, at a fuel rate supply of 2.72 t/h, calcium sulphide starts to form, primarily by combining with sulphur dioxide.

$$CaO + SO_2 \rightarrow CaS + \frac{3}{2}O_2 \tag{6.24}$$

The net reaction is:

$$C_2H_4 + 2CaO + 2SO_2 \rightarrow 2CaS + 2CO_2 + 2H_2O \tag{6.25}$$

Accordingly, the SO_2 decreases fast in this region.

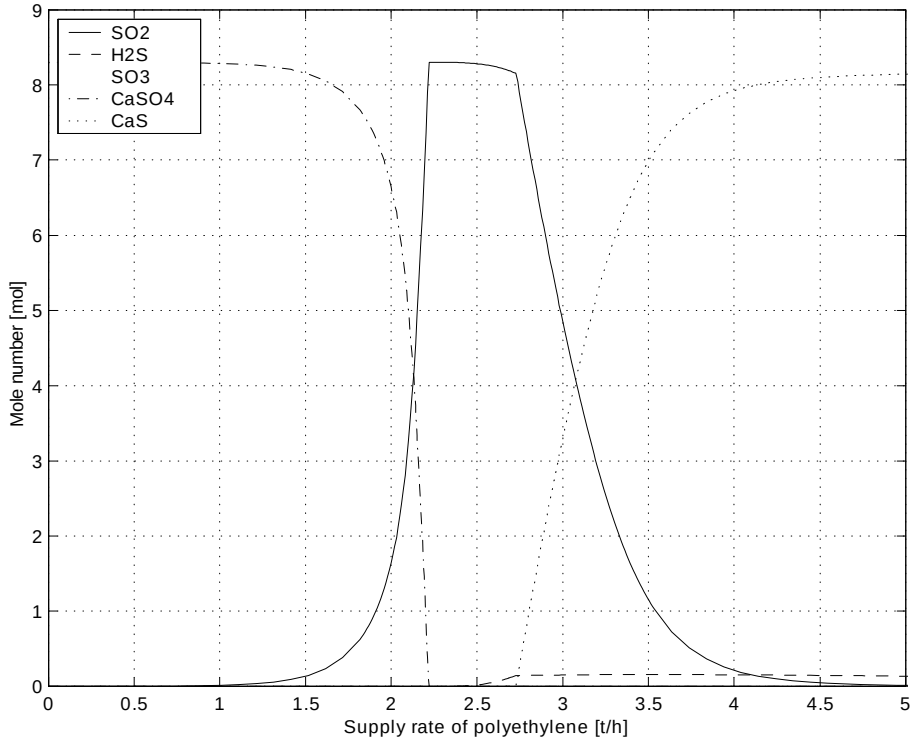

Figure 6.3: Absolute amount of all sulphur containing compounds as a function of fuel supply rate.

The absolute amounts of all sulphur containing compounds at equilibrium are shown in Figure 6.3. From this figure it is easy to see that under oxidizing conditions, no transfer of sulphur from solid to gas phase takes place; under moderate reducing conditions sulphur is transformed from solid (sulphate) to gas phase (mainly SO_2); and under strongly reducing conditions, sulphur is transferred from gaseous to solid state (CaS). SO_3(g) never reaches concentrations comparable to the other sulphur compounds, which is not surprising, since this would require oxygen in excess.

Under moderate reducing conditions, the relative amount of CaO in the solids will increase. Then, if the total thermal energy supply to the kiln system is not increased in order to increase the formation of C_3S (see Table 2.3), this will probably increase the concentration of free lime in the clinker, which is negative for the clinker quality. Simultaneously sulphur, mainly in the form of SO_2, is transferred from the rotary kiln cycle to the precalciner. Further up in the precalciner, the kiln gas will gradually mix with the oxygen rich co-flowing gas from the tertiary air side (see Figure 5.1), resulting in oxidizing conditions. The SO_2 will then react according to Equation 3.24 (whereas any H_2S will be oxidized). This means that gas phase sulphur is transferred to sulphate in

the meal and is returned to the kiln inlet zone for a new cycle in the precalciner. The net effect is a transient build-up of sulphur in the precalciner. In the end this leads to deposits and eventually blockages. This is exactly what has been experienced in full-scale trials (see Chapter 5).

The CaS formed under strongly reducing conditions will contaminate the clinker and deteriorate the product quality, hence such operating conditions can not be accepted. The effects of strongly reducing conditions have not been experienced in full-scale trials because of relatively low fuel supply rates ($\leq$ 2 t/h). But this calculation indicates what would happen if polyethylene was supplied at a rate of about 2.5 t/h or more.

The calculation discussed above was based on pure ethylene as reburning fuel. Other fuels may behave somewhat differently regarding temperature profile and stoichiometric air/fuel ratios, but are supposed to follow the same general pattern as far as the sulphur chemistry is concerned.

Another point to be made is that, according to the results of the equilibrium analysis, the sulphate concentration in the precalcined meal is supposed to increase continuously. However, full-scale experiments have shown that the sulphate concentration tends to stabilize at a certain high concentration (say 6 %). This suggests that the real process is controlled by a mass transfer rate, i.e. the process does not take place infinitely fast, as is assumed in the equilibrium analysis. However, this does not alter the general conclusion that a reducing atmosphere in the rotary kiln, initiated by fuel supply at the kiln inlet, drives the kiln process towards unacceptable operating conditions.

6.2.1 Estimation of energy transfer during reducing conditions

The reaction given by Equation 3.24 is exothermic, whereas the reverse reaction is of course endothermic. This means that under reducing conditions not only mass (SO_2), but also energy is transferred from the kiln to the precalciner. Under normal operating conditions, the SO_3 content of the precalcined meal is about 2 %, whereas it may reach values of 5-7 % when the operation is disturbed.

Assuming that all energy required to decompose sulphate is taken from the solid material, and that all SO_2 transported to calciner is returned to the kiln as sulphates, the increase in concentration of SO_3 in precalcined meal should be proportional to the increase in energy transfer. Figure 6.4 shows calculated values of energy transfer (both as coal equivalents and as a percentage of the total thermal energy supply rate to the kiln system) as a function of SO_3 concentration increase in precalcined meal. Sulphur may exist as different sulphates, hence the decomposition energy of both potassium, sodium and calcium sulphate are shown. (The actual distribution of sulphur between the three is not known.)

Decomposition of potassium sulphate requires more energy than sodium sulphate, which in turn requires more energy than do calcium sulphate. A 4 % increase in SO_3 concentration in precalcined meal means that energy equivalent to 1.7–2.7 t/h of coal

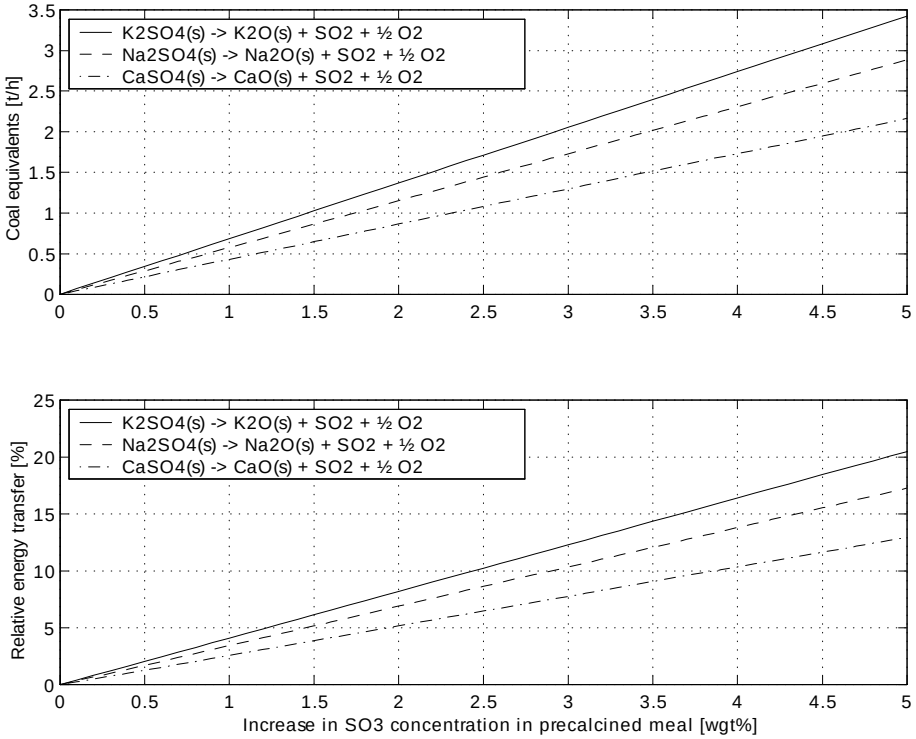

Figure 6.4: Calculated energy transfer from kiln to precalciner as a function of SO_3 increase in precalcined meal.

is transferred from the kiln to the calciner. This corresponds to 10–17 % of the total thermal energy supplied to the kiln system. The fact that this is more than what has been experienced in full-scale trials, can be explained by some of the reaction energy coming from the gas phase instead of the solids phase: The part of the reaction energy that is taken from the kiln gas, causes the gas temperature to decrease, and then no net energy is transferred from the kiln to the precalciner. It is difficult to say what fraction of the reaction energy that is taken from the solid material, and what fraction that is taken from the kiln gas. But any energy contribution to the sulphate decomposition reaction from the solid material is equivalent to a net transfer of energy from the rotary kiln to the precalciner. The analysis above simply determines the maximum energy transfer.

This equilibrium study indicates that supplying fuel in the kiln inlet zone is highly undesirable as far as the operation of the kiln is concerned. It also explains the phenomena observed in Test B, described in Chapter 5. The calculated numeric values are of course not fully correct, since the effects of non-perfect mixing and finite rate chemistry are neglected. Nevertheless, this analysis elucidates the qualitative behaviour of the chemistry with increasing amounts of reburning fuel supplied at the kiln inlet.

Chapter 7

Thermogravimetric analyses

The equilibrium analysis in Chapter 6 indicated that contact between fuel and precalcined meal under reducing conditions will cause the sulphates of the meal to decompose. This type of behaviour should be possible to demonstrate in the laboratory using thermogravimetric analysis (TGA).

In a thermogravimetric analysis, the sample is placed in a furnace and heated according to a specified temperature program; and simultaneously the weight loss of the sample is recorded by means of a balance. During the analysis, a purge gas flows through the furnace in order to expose the sample to a certain atmosphere; air, oxygen, nitrogen and argon are typical purge gases. The output from the TGA is the sample mass as a function of temperature and time, and it can be used to characterize, and compare, for instance various types of fuels.

The idea of using TGA in this work, is as follows:

- TGA of a fuel in an inert atmosphere will release the moisture and the volatiles, whereas the char and the ash fraction will remain in the sample.

- TGA of a precalcined meal in an inert atmosphere will expel moisture and decarbonate the rest of the calcium carbonate in the meal. Provided the temperature is kept sufficiently low, sulphates present in the meal, which are relatively stable, will remain in the meal.

- TGA of a blend of fuel and precalcined meal in an inert atmosphere will, in addition to the reactions mentioned above, promote reactions between sulphates in the precalcined meal and fuel fractions present in the volatiles and/or in the char fraction of the fuel.

- Because of reactions between sulphates and fuel fragments, the mass loss recorded in the TGA of the fuel/meal blend is expected to exceed the weighted mass loss of the separate runs, in which such reactions are of course not occuring. Accordingly,

Table 7.1: Proximate analysis (dry basis) of the the pulverized bituminous coal used in the experiments.

Parameter	**Unit**	**Coal**	**Tyres**
Volatile matter	%	40.28	62.64
Fixed carbon	%	53.67	32.20
Ash	%	6.06	5.16
Sum	%	100.01	100
Sulphur	%	1.60	1.80

the difference in mass loss should be approximately equal to the SO_3 content of the precalcined meal.

- If the same analyses are performed in an oxidizing atmosphere, no significant difference in mass loss should be detected. This is because the fuel will be oxidized by the oxygen of the heating medium instead of reacting with the precalcined meal.

7.1 Experimental details

Following the idea outlined above, TGA was carried out using a precalcined meal and two different fuels; pulverized coal and pulverized tyres.

7.1.1 Meal and fuel analyses

The precalcined meal, taken from Norcem's Kiln 6, contained 5.2 % of sulphur, measured as SO_3; a meal with a rather high SO_3 concentration was selected to make it easier to demonstrate the expected effect. The degree of calcination was 95.0 %.

A bituminous coal supplied by Leco® was used, see Table 7.1, where also the proximate analysis of the tyre rubber is given.

7.1.2 Equipment

TGA equipment from Perkin-Elmer was used:

- Thermogravimetric Analyzer, TGA 7
- Thermal Analysis Controller, TAC 7/DX
- Thermal Analysis Gas Station, TAGS
- Software, Pyris 2.00 (installed on a personal computer)

Table 7.2: Method used in the TGA experiments.

Step	**Description**	**Time** [min]	**Temperature** [°C]	**Heating rate** [°C/ min]
1	Hold	60	25	0
2	Heat	4.25	25–110	20
3	Hold	5	110	0
4	Heat	42	110–950	20
5	Hold	60	950	0

The TGA 7 microbalance is capable of detecting weight changes as small as 0.1 μg, and it has a maximum capasity of 1300 mg. The furnace functions both as a heater and a resistance thermometer, detecting its own temperature. A chromel-alumel thermocouple is located in close proximity to the sample material in the furnace and is supposed to provide an accurate sample temperature during the analysis. The maximum temperature of the TGA 7 Standard Furnace is 1,000 °C, but the temperature never exceeded 950 °C in the runs.

N_2 and air in separate gas sylinders were connected to the system and could be used interchangably.

An analytical balance from Mettler (AE 240 Dual Range Balance) was used to weigh the samples.

7.1.3 Experimental procedure

The temperature program (termed 'method') is shown in Table 7.2. Inititally the system is flushed with nitrogen to remove any oxygen present; in the second/third step free water is expelled; and in the fourth/fifth step volatiles are driven off and, provided there are oxidizing conditions, fixed carbon is oxidized. This method was used in all runs, shown in Table 7.3. N_2 was used to create a reducing atmosphere (Run 1, 2, 3, 7 and 8), and air was employed in the cases with oxidizing conditions (Run 4, 5, 6, 9 and 10).

7.2 Results and discussion

The initial and final sample masses of the various runs are given in Table 7.3.

7.2.1 Coal runs

Reducing conditions

Figure 7.1 shows the mass loss curves and time derivatives of meal and coal under reducing conditions (run 1, 2 and 3).

Table 7.3: TGA runs. (In all meal/fuel blends, the fuel mass was 1.000 g.)

Run	**Sample**	**Hot gas**	**Initial mass**	**Final mass**	
			[g]	[g]	[%]
1	Meal	N_2	15.507	14.570	94.0
2	Coal	N_2	3.265	1.915	58.7
3	Meal + coal	N_2	17.853	15.744	88.2
4	Meal	Air	17.738	16.565	93.4
5	Coal	Air	3.837	0.195	5.1
6	Meal + coal	Air	17.834	15.787	88.5
7	Tyres	N_2	4.080	1.350	33.1
8	Meal + tyres	N_2	16.240	13.679	84.2
9	Tyres	Air	4.147	0.514	12.4
10	Meal + tyres	Air	16.279	14.241	87.5

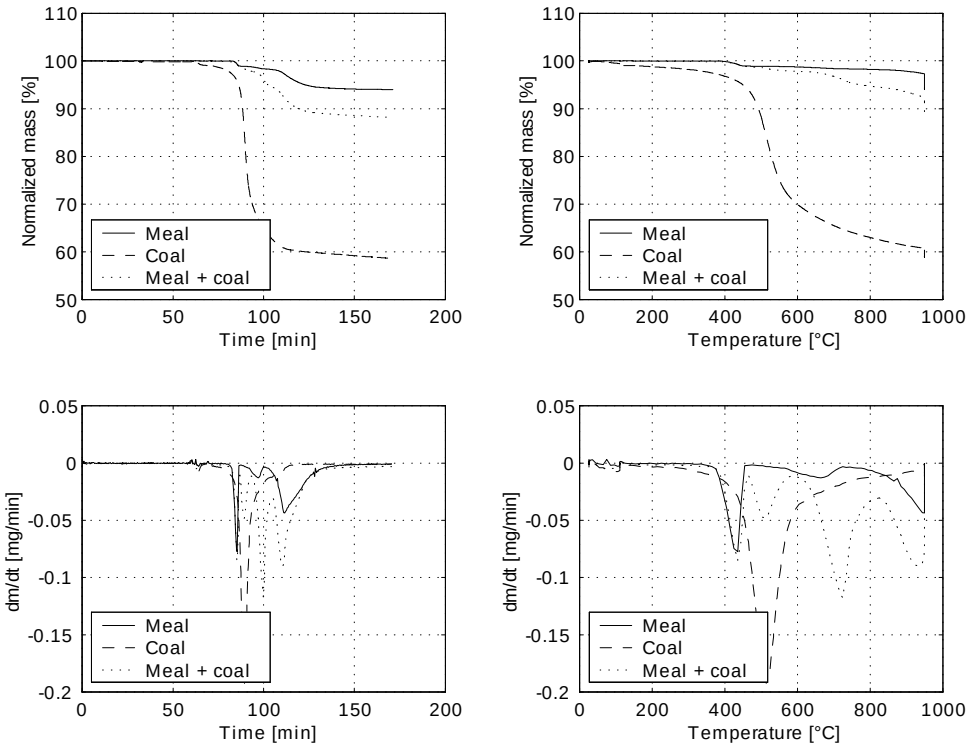

Figure 7.1: Mass loss curves (top) and time derivatives (bottom) of meal and coal as a function of time (left) and temperature (right) under reducing conditions (N_2).

The precalcined meal decomposes in three stages: There are peaks in the derivative curves at about 450, 650 and 900 °C. The first two peaks presumably correspond to dehydration of hydroxides, such as:

$$Mg(OH)_2 \longrightarrow MgO + H_2O \tag{7.1}$$

$$Ca(OH)_2 \longrightarrow CaO + H_2O \tag{7.2}$$

Hydroxides are not found in precalcined meal immediately after burning, but may have been formed during storage[1] of samples. (According to Lea [151], calcium hydroxide starts to decompose at about 400 °C.) The third peak represents the calcination of the calcium carbonate that remained in the precalcined meal after the precalcination, see Equation 2.5.

The coal decomposes in two stages: First, water is expelled at about 100 °C; secondly, volatiles are driven off at about 500 °C. The final mass given in Table 7.3 (58.7 %) corresponds well to the sum of ash and fixed carbon reported in Table 7.1 (59.7 %). The difference can be explained by the moisture content of the coal.

The mixture of coal and meal seems to decompose in five stages — presumably the same five steps as the two separate runs of coal and meal — this will however be discussed more thoroughly below.

Oxidizing conditions

Figure 7.2 shows the mass loss curves and time derivatives of meal and coal under oxidizing conditions (run 4, 5 and 6).

As in Run 1, the precalcined meal decomposes in three stages, and the total mass loss in Run 4 is about the same as in Run 1. This is reasonable, because no chemical reactions between the solids and the gas phase were expected to occur under reducing or oxidizing conditions.

In Run 5, there is one additional stage compared to Run 2: oxidation of fixed carbon. This results in a higher total mass loss; only about 5 % of the initial material is left after burnout, which corresponds well to the 6 % ash fraction determined in the proximate analysis given in Table 7.1. In Figure 7.2, however, the release of volatiles and oxidation of fixed carbon interfere with each other, so the volatiles peak is seen as a 'shoulder' on the fixed-carbon peak, which has a maximum around 650 °C.

The mixture of meal and coal behaves somewhat differently under oxidizing conditions than in a reducing atmosphere: After the inital drying and release of volatiles, there is an increase of mass at about 500–750 °C. This is probably due to reactions between calcium

[1] The meal had been stored for about 6 months before it was used in this analysis.

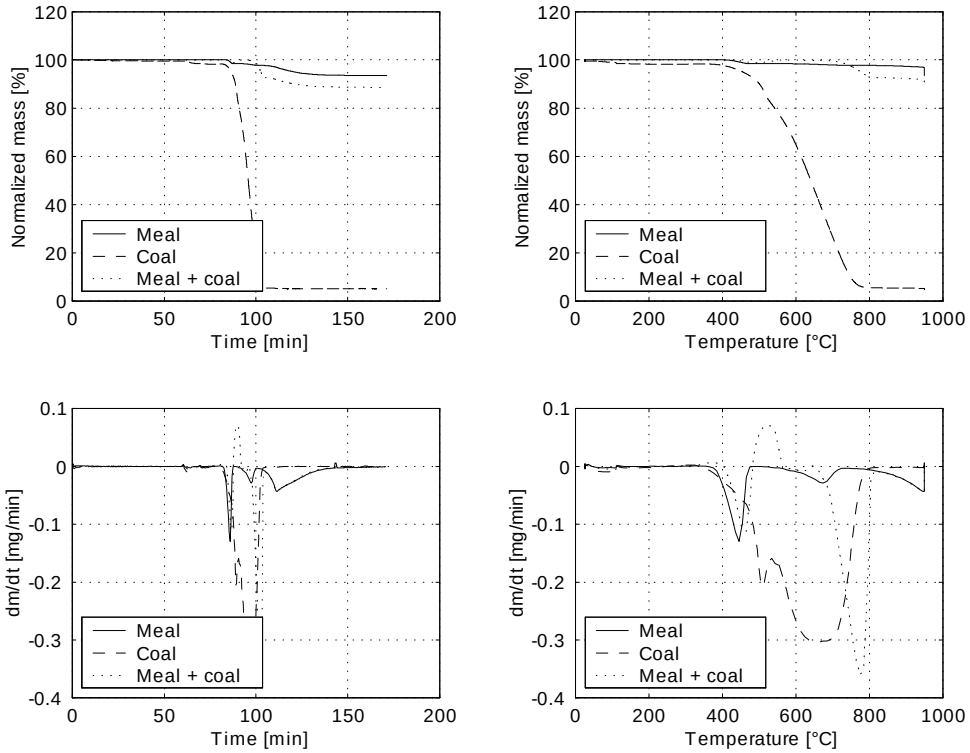

Figure 7.2: Mass loss curves (top) and time derivatives (bottom) of meal and coal as a function of time (left) and temperature (right) under oxidizing conditions (air).

oxide and carbon dioxide, the latter being formed during oxidation of coal:

$$\mathrm{C(s)}+\frac{1}{2}\mathrm{O_2} \longrightarrow \mathrm{CO} \tag{7.3}$$

$$\mathrm{C(s)} + \mathrm{O_2} \longrightarrow \mathrm{CO_2} \tag{7.4}$$

$$\mathrm{CO}+\frac{1}{2}\mathrm{O_2} \longrightarrow \mathrm{CO_2} \tag{7.5}$$

$$\mathrm{CO_2}+\mathrm{CaO(s)} \longrightarrow \mathrm{CaCO_3(s)} \tag{7.6}$$

$$\mathrm{CO_2}+\mathrm{MgO(s)} \longrightarrow \mathrm{MgCO_3(s)} \tag{7.7}$$

The final mass of the meal/coal mixture is a bit higher in Run 6 (88.5 %) than in Run 3 (88.2 %). This means that — despite the char oxidation taking place under oxidizing conditions — more mass has been lost under reducing conditions, suggesting that interactions between meal and fuel, such as sulphate decomposition, has occured.

Composite curves

The decomposition of sulphates is not easily identified in Figure 7.1, as it is probably hidden behind one of the peaks that can be seen in the derivative curve plots. To throw some light on this, a composite curve (function) is defined as the weighted average of the separate meal and fuel runs, $m_{composite}$:

$$m_{composite}(t) = \frac{m^0_{meal,mix}}{m^0_{meal}} m_{meal}(t) + \frac{m^0_{fuel,mix}}{m^0_{fuel}} m_{fuel}(t) \tag{7.8}$$

Here, m^0_{meal} and m^0_{fuel} is the initial mass of meal and fuel when these substances are analyzed separately; $m^0_{meal,mix}$ and $m^0_{fuel,mix}$ is the initial mass of meal and fuel in the meal/fuel blend; and m_{meal} and m_{fuel} is the time dependent mass of meal and fuel in the separate runs.

This composite curve can be compared to the curve representing the mix of fuel and meal, to check whether some other reactions have taken place in the latter case.

Figure 7.3 reveals two clear differences between reducing and oxidizing conditions as far as the mass loss is concerned:

- Under oxidizing conditions the total mass loss of the composite curve is very close to the total mass loss of the 'Real' curve, i.e. the curve representing the mixture of fuel and meal. Under reducing conditions, however, there is a difference in final mass of about 4 %. Keeping in mind that the SO_3 content of the precalcined meal was about 5.2 %, it seems very likely that the difference in mass loss is due to sulphate decomposition (77 % of the sulphate is decomposed). A 100 % conversion of sulphates to gaseous sulphur was not to be expected, because a perfect mixture of meal and fuel particles is not attainable.

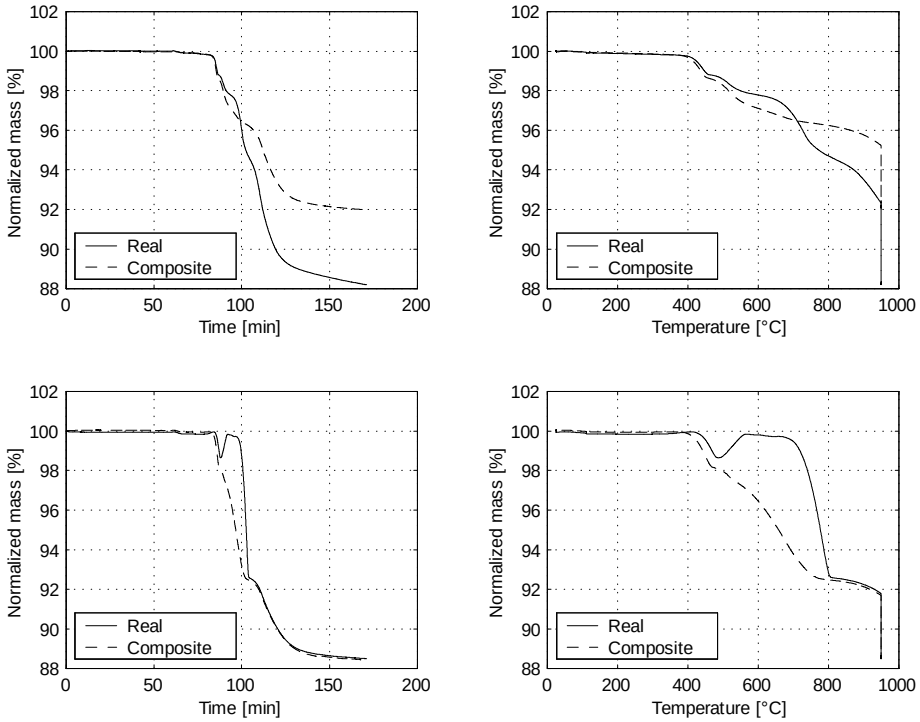

Figure 7.3: Mass loss curves of meal and coal under reducing (top) and oxidizing (bottom) conditions, as a function of time (left) and temperature (right).

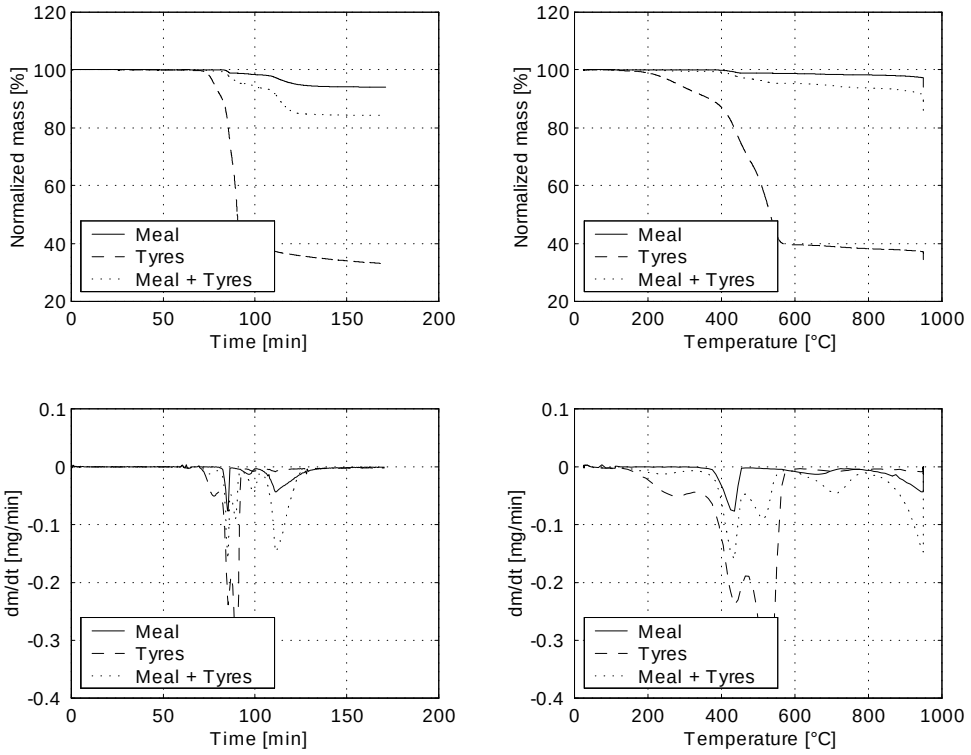

Figure 7.4: Mass loss curves (top) and time derivatives (bottom) of meal and tyres as a function of time (left) and temperature (right) under reducing conditions (N_2).

- The temporary mass increase, due to carbonation of free lime (and possibly magnesium oxide), is clearly seen in the 'Real' curve, however not in the 'Composite' curve. This is of course due the lack of contact between CO_2 and CaO (or MgO) when fuel and meal are analyzed separately.

7.2.2 Tyre runs

Also the interaction between pulverized tyres and precalcined meal was investigated. Four more runs were executed, using nitrogen (Run 7 and 8) and air (Run 9 and 10) as heating gas.

Reducing conditions

The mass loss curves and time derivatives of meal and tyres under reducing conditions (Run 1, 7 and 8) is shown in Figure 7.4.

The meal curve for reducing conditions is the same as the one used in Run 1.

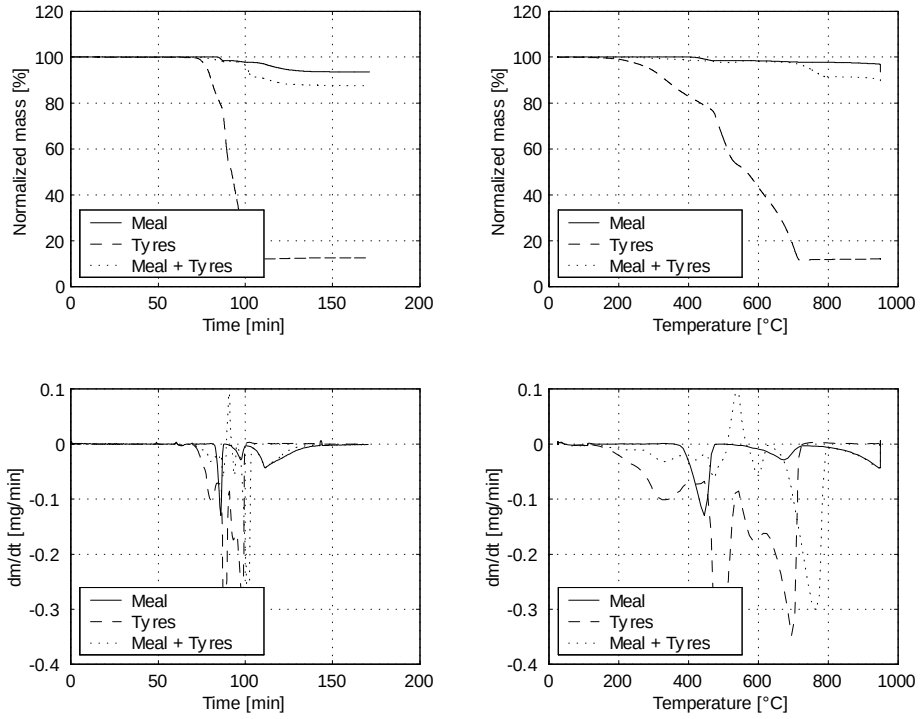

Figure 7.5: Mass loss curves (top) and time derivatives (bottom) of meal and tyres as a function of time (left) and temperature (right) under oxidizing conditions (air).

Tyres decompose in three stages, which can be seen as three peaks on the derivative curves given in Figure 7.4; one peak at about 280 °C, one at about 430 °C and one at about 530 °C. This is in very good agreement by an analysis performed by Atal and Levendis [152]; the three peaks correspond to pyrolysates of butadiene, lighter pyrolysates of polystyrene, and heavy pyrolysates of polystyrene, respectively.

Compared to coal, the tyre sample loses more mass under reducing conditions. This is because tyres have a higher fraction of volatiles. There is pretty good agreement between the final mass of the tyre sample in Run 7 (33.1 %) and the sum of the fixed carbon and ash in the tyre sample (37.3 %), see Table 7.1.

The curve representing the mixture of meal and tyres (Run 8) seems to contain the same steps as the curves of Run 1 and 7, as expected. But, as for the coal analysis, this will be discussed into more detail below.

Oxidizing conditions

Figure 7.5 shows the results from the TGA runs with air (Run 4, 9 and 10).

The meal curve is the same as in Run 4.

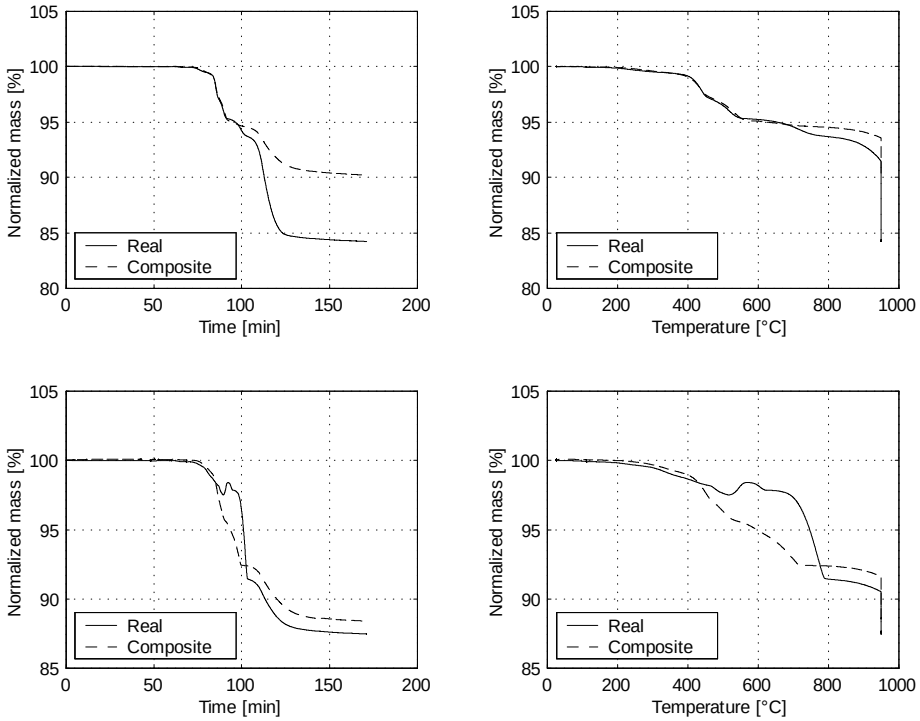

Figure 7.6: Mass loss curves of meal and tyres under reducing (top) and oxidizing (bottom) conditions, as a function of time (left) and temperature (right).

Under oxidizing conditions, tyres decompose in four stages, i.e. one more than under reducing conditions. This fourth stage, seen on the derivative curve as a peak at about 700 °C, probably corresponds to oxidation of carbon black [152]. Because of the char oxidation, the total mass loss is higher in Run 9 (87.6 %) than in Run 7 (66.9 %), see Table 7.3. However, the final mass under oxidizing conditions (12.4 %) is considerably higher than the ash fraction determined in the proximate analysis (5.16 %). There is no obvious reason for this.

Run 10 reveals that the temporary mass increase at about 550 °C occurs for the meal/tyres mix as it did in the meal/coal run (Run 6). The same reactions are supposed to apply. As in the coal analyses, the final mass under oxidizing conditions (87.5 %) is higher than under reducing conditions (84.2 %). Again, this suggests that reactions between meal and fuel have occured.

Composite curves

Equation 7.8 is now employed on the meal/tyres mix; the result is given in Figure 7.6.

As in the meal/coal runs, there is a significant difference in total mass loss under

reducing and oxidizing conditions, the difference being about 6 %. Since this is more than the SO_3 content of the precalcined meal, it appears that some other reactions between meal and tyres have occured in addition to the sulphate decomposition. This is supported by the fact that under oxidizing conditions there is a difference in total mass loss of about 1 % between the 'Real' and 'Composite' curve. What reactions that have occured is an open question.

This TGA has substantiated that interactions between meal and fuel will interfere with the internal circulation of sulphur in the kiln system.

Chapter 8

Flow calculations

The analyses peformed in Chapter 6 and 7 explain why close contact between precalcined meal, kiln gas and fuel will cause a disturbance in the internal material cycles in the kiln system. As was shown in Chapter 5, such disturbances tend to occur when alternative fuels are fed to the dust settling chamber (i.e. the kiln inlet zone). In this chapter, a CFD analysis of this chamber is carried out in order to investigate to what extent close contact between precalcined meal and different fuel particles can be expected.

8.1 CFD and `Fluent`

Fluid flow, heat transfer and other related processes are governed by certain physical laws. Conservation of mass, chemical species, energy, momentum, turbulence kinetic energy and dissipation rate all can be expressed in terms of a general differential equation (here given in Cartesian coordinates):

$$\frac{\partial}{\partial t}\left(\rho\phi\right) + \frac{\partial}{\partial x_i}\left(\rho u_i \phi\right) = \frac{\partial}{\partial x_i}\left(\Gamma_\phi \frac{\partial \phi}{\partial x_i}\right) + S_\phi \tag{8.1}$$

Here, ϕ is the the general variable to be solved, t is time, x_i is position, ρ is density, u_i is velocity, Γ_ϕ is a diffusion coefficient, and S_ϕ is a source term. Equation 8.1 has to be solved numerically, i.e. the equation must be discretized. The control volume formulation is often employed for this purpose. In the control volume formulation, the calculation domain is divided into a finite number of control volumes (cells), each cell surrounding a point. The points constitute a grid. The differential equation is integrated over each control volume, and piecewise profiles expressing the variation of the general variable ϕ between the grid points are used to evaluate the integrals. Details on the treatment of the various terms in the general differential equation are not given here, but can be found for instance in the textbook of Patankar [153].

In general, a CFD analysis involves the following steps:

Table 8.1: Boundary conditions for the CFD calculations.

Flow rate	100,000	Nm^3/h
Inlet velocity	22.6	m/s
Temperature	1200	°C
Turbulence intensity	10	%
Characteristic length	3.64	m
Heat loss	0	W/m^2

1. Geometry definition
2. Grid generation
3. Case definition, i.e. specification of models, chemical species, physical constants and boundary conditions for the problem to be solved
4. Computation, i.e. an iterative procedure for solving the discretized equations
5. Postprocessing, e.g. graphically displaying the calculated fields

FLUENT, which is used in this work, is a commercial program package developed for solving CFD problems. A detailed description of the models used can be found in the FLUENT manuals [154].

8.2 CFD analysis of the dust settling chamber

8.2.1 Geometry and grid generation

The geometry and the 3D-grid used in the calculations are shown in Figure 8.1. The dark area in the front end is where the kiln gas enters the reactor. The off-gas exits through the upper horizontal, rectangular plane. The solid fuel inlet is in the middle of the lower horizontal, rectangular plane (see also Figure 5.1). The meal phase is not included in the analysis.

8.2.2 Flow field calculations

Merely the gas flow field is considered in the calculations, i.e. no chemical reactions are included in the analysis. The standard k-ϵ model is used for the turbulence calculations. Adiabatic walls are chosen, and the characteristic length of the turbulent eddies is set equal to the gas inlet diameter. Boundary conditions for the gas phase are summarized in Table 8.1.

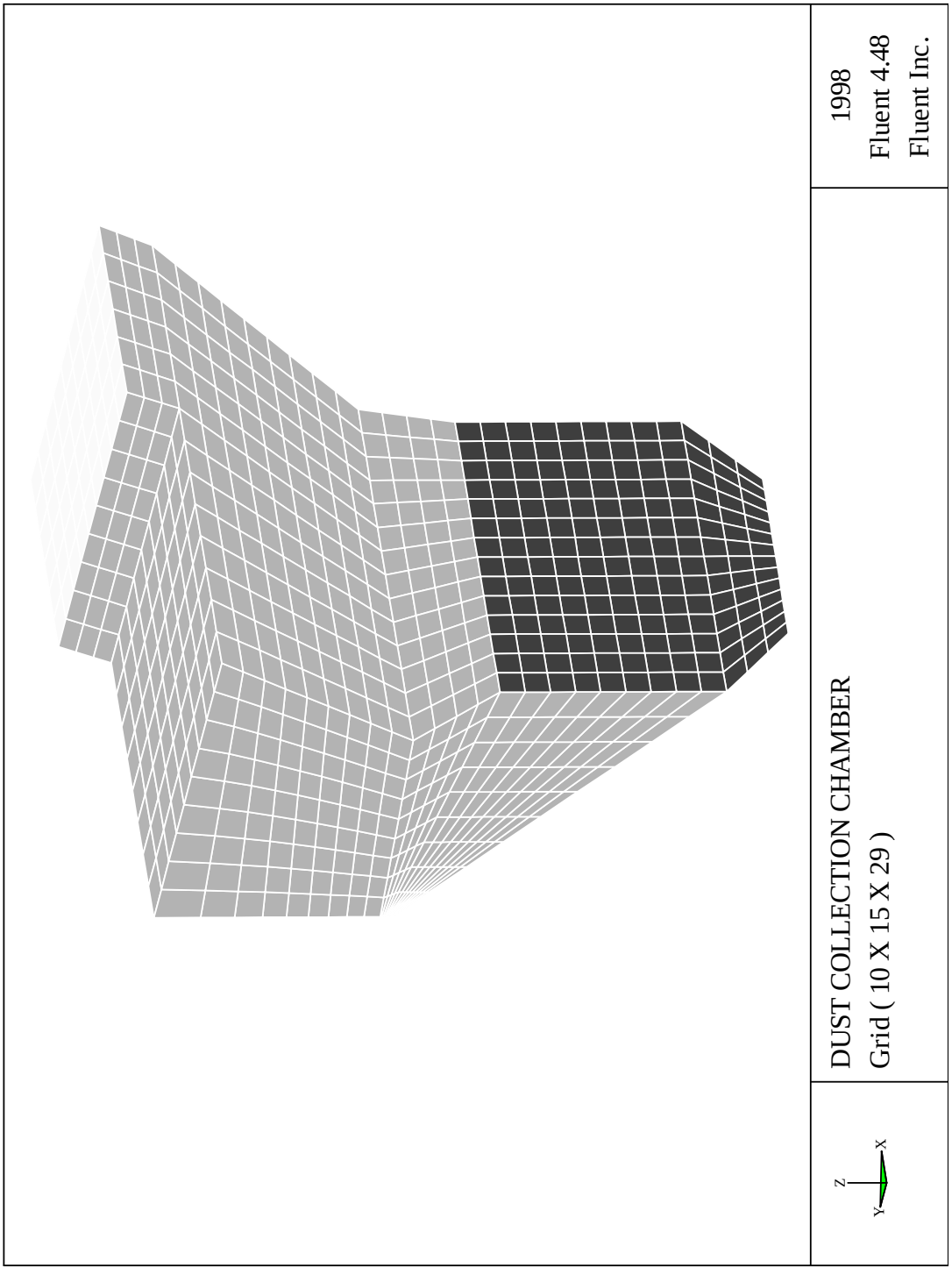

Figure 8.1: Dust settling chamber, geometry and grid used in the calculations.

Part of the flow field is shown in Figure 8.2. A recirculation zone above the constriction, near the front-end wall, is clearly indicated. The vertical velocity component is negative in this area, meaning that fuel particles following streamlines that run through this area, tend to fall down into the kiln.

8.2.3 Particle tracking

The track followed by the fuel particles can be examined by utilizing FLUENT's capability of simulating solid particles dispersed in the gas phase. A Lagrangian formulation that includes the inertia, hydrodynamic drag and gravity forces acting on a spherical particle is used [154]. The particles are taken as inert, i.e. combustion is not considered, which means that the mass loss of the particles due to devolatilazation and combustion is not taken into account. Hence, the simulations are conservative. In spite of this simplification, it should be possible to compare the qualitative behaviour of different fuel particles in the dust settling chamber. Coupling between the dispersed and the continuous phase is included in the calculation procedure, even though this is of minor importance to the particle tracks.

The boundary conditions are defined in such a way that particles colliding with the bottom of the chamber are trapped; particles entering the inlet zone are trapped; particles hitting a vertical wall are reflected; and particles entering the outlet zone escape.

The fuel particles differ in density, size and inlet velocity. Besides, the exact inlet position may vary over the entire inlet cross-section. Table 8.2 summarizes the fuels that have been simulated. In each case, nine particles are evenly distributed across the inlet cross-section. Because the actual inlet velocity is not known excactly, different inlet velocities are simulated for all fuels, giving a total of 30 cases. For each particle, the trajectory is calculated 100 times, using FLUENT's Discrete Random Walk (DRW) model [154] in order to include the stochastic effect of turbulence on the particle trackings. The average percentage of particles that is entrained by the kiln gas in the various cases is given in the table. Some particle tracking examples are given in Appendix D.

The calculations imply that car tyres, plastic strips and RDF is not conveyed by the kiln gas to the precalciner, even if the initial vertical velocity is 0 m/s. It is also seen that saw dust can be expected to be entrained by the kiln gases, even at a very high vertical inlet velocity. Plastic particles are supposed to be entrained when the inlet velocity is low (which is likely), but not when it is high (less likely). However, small particles may form agglomerates, leading to larger effective diameters. In such cases, entrainment is impeded. A preliminary conclusion is that it is very difficult to ensure complete entrainment of particles in the dust settling chamber. Hence, close contact between fuel, meal and gas can be expected to occur for almost any type of fuel used.

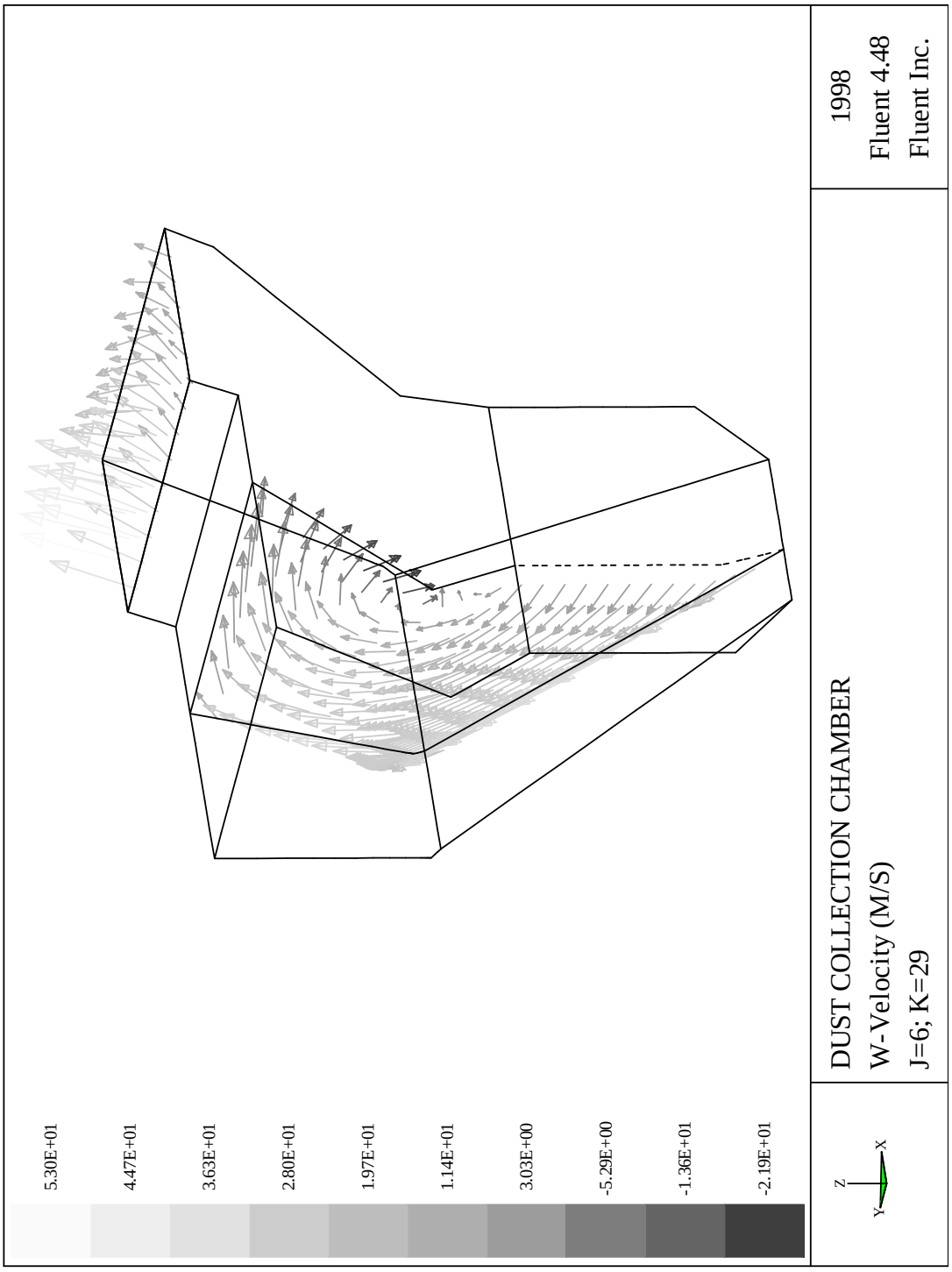

Figure 8.2: Modelled flow field in the dust collection chamber (slices j=6 and k=29 shown).

Table 8.2: Dispersed phase simulation cases. For each inlet velocity, the percentage of particles entrained by the kiln gas is given.

Fuel	**Hydr. diam.**	**Density**	**Inlet velocity**				
	[mm]	[kg/m^3]	0 m/s	-1 m/s	-3 m/s	-5 m/s	-10 m/s
1 Saw dust	2	800	100	100	100	100	85
2 Crushed plastic	5	900	100	100	56	0	0
3 Plastic screw cap	30	100	100	100	76	9	0
4 RDF	30	250	23	0	0	0	0
5 Plastic strip	50	250	1	0	0	0	0
6 Shredded tyre	30	1000	0	0	0	0	0

8.3 Experimental determination of entrainment velocity

The velocity required for entrainment of the various reburning fuels has also been investigated in the laboratory.

8.3.1 Experimental setup

In order to establish the relationship between fuel type and 'entrainment velocity' - expressed as a correlation between Reynolds number and drag factor - an experimental rig was constructed, see Figure 8.3. The rig consists of a vertical, transparent plastic tube smoothly connected to a steel tube by means of a removable muff. The plastic tube is equipped with a fine grating at the bottom and a coarse grating at the top. Air is supplied at the back end of the steel tube, which is equipped with a rotameter, allowing gas flow to be measured.

In an experiment, the sample is placed on the lowest grating, and air at ambient temperature is supplied at a steadily increasing rate. The flow rate at which the sample starts to lift is recorded. At higher flow rates the sample is entrained by the air and stays at the top of the transparent tube, where it is held back by the upper grating. Then the air flow is gently reduced, and the rate at which the sample starts to drop is recorded as well.

A total of 36 samples were prepared to examine the effect of differences in mass, shape (i.e. different diameters, projected areas and specific surface areas) and density. A reference experiment using spheres was also performed. Details of the various samples used in the experiments can be found elsewhere [12].

Data for some representative fuel samples are given in Table 8.3, and the drag coefficients calculated from the experiments are given in Figure 8.4. Realizing that the the gas flow rate out of the rotary kiln is typically 100,000 Nm^3/h, with a temperature of typi-

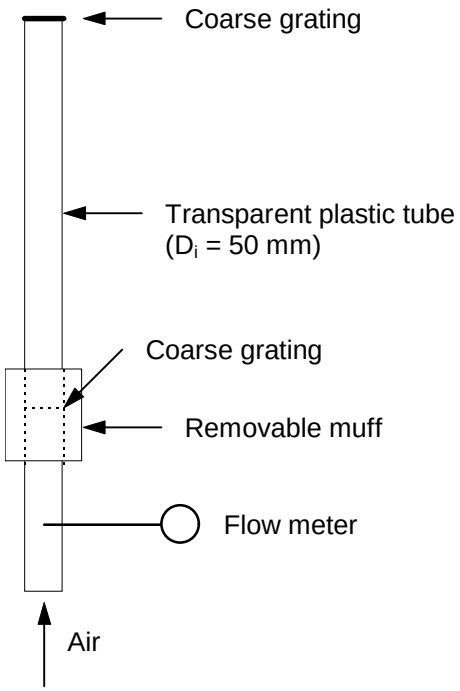

Figure 8.3: Experimental setup.

Table 8.3: Measured entrainment velocity (at 298 K) and calculated reynolds number for various fuel samples.

Fuel sample	m [g]	D_h [mm]	φ [–]	Re [–]	C_D [–]
Crushed plastic	0.20	2	0.23	$3.5{\cdot}10^2$	119.55
RDF, high spericity	8.83	30	0.99	$1.7{\cdot}10^3$	171.89
Plastic screw cap	2.83	30	0.21	$4.4{\cdot}10^4$	13.61
RDF, low spericity	5.57	35	0.73	$1.2{\cdot}10^4$	2.49
Plastic strip	3.16	3	0.13	$1.4{\cdot}10^4$	1.28
Shredded tyre	15.04	37	0.59	$5.1{\cdot}10^4$	0.06

cally 1200 °C, and that the smallest cross-section in the dust-settling chamber is about 8 m^2, it can be shown that neither chopped car tyres nor large pieces of shredded plastic will be entrained. Small plastic pieces, though, will probably be entrained. Furthermore, screw caps and RDF with high sphericities may be entrained, but not RDF with low sphericitites. These experimental results are in agreement with the results from the CFD calcualtions.

8.4 Proposal of mechanism

Based on the experience from full-scale trials (Chapter 5), the thermodynamic equilibrium calculations (Chapter 6), the TGA work (Chapter 7), the CFD computations (Section 8.2) and the entrainment velocity measurements executed in a lab-scale rig (Section 8.3), a mechanism explaining the observed phenomena can now be constructed, see Figure 8.5. If this mechanism is correct, logical consequences are:

- The feeding point must be relocated to a position where entrainment of the fuel particles is facilitated. The kiln riser duct could be such a location. (However, this is likely to lead to a lower NO_x reduction because the residence time for the fuel in a reducing atmosphere is reduced.)
- From a fluid dynamic point of view, the fuel particles should have a rather low density, a small hydraulic diameter and a sphericity close to 1. Large, dense particles, for instance car tyre pieces, can not be expected to be entrained anywhere in the calciner because no place is the gas velocity high enough to ensure entrainment.

The proposed mechanism was tested in new full-scale experiments. This is the subject of Chapter 9.

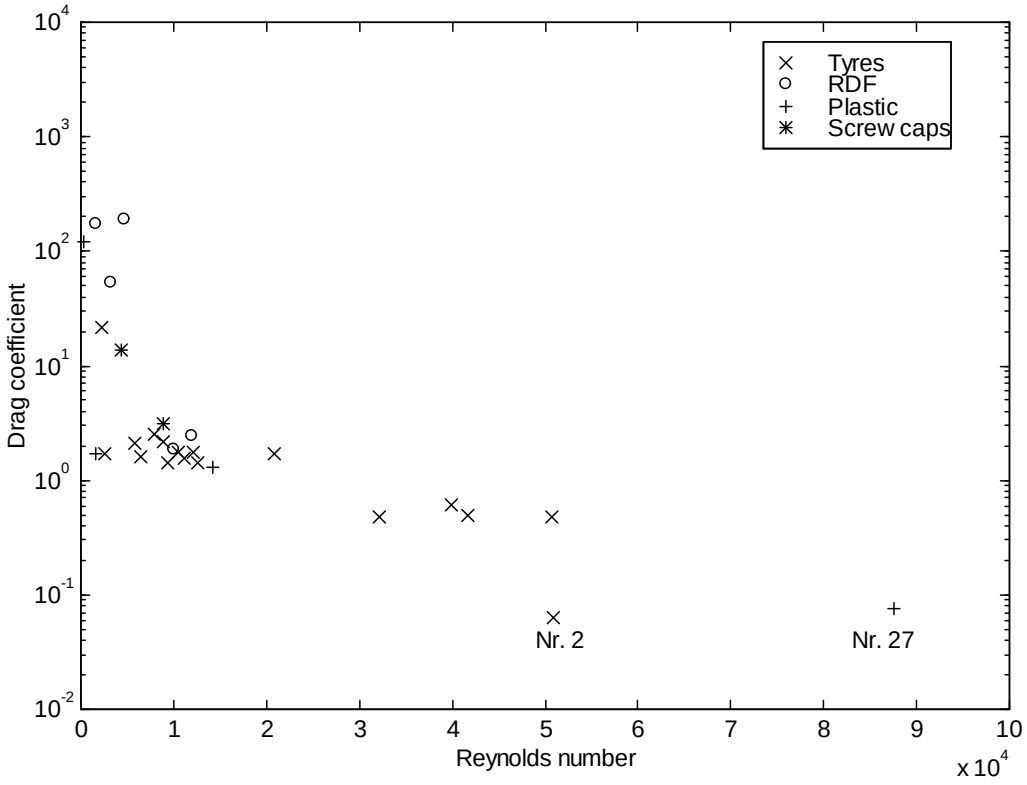

Figure 8.4: Drag coefficient as function of reynolds number of various fuel particles.

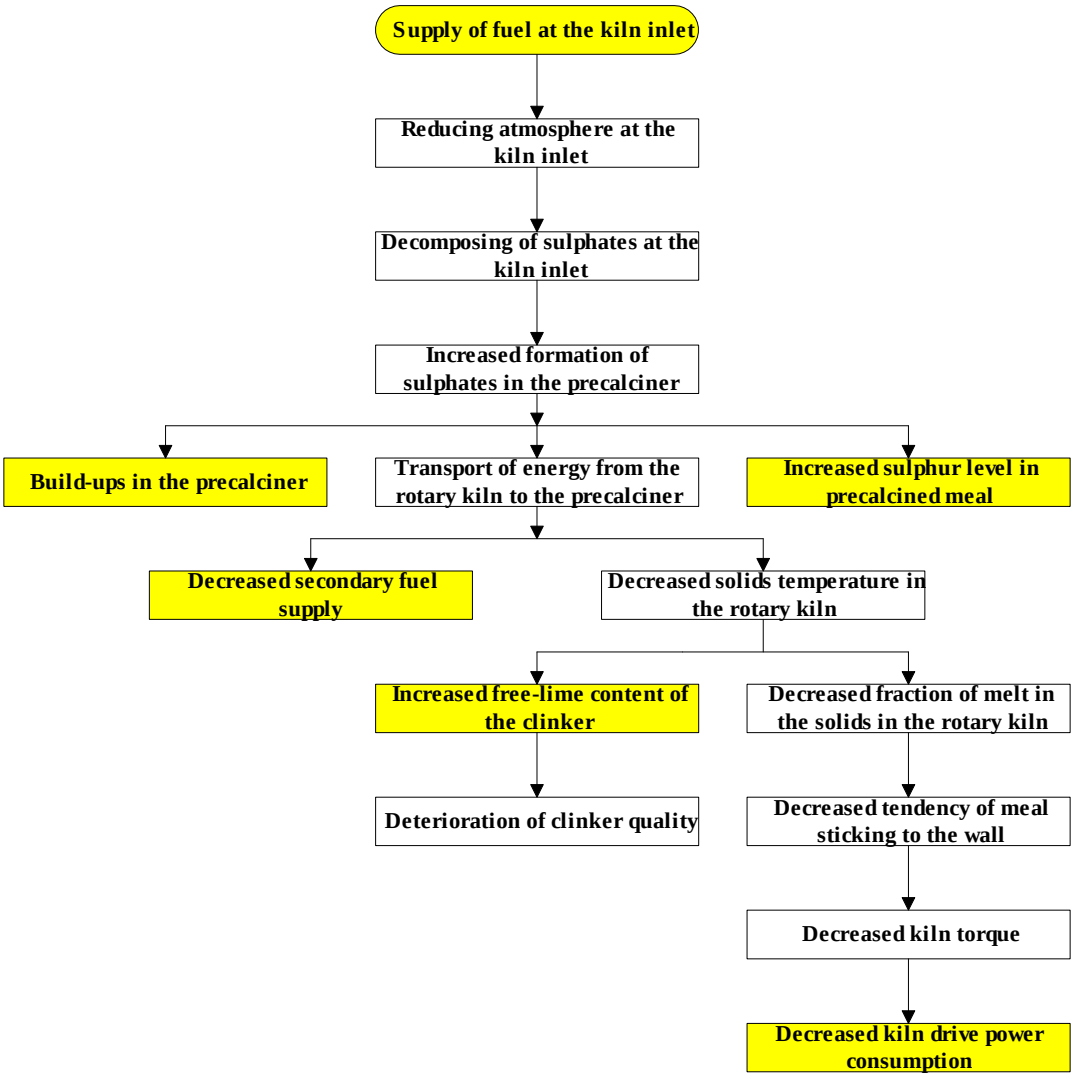

Figure 8.5: Proposal of mechanism explaining observed phenomena (hatched boxes).

Chapter 9

Full-scale experiments II

In this chapter, three new full-scale trials supplying plastic, RDF and biomass to the kiln riser duct are discussed. The purpose of the experiments was to reduce the NO_x formed in the rotary kiln by means of staged combustion, but also to test the mechanism described in Section 8.4.

The experiments were conducted in March 1998; key values for the kiln operation are given in Table 9.1. Some results from the trials have been reported previously [19, 11].

9.1 Experimental details

9.1.1 Experimental procedure

Based on experience from experiments and calculation results, a new feeding point for alternative fuels was selected. A new duct was installed, running from the conveyor belt to the kiln riser duct, and the duct was equipped with a rotating feeder to ensure stable, continuous feeding. The new feeding system is shown in Figure 9.1.

The experimental procedure was basically the same as the one used in Test A and B, as described in Subsection 5.1.1. However, far more meal samples were collected; this was done in order to investigate the internal material circulation in the system — a topic that

Table 9.1: Experimental conditions (average values) for Test C, D and E.

Parameter	**Unit**	**Test C**	**Test D**	**Test E**
Clinker production	t/d	3589	3202	3500
Total specific fuel consumption	MJ/(kg clinker)	3.2	3.4	3.2
Degree of calcination in the precalciner	%	92	94	94
Fuel fraction in the precalciner	MJ/MJ	0.56	0.54	0.55
Nominal feed rate of alternative fuel	t/h	2.0	2.0	2.0

is further discussed in Chapter 10.

9.1.2 Fuel analyses

Three fuels, plastic, RDF and biomass, were tried out, see Table 9.2. The plastic used in Test C was a mix of PP (presumably from plastic cans) and PET (presumably from soft drink bottles), the former constituting the largest fraction. This plastic mix was ground to a typical size of 5mm × 5mm × 2mm, i.e. rather small particles. The bulk density was about 500 kg/m^3. The RDF was derived from municipal waste; its main constituents were paper, plastic and biomass. (It had been dried and made into briquettes by the supplier.) The bulk density was about 250 kg/m^3. The biomass was a fine sawdust from a local sawmill. It was very dry, and had a very low bulk density of approximately 100 kg/m^3.

The pulverized coal mix used in the primary and secondary burner during the trials, was a blend of 80–100 % of a bituminuos coal and 0–20 % of a high-sulphur petroleum coke. Characteristics of the coal mix are given in Table 9.2. (In Test C, two different coal blends were used; accordingly, two analyses are given.)

The analyses of the solid and liquid hazardous waste used in the three tests, are given in Table 9.3.

In addition to proximate analyses, ultimate analyses[1] of all fuels were also carried out. The results are given in Table 9.4 and 9.5.

The following points can be made about the fuels:

- The coal mix contains relatively much nitrogen, this is a considerable source for fuel NO_x formation.
- Plastic and biomass contains very little nitrogen, making them suitable for reducing fuel NO_x formation.
- RDF and biomass have a very similar composition. This is because RDF contains a large fraction of paper.
- The rather high oxygen content of the RDF, biomass and SHW is due to the chemical structure of cellulose, hemicellulose and lignin.

[1] In an ultimate analysis, which is a standard analysis for solid fuel characterization, the content of the elements C, H, O, S and N as well as moisture and ash in the fuel is determined.

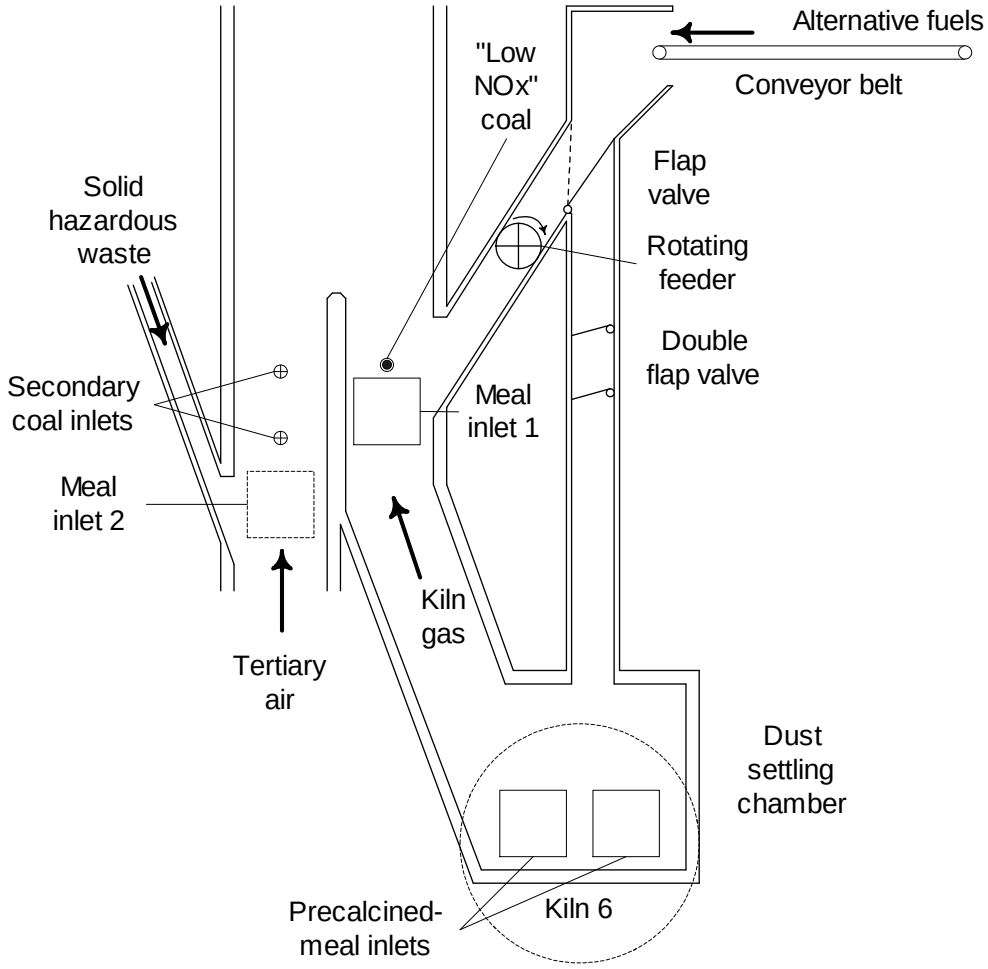

Figure 9.1: Principle drawing of system for feeding alternative fuels into the kiln riser duct and kiln inlet.

Table 9.2: Proximate analysis and heating value of the alternative fuels and the pulverized-coal mix used in Test C, D and E.

Parameter	**Unit**	**Plastic**	**RDF**	**Sawdust**	**Coal$_C$**		**Coal$_D$**	**Coal$_E$**
Moisture	%	0.4	8.3	7.7	1.5	1.0	1.0	1.1
Volatile matter	%	95.9	71.1	76.6	25.5	22.8	23.0	23.3
Fixed carbon	%	1.7	10.3	15.0	57.4	61.9	62.5	61.3
Ash	%	2.0	10.3	0.7	15.7	14.3	13.6	14.3
Sum	%	100.0	100.0	100.0	100.1	100.0	100.1	100.0
Lower heating value	MJ/kg	37.00	18.43	17.02	26.53	28.08	28.25	27.83

Table 9.3: Proximate analysis and heating value of the hazardous waste used in Test C, D and E.

Parameter	**Unit**	**SHW$_C$**	**SHW$_D$**	**SHW$_E$**	**LHW$_C$**	**LHW$_{D/E}$**
Moisture	%	7.8	15.6	12.0	–	–
Volatile matter	%	64.1	61.7	60.7	–	–
Fixed carbon	%	10.6	7.8	9.5	–	–
Ash	%	17.5	15.0	17.9	–	–
Sum	%	100.0	100.0	100.0	–	–
Lower heating value	MJ/kg	15.93	15.28	16.62	14.93	14.31

Table 9.4: Ultimate analysis of the alternative fuels and the pulverized-coal mix used in Test C, D and E.

Parameter	**Unit**	**Plastic**	**RDF**	**Sawdust**	**Coal$_C$**		**Coal$_D$**	**Coal$_E$**
Moisture	%	0.4	8.3	7.7	1.5	1.0	1.0	1.1
C	%	80.2	44.2	44.8	69.4	72.4	72.9	72.3
H	%	13.4	6.6	5.8	4.0	3.9	3.9	3.9
O	%	3.7	29.1	40.8	7.2	5.4	5.6	5.5
S	%	0.2	0.5	0.2	0.5	1.5	1.4	1.4
N	%	0.1	1.0	0.1	1.8	1.6	1.7	1.6
Ash	%	2.0	10.3	0.7	15.7	14.3	13.6	14.3
Sum	%	100.0	100.0	100.1	100.1	100.1	100.1	100.1

Table 9.5: Ultimate analysis of the hazardous waste used in Test C, D and E.

Parameter	**Unit**	**SHW$_C$**	**SHW$_D$**	**SHW$_E$**	**LHW$_C$**	**LHW$_{D/E}$**
Moisture	%	7.8	15.0	17.9	–	–
C	%	36.8	34.2	36.8	48.7	38.6
H	%	5.9	4.7	5.2	7.6	8.3
O	%	29.8	29.3	26.4	21.2	29.4
S	%	1.6	0.9	1.2	1.4	1.7
N	%	0.6	0.5	0.6	1.5	2.1
Ash	%	17.5	15.6	12.0	–	–
Sum	%	100.0	100.2	100.1	–	–

Table 9.6: Experimental results (average values).

	Unit	Test C		Test D		Test E	
Feed rate of alternative fuel	t/h	0.0	2.0	0.0	2.0	0.0	1.5
Secondary coal feed rate	t/h	8.8	6.5	8.4	6.9	8.2	7.0
Clinker production	t/d	3605	3578	3300	3435	3538	3457
Total specific fuel consumption	MJ/(kg cli)	3.2	3.3	3.4	3.3	3.2	3.2
Fuel fraction in the precalciner	MJ/MJ	0.56	0.57	0.55	0.55	0.55	0.55
NO_x content in the kiln inlet	mg/Nm^3	386	231	566	854	403	358
NO_x content in the stack gas	mg/Nm^3	566	449	770	851	667	655
NO_x reduction, kiln inlet	%	+40		+34		+11	
NO_x reduction, stack	%	+21		+10		+2	

9.2 Results and discussion

9.2.1 NO_x reduction

Table 9.6 lists some of the key figures from Test C, D and E. The NO_x concentration in the kiln inlet was very low during all the tests, in fact it was lower than the concentration in the stack gas most of the time. This is likely to be due to an extraordinary low temperature in the kiln burning zone. There is no obvious reason for this. However, by using MEBCEM to calculate the equivalence ratios in the system, it appears that the low NO_x levels are due to rather low equivalence ratios in the system. This can be seen in Figure 9.2, which shows the relation between NO_x concentration at the kiln inlet and the equivalence ratio of the kiln/precalciner for six independent full-scale trials. At the highest equivalence ratios, the NO_x concentration is very low. This is in accordance with the theory, which says that the excess air should be as low as possible in order to minimize the NO_x emissions. It is also interesting to see that the NO_x band is much more narrow at high equivalence ratios. Furthermore, the figure indicates that the kiln system is operated non-optimally a large part of the time, i.e. when the equivalence ratio is low.

The results from the plastic trial, Test C, are given in Figure 9.3–9.5[2]. The reduction in the secondary coal supply corresponds well to the plastic supply, and the NO_x concentration in the stack gas is reduced by 21 % for a plastic supply rate of 2 t/h (see Figure 9.4). During the plastic supply, a drop in the kiln inlet NO_x level is seen. This 'spike', which is caused by an extraordinary high equivalence ratio, explains the minimum value of the NO_x conversion ratio, as seen in Figure 9.5.

In Test C, it was experienced that the plastic particles had a tendency of sticking to the walls of the precalciner, possibly causing damages on the furnace lining. This suggests that lining qualities more resistant to high temperatures, ought to be considered for use in

[2]Due to some problems with the electronic data collection system, the data had to entered manually. Hence, only hourly averages are given.

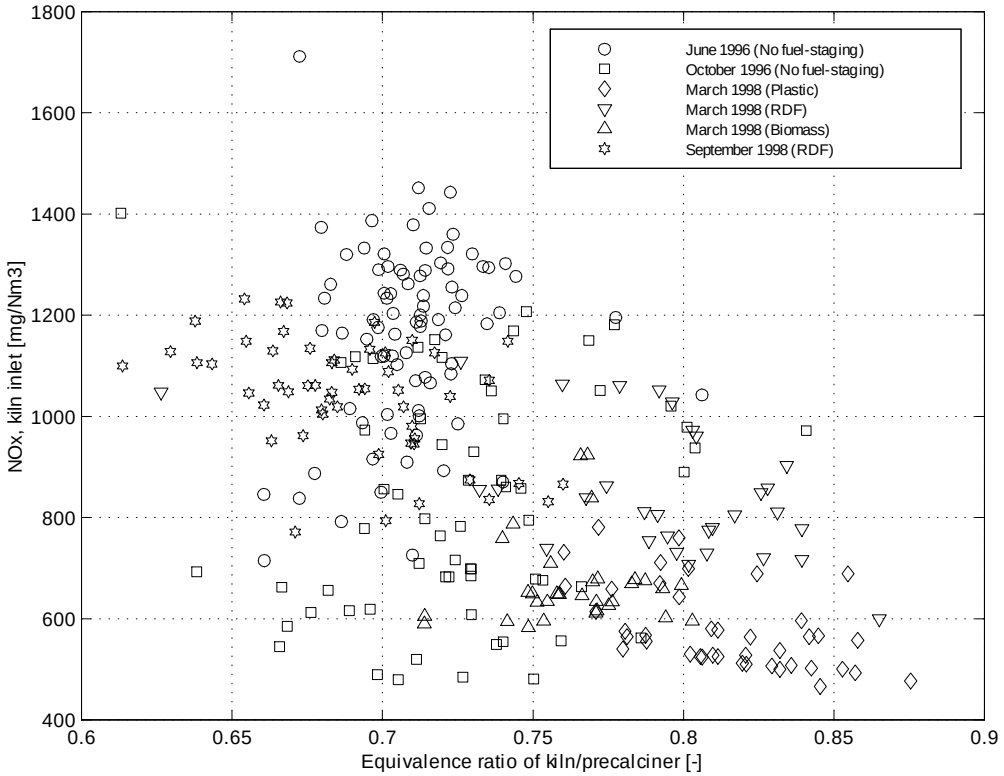

Figure 9.2: Relation between NO_x level at the kiln inlet and equivalence ratio of the kiln/precalciner.

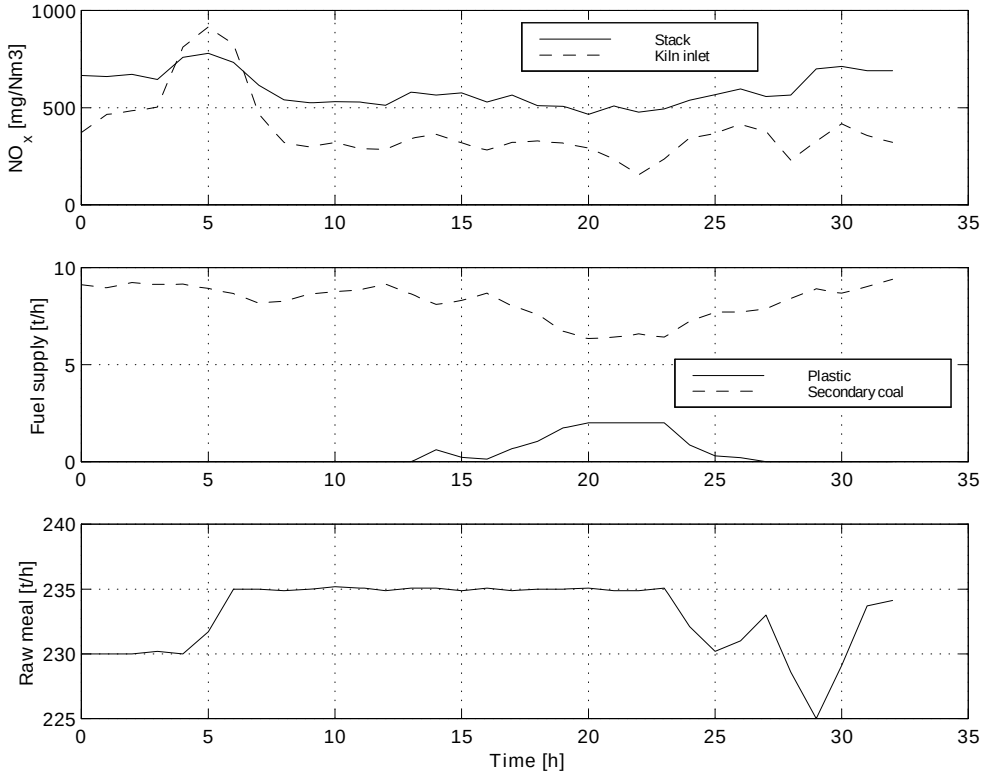

Figure 9.3: NO_x concentration in the kiln inlet and in the stack during supply of secondary coal, plastic and raw meal, Test C.

the precalciner if pure plastic is to be burned. Furtermore, a few agglomerates of plastic and preheated meal were found in the dust settling chamber during the experiments, indicating that melted plastic tend to mix with preheated meal and form agglomerates that are not easily entrained. However, because this tendency is not very pronounced, it is not likely to impede the use of plastic in the kiln riser duct.

The results from the RDF trial, Test D, are given in Figure 9.6–9.8[3]. In this trial, there is no reduction in the NO_x concentration in the stack gas (see Figure 9.7). This is not surprising since the heating value of the RDF is only the half of that of plastic. Thus, no reducing zone is formed, and the NO_x is not converted to N_2.

The results from the sawdust trial, Test E, are given in Figure 9.9–9.11. Nor in this trial is there any reduction in the stack gas NO_x concentration. Again, this is explained by the low heating value of the fuel. (Besides, due to the very low bulk density of the sawdust, a feeding rate of 2 t/h was never reached. The volumetric feeding rate capacity

[3]Due to some problems with the electronic data collection system, the data had to entered manually. Hence, only hourly averages are given.

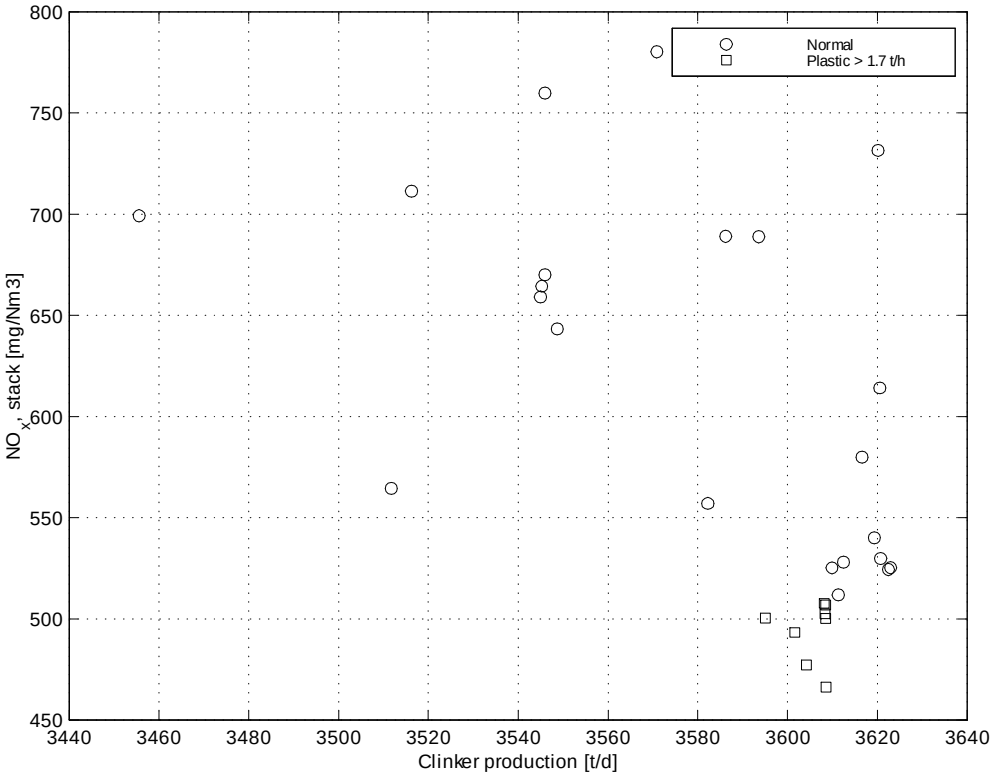

Figure 9.4: NO_x concentration in the stack gas versus clinker production, Test C.

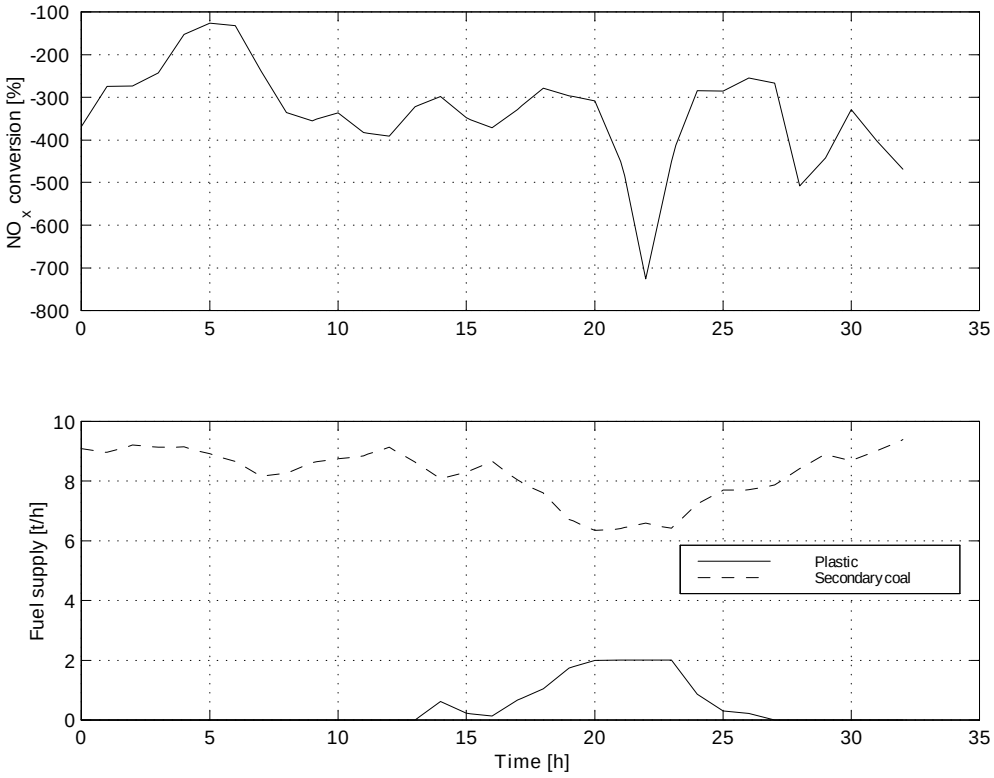

Figure 9.5: Calculated NO_x conversion in the precalciner, Test C.

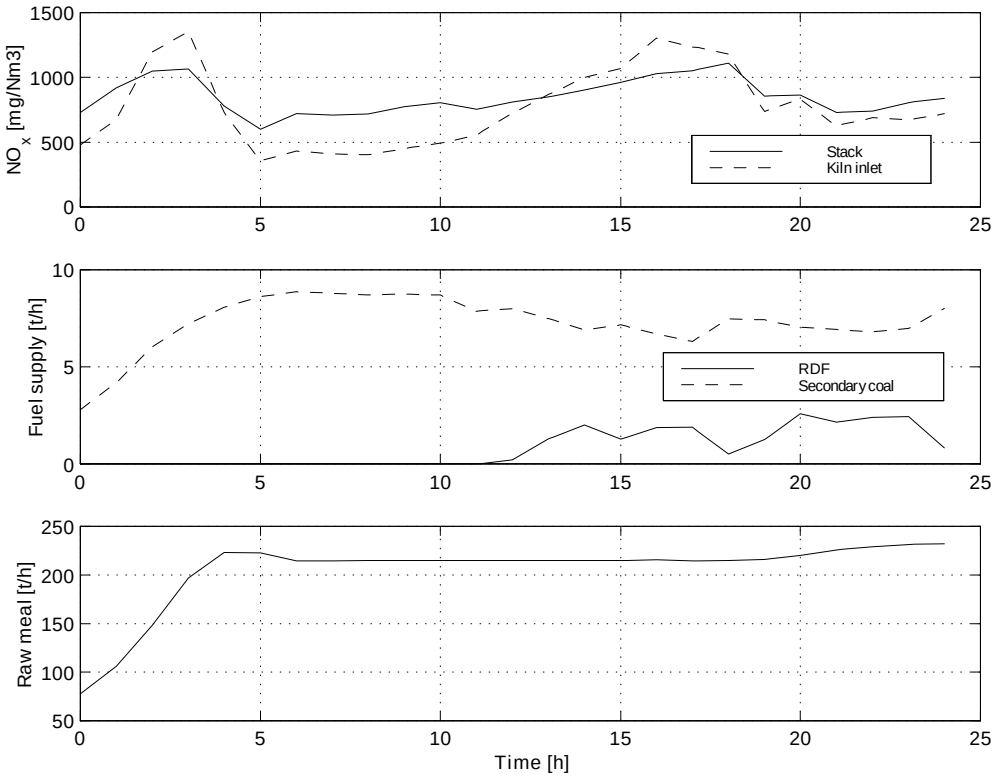

Figure 9.6: NO_x concentration in the kiln inlet and in the stack during supply of secondary coal, RDF and raw meal, Test D.

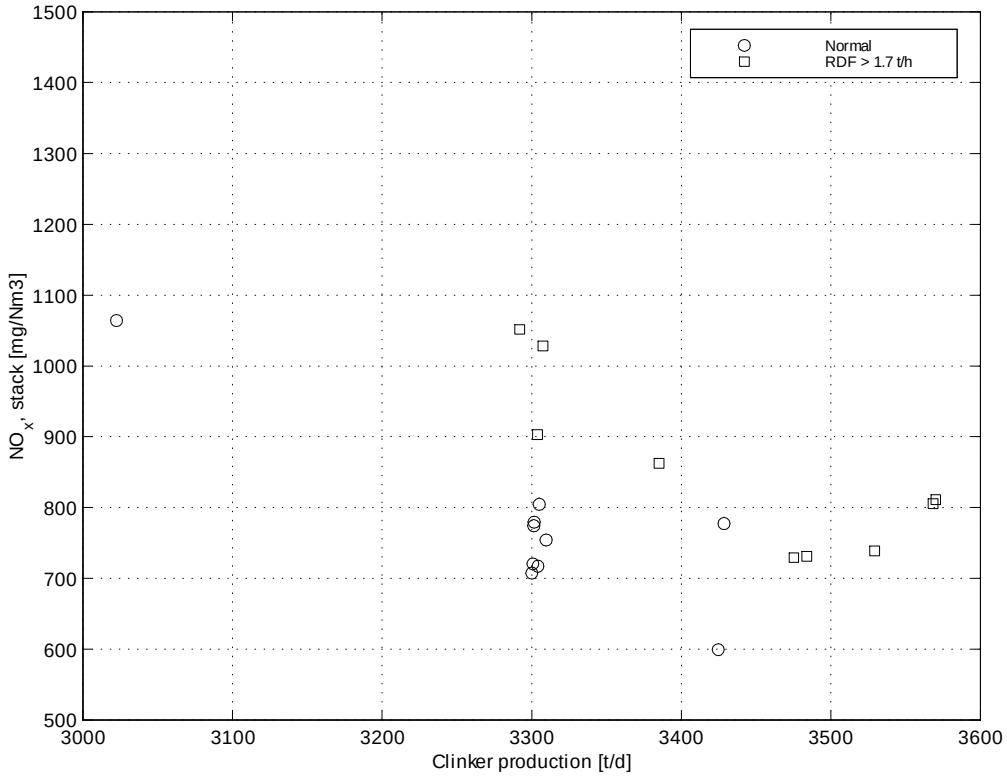

Figure 9.7: NO_x concentration in the stack gas versus clinker production, Test D.

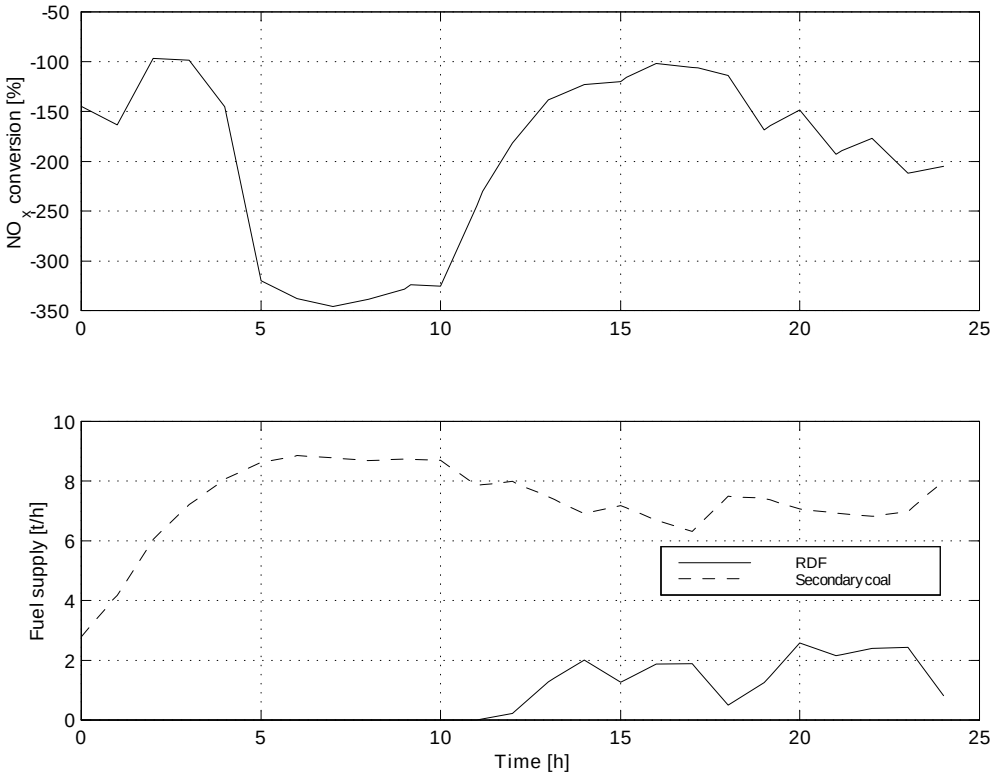

Figure 9.8: Calculated NO_x conversion in the precalciner, Test D.

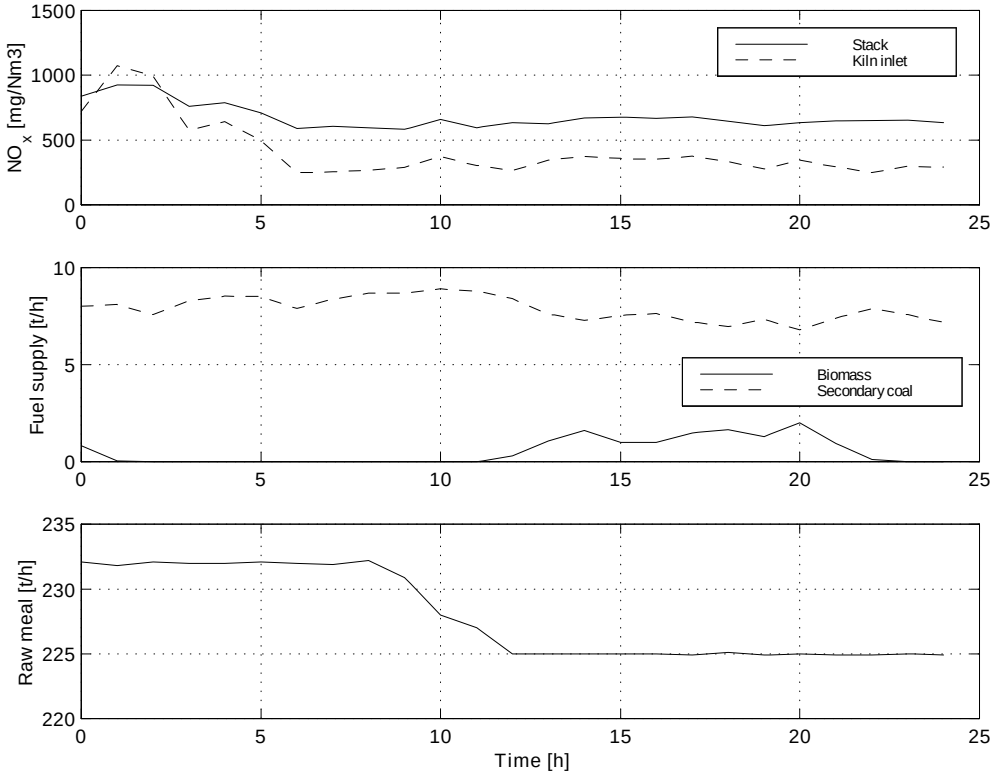

Figure 9.9: NO_x concentration in the kiln inlet and in the stack during supply of secondary coal, biomass and raw meal, Test E.

of the feeding system limited the sawdust supply to about 1.5 t/h.)

9.2.2 NO_x formation mechanism distribution and fuel-N conversion

It is of great interest to be able to quantify the NO_x formed in the rotary kiln (which is believed to be mainly thermal NO_x) relative to the NO_x formed downstream of the kiln (which is mainly fuel-NO_x). This requires a mass balance of the rotary kiln system, since the flow of exit gas from the rotary kiln is unknown and very difficult to measure due to the high temperature and dust concentration. In this connection, MEBCEM is useful. Furthermore, it would be of great value to be able to calculate the conversion of fuel-N to NO_x in the precalciner. There seems to be little information on these process properties in the literature.

Figure 9.12 shows a calculation of NO_x formed in the rotary kiln ('Thermal NO_x') and NO_x formed downstream of the kiln ('Fuel- and feed-NO_x'), based on measured NO_x

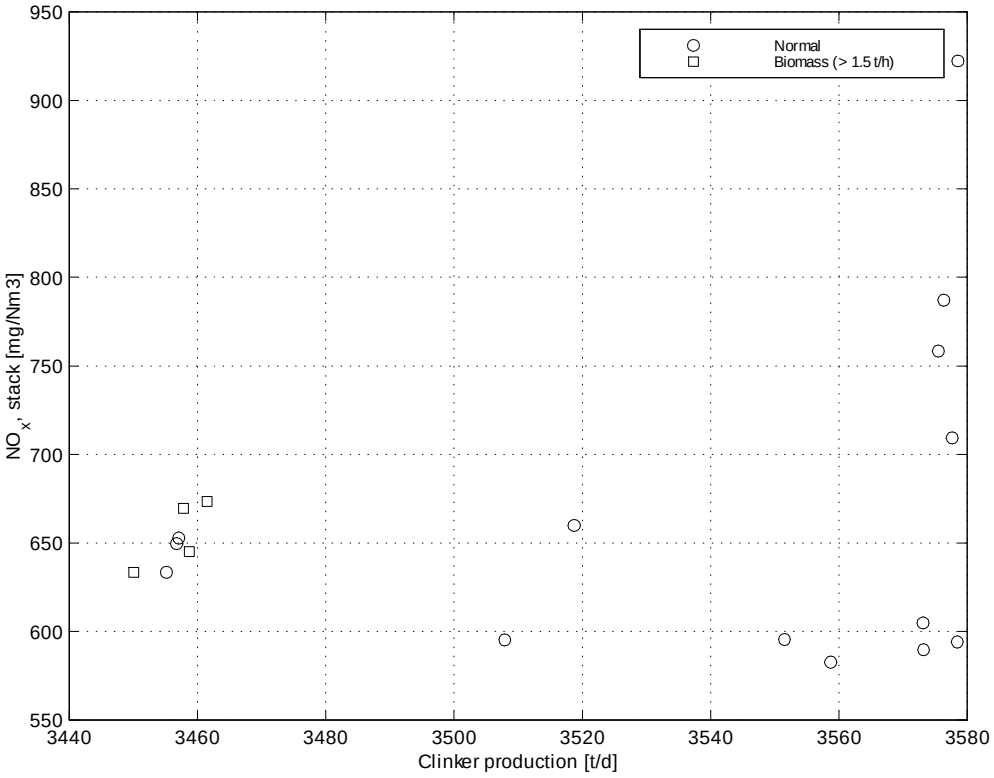

Figure 9.10: NO_x concentration in the stack gas versus clinker production, Test E.

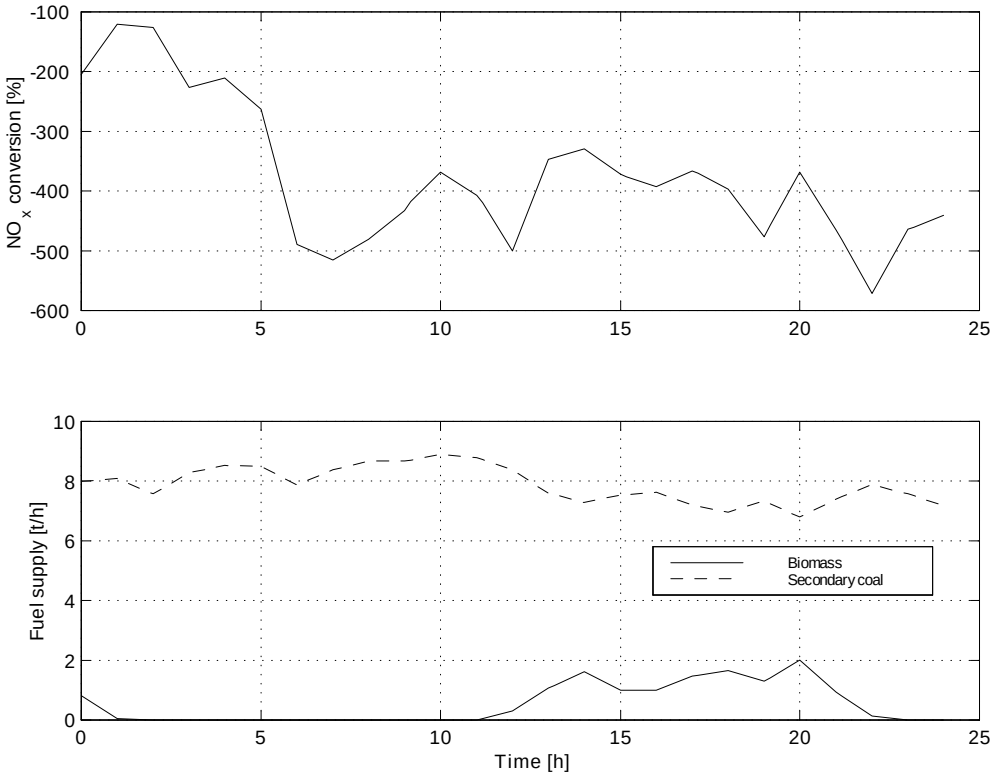

Figure 9.11: Calculated NO_x conversion in the precalciner, Test E.

concentration at the kiln inlet and in the chimneys during Test C, D and E. MEBCEM has been used to calculate the mass flow out of the kiln and in the chimneys. The total mass flow of NO_x out of the chimney is set to 100 %, then the percentage formed in the kiln ('Thermal NO_x') is calculated by taking the ratio of inlet NO_x to stack NO_x, and finally the percentage formed in the precalciner/preheater ('Fuel- and feed- NO_x') is calculated by difference. It is interesting to see that a major part of the emissions from this cement kiln seems to be due to NO_x formation in the precalciner. This is an interesting observation, since the general view seems to be that thermal NO_x formation is the dominant mechanism [44, 155]; Smart *et al.* [44] claims that 70 % of the NO_x is thermal NO_x, and Gardeik *et al.* [46] found that only 20 % of the NO_x was formed in the secondary combustion zone. The present analysis roughly gives the opposite result, i.e. that about 70 % of the NO_x is formed in the precalciner. But, of course, this percentage will vary from plant to plant, and to a certain extent it will vary with time in a particular plant.

Figure 9.13 shows the fuel-N conversion for the same three trials. The conversion is fairly constant and is in the range of 25 to 35 %. Fluctuations are to be expected due to the varying conditions in the precalciner; calculations show that the fuel-N conversion increases with decreasing equivalence ratio on the tertiary air side of the precalciner (i.e. where the secondary fuel is supplied). This explains the difference between the runs.

9.2.3 Impact on the internal material cycles

The impact of alternative fuel supply in the kiln riser duct on various measures related to the internal material circulation is shown in Figure 9.14, 9.15 and 9.16 for Test C, D and E, respectively.

In all tests, the weight percentage of SO_3 in precalcined meal was high — both before, during and after the supply of alternative fuels. No changes in the SO_3 level can be attributed to the supply of plastic, RDF or sawdust.

Also the weight percentage of free lime in the clinker product was fairly high in all experiments. Indeed, in Test C the maximum value of free CaO coincides with the maximum value of plastic supply. But another high free-CaO value is reached after the plastic supply is ended, so there is no significant correlation between the two variables. In Test D and E, the correlation is even less.

The kiln drive current was reduced by about 8 % in Test C; in Test D the reduction was on average 9 %; whereas in Test E, there was in fact an increase of about 15 %. However, none of these variations can be attributed to the supply of alternative fuel.

9.2.4 Fuel particle requirements

The experience and insight gained from experiments and calculations may be utilized to specify the characteristics of fuel particles used for the purpose of staged combustion in

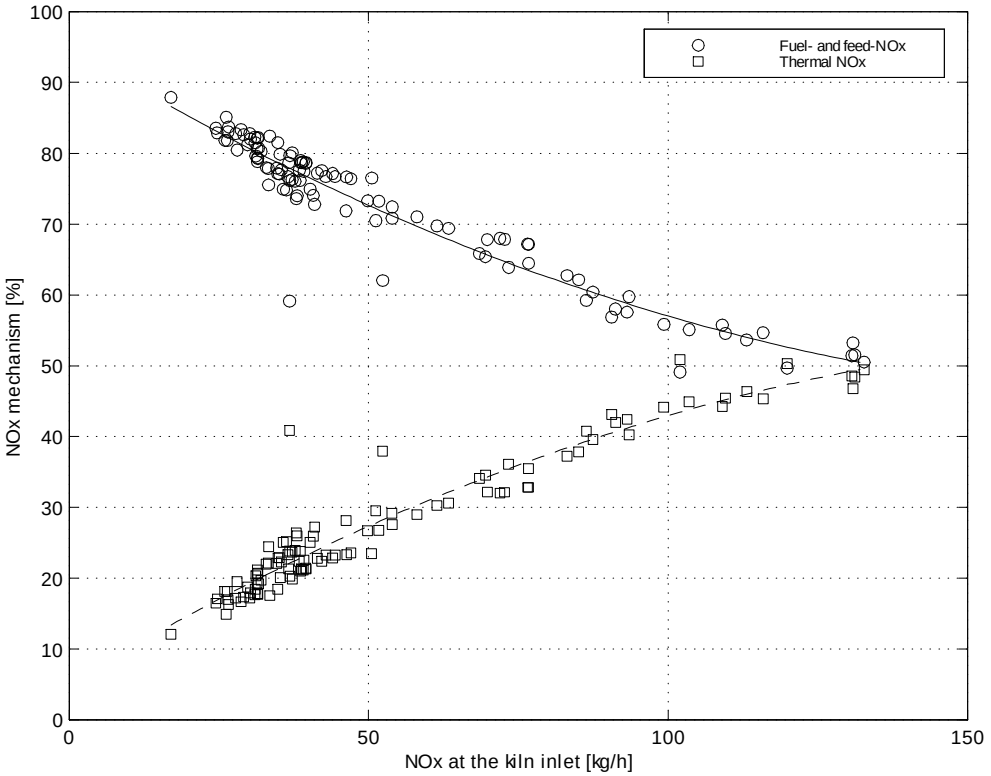

Figure 9.12: NO_x formed in the rotary kiln ('Thermal NO_x') and in the precalciner ('Fuel- and feed-NO_x'); Test C, D and E.

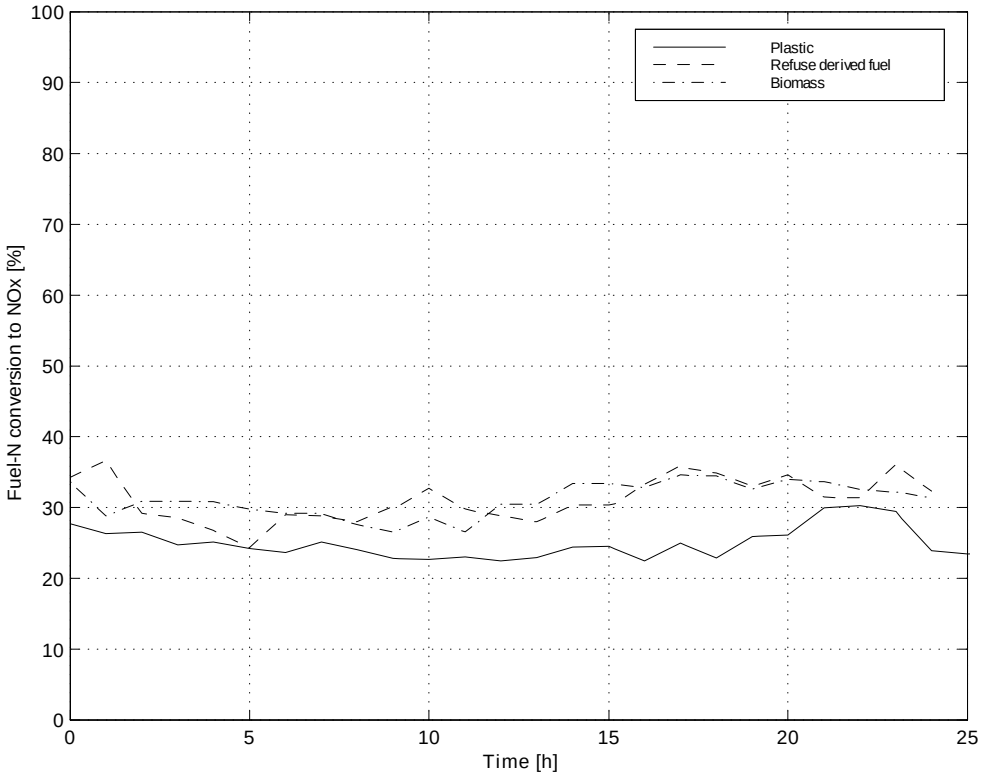

Figure 9.13: Conversion of fuel nitrogen to NO_x in the precalciner; Test C, D and E.

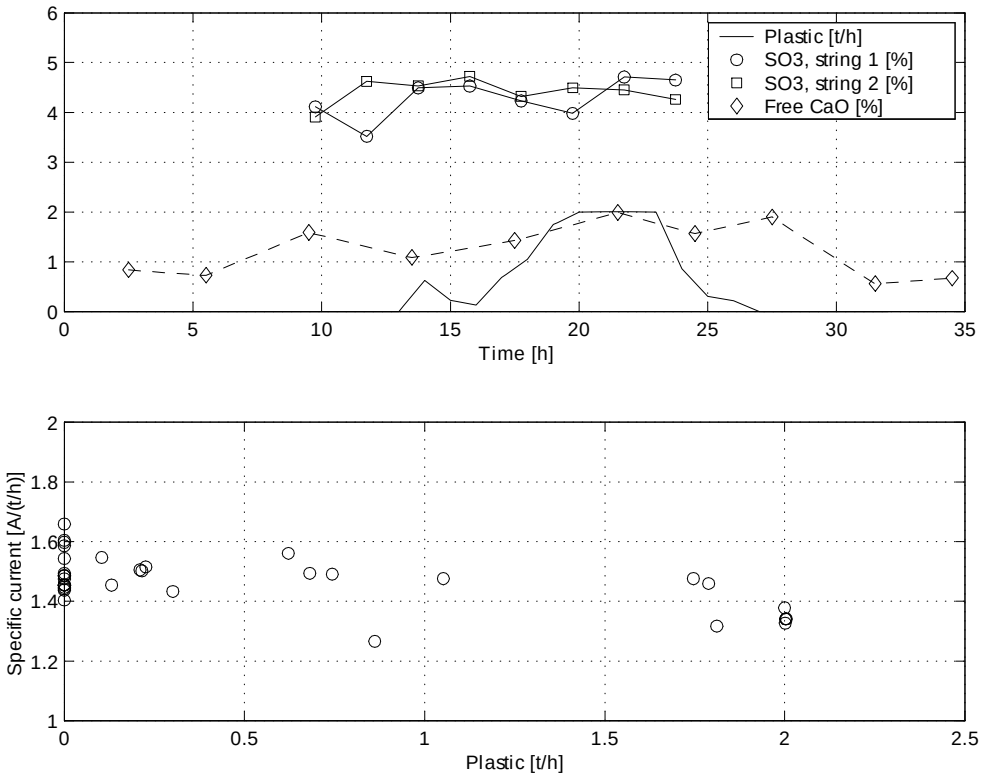

Figure 9.14: Free CaO in clinker, sulphur in precalcined meal and current consumption by kiln rotation, Test C.

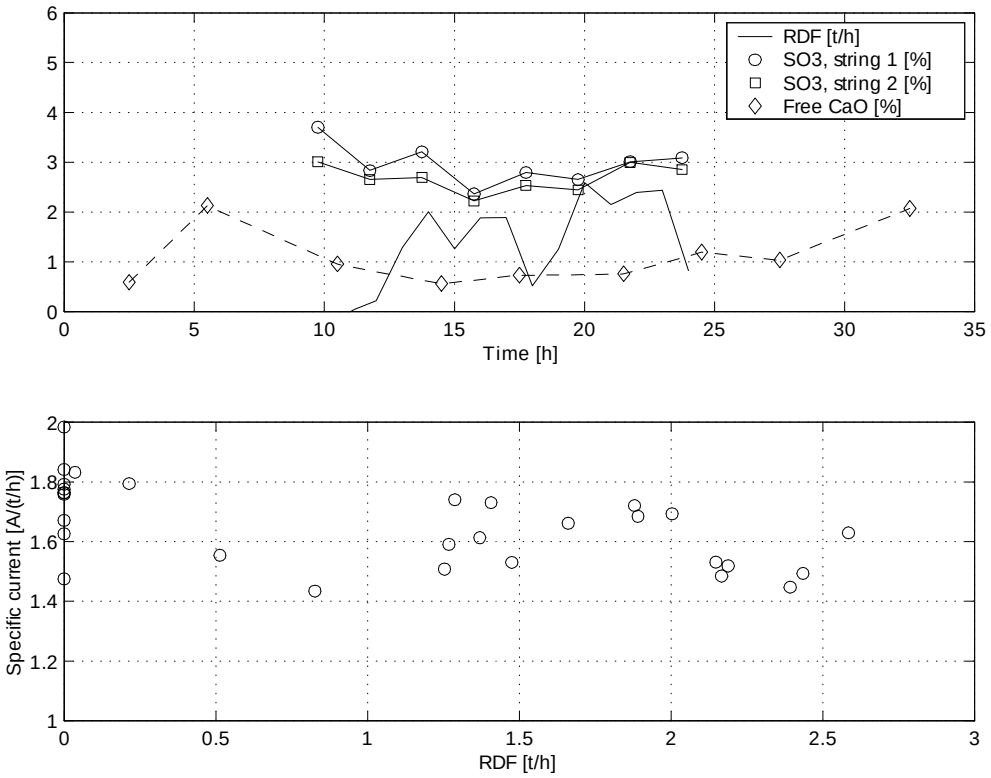

Figure 9.15: Free CaO in clinker, sulphur in precalcined meal and current consumption by kiln rotation, Test D.

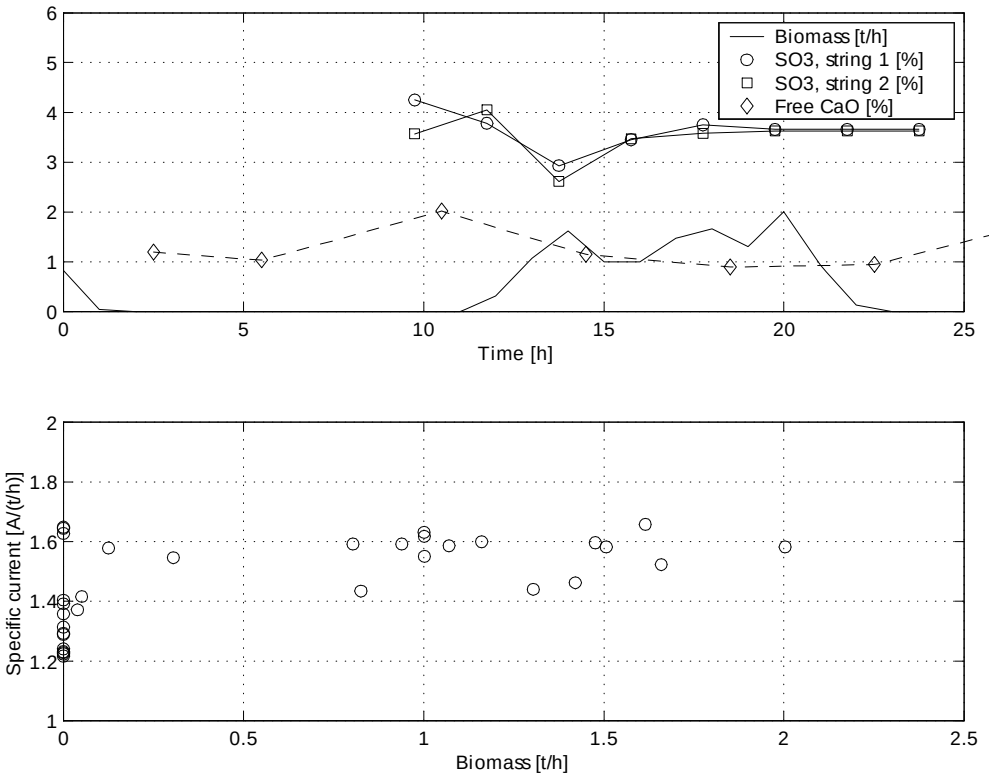

Figure 9.16: Free CaO in clinker, sulphur in precalcined meal and current consumption by kiln rotation, Test E.

the precalciner:

- Fluid mechanical requirements:
  - *Diameter, density and shape:* The particles should be small and light and have a high sphericity in order to be easily entrained by the kiln gases.
  - *Inlet velocity and -angle:* The inlet velocity and -angle may be decisive of the particle track. This is particularly relevant to particles with a 'critical' diameter, density and/or shape. For very small and light particles, such as sawdust, this is not relevant because of the low momentum of such particles.
  - *Agglomeration/melting tendency:* Particles that easily melt and agglomerate should be avoided because they are difficult to entrain.

  The excact fluid mechanical requirements depend on the kiln gas velocity and temperature.The flow field of the feeding point area can be examined by means of a CFD analysis in order to decide whether a given particle will be entrained or not.

- Combustion requirements:
  - *Burning rate:* Burnout of the particle before the precalciner exit is essential in order to avoid increased CO emissions. In this connection the residence time and the temperature of the particles inside the precalciner, as well as the local atmosphere experienced by the particles, is of key importance. This means that different precalciner designs may give very different fuel requirements.
  - *Heating value:* The fuel should have a high heating value in order to be a proper substitute for pulverized coal. Besides, for a given feed rate, the NO_x reduction capacity increases with the heating value (due to a higher reduction in fuel-NO_x formation from the secondary coal), a fact that further emphasizes this requirement.

- System requirements:
  - *Burning rate:* Particles with a very high burning rate tend to cause high temperatures locally that may damage the furnace lining. If such particles are to be used, bricks with high thermal stability must be employed.
  - *Homogeneity:* Very often the feeding system, for instance rotary feeders, will put limits on the particle quality. This means that 'pollutants' such as stones, metals, etc. should be absent — even though such objects may be of little risk to the process in other respects.
  - *Bulk density:* Fuels with a very low bulk density are expensive to handle. Thus they should be avoided.

- Process requirements:
  - *Low/stable content of circulating substances:* The fuel should not have a very high content of circulating elements, such as S, K, Na and Cl. For example, PVC contains too much chlorine, and some biofuels, such as bark, tend to contain too much alkalies. Equally important is the demand for a stable content of such elements; large fluctuations may induce unwanted disturbances to the kiln system.
  - *Low 'pollutant' content:* The fuel should have acceptably low levels of 'pollutants', for instance heavy metals.

Chapter 10

Calculation of internal material cycles

In this chapter, the internal circulation of sulphur, alkalis and chlorine in the kiln system is calculated by means of program routine based on MEBCEM. It is also shown how the intensity of the internal cycles may be reduced by controlling the input of the circulating elements. Data from Test C is used in the calculation examples.

10.1 Sulphur, alkalies and chlorine in the system

Sulphur enters the system through the raw meal and through the various fuels used in the combustions processes. Both raw meal and coal has a typical S content of 0.4 % (measured as S; corresponding to about 1 % measured as SO_3). However, if petcoke is used (mixed with coal), the fuel sulphur increases, since petcoke typically contains 5 % S. The main part of the sulphur leaves the system as part of the clinker product. But some sulphur is released to the surroundings as SO_2, mainly because of oxidations of pyrrite (FeS_2) in the preheater. The SO_2 concentration is highest in the off-gas from string 1. This is due to the off-gas from the string 2 preheater being utilized in the raw meal mill as a drying medium — in this process presumably about 85 % of the sulphur in the gas is absorbed in the raw materials. The dust from the ESP's, which contains some sulphur, mainly in the form of sulphates, is mixed with the raw meal and then returned to the cyclone tower.

The alkalies are supplied mainly as part of the raw meal. The fuel ash also contains alkalies, but the amount in the ash only goes up to a fraction of the amount in the raw meal, since the raw meal flow is so much larger than the fuel flow. The alkalies leave the system mainly as alkali sulphates in the clinker.

The chlorine content of the raw meal is very low, usually ranging from 0.01 to 0.1 % on a mass basis. The chlorine content of the fuel is largely dependent on fuel type; coal

contains only small amounts of chlorine, whereas hazardous waste typically contains 0.5-2 % chlorine. Alternate fuels, such as RDF and plastic, may also contain considerable amounts of chlorine. The chlorine leaves the system as part of the clinker and the ESP dust (which is subsequently returned to the cyclone tower). However, some chlorine is released to the surroundings as HCl in the off-gas from string 1; the chlorine in the off-gas from string 2 is efficiently absorbed in the raw meal mill during the drying process.

10.2 Calculation of circulating compounds

In Chapter 4, the development of MEBCEM was described. MEBCEM is used as a basis for the calculation of circulating compounds.

The raw material processed in the kiln system contains a large fraction that is not chemically specified in MEBCEM. This fraction, which constitutes about 67 % of the raw meal, contains S, K, Na and Cl.

MEBCEM requires the elemental fuel composition[1] of all fuels as input data. This means that S is specified. The elements K, Na and Cl are all a part of the fuel ash, which is part of the fuel composition vector.

The major gas species generally considered in MEBCEM are CO_2, O_2, N_2, H_2O and CO. In other words, circulating elements like S, K, Na and Cl are not taken into consideration in MEBCEM. However, the concentration of S, K, Na and Cl are believed to be rather small in most of the kiln system. Thus, treating these elements as minor gas species should be acceptable. On the other hand, the concentration of circulating elements in the off-gas from the rotary kiln may be considerable due to the accumulation tendency in the precalciner. However, this is partly handled through an extra component in the gas composition vector, which is implemented in MEBCEM for this particular location in the kiln system.

The remaining subsections in this section deal with the development of a new model, called CIRCCEM[2] which is used to calculate the circulation of S, K, Na and Cl in the system.

10.2.1 Assumptions and simplifications

A number of prerequisites, assumptions and simplifications are made in order to obtain a tractable model:

- The basis for the model to be developed is MEBCEM. MEBCEM is a steady state model; accordingly, the calculation of circulating compound also has to be performed

[1] C, H, O, S, N, ash and moisture, i.e. ultimate analysis.

[2] CIRCCEM is an acronym for Calculation of ciRculating Compounds in a CEMent kiln system.

on a steady state basis. This means that transient phenomena, such as run-ups and shutdowns, can not be modelled well.

- The fraction of precalcined meal in the meal out of a cyclone is assumed equal to the fraction of precalcined meal in the dust out of the same cyclone. In reality, the fraction is likely to be somewhat higher in the dust because the dust probably has a higher fraction of small particles, which are believed to be more readily calcined.
- The gas flow out of the preheater is assumed equally divided between string 1 and 2. In reality there may be small (typically a few percent) deviations from this.
- The concentration of dust downstream of the ESP's is neglected, i.e. taken as zero. This is justified by the high efficiency of the ESP's (typically $> 99{,}9$ %).
- The ratio of dust entering the coal mill to dust entering ESP 4 is assumed equal to the ratio of gas entering the coal mill to gas entering ESP 4. This is a reasonable assumption since the two gas flows are originating from string 1 of the cyclone tower.
- The time delay related to the transport of ESP dust from the ESP's to the re-injection into the cyclone tower is neglected. This means that the ESP dust that is mixed with fresh raw meal is identical in composition to the dust from ESP 3 and ESP 4, and that the residence time in the silo containing fresh raw meal and ESP dust is neglected. The real residence time in the silo depends on the charge level in the silo, but is typically less than one hour. (The silo capacity is 250 tons, and a typical feed rate of raw meal is 220 tons per hour.)

10.2.2 Preheater mass balance modifications

The output from MEBCEM is stored in a datafile[3], which contains most of the mass flows required for calculating the circulating substances. However, MEBCEM treats the preheater (i.e. the three upper cyclone stages in string 1 and 2) as one reactor unit. Such a model is not adequate if the elemental distribution in the various cyclone stages is to be described. Hence, a splitting up of the preheater, in which both meal, gas and dust flows are considered, is required[4]. A schematic of the (macroscopic) flow process in the preheater/precalciner is shown in Figure 10.1.

Now, let A and B denote mass flow of uncalcined and calcined meal, respectively, and let indexes D and K designate 'dust' and 'kiln', respectively. Assuming that the the cyclone efficiency $\eta_{\#}$ of cyclone stage # ($\# \in \{1, 2, 3, 4\}$) is the same for both calcined and uncalcined meal, the following equations result:

$$\eta_1 = 1 - \frac{A_{\mathrm{D1}}}{A_0 + A_{\mathrm{D2}}} \tag{10.1}$$

[3] `rdata#.mat`, where `#` corresponds to the dataset ID

[4] This improved model of the preheater is to be implemented in future versions of `MEBCEM`.

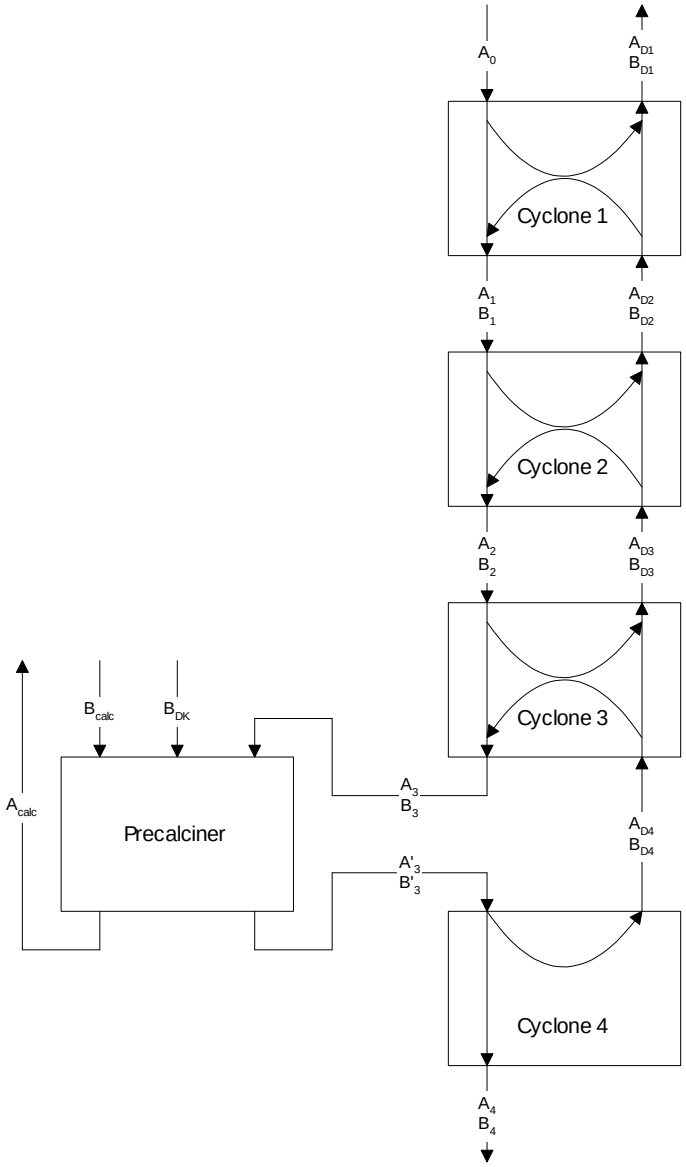

Figure 10.1: Diagram showing the flow process in the cyclone tower.

$$\eta_1 = 1 - \frac{B_{\mathrm{D1}}}{B_{\mathrm{D2}}} \tag{10.2}$$

$$\eta_2 = 1 - \frac{A_{\mathrm{D2}}}{A_1 + A_{\mathrm{D3}}} \tag{10.3}$$

$$\eta_2 = 1 - \frac{B_{\mathrm{D2}}}{B_1 + B_{\mathrm{D3}}} \tag{10.4}$$

$$\eta_3 = 1 - \frac{A_{\mathrm{D3}}}{A_2 + A_{\mathrm{D4}}} \tag{10.5}$$

$$\eta_3 = 1 - \frac{B_{\mathrm{D3}}}{B_2 + B_{\mathrm{D4}}} \tag{10.6}$$

$$\eta_4 = 1 - \frac{A_{\mathrm{D4}}}{A_3^{'}} \tag{10.7}$$

$$\eta_4 = 1 - \frac{B_{\mathrm{D4}}}{B_3^{'}} \tag{10.8}$$

In addition, the following balance equations for the components can be produced:

$$A_0 + A_{\mathrm{D2}} = A_1 + A_{\mathrm{D1}} \tag{10.9}$$

$$B_{\mathrm{D2}} = B_1 + B_{\mathrm{D1}} \tag{10.10}$$

$$A_1 + A_{\mathrm{D3}} = A_2 + A_{\mathrm{D2}} \tag{10.11}$$

$$B_1 + B_{\mathrm{D3}} = B_2 + B_{\mathrm{D2}} \tag{10.12}$$

$$A_2 + A_{\mathrm{D4}} = A_3 + A_{\mathrm{D3}} \tag{10.13}$$

$$B_2 + B_{\mathrm{D4}} = B_3 + B_{\mathrm{D3}} \tag{10.14}$$

$$A_3^{'} = A_4 + A_{\mathrm{D4}} \tag{10.15}$$

$$B_3^{'} = B_4 + B_{\mathrm{D4}} \tag{10.16}$$

$$A_3 = A_3^{'} + A_{\mathrm{calc}} \tag{10.17}$$

$$B_3 + B_{\mathrm{calc}} + B_{\mathrm{DK}} = B_3^{'} \tag{10.18}$$

The calcination in the precalciner gives the following equations, where $w_{\mathrm{CaCO_3}}$ is the mass fraction of calcium carbonate in the raw meal:

$$B_{\mathrm{calc}} = A_{\mathrm{calc}} \left(1 - \frac{M_{\mathrm{CO_2}}}{M_{\mathrm{CaCO_3}}} w_{\mathrm{CaCO_3}}\right) \tag{10.19}$$

$$\eta_{\mathrm{calc}} = 1 - \left(\frac{M_{\mathrm{CaCO_3}}}{M_{\mathrm{CO_2}} w_{\mathrm{CaCO_3}}} - 1\right) \left(\frac{A_4 + B_4}{A_4 \left(1 - \frac{M_{\mathrm{CO_2}}}{M_{\mathrm{CaCO_3}}} w_{\mathrm{CaCO_3}}\right) + B_4} - 1\right) \tag{10.20}$$

The result is a system of 20 unknowns (A_0, B_{DK}, η_1, η_3, η_3, η_4 and η_{calc} are known) in 20 equations, which may be solved by means of linear algebra. This is shown in Appendix E.

The extended mass balance results in an outflow of precalcined meal from the fourth cyclone stage that is slightly (about 3 %) lower than the flow value of precalcined meal calculated in MEBCEM. Furthermore, MEBCEM neglects the dust concentration in the off-gas from the preheater. This simplification is removed here, i.e. dust flows are considered — not only in the preheater, but also downstream (with regard to the gas phase) of the preheater[5]. The discrepancies are, however, within an acceptable range. The filter dust from ESP 3, ESP 4 and the coal mill filter are calculated in the following way:

$$m_{\mathrm{D,CM}} = m_{\mathrm{D,c1,s1}} \frac{m_{\mathrm{G,CM,in}}}{m_{\mathrm{G,c1,s1}}} \tag{10.21}$$

$$m_{\mathrm{D,ESP4}} = m_{\mathrm{D,c1,s1}} - m_{\mathrm{D,CM}} \tag{10.22}$$

$$m_{\mathrm{D,ESP3}} = m_{\mathrm{D,c1,s2}} \tag{10.23}$$

Apart from the extensions presented above, no other modification of the MEBCEM main mass balance is required. The resulting model for calculation of circulating compounds is shown in Figure 10.2.

10.2.3 Mass flow of circulating elements

The mass flow of a circulating component in a flow/position j is calculated:

- ...either by using mass flow data from MEBCEM and concentration data from meal and fuel analyses:

$$\begin{aligned} \dot{m}_{k,i} &= w_{k,j} \dot{m}_i \\ k &\in \{SO_3, K_2O, Na_2O, Cl\} \end{aligned} \tag{10.24}$$

- ...or by applying mass balances:

$$\sum_k \dot{m}_{k,i} = \sum_j \dot{m}_{k,j} \tag{10.25}$$

Here, summation is performed over i inlet flows and j outlet flows. The calculations are not shown in detail here, but can be found elsewhere [18].

[5] However, downstream of the ESP's the dust concentrations are neglected; see the subsection on assumptions and simplifications.

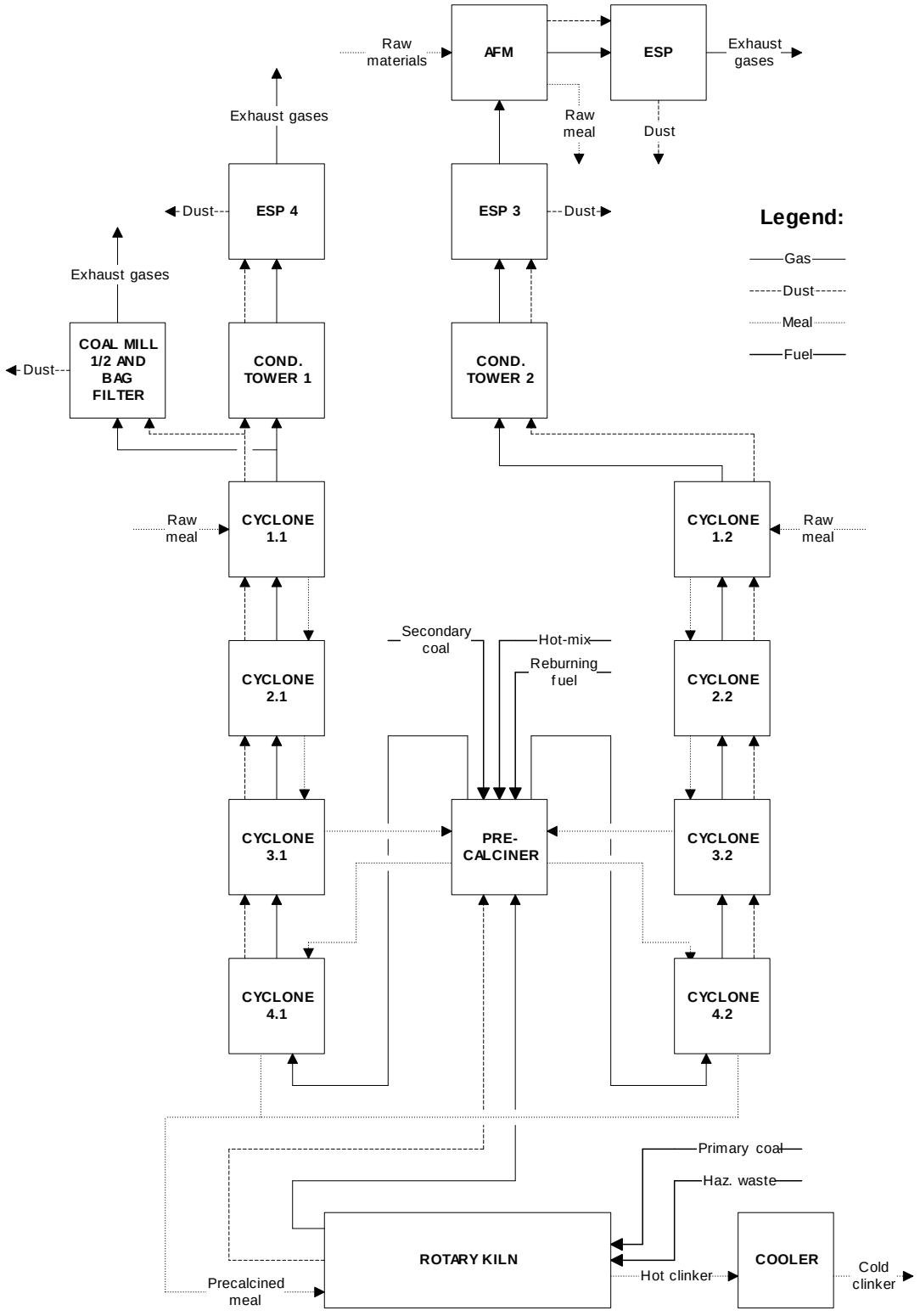

Figure 10.2: Model of the precalciner cement kiln system used for calculating circulating substances.

10.2.4 Total mass imbalance

The total imbalance ε_k and the percentage total imbalance $p_{\varepsilon,k}$ of a circulating component k in the system may be calculated by comparing the calculated total inflow and outflow. Summing over i inflows and j outflows gives:

$$\varepsilon_k \triangleq \sum_i \dot{m}_{k,i} - \sum_j \dot{m}_{k,j} \qquad \forall k \tag{10.26}$$

$$p_{\varepsilon,k} \triangleq \frac{\sum_i \dot{m}_{k,i} - \sum_j \dot{m}_{k,j}}{\sum_i \dot{m}_{k,i}} 100\ \% \qquad \forall k \tag{10.27}$$

$$k \in \{\mathrm{SO_3}, \mathrm{K_2O}, \mathrm{Na_2O}, \mathrm{Cl}\}$$

Errors are introduced both through the use of emission monitoring equipment and through the chemical analyses of the samples, leading to mass imbalances. In addition to these phenomena, the imbalance will depart from zero whenever the process is not at steady state, i.e. when there is (a positive or negative) accumulation of mass inside a reactor unit. Perturbations frequently occur in a cement kiln system; hence, a perfect balance between in- and outflows can never be expected.

10.2.5 Interpolation of data

MEBCEM calculations are based on, and generate, hour (or minute) averaged values. The time vectors pertaining to the samples collected for chemical analysis, on the other hand, in general do not correspond to the MEBCEM time vector. In order to be able to combine MEBCEM data and circulation data, an adequate interpolation procedure has to be developed.

Let $\mathbf{t_M}$ be the MEBCEM time vector, and let $\mathbf{t_S}$ be a sample time vector[6]:

$$\mathbf{t_M} = [t_{M,0}, ..., t_{M,N}] \tag{10.28}$$

$$\mathbf{t_S} = [t_{S,0}, ..., t_n] \tag{10.29}$$

The following condition applies:

$$t_{M,0} \leq t_{S,0} \leq t_{S,n} \leq t_{M,N} \tag{10.30}$$

The corresponding data vectors are:

$$\mathbf{x_M} = [x_M(t_{M,0}), ..., x_M(t_{M,N})] \tag{10.31}$$

$$\mathbf{x_S} = [x_S(t_{S,0}), ..., x_S(t_{S,n})] \tag{10.32}$$

[6] There is one time vector for each sampling position.

Now, the following constraint, which in practice always will be met, is introduced:

$$\dim(\mathbf{t_M}) \geq \dim(\mathbf{t_S}) + 2 \tag{10.33}$$

Each sample time vector is now expanded by by adding a new first element $t_{M,0}$ and a new last element $t_{M,N}$. This gives a new sample time vector:

$$\mathbf{t_{S,new}} = [t_{M,0}, t_{S,0}, ..., t_{S,n}, t_{M,N}] \tag{10.34}$$

The sample vector itself is then expanded accordingly, simply using the values of the adjacent elements:

$$x_S(t_{M,0}) = x_S(t_{S,0}) \tag{10.35}$$
$$x_S(t_{M,N}) = x_S(t_{S,n}) \tag{10.36}$$
$$\mathbf{x_{S,new}} = [x_S(t_{M,0}), x_S(t_{S,0}), ..., x_S(t_{S,n}), x_S(t_{M,N})] \tag{10.37}$$

And it follows that:

$$\dim(\mathbf{x_M}) \geq \dim(\mathbf{x_{S,new}}) \tag{10.38}$$

Now the interpolation can be performed. There is no evident reason for using a complex, e.g. a quadratic, interpolation scheme; hence a linear scheme is chosen. The result of the interpolation is a new sample vector:

$$\mathbf{x_{S,inter}} = [x_{S,inter}(t_{M,0}), x_{S,inter}(t_{M,1}), ..., x_{S,inter}(t_{M,N-1}), x_{S,inter}(t_{M,N})] \tag{10.39}$$

And, because the sample time vector is now identical to the MEBCEM time vector, we have:

$$\dim(\mathbf{x_M}) = \dim(\mathbf{x_{S,inter}}) \tag{10.40}$$

Figure 10.3 shows an example of applying the interpolation procedure on experimental data. Typically, an error of 0–2 % is introduced. In general, the interpolation procedure tends to smoothen the data, i.e. the error is largest when there are rapid changes in the raw data. It should be pointed out that the tails in the first and last part of the curves are due to the inital expansion of the sample data vector. In the analysis of the species circulation phenomena, these parts of the curves are not used; they are only included in the calculations for technical reasons.

10.2.6 Program implementation

The models presented in the preceding sections are implemented in MATLAB® in a program called CIRCCEM. Details of the program structure and the source code of CIRCCEM is not given here, but can be found elsewhere [18]. A brief description is, however, given in Appendix F.

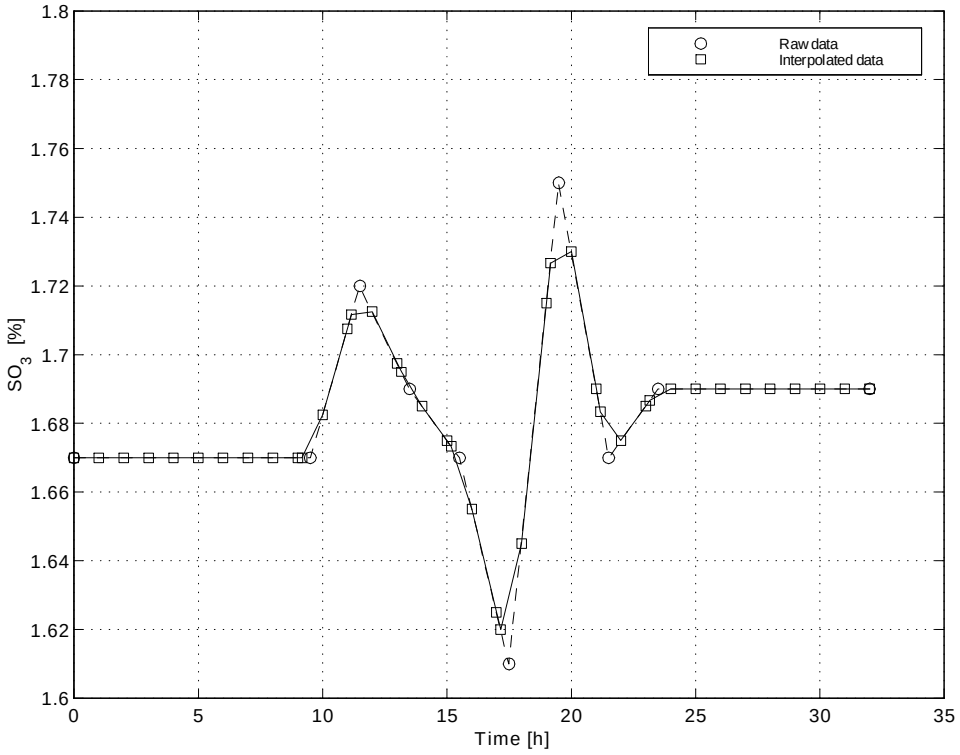

Figure 10.3: Interpolation of experimental data.

10.3 Some calculation results

MEBCEM and CIRCCEM have been used to calculate the internal circulation of S, K, Na and Cl during a full-scale trial on Kiln 6. Here, some results are presented and discussed. More details can be found elsewhere [19].

10.3.1 Meal and dust distribution in the cyclone tower

The distribution of meal and dust in the cyclone tower is shown in Figure 10.4 and 10.5, respectively. (The distribution in string 1 was essentially the same as in string 2. Hence, the flow values of string 1 and 2 were added in order to minimize the number of plots.)

The upper part of Figure 10.4 shows that the raw meal accumulates in the upper part of the cyclone tower; in fact the flow of raw meal leaving cyclone stage 1 is about 20 % higher than the raw meal supply. This is due to the cyclone efficiencies being lower than 100 %, i.e. meal is convected with the gas flow from lower cyclone stages. The large difference between cyclone stage 3 and 4 is due to the calcination reactions occuring in the precalciner. This also explains that the accumulation tendency is reversed for the calcined meal, as can be seen in the lower part of Figure 10.4.

In the upper part of Figure 10.5, the raw meal dust flow is observed to decrease with increasing cyclone stage number. This is due to the calcination reactions in the precalciner and the cyclone efficiencies being lower than 100 %. However, the dust flow out of stage 1 is lower than out of stage 2 and 3. This is due to the high efficiency of stage 1 (95 %) compared to the other stages (80 %).

The lower part of Figure 10.5 shows that the flow of calcined dust increases with increasing cyclone stage number, as could be expected from the cyclone efficiencies and the calcination reactions. The calcined-dust flow out of cyclone stage 1 is very low, due to the high efficiency of this stage.

The total meal flow, i.e. the sum of raw meal and calcined meal, and the total dust flow are shown in Figure 10.6.

10.3.2 Total component imbalances

Figure 10.7–10.10 show the percentage imbalance of S, K, Na and Cl.

The total inflow of S (Figure 10.7) is on average 6.7 % higher than the total outflow. This may be due to a systematic error in the analysis of raw meal or clinker, since the meal and clinker represents the main part of the sulphur flow into and out of the system, respectively. The error in the main mass balance for the meal/clinker is apparently too small to explain the discrepancy. Another reason could be an accumulation of sulphur in the kiln system.

The total outflow of K (Figure 10.8) is about 5 % lower than the total inflow. Again, this may be due to an error in the analysis of raw meal or clinker, since (as was the case

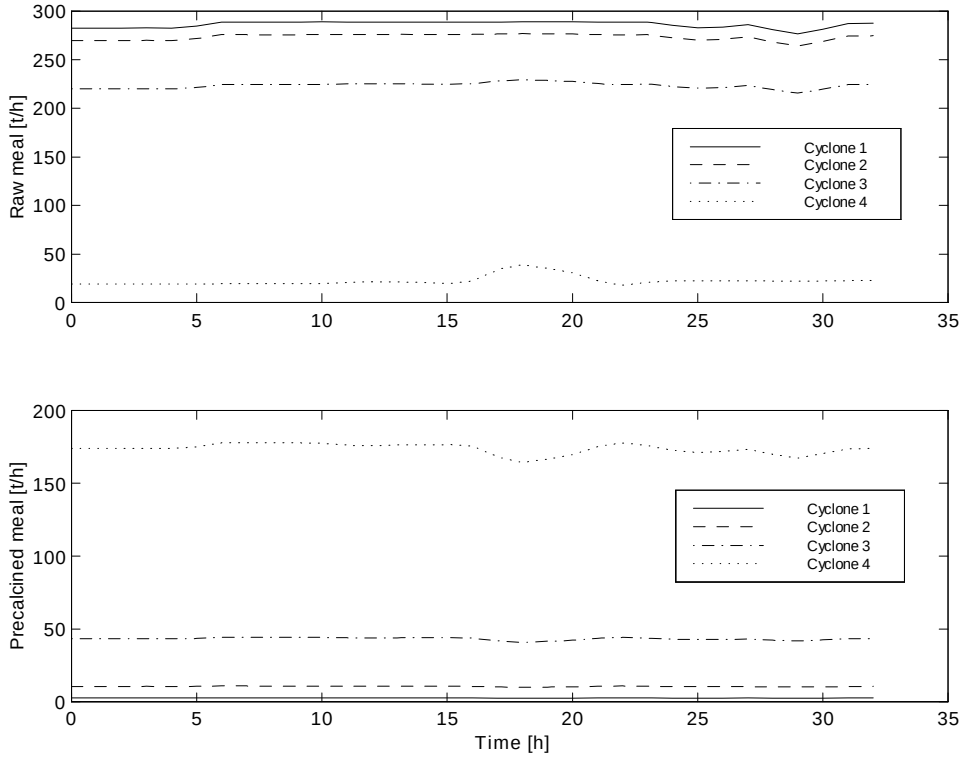

Figure 10.4: Meal distribution in the cyclone tower (string 1 and 2).

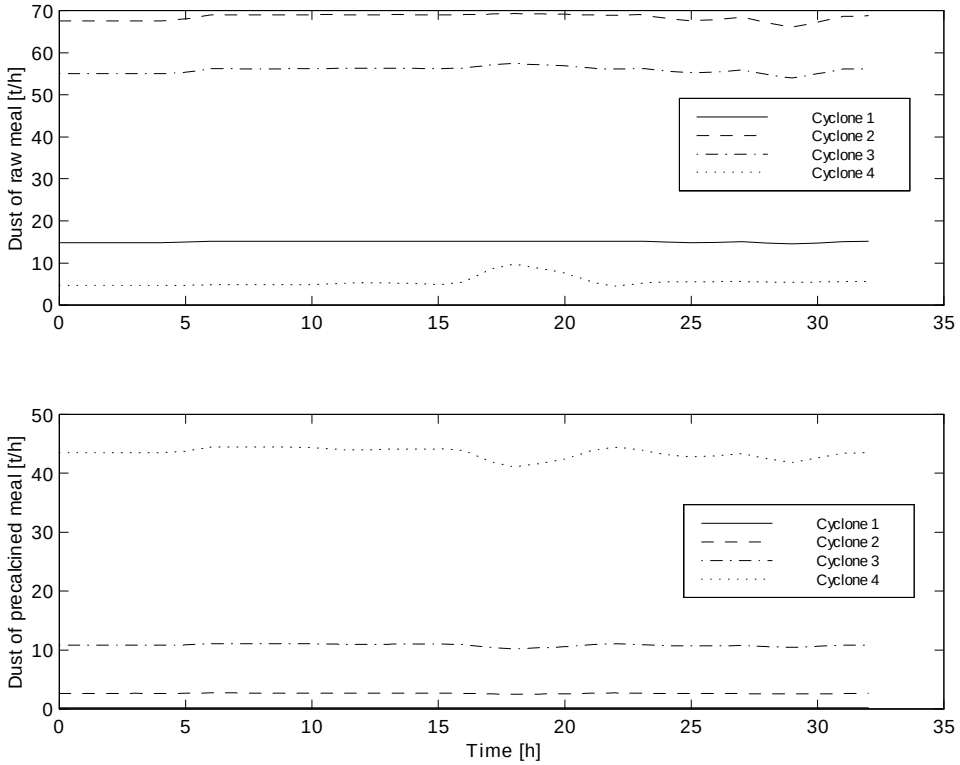

Figure 10.5: Dust distribution in the cyclone tower (string 1 and 2).

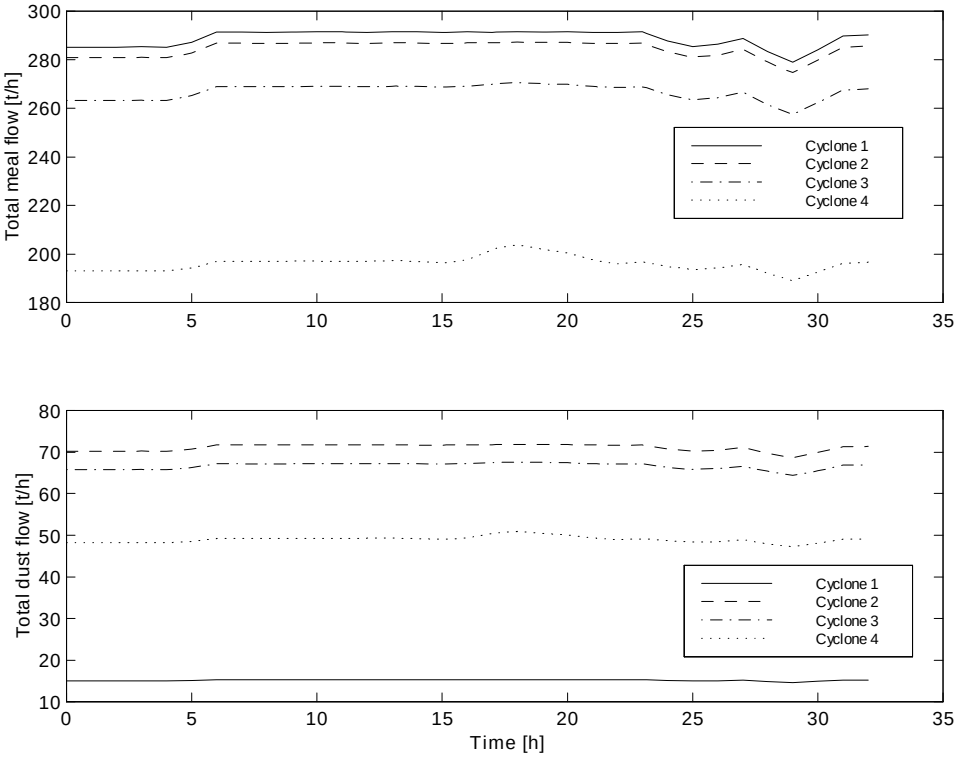

Figure 10.6: Total meal and dust distribution in the cyclone tower (string 1 and 2).

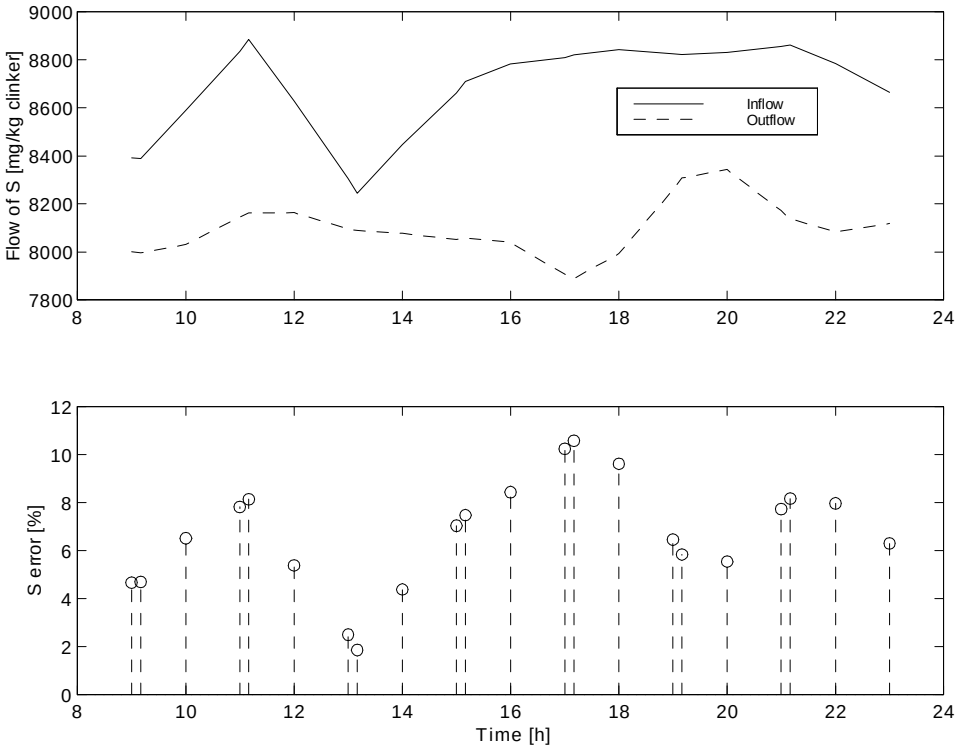

Figure 10.7: Sulphur mass imbalance calculated with MEBCEM/CIRCCEM.

for sulphur) the meal and clinker represents the main part of the potassium flow into and out of the system, respectively. The error in the main mass balance for the meal/clinker is too small to explain the discrepancy.

The mean sodium imbalance (Figure 10.9) is 7.4 %, but the variation is much larger than in the case of sulphur and potassium. This may be due to the fact that lower concentration gives a lower reliability in the analysis results.

Even though the discrepancy between inflow and outflow is significant in the S, K and Na calculations, the imbalance is within acceptable limits, i.e. the results may used for instance in a diagnosis of the kiln system.

When it comes to the Cl imbalance (Figure 10.10), the picture is different, however. It is evident that the chlorine inflow is much lower than the outflow. Furthermore, there seems to be very little correlation between the inflow and outflow. In this case, accumulation of chlorine in the system is a more likely explanation. This will be further addressed in the following section on the internal distribution of circulating substances.

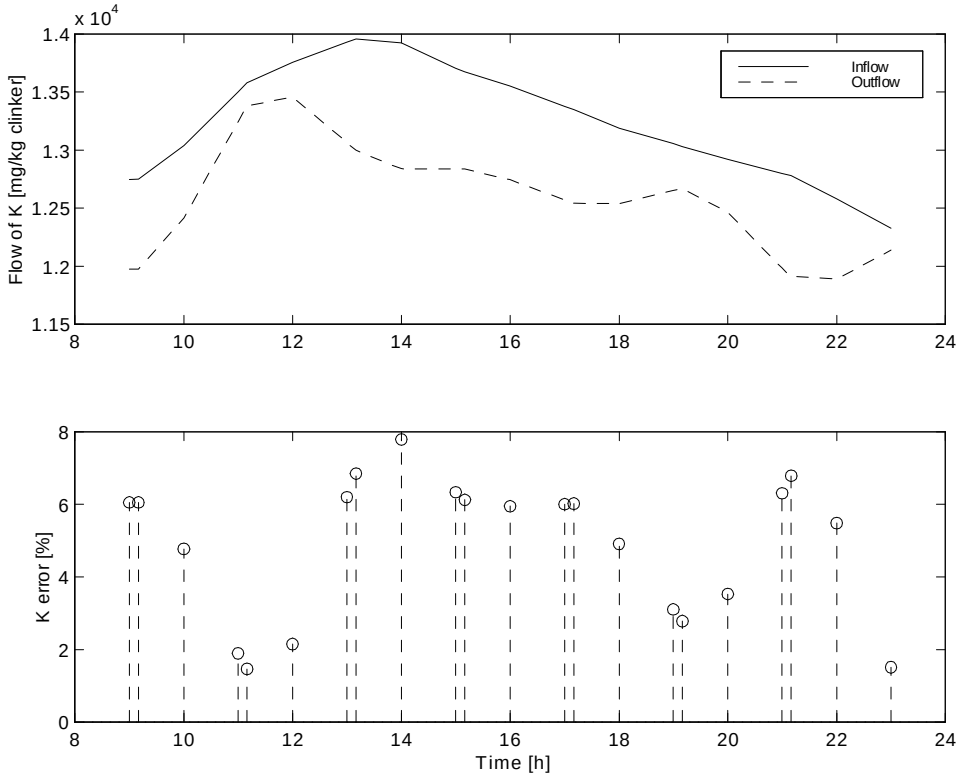

Figure 10.8: Potassium mass imbalance calculated with MEBCEM/CIRCCEM.

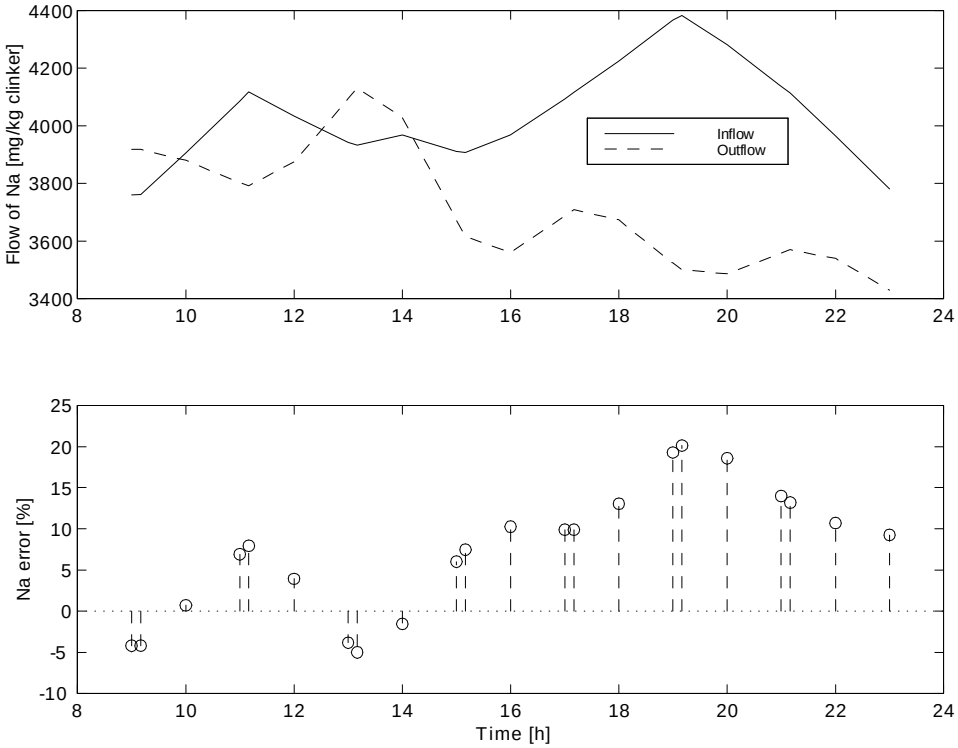

Figure 10.9: Sodium mass imbalance calculated with MEBCEM/CIRCCEM.

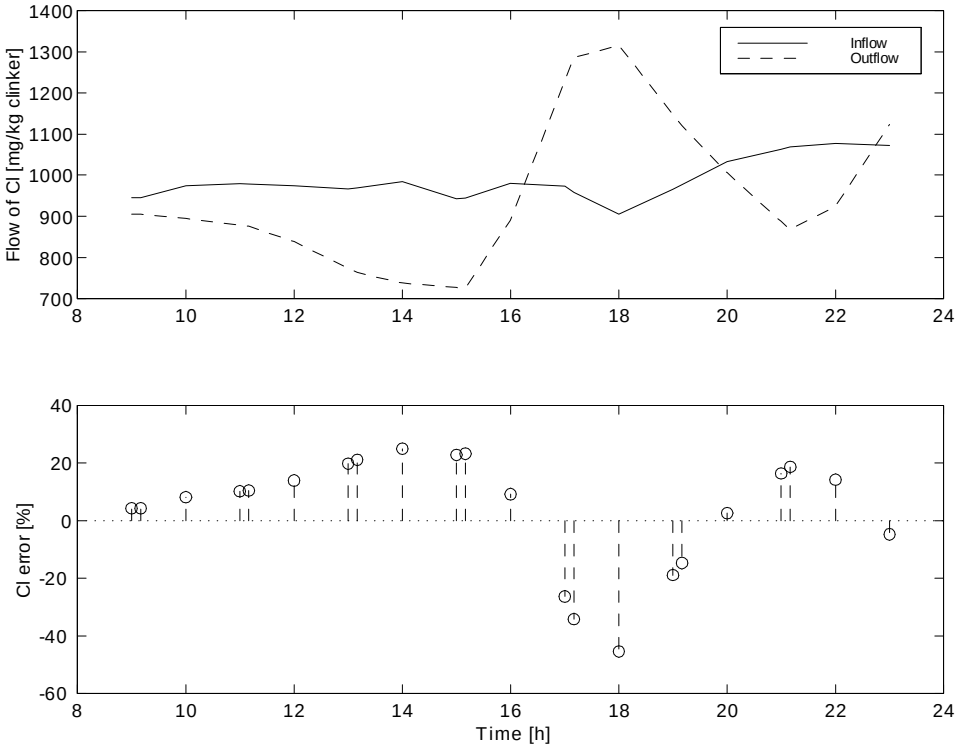

Figure 10.10: Chlorine mass imbalance calculated with MEBCEM/CIRCCEM.

10.3.3 Internal circulation

Figure 10.11–10.18 show the internal distribution of S, K, Na and Cl in the kiln system.

Figure 10.11 reveals that there is a substantial amount of sulphur locally accumulated in the meal in the lower part of the cyclone tower, the flow rate in the lowest stage being about three times the flow rate in the uppermost stage. There are only minor differences between stage 1 and 2, whereas the flow rate in stage 3 is somewhat higher. This is due to the fraction of precalcined meal being higher in this stage, see Figure 10.4. The precalcined meal contains more sulphur than raw meal because SO_2 reacts with CaO and O_2 to produce calcium sulphate in the precalciner.

The fact that the precalcined meal going into the kiln has a much higher S content than the meal leaving cyclone stage 3 (see Figure 10.11), means that the kiln gas carries a large amount of S from the kiln to cyclone stage 4. This can be seen in Figure 10.12, where the S flow in the gas/dust is shown. Furthermore, the gas/dust sulphur flow out of cyclone stage 4 is higher than out of the other cyclone stages. This is not surprising, since the dust from stage 4 is mostly precalcined meal. The high S load in the kiln gas and in the precalciner gas reflects the intensity of the internal sulphur circulation.

Also the potassium curves, see Figure 10.13, shows an accumulative effect in the lower part of the cyclone tower, but the effect is not as pronounced as is the case for the sulphur distribution. An explanation to this is that the intensity of the potassium circulation between the kiln and the precalciner is only about the half of the sulphur circulation. This may be observed in Figure 10.14, where the difference between the K flow in the kiln gas/dust and in the gas/dust from the precalciner is less than the corresponding difference for S, as seen in Figure 10.12.

Looking at the absolute values, the sodium flow inside the system is lower than the potassium flow because of the general lower concentration in the meal. However, as seen in Figure 10.15, the difference between the various cyclone stages is much less than in the potassium case. In fact, there seems to be no significant differences between the stages as far as the Na flow rate in meal is concerned. On the other hand, the concentration of Na in the different stages shows a clear increase as one procedes down the cyclone tower. The explanation to these apparently contradictory phenomena is that the meal flow is higher in the upper stages than in the lower stages, due to the calcination of the meal. In other words, the 'accumulation' of sodium in the lower cyclones, as observed in the meal analysis, is not an accumulation caused by chemical reactions involving sodium, but rather a consequence of the flow pattern in the cyclone tower. Interestingly, this was not the case for potassium, see Figure 10.13.

The upper part of Figure 10.16 shows that the sodium flow in the kiln gas is considerably lower than in the precalciner gas. This means that Na is a less intensively circulating compound than K. The Na flow out of the preheater is low, due to the high efficiency of the upper cyclone stage. This is also seen in the lower part of the figure.

Figure 10.17 shows that the internal flows of chlorine are very large compared to the

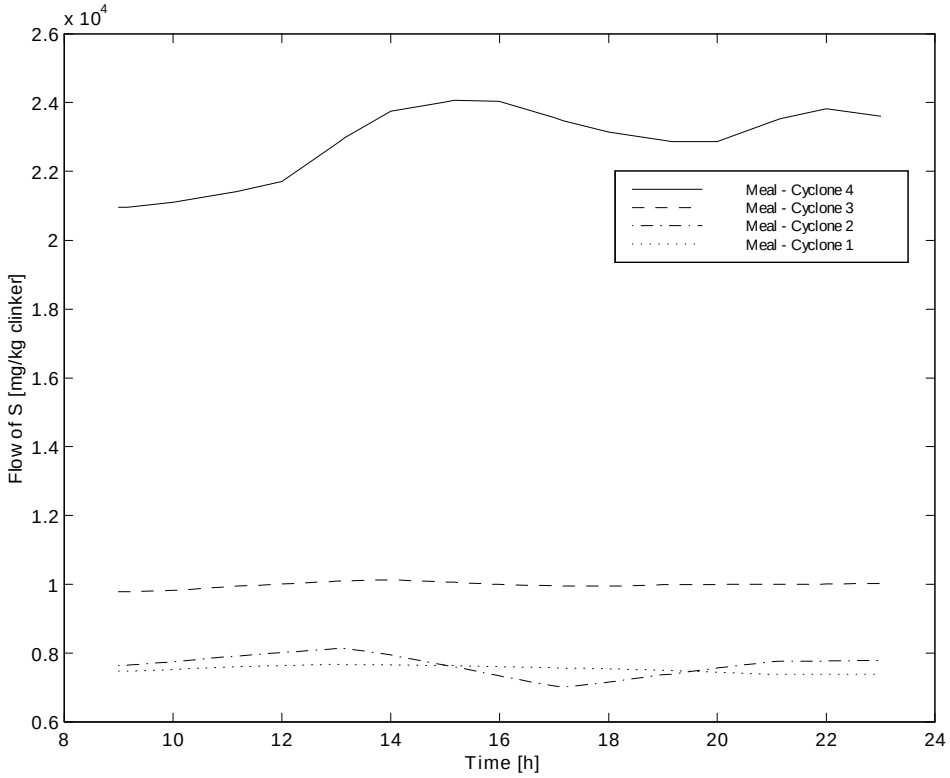

Figure 10.11: Internal distribution of sulphur in the meal.

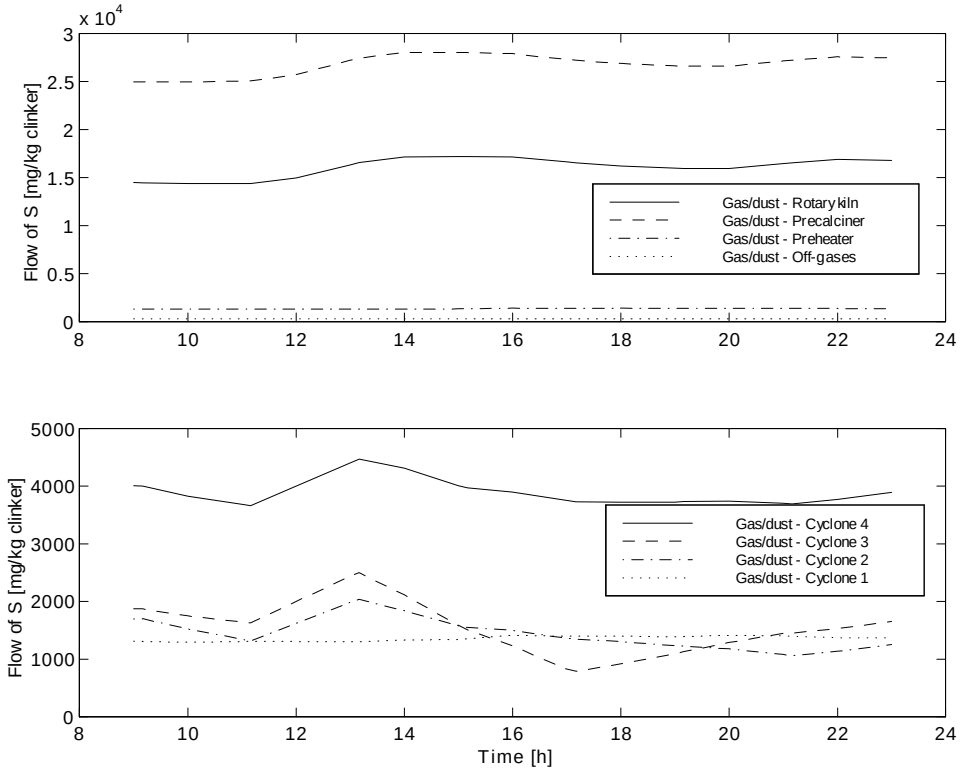

Figure 10.12: Internal distribution of sulphur in the gas/dust.

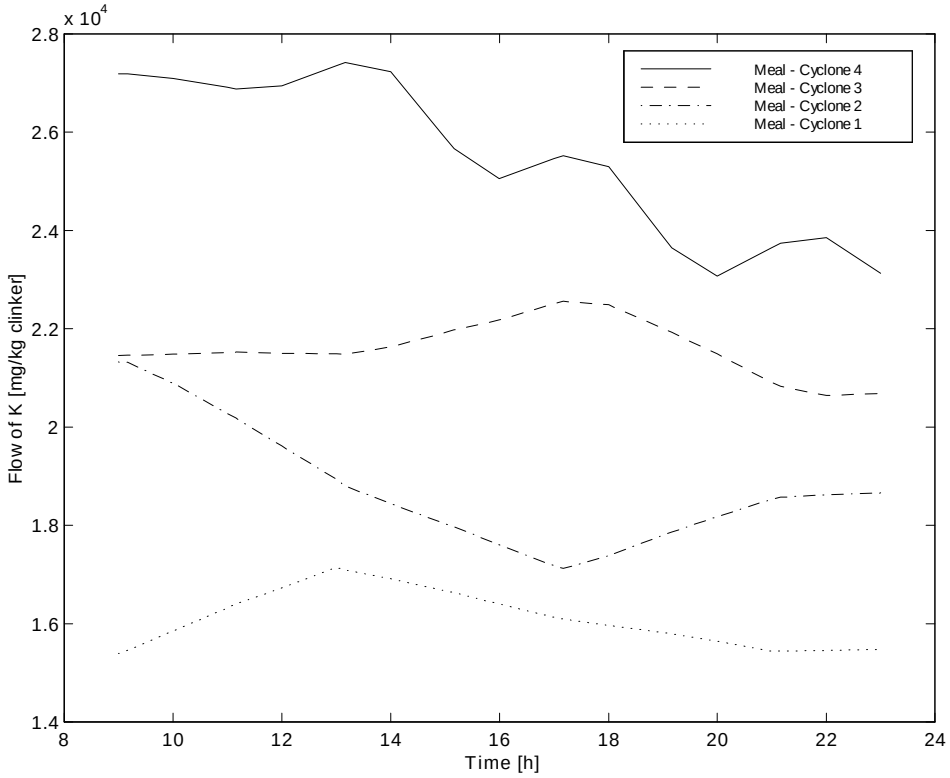

Figure 10.13: Internal distribution of potassium in the meal.

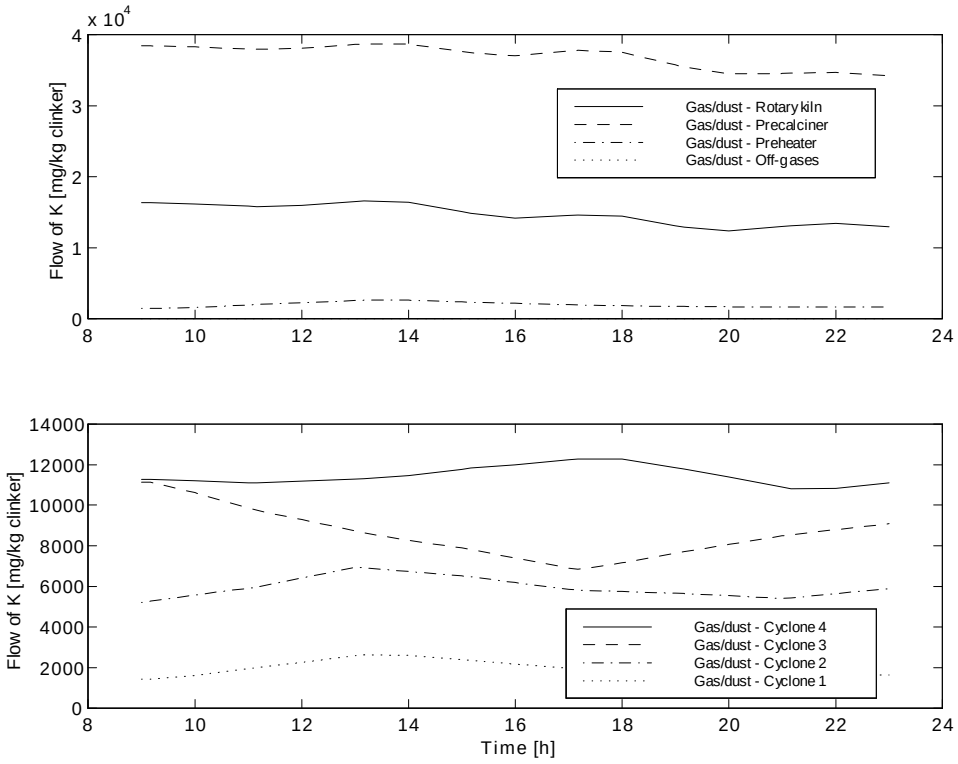

Figure 10.14: Internal distribution of potassium in the gas/dust.

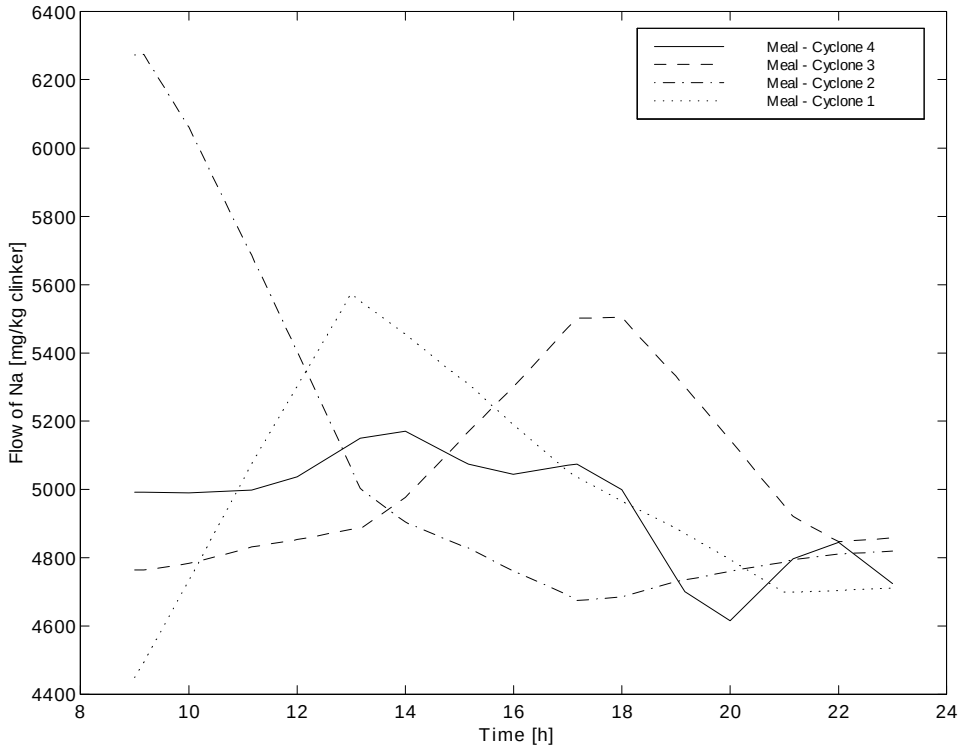

Figure 10.15: Internal distribution of sodium in the meal.

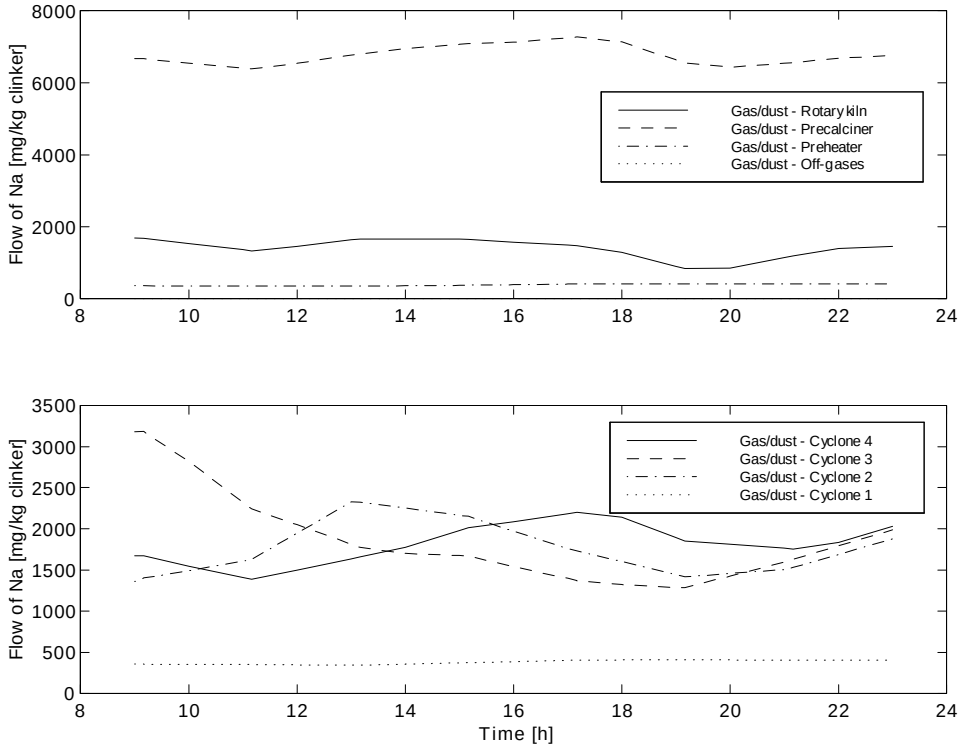

Figure 10.16: Internal distribution of sodium in the gas/dust.

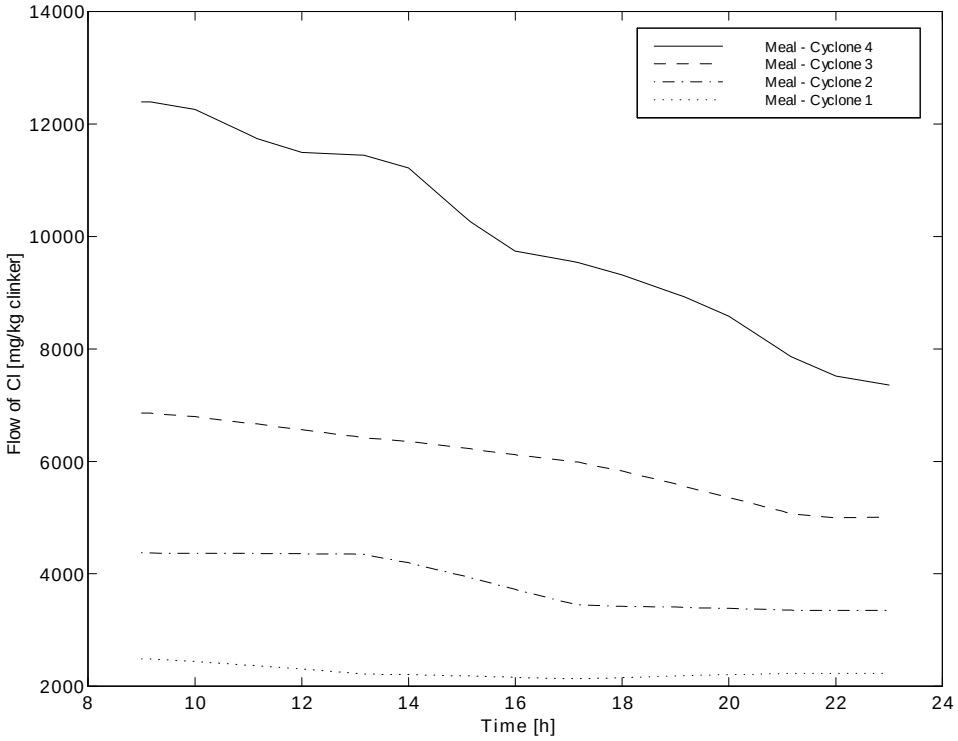

Figure 10.17: Internal distribution of chlorine in the meal.

total inflow (or outflow); for instance, the flow of chlorine in precalcined meal is more than 20 times higher than the total inflow of chlorine. This means that there is a large buffer of chlorine in the kiln system, and that the intensity of the chlorine circulation is very high compared to the other circulating components. Changes in the chlorine buffer — possibly driven by temperature changes — is a dynamic process which will have significant effects on the total chlorine balance. For this reason, it is almost impossible to obtain a balanced chlorine calculation.

Another striking phenomenon is that the meal-chlorine flows out of the cyclones are continously decreasing throughout the trial. This may indicate that the cyclones are in fact being emptied of chlorine. It should be mentioned here, that if the 'chlorine process' is non-steady, then the gas/dust chlorine flows out of the cyclone, shown in Figure 10.18, are too high. This is because these values are calculated assuming steady conditions. If the system is being emptied of chlorine, this is an explanation to why there is such a large discrepancy between total inflow and total outflow of chlorine, as seen in Figure 10.10.

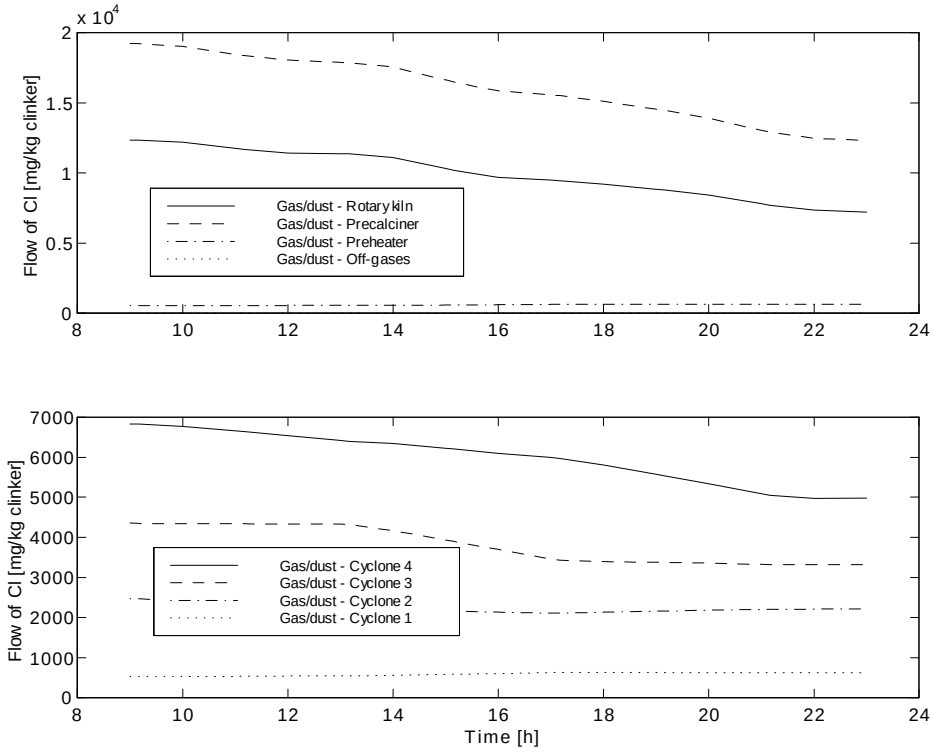

Figure 10.18: Internal distribution of chlorine in the gas/dust.

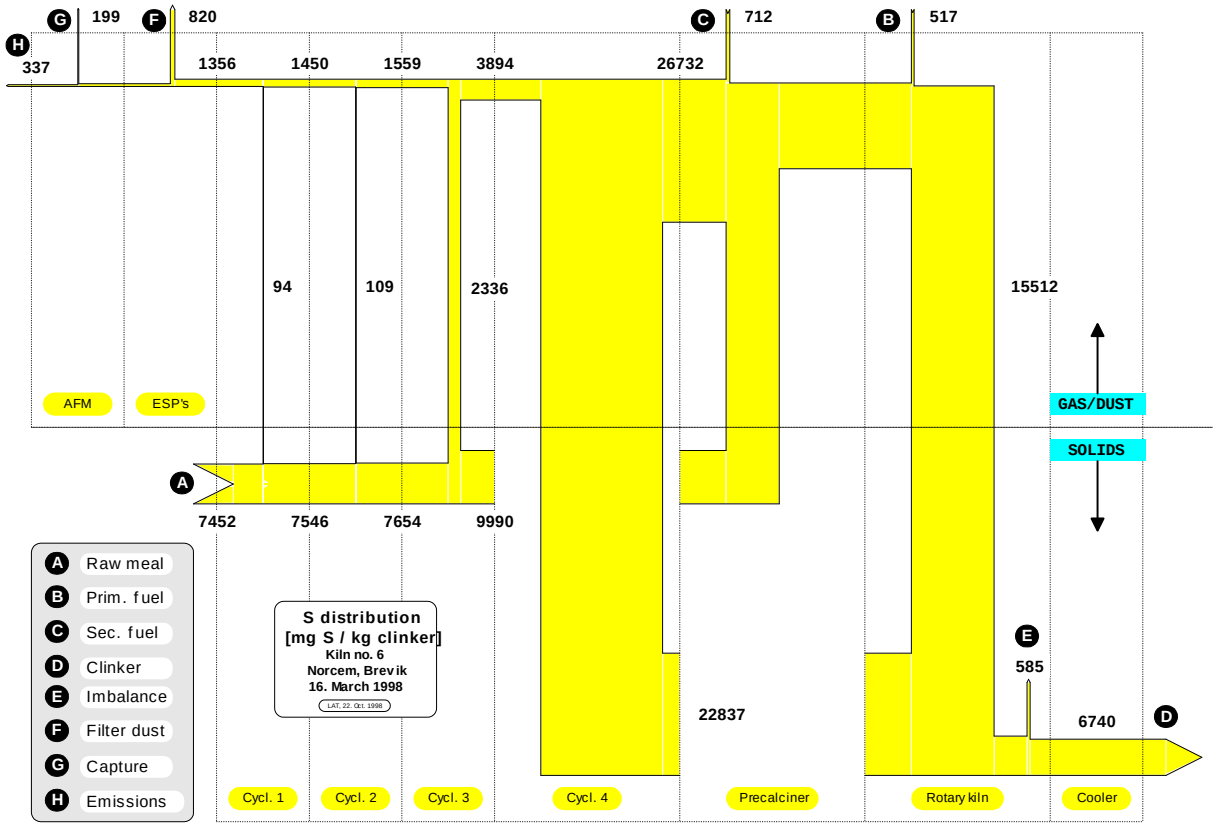

Figure 10.19: Sulphur circulation diagram.

10.4 Material flow diagrams and measures

Flow diagrams of the inflow, outflow and internal flow of the circulating components in the kiln system are given in Figure 10.19–10.22. The diagrams are produced by averaging the data from the full-scale trial presented in the previous section.

Sulphur, alkalies and chlorine circulate with different intensities. Several useful measures describing the circulation can be introduced, making it easier to compare the behaviour of various components in the system.

The *evaporation*[7] *factor* E_k of a given component k is the ratio of the rate of evaporation in the rotary kiln, $m_{k,\text{evap}}$, and the flow rate of this component into the kiln in

[7] 'Evaporation' is a somewhat misleading term, since what happens in the burning zone of the rotary kiln is not only evaporation (e.g. of alkali chlorides), but also decomposition (e.g. of sulphates).

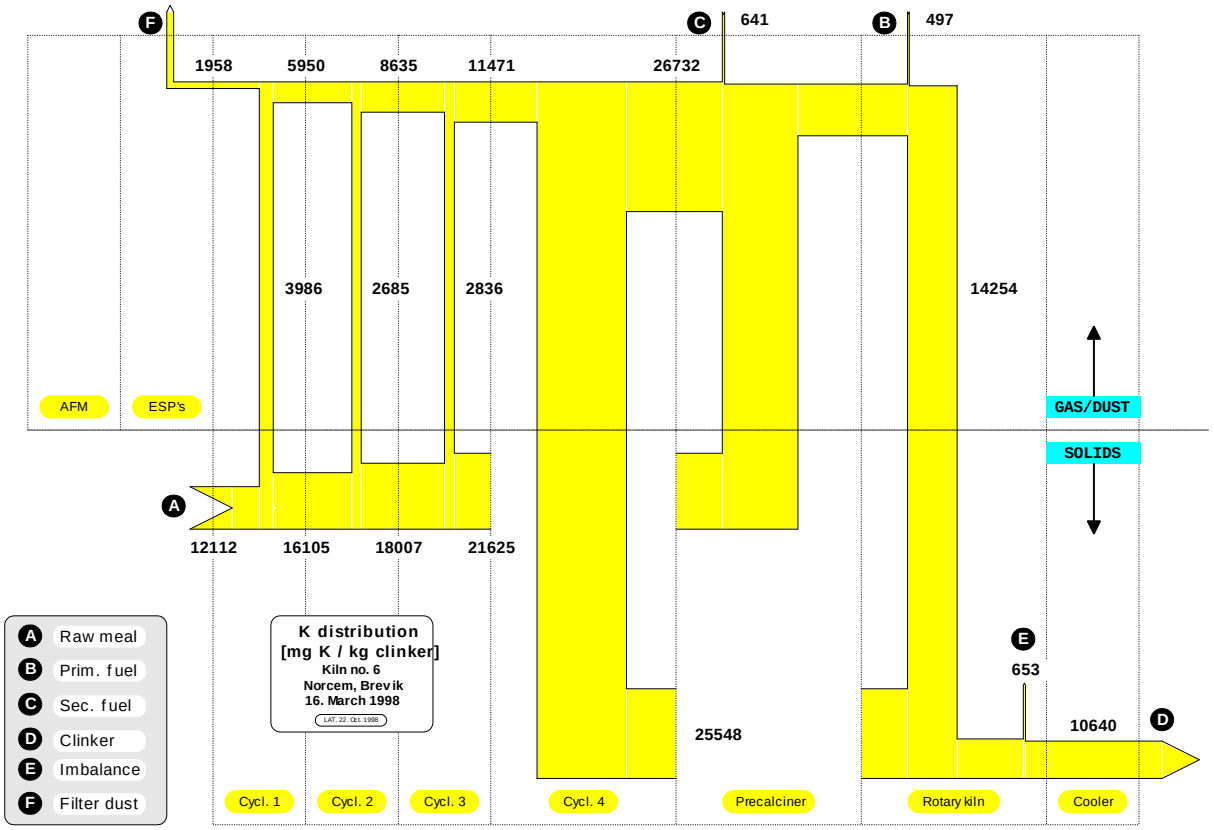

Figure 10.20: Potassium circulation diagram.

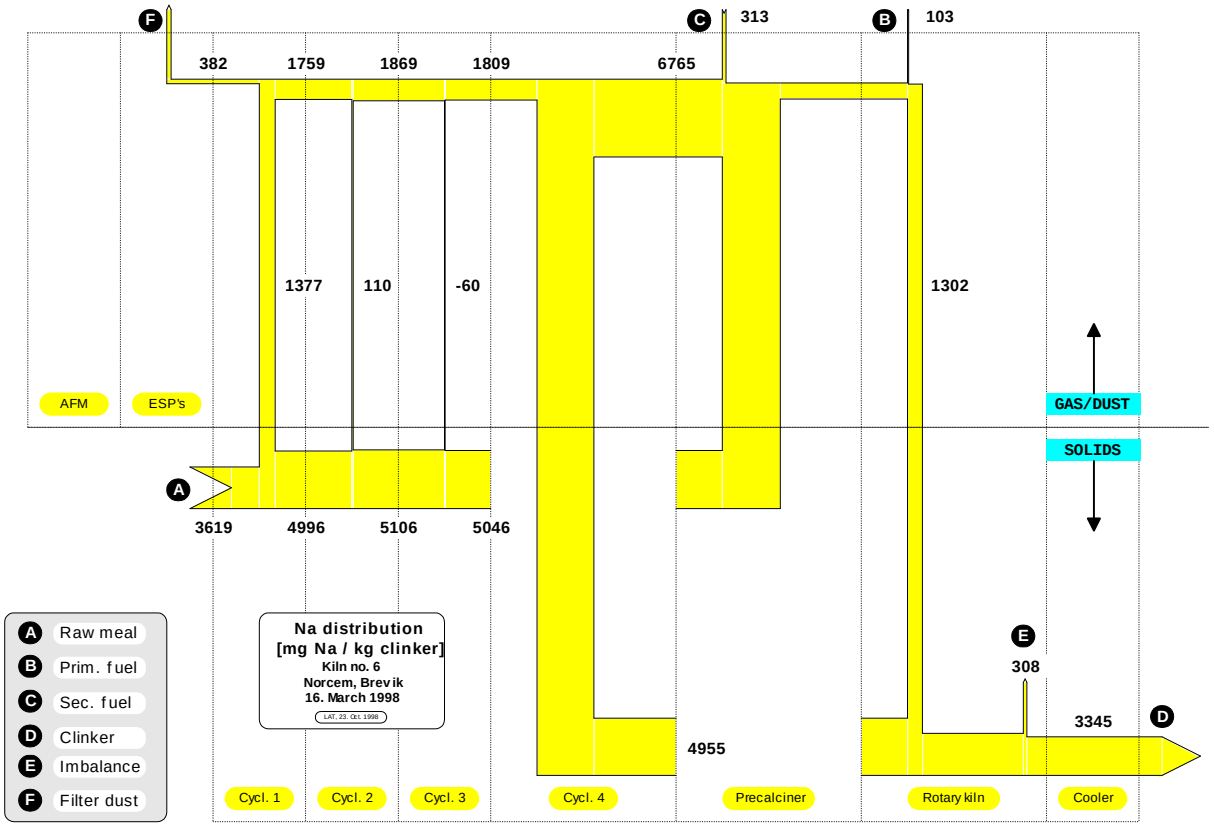

Figure 10.21: Sodium circulation diagram.

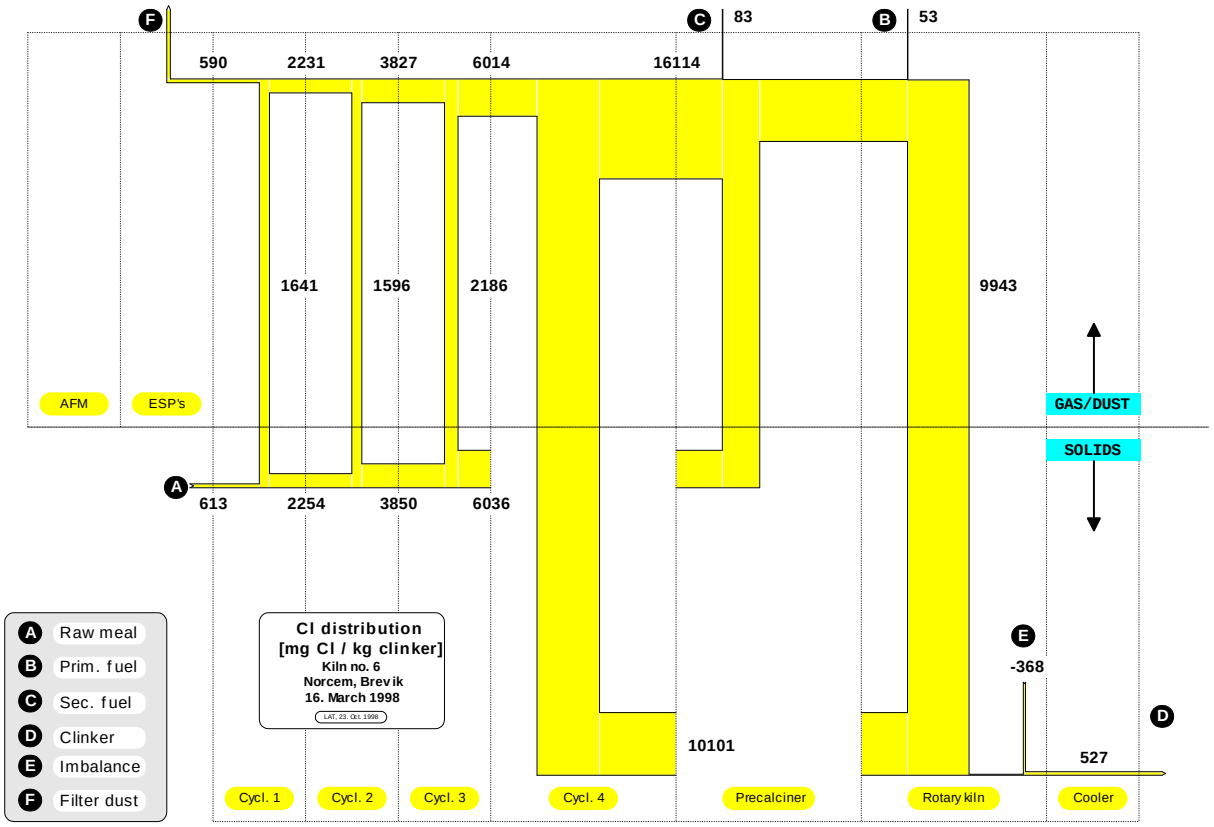

Figure 10.22: Chlorine circulation diagram.

precalcined meal, $m_{k,\mathrm{calc}}$ [156, 157]:

$$\begin{aligned} E_k &\triangleq \frac{\dot{m}_{k,\mathrm{evap}}}{\dot{m}_{k,\mathrm{calc}}} \\ k &\in \{\mathrm{SO_3}, \mathrm{K_2O}, \mathrm{Na_2O}, \mathrm{Cl}\} \end{aligned} \tag{10.41}$$

The *circulation factor* C_k of a given component k is the ratio of the flow rate of this component into the kiln in precalcined meal and the total inflow of the component into the kiln and the precalciner (which is the sum of the inflows along with the primary fuels, $m_{k,\mathrm{prim}}$, the secondary fuels, $m_{k,\mathrm{sec}}$, and the preheated meal, $m_{k,\mathrm{preh}}$) [156]:

$$\begin{aligned} C_k &\triangleq \frac{\dot{m}_{k,\mathrm{calc}}}{\dot{m}_{k,\mathrm{prim}} + \dot{m}_{k,\mathrm{sec}} + \dot{m}_{k,\mathrm{preh}}} \\ k &\in \{\mathrm{SO_3}, \mathrm{K_2O}, \mathrm{Na_2O}, \mathrm{Cl}\} \end{aligned} \tag{10.42}$$

The *residual factor* R_k of a given component k is the ratio of the flow rate of this component in the clinker and the total inflow of the component into the kiln and the precalciner:

$$\begin{aligned} R_k &\triangleq \frac{\dot{m}_{k,\mathrm{cli}}}{\dot{m}_{k,\mathrm{prim}} + \dot{m}_{k,\mathrm{sec}} + \dot{m}_{k,\mathrm{preh}}} \\ k &\in \{\mathrm{SO_3}, \mathrm{K_2O}, \mathrm{Na_2O}, \mathrm{Cl}\} \end{aligned} \tag{10.43}$$

The *cyclone valve factor* $V_{i,k}$ of a given component k can be defined as the ratio of the gas/dust flow of this component out of cyclone stage i and out of the kiln:

$$\begin{aligned} V_{i,k} &\triangleq \frac{\dot{m}_{G/D,i,k}}{\dot{m}_{G/D,\mathrm{ki\,ln},k}} \\ k &\in \{\mathrm{SO_3}, \mathrm{K_2O}, \mathrm{Na_2O}, \mathrm{Cl}\} \\ i &\in \{1, 2, 3, 4\} \end{aligned} \tag{10.44}$$

Table 10.1 and Figure 10.23 show the various circulation measures based on the circulation diagrams in Figure 10.19–10.22. (The imbalances are neglected in the calculations.)

The high intensity of the chlorine circulation, in terms of evaporation rate, is evident. This is also reflected in the low residual factor of chlorine. The sulphur circulation factor is, however, higher than the chlorine circulation factor. The explanation to this is that 60 % of the chlorine flow from the kiln to the precalciner, is in fact passed on to the preheater cyclone stage 3; the corresponding fraction for sulphur is only 24 % (see Figure 10.19 and 10.22). This is due to the thermal stability of sulphates being higher than that of chlorides. Relative to chlorine, sodium is an extreme in the opposite direction; it exhibits the lowest tendency to evaporate in the kiln and to circulate in the system. The general trend of the cyclone valve factors is, as expected, that they increase with increasing cyclone number, see Figure 10.23.

Table 10.1: Evaporation, circulation and residual factors of the circulating components in the kiln system.

Component, k	E_k	C_k	R_k
SO_3	0.68	2.03	0.60
K_2O	0.58	1.12	0.47
Na_2O	0.26	0.91	0.61
Cl	0.98	1.64	0.09

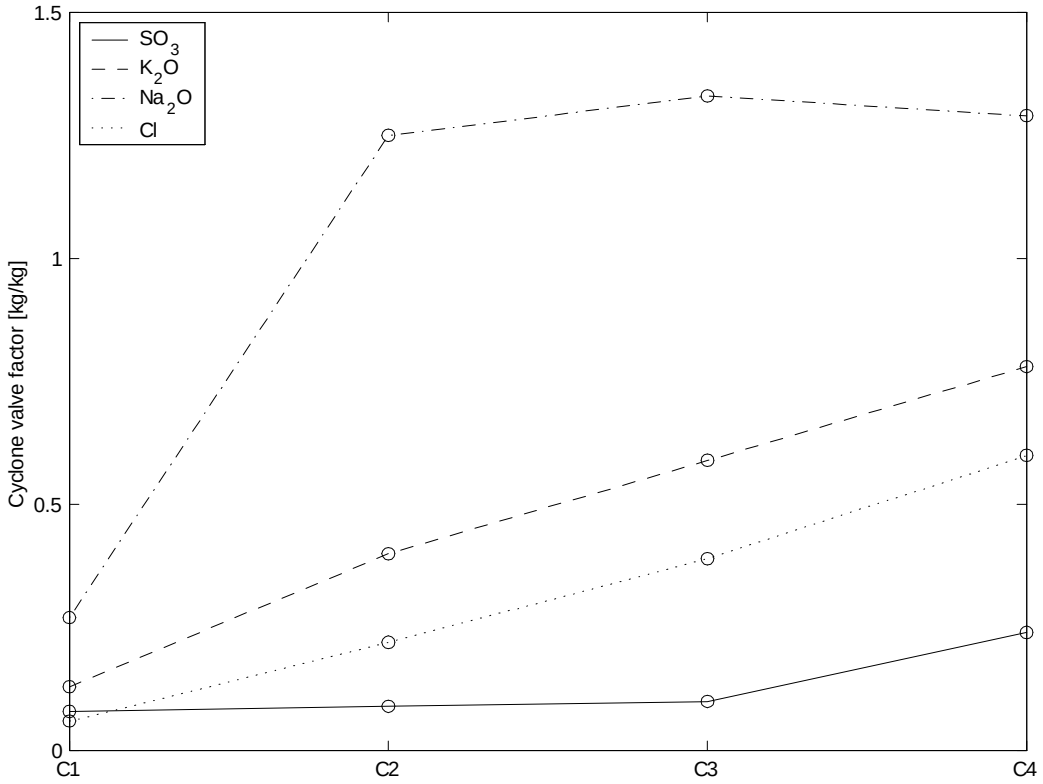

Figure 10.23: Cyclone valve factors for cyclone 1–4.

10.5 Control of the internal material cycles

When the circulation factor is high, the risk of getting problems with buildups in the cyclone tower is also high (see Subsection 3.3.4). It is known from analyses that the deposits have high concentrations of circulating substances. Hence, it is desirable to reduce the intensity of the circulation, i.e. to control the internal material cycles. This is particularly important when staged combustion is to be applied.

10.5.1 Degree of sulphatization

An important parameter describing the potential circulation intensity in the kiln system is the degree of sulphatization of the alkalies in the clinker. This can be defined as:

$$SD_{out} \triangleq \frac{\dot{n}_{\mathrm{SO_3,cli}}}{\dot{n}_{\mathrm{K_2O,cli}} + \dot{n}_{\mathrm{Na_2O,cli}} - 2\dot{n}_{\mathrm{Cl,cli}}} 100\ \% \tag{10.45}$$

Theoretically, when SD_{out} is 100 %, all of the alkalies, except for the part combined with chlorine, are bound as sulphates. First, arcanite (K_2SO_4) is formed, then thenardite (Na_2SO_4) follows, and — if there is still more sulphur in the system — anhydrite ($CaSO_4$) is formed [134]. This means that when $SD_{out} > 100$ %, the sulphur circulation in the system is intensified, because calcium sulphates are more volatile than alkali sulphates. Then an accumulation of sulphur in the tower is to be expected. When $SD_{out} < 100$ %, there is not enough sulphur to balance the alkalies. This means that the alkalies will combine with the clinker minerals, which may deteriorate the clinker quality.

In Kiln 6, SD_{out} varies a lot; sometimes it is as low as 100 %, sometimes it is as high as 130–140 %. This means that the balance between sulphur and alkalies in the kiln system is frequently disturbed, which is disadvantageous for the operation of the kiln. It also means that when the circulation is intense, one should in fact distinguish between two possible reasons: 1) a high degree of sulphatization and 2) a 'short-circuit' of the sulphur cycle initiated by staged combustion at the kiln inlet. It should be possible to counteract the negative impact of the latter by avoiding the former. In other words, if the sulphatization degree of the clinker could be controlled, it would be easier to maintain a stable kiln operation, which is particularly important during staged combustion. SD_{out} is a function of the composition of the in-flowing materials. Hence, the sulphur, alkalies and chlorine in the flows entering the kiln system should be controlled.

Another sulphatization degree, based on the various inflows to the system, can be defined as:

$$SD_{in} \triangleq \frac{\sum\limits_i \left(\dot{n}_{\mathrm{SO_3}}\right)_i - \dot{n}_{\mathrm{SO_3,off-gas}}}{\sum\limits_i \left(\dot{n}_{\mathrm{K_2O}} + \dot{n}_{\mathrm{Na_2O}}\right)_i - \sum\limits_i 2\left(\dot{n}_{\mathrm{Cl}}\right)_i} 100\ \% \tag{10.46}$$

Here, summation is performed over i inlet flows. A basic prerequisite for the validity of this definition is that the gas emissions of alkalies and chlorine are negligible compared to

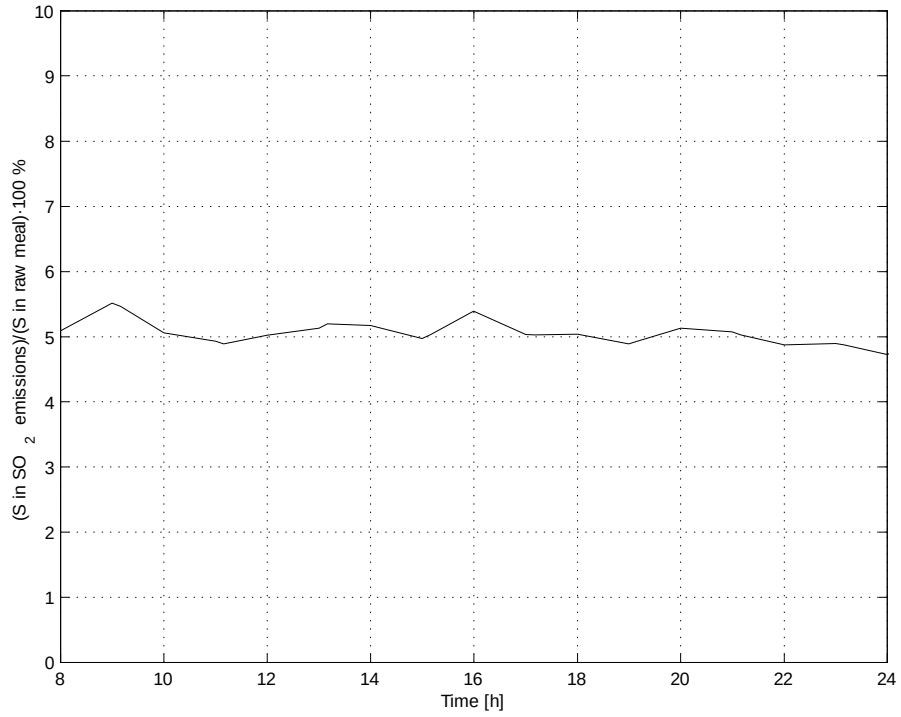

Figure 10.24: Relationship between sulphur in off-gas and sulphur in raw meal.

the corresponding species discharged with the clinker. This assumption should be justified by the reasoning in Section 3.3.

Because the sulphur originating from the various fuels is efficiently trapped by the meal in the precalciner, practically no fuel sulphur is emitted to the surroundings (see Section 3.3) — the SO_2 emissions originate almost entirely from the raw meal; hence:

$$\dot{n}_{\mathrm{SO_3,off-gas}} = f\left(\dot{m}_{\mathrm{SO_3,meal}}\right) \tag{10.47}$$

Figure 10.24 demonstrates a more or less linear relationship between meal SO_3 and SO_2 in the off-gas; and the proportionality constant is about 0.05.

Provided the kiln process is stable, the following relationship results:

$$SD_{in} \approx SD_{out} \tag{10.48}$$

Figure 10.25 shows SD_{in} and SD_{out} based on the data used previously in this chapter. A fairly good agreement between the two is seen. And the more stable the circulation intensity is, the better agreement can be expected. This means that if the sulphatization degree based on the inlet materials can be controlled, it is possible to improve the stability of the kiln operation.

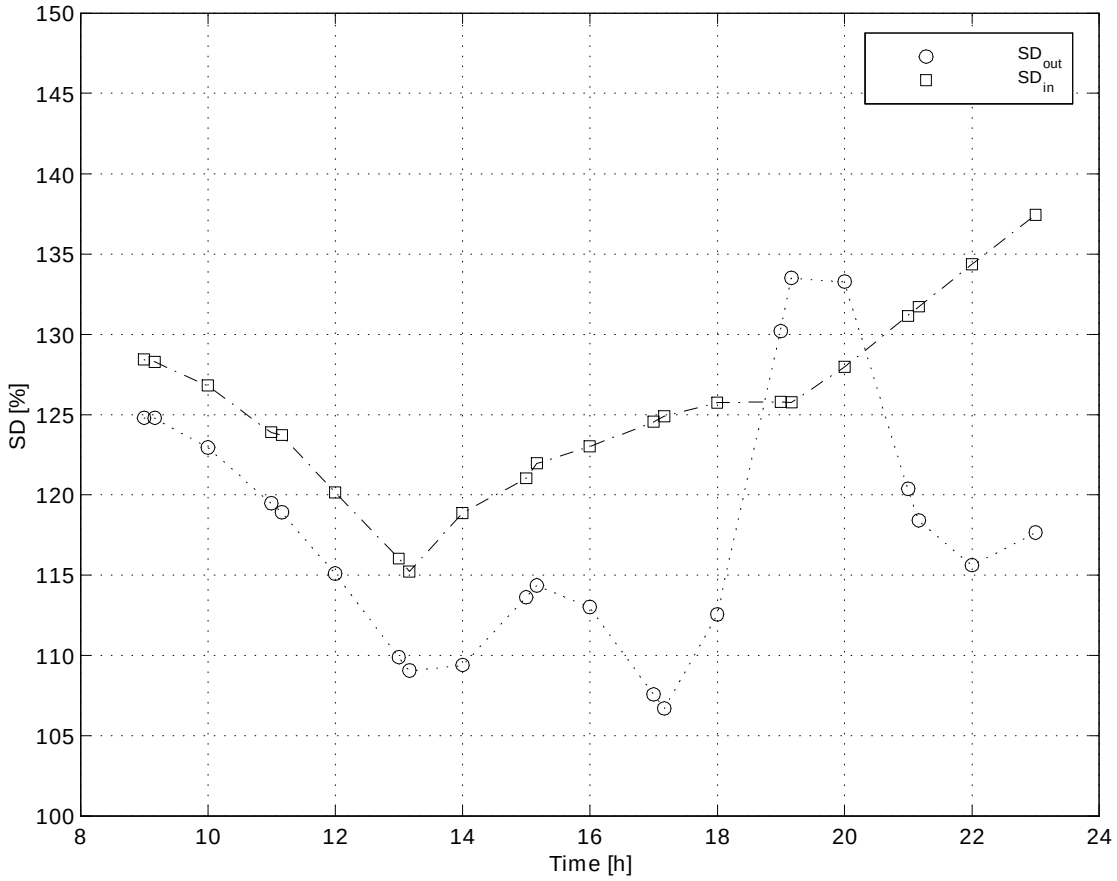

Figure 10.25: Sulphatization degree based on inlet flows, SD_{in}, and clinker, SD_{out}.

As was seen in Chapter 9, there are two main sources of sulphur; the raw meal and the fuels. Since petcoke, which is a high-sulphur fuel compared to coal, is often used in cement plants, it is possible to control the fuel sulphur input to the system by adjusting the petcoke fraction of the total fuel input. (Adjusting the meal sulphur is a more demanding task, but it is certainly possible.) In the next subsection, a procedure is developed for the purpose of optimizing the degree of sulphatization.

10.5.2 Procedure for obtaining the right sulphatization degree

Assume that the main fuel used is a mix of coal and petcoke, and that the following information is available from chemical analyses and from the monitoring system of the plant:

- The inflow of raw meal
- The inflow of all fuels
- The lower heating value of coal and petcoke
- The content (mass fraction) of the circulating components, SO_3, K_2O, Na_2O and Cl, in raw meal
- The content of the circulating components in all fuels
- The current setpoint percentage of petcoke in the coal/PC mix

Based on this information, the following procedure can be constructed:

1. Choose the target sulphatization degree $SD_{in,\text{target}}$.
2. Calculate the coal-mix energy input rate:
$$\dot{H}_{\text{in,coal/PC}} = \hat{H}_{b,\text{coal}}\dot{m}_{\text{coal}} + \hat{H}_{b,\text{PC}}\dot{m}_{\text{PC}} \tag{10.49}$$
3. Calculate the total inflow of the circulating components, k, by summing over all inflows, i:
$$\begin{aligned} \dot{m}_{k,\text{in}} &= \sum_i \dot{m}_{k,\text{in},i} \qquad \forall k \\ k &\in \{\text{K}_2\text{O}, \text{Na}_2\text{O}, \text{Cl}\} \end{aligned} \tag{10.50}$$
4. Calculate the inflow of SO_3 in meal and all fuels, except for the coal/PC mix:
$$\dot{m}_{\text{SO}_3,\text{in,net}} = \sum_{\substack{i\neq\text{coal},\\ i\neq\text{PC}}} \dot{m}_{\text{SO}_3,\text{in},i} \tag{10.51}$$

5. Transform the mass flows into mole flows when necessary:

$$\dot{n}_i = \frac{\dot{m}_i}{M_i} \qquad \forall i \tag{10.52}$$

6. Calculate the SO_3 loss with the off-gas, using Equation 10.47.

7. Calculate the target inflow of SO_3 by setting $SD_{in} = SD_{in,\text{target}}$ and applying Equation 10.46:

$$\dot{n}_{\text{SO}_3,\text{in,target}} = \sum_i \left(\dot{n}_{\text{SO}_3}\right)_i = \frac{SD_{in,\text{target}}}{100\ \%} \left[\sum_i \left(\dot{n}_{\text{K}_2\text{O}} + \dot{n}_{\text{Na}_2\text{O}}\right)_i - \sum_i 2\left(\dot{n}_{\text{Cl}}\right)_i\right] + \dot{n}_{\text{SO}_3,\text{off-gas}} \tag{10.53}$$

8. Transform the mole flow of SO_3 into mass flow by using Equation 10.52.

9. Calculate the target mass flow of SO_3 entering the system with coal/PC:

$$\dot{m}_{\text{SO}_3,\text{coal/PC,target}} = \dot{m}_{\text{SO}_3,\text{in,target}} - \dot{m}_{\text{SO}_3,\text{in,net}} \tag{10.54}$$

10. Calculate the target mass flow of PC and raw coal, respectively:

$$\dot{m}_{\text{PC,target}} = \frac{\dot{m}_{\text{SO}_3,\text{coal/PC,target}} - w_{\text{SO}_3,\text{coal}}\dot{m}_{\text{coal/PC}}}{w_{\text{SO}_3,\text{PC}} - w_{\text{SO}_3,\text{coal}}} \tag{10.55}$$

$$\dot{m}_{\text{coal,target}} = \dot{m}_{\text{coal/PC,initial}} - \dot{m}_{\text{PC,target}} \tag{10.56}$$

11. Calculate the new PC setpoint:

$$SP_{PC}^{\text{new}} = \frac{\dot{m}_{\text{SO}_3,\text{coal/PC,target}}}{\dot{m}_{\text{coal/PC}}} 100\ \% \tag{10.57}$$

12. Calculate the new coal-mix energy input rate:

$$\dot{H}_{\text{in,coal/PC}}^{\text{new}} = \hat{H}_{b,\text{coal}}\dot{m}_{\text{coal,target}} + \hat{H}_{b,\text{PC}}\dot{m}_{\text{PC,target}} \tag{10.58}$$

13. Calculate the new heating value of the coal mix:

$$\hat{H}_{b,\text{coal/PC}} = \frac{\dot{H}_{\text{in,coal/PC}}^{\text{new}}}{\dot{m}_{\text{coal,target}} + \dot{m}_{\text{PC,target}}} \tag{10.59}$$

14. Update the mass flow of the coal mix, satisfying the energy balance:

$$\dot{m}_{\text{coal}}^{\text{new}} = \frac{\dot{H}_{\text{in,coal/PC}}}{\hat{H}_{b,\text{coal/PC}}} \tag{10.60}$$

15. Calculate the error in the coal mix energy input rate:

$$\varepsilon_H = \dot{H}^{\text{new}}_{\text{in,coal/PC}} - \dot{H}_{\text{in,coal/PC}} \tag{10.61}$$

16. If $\varepsilon_H > \varepsilon_H^{\max}$ (where $\varepsilon_H^{\max}$ is some small value), repeat steps 3–5 and steps 7–15.
    If $\varepsilon_H \leq \varepsilon_H^{\max}$, stop.

This procedure has been implemented in MATLAB® and tested on experimental data. The result of the calculation example is shown in Figure 10.26. In this case, the real sulphatization degree (indicated with a dashed line in the figure) was 137 %, which is rather high. The PC setpoint was 20 %. For each value of $SD_{in,\text{target}}$, a new PC setpoint has been calculated. Increasing $SD_{in,\text{target}}$ to 140 % allows an increase in the PC setpoint to about 23 %. However, an SD_{in} value of less than about 120 % is not possible to obtain because then the minimum PC setpoint (0 %) is reached. In accordance with this, the new sulphatization degree, SD_{in}^{new}, is equal to the target value, $SD_{in,\text{target}}$ in the SD_{in} interval from 120 to 140 %. However, below this interval, a lower, constant SD_{in}^{new} value of 120 % is reached.

In this particular case, the starting point was not good. However, in situations where the actual sulphatization degree is low, something which frequently occurs in the present plant, the demonstrated procedure may be used to increase the PC supply, resulting in a more stable kiln system and improved economy of the plant. (In cement works with a low input of raw meal sulphur, this aspect is even more important.)

It is also interesting to investigate the impact of the chlorine mass flow into the system. In this particular case, the liquid hazardous waste contains most of the chlorine fed to the system, whereas solid hazardous waste carries most of the remaining. However, the Cl concentration in LHW and SHW tends to vary a lot. Figure 10.27 shows what happens to the PC setpoint when the Cl content of LHW varies from 0 to 3 %, which is the typical variation interval. (The actual SD_{in} value, indicated by the dashed line, is no longer constant because the chlorine input is varied.) An $SD_{in,\text{target}}$ value of 115 % is chosen, i.e. below the lower limit of 120 % which applied when the LHW contained 2.3 % Cl. It is clear that the target value of the sulphatization degree (115 %) can be reached when the Cl content of the LHW is low (<0.6 %). This demonstrates that the Cl input can be crucial for obtaining a stable kiln system.

Adjustment of the alkali input is the third and last possibility of controlling the sulphatization degree. In cases where the sulphatization degree is high, and at the same time the total input of circulating elements is relatively low, it is possible to reduce the sulphatization degree and hence the circulation intensity by supplying alternative fuels rich in alkalies. (Corrective ingredients rich in alkalies could of course also be used for this purpose.) For instance, bark might be tried out in such a context.

In the calculation procedure outlined above the high sulphur content of PC is utilized to stabilize the kiln. However, the main reason for the fluctuations in the sulphatization

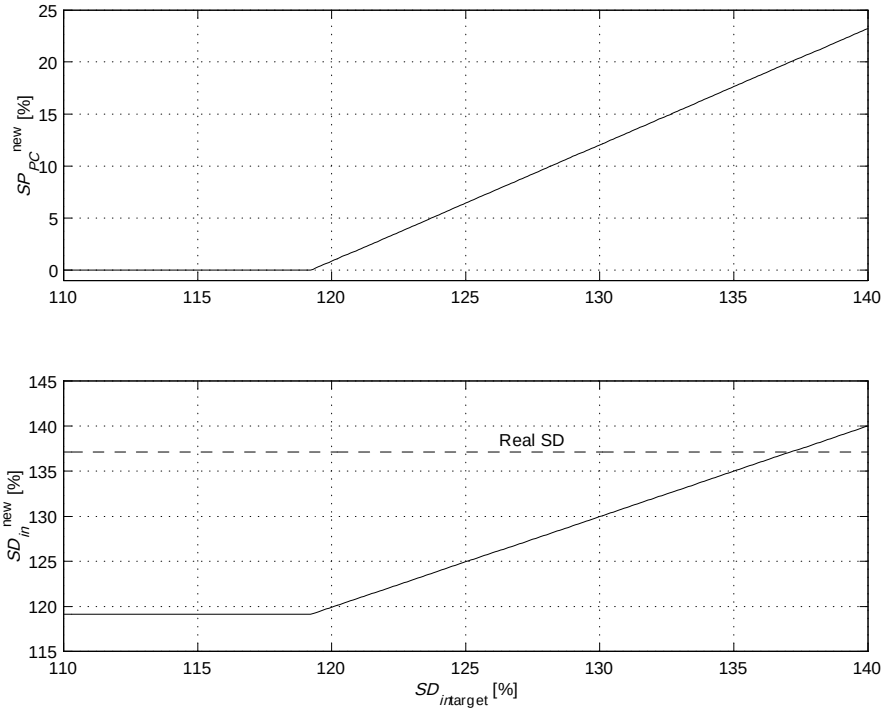

Figure 10.26: Calculation of new setpoint for the petcoke supply as a function sulphatization degreee.

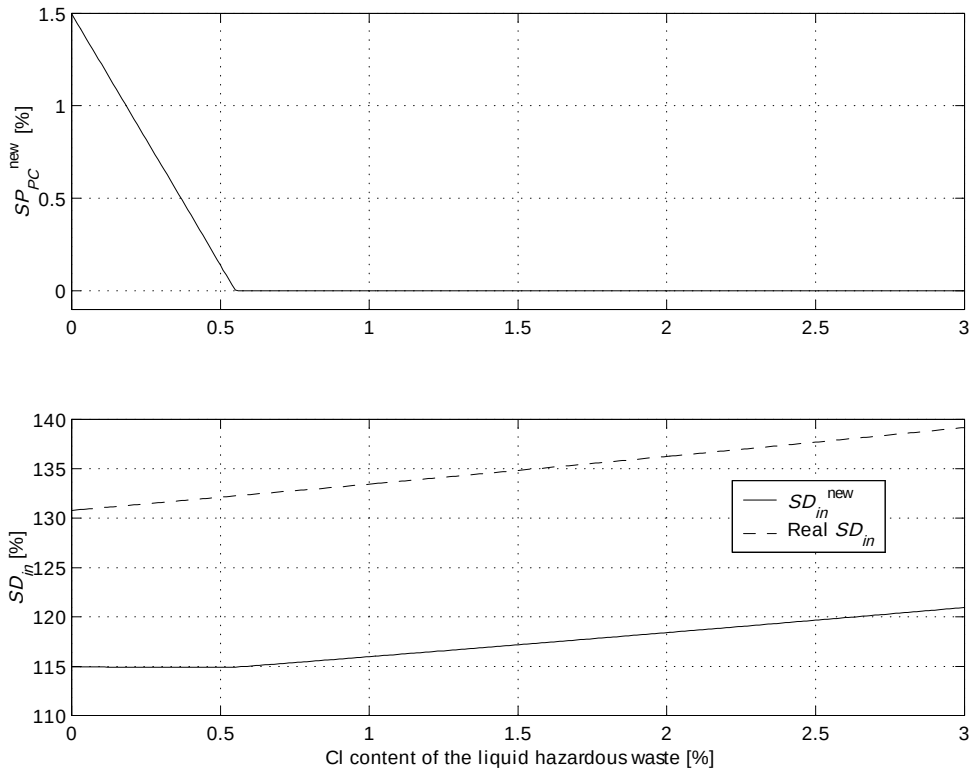

Figure 10.27: Impact of varying chlorine content in LHW on the calculated PC setpoint and the sulphatization degree.

degree is the varying amount of sulphur and alkalies in the raw meal. And it was seen that often it may be impossible to bring the sulphatization degree down to an acceptable level simply by adjusting the PC setpoint. But if the variation in the raw meal composition could be controlled, the SD_{out} fluctuations could be avoided, or at least cut down appreciably. Mortensen *et al.* [156, 157] showed that by constructing a block model for each of the mine sectors involved, they were able to determine the total tonnage and the average quality, i.e. CaO and sulphur content, of the mine sectors. Subsequently, this information was utilized in a system for operational production control of the plant. Thereby, they were able to optimize the use of high sulphur petroleum coke. However, this strategy is more demanding than simply adjusting the PC setpoint.

If the sulphatization degree in a kiln system is very high or very low, increased circulation intensity results. This means that the system is more sensitive to influences induced by for instance supply of reburning fuel at the kiln inlet or in the calciner. Therefore, control of sulphatization degree, and hence the input of circulating species, is crucial when it comes to optimization of staged combustion.

Indirectly the sulphatization degree also affects the NO_x formation in the system because the temperature profile of the kiln is likely to be somewhat dependent on the intensity of the material circulation.

Chapter 11

Full-scale experiments III

In this chapter, a new full-scale trial, feeding whole car tyres at the kiln inlet, is discussed. The purpose of the experiments was to examine the impact of whole car tyres on the process. Because the supply rate was kept low, overall reducing conditions were avoided ($\lambda > 1$). This made it possible to explore the potential of NO_x reduction through lean reburning, a variant of staged combustion discussed in Subsection 3.1.6.

The experiment was conducted in October 1998; key values for the kiln operation are given in Table 11.1.

11.1 Experimental details

11.1.1 Experimental procedure

The feeding system was modified to enable feeding of whole car tyres, i.e. the vertical duct was enlarged, and a horizontal, slightly inclined, tyre feed chute was installed and connected to the vertical duct. Otherwise, the system was identical to the one shown in Figure 9.1.

The tyres were supplied to the feeding chute manually, at a rate of up to 1 t/h. In contrast to Test A–E, this was a long-term test, running over 10 days. Samples of

Table 11.1: Experimental conditions (average values) for Test F.

Parameter	**Unit**	**Test F**
Clinker production	t/d	3133
Total specific fuel consumption	MJ/(kg clinker)	3.4
Degree of calcination in the precalciner	%	95
Fuel fraction in the precalciner	MJ/MJ	0.50
Nominal feed rate of alternative fuel	t/h	1.0

Table 11.2: Characteristics of the fuels used in Test F. (Only the rubber part of the tyre was analyzed; the cord was removed.)

Parameter	**Unit**	**LHW_F**	**SHW_F**	**Rubber**	**$Coal_F$**
Moisture	%	–	–	0.31	1.63
Volatile matter	%	–	–	62.45	29.88
Fixed carbon	%	–	–	32.10	51.86
Ash	%	–	–	5.14	16.58
Sum	%	–	–	100.0	100.0
Lower Heating value	MJ/kg	14.7	17.2	35.8	26.90

precalcined meal were taken every other hour and analysed for SO_3 content and degree of precalcination. Clinker samples were also taken, and analysed for free CaO and SO_3 content.

11.1.2 Fuel analyses

The pulverized coal mix used in the primary and secondary burner during the trials, was a blend of 75–100 % of a bituminuos coal and 0–25 % of a high-sulphur petroleum coke. Accordingly, the sulphur content of the coal mix varied from 0.92 to 1.92 %. Liquid and solid hazardous waste were also used in the trial, as in Test A–E. Fuel analyses of the various fuels are given in Table 11.2. Proximate analyses of solid and liquid hazardous waste were not carried out, since these were believed to give nearly the same values as those given in Table 9.3. For the same reason, ultimate analyses of the various fuels were not carried out.

Car tyre rubber typically contains 95 % hydrocarbons [158, 159, 160], hence only small amounts of oxygen, sulphur, nitrogen, ash and moisture are present. Different manufacturers use different rubber types; natural rubber, styrene-butadiene rubber or polybutadiene rubber are usually the main components. Carbon black is a common additive [161, 152].

11.2 Results and discussion

Table 11.3 lists some of the key figures from Test F. Unfortunately there were several interruptions to the production process during the test period, as can be seen in Figure 11.1. However, these interruptions were not caused by the tyre supply.

As in Test C–E, the NO_x concentration in the kiln inlet was low during the test. Again, by using MEBCEM to calculate the equivalence ratios in the system, it appears that the low NO_x level is due to rather low equivalence ratios in the system, see Table 11.3.

At no time during the trial was there an overall reducing atmosphere in the kiln inlet. Nevertheless, a NO_x reduction of 25 % was achieved. This means that local reducing zones in the kiln must have been formed and reduced the NO_x generated in the primary zone. This demonstrates that lean reburning using car tyres may be an effective means of reducing NO_x emissions. Furthermore, the NO_x reduction seems to be independent of clinker production rate, see Figure 11.2.

With a tyre feeding rate of 1 t/h, the NO_x concentration in the kiln inlet is reduced by 40 %. This is not surprising, since most of the NO_x reduction is accomplished in the rotary kiln, in contrast to what happened in Test A–E. In good agreement with this, Figure 11.3 shows that the NO_x conversion is always negative, which means that there is always a net production of NO_x in the precalciner.

The SO_3 level in the precalcined meal was rather high, about 4 %, before the trial started. This was probably due to the degree of sulphatization (see Subsection 10.5.1) being as high as 110 %. During the tyre supply, the SO_3 concentration grew even higher and reached a maximum level of 6 %, as can be seen in Figure 11.4. This naturally caused problems with deposits in the kiln inlet zone and in the lower part of the tower. The average concentration of SO_3 when tyres were fired at a rate of 1 t/h, was 4.1 %. During tyre supply breaks, the SO_3 level was quickly reduced to an average of about 2.5 %. Hence, it is obvious that the tyres disturbed the internal sulphur cycle in the kiln system, in spite of overall oxidizing conditions. On the other hand, the free-lime level in the clinker was apparently not impacted by the tyre supply; it was below 2 % most of the time.

Figure 11.5 shows that the specific kiln current was reduced by about 10 %, from an average of 1.8 when no tyres were fired to an average of 1.6 A/(t/h) when a feeding rate of 1 t/h was applied. This may be due to an altered temperature profile in the rotary kiln, and is presumably related to the changes in the material cycles.

Table 11.3: Experimental results (average values).

	Unit	**Test F**	
Feed rate of tyres	t/h	0.0	1.0
Secondary coal feed rate	t/h		
Clinker production	t/d	3101	3066
Total specific fuel consumption	MJ/(kg cli)	3.5	3.4
Fuel fraction in the precalciner	MJ/MJ	51.1	48.9
Equivalence ratio, rotary kiln	–	0.70	0.69
Equivalence ratio, reburning chamber	–	0.70	0.79
NO_x content in the kiln inlet	mg/Nm^3	456	272
NO_x content in the stack gas	mg/Nm^3	646	487
NO_x reduction, kiln inlet	%	40	
NO_x reduction, stack	%	25	

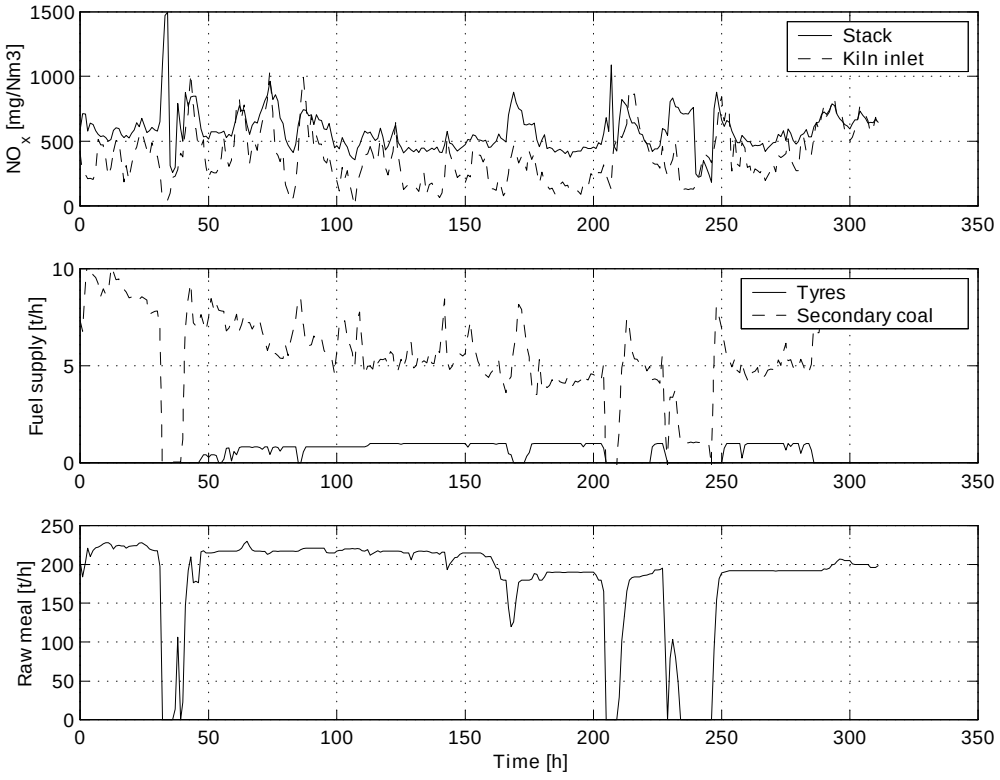

Figure 11.1: NO_x concentration in the kiln inlet and in the stack during supply of secondary coal, tyres and raw meal, Test F.

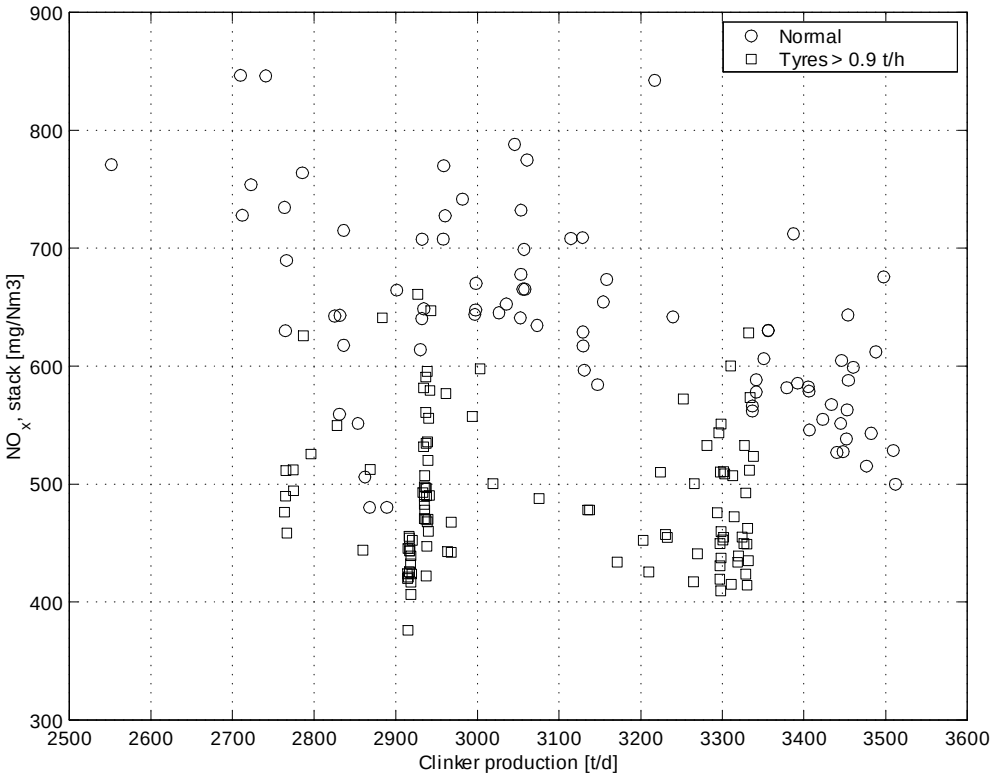

Figure 11.2: NO_x concentration in the stack gas versus clinker production, Test F.

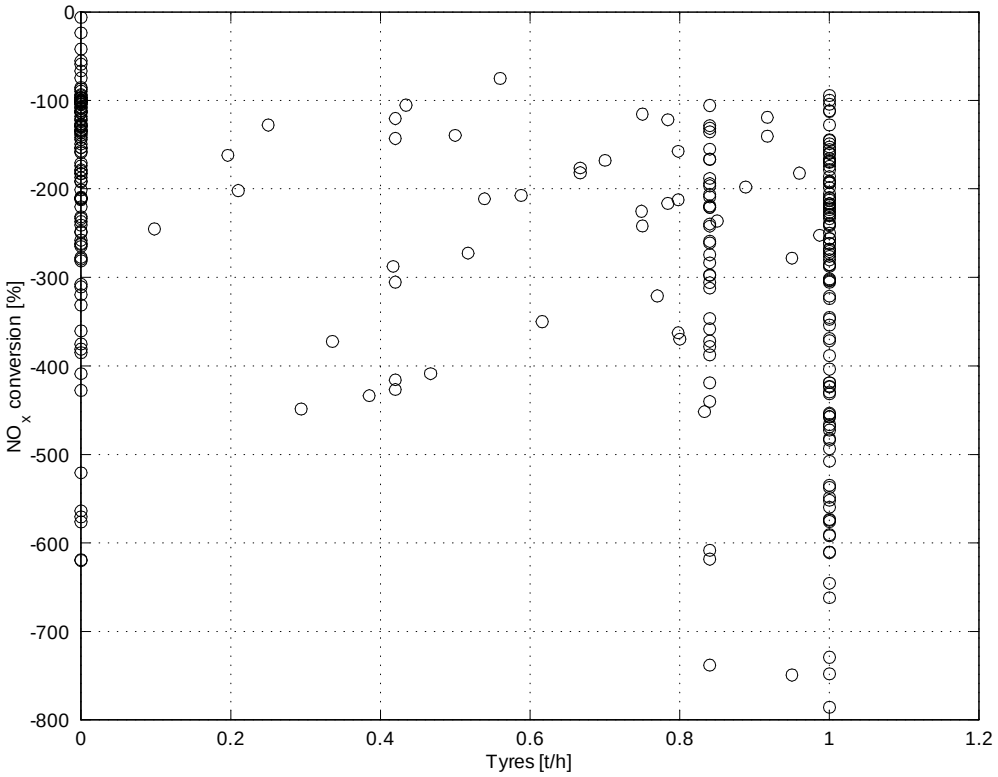

Figure 11.3: Calculated NO_x conversion in the precalciner, Test F.

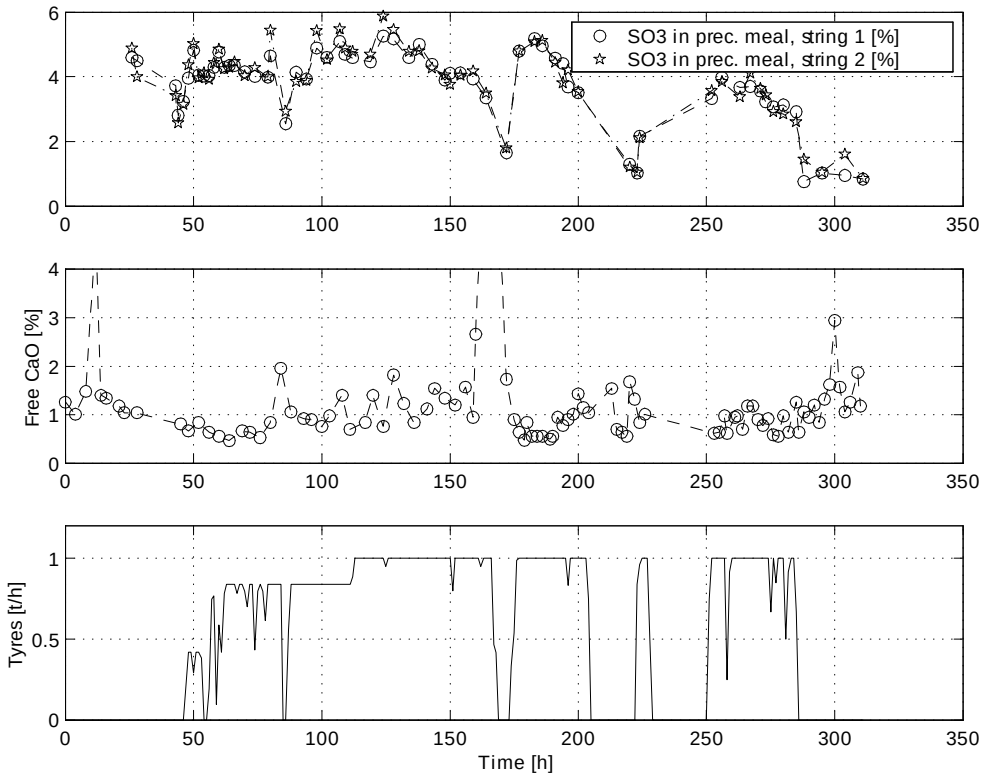

Figure 11.4: Sulphur in precalcined meal and free CaO in clinker, Test F.

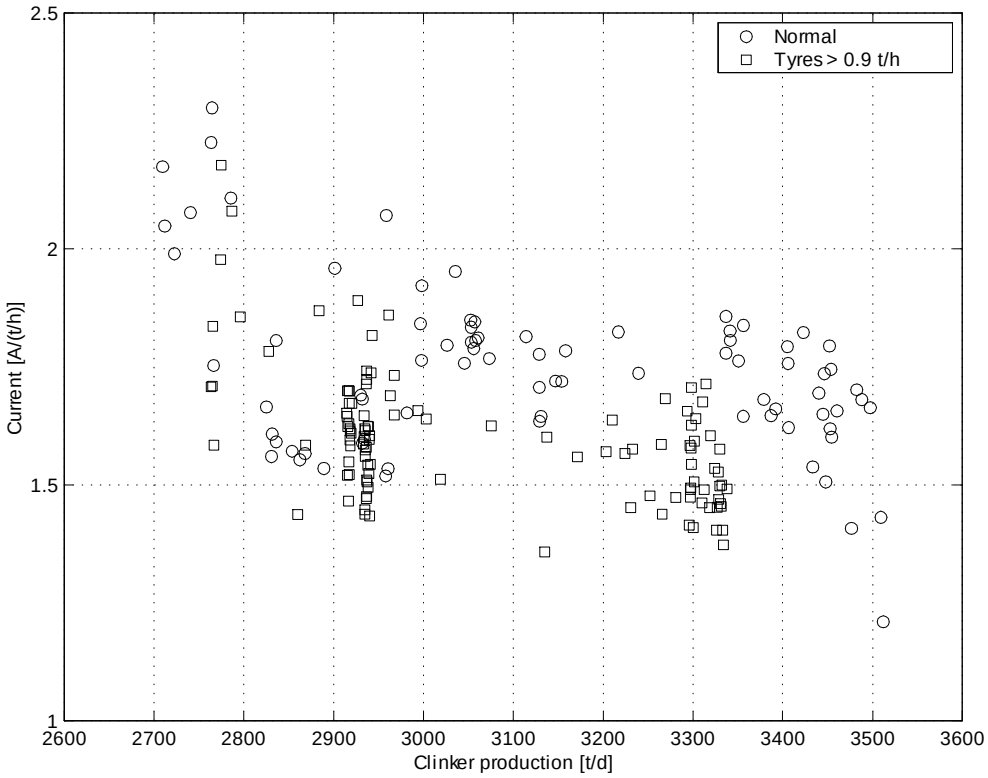

Figure 11.5: Current consumption by kiln rotation as a function of clinker production rate and supply rate of car tyres, Test F.

Chapter 12

Conclusions

12.1 Summary

Cement kilns generate high emissions of NO_x. This is due to the special process conditions prevailing in cement kilns: High gas temperatures, oxidizing conditions and long residence times promote thermal NO_x formation, and the extensive use of nitrogen-containing fuels leads to fuel-NO_x formation. In a cement kiln, staged combustion may be employed by adding fuel to the kiln exhaust gas, either at the kiln inlet or in the precalciner. Through this, a reducing zone is generated, and reduction of the NO_x formed in the primary zone, occurs.

In this work, the relations between staged combustion and the internal material circulation in the kiln system has been in focus. Mathematical modelling has been applied, and full-scale trials on Kiln 6 at the Norcem cement works in Brevik, Norway, have been conducted. The conclusions to be drawn apply to the particular kiln system that has been studied in this work, and hence can not in general be taken as valid for other cement kilns.

The major findings can be stated as follows:

- A mass and energy balance of a precalciner cement kiln system, MEBCEM, has been implemented in MATLAB®, and used as a tool for analysis of the kiln system, planning of experiments and interpretation of experimental data. The mass balance part of the model has been calibrated and validated by means of experimental data, and the prediction abilities can be regarded as satisfactory provided the process is at steady state.

- By using MEBCEM, it is possible to quantify the effect of NO_x reduction measures, of which staged combustion is an example.

- In the literature, thermal NO_x formed in the primary burning zone is claimed to be the major source of NO_x emissions from cement plants. However, in the kiln

that has been studied in this work, the NO_x formation in the precalciner, which is mainly fuel-NO_x formation, dominates over NO_x formed in the rotary kiln. Only at the highest primary NO_x levels are the contributions from the two mechanisms of the same order. This suggests that in some cement kilns, it is appropriate to focus on the NO_x formation in the precalciner, rather than in the main burner, when NO_x reduction measures are to be implemented.

- In this kiln system, the conversion of fuel-nitrogen to NO_x amounts to about 30 %. Apparently, there is no information on this topic in the literature.

- Two full-scale trials supplying plastic waste in the kiln inlet (Test A and B), have been conducted. A NO_x reduction of up to 40 % was achieved when plastic was supplied to the kiln inlet at a rate of 2 t/h, corresponding to about 15 % of the total energy input to the process. This demonstrates the potential of staged combustion. The NO_x reduction is probably due to a combination of homogeneous reactions (reburning reactions involving hydrocarbon radicals), heterogeneous-catalytic reduction (CaO catalysed reduction of NO with CO) and heterogeneous reduction (reduction of NO by solid carbon).

- When solid fuels are supplied at the kiln inlet, the internal material cycles as well as the energy distribution in the kiln system may change. In one of the trials (Test B), an increased SO_3 level in precalcined meal, reduced kiln power consumption and increased free-lime concentration in clinker were experienced. Such disturbances to the kiln operation are unaccaptable and may impede the application of staged combustion.

- A program for thermodynamic equilibrium analysis of the sulphur chemistry at the kiln inlet, SEACEM, has been implemented in MATLAB®. The program has been validated against data published in the literature.

- The SEACEM analysis indicated that close contact between fuel, precalcined meal and kiln gas is highly undesirable, because sulphates tend to decompose under reducing conditions. This leads to an accumulation of sulphur in the precalciner, and subsequently to deposits in the precalciner, in the lower cyclone stages of the preheater tower and in the feed-end housing. Due to the endothermicity of the appurtenant chemical reactions, a transfer of energy from the kiln to the precalciner also takes place when reducing conditions are prevailing. This is equivalent to a net reduction in the energy input to the system, and the consequence is unsufficient "burning" of the clinker, and increased free lime concentrations are seen. In extreme cases, sulphides are formed in the solid material; this is unacceptable for the clinker quality.

- Thermogravimetric analyses of precalcined meal, pulverized coal and car tyres have been carried out. A method to investigate the impact of reducing conditions was developed and successfully applied. The experiments clearly indicated that a reducing atmosphere promoted reactions between fuel fragments and SO_3 in the meal, and thus confirmed the results obtained in full-scale trials and in equilibrium calculations.

- CFD calculations have been conducted with FLUENT®, and laboratory experiments for the determination of entrainment velocity for various alternative fuels have been carried out. Through this, it was demonstrated that, in the kiln system that was studied, contact between fuel, precalcined meal and kiln gas is unavoidable. In accordance with these findings, the feeding-system for alternative fuels was rebuilt, and a new feeding point location, in the kiln riser duct, was chosen.

- In three additional experiments (Test C, D and E) with the new feeding point location — where precalcined meal, reburning fuel and kiln gas was not brought into simultaneous contact — operational impacts were avoided. However, the NO_x reduction efficiency in the plastic trial (Test C) was reduced to about 20 %, probably due to a diminished reburning zone and possibly a decreased heterogeneous-catalytic NO_x reduction. In the trials with RDF (Test D) and biomass (Test E), no significant reduction in NO_x emissions were seen. This was due to limitiations regarding the feeding system: Because of the low bulk density of these fuels, the supply rates were too low to set up reducing conditions in the kiln riser duct.

- In a long-term trial (Test F), running over 10 days, an average NO_x reduction as high as 25 % was achieved with a tyre feeding rate of 1 t/h. In this trial, the global eqivalence ratio was always below 1, i.e. there were always oxidizing conditions in the rotary kiln. Hence, the potential of lean reburning was demonstrated. However, also in this trial the internal sulphur cycle was disturbed, probably due to the locally existing reducing zones in the rotary kiln.

- The fact that lean reburning in the rotary kiln (Test F), but not in the kiln riser duct (Test D and E), efficiently reduced NO_x, may be due to longer residence time under reducing conditions and a higher temperature. However, the effect of heterogeneous-catalytic reduction (which was not present in Test D and E) is also a possible explanation.

- Based on the experimental and theoretical work, a mechanism explaining the phenomena observed in the experiments has been suggested.

- A program for the quantification of internal material cycles in the kiln system, CIRCCEM, has been implemented in MATLAB®. The program combines outputs from MEBCEM with meal and gas sample analyses to calculate the circulation of

sulphur, sodium, potassium and chlorine. For S, K and Na, the balance errors were about 7, 5 and 7 %, respecively, which is considered as good results. The Cl imbalance, however, was much larger. The very intense circulation of chlorine explains why it is difficult to obtain a material balance for chlorine in a cement kiln system.

- It is of great importance to be able to control the internal material circulation. In this context, a sulphatization degree based on incoming materials has been defined. This number should be about 100 % in order to minimize the intensity of the internal material cycles. When the process runs at steady state, the sulphatization degree based on incoming materials should equal the sulphatization degree based on the clinker product. If this is true, the former may be used to control the latter. A quite good correlation between the two measures has been demonstrated.

- It has also been shown that the chlorine supply to the system may have a considerable impact on the value of the sulphatization degree. Hence, the chlorine contribution should in general not be neglected when the sulphatization degree is calculated.

- A procedure for optimizing the sulphatization degree has been developed. In this procedure, the supply of petcoke, which contains a considerable part of the incoming sulphur, is adjusted to meet some specified sulphatization degree requirement. Application of the procedure may reduce negative impacts of staged combustion, because the intensity of the internal material cycles is reduced.

12.2 Main conclusions

The questions asked in the problem statement, given in Section 1.2, can now be answered:

1. What characterizes the operational disturbances?

   When fuels are supplied at the kiln inlet, the concentration of sulphates in the precalcined meal increases, the free-lime concentration in the clinker tends to increase and there is an increased tendency of build-ups in the precalciner and in the kiln inlet. Furthermore, the power consumption of the kiln is often seen to decrease, and the secondary fuel supply is sometimes reduced.

2. Why do the operational impacts occur?

   Supply of fuel at the kiln inlet leads to reducing conditions. This promotes the decomposition of sulphates in the precalcined meal, and impedes capture of gaseous sulphur oxides by the meal. Hence, sulphur is transported by the kiln gas from the kiln to the precalciner, where sulphur dioxide is converted to sulphate under

oxidizing conditions and returned to the kiln. The increased level of sulphates in the precalciner leads to deposit formation. Because decomposition of sulphates is an endothermic process, the altered sulphur circulation also implies a transfer of energy from the solids in the rotary kiln to the precalciner. Accordingly — since the secondary coal is automatically controlled by the calciner temperature — the secondary coal supply is reduced. Reduced solids temperature in the kiln, caused by the energy transfer, impedes the burning of the clinker, and the concentration of free lime in the clinker increases. A reduced solids temperature may also result in a lower melt fraction, so that the tendency of the meal sticking to the kiln wall is reduced, and thus the kiln torque is reduced, which is equivalent to a lower kiln power consumption.

3. How can the disturbances be minimized?

   Disturbances to the process during supply of reburning fuels are reduced by avoiding contact between precalcined meal, fuel and kiln gas. This may be done by moving the fuel feeding point to an appropriate location, a strategy that has been demonstrated in this work. Another possibility, which has not been tried out in the present work, is to gasify the solid fuels in an external reactor and then introduce the product gas at the kiln inlet. Moreover, keeping the sulphatization degree at a value of about 100 % will reduce the intensity of the material circulation and hence reduce the disturbance of the kiln process.

The main conclusion is that, by selecting fuels with appropriate characteristics and choosing a favourable feeding position, NO_x reduction by staged combustion in this type of kiln system, is indeed possible. However, for kilns with a distribution of circulating species comparable to that of Kiln 6, solid fuel supply to the kiln inlet can not be advocated, since this inevitably introduces operational disturbances. Instead, the feeding-point should be located so as to provide minimal contact between fuel and precalcined meal. This solution lowers the NO_x reduction efficiency, but operational disturbances are minimized.

12.3 Further work

In the present work, three computer programs were written, serving as tools for investigating the impact of staged combustion on the production process. Further development and utilization of these programs is required. Some more experimental and theoretical work is also desirable. The following is a list of tasks that are on the agenda:

- Several of the models in MEBCEM should be put on-line to provide support for the kiln operators. Examples of important properties that should be calculated are tertiary air flow, secondary air flow, various equivalence ratios and various thermal efficiencies.

- The energy balance part of MEBCEM should be calibrated and validated.
- MEBCEM and CIRCCEM are codes adapted to the Kiln 6 process at the Brevik works. Some modifications would allow other kiln systems to be analyzed as well.
- CIRCCEM calculates the distribution of S, K, Na and Cl. Some minor modifications to the program would enable the calculation of other components as well. For instance, the distribution of mercury (Hg), which is a rather volatile metal that is partly emitted to the surroundings, would be possible to calculate using a slightly modified version of CIRCCEM.
- The petcoke optimization procedure should be put on-line to provide operator support.
- Advanced reburning, using for instance refuse derived fuel in combination with urea prills, should be tried out. More strict NO_x regulations are to be expected in the near future, and advanced reburning may be an interesting alternative or supplement to other NO_x reduction measures in the cement kiln system.
- Supplying large amounts of alternative fuels to the precalciner — particularly when solid fuels are fed to the kiln side and the tertiary air side of the precalciner simultaneously — may give rise to burnout problems, indicated by increased CO emissions. There is also a risk of generating high temperatures locally, possibly damaging the kiln lining, especially when plastic fuels are used. Limitations of this kind should be assessed.
- If solid fuels are gasified in a separate reactor and the gas subsequently injected in the precalciner, several of the problems related to staged combustion of solid fuels could be eliminated. Hence, the potential of applying external gasification [162] of alternative fuels, followed by staged combustion in the precalciner, should be evaluated.
- This work has focused on impact on the process conditions, and only to some extent on the impact on the clinker quality (free lime and sulphate content). It is recommended that effects on for instance clinker microstructure is investigated more thoroughly.

In Norway, as in many other countries, more strict regulations on pollutant emissions from cement kilns are to be expected in the future. Accordingly, in the cement industry there is a continuous work going on to reduce the emission of pollutants, including NO_x, and there is a constant need for more research in this area. It is the author's hope that the present thesis is a contribution in the right direction.

Appendix A

Precalciner kiln systems

Table A.1 gives an overview of precalciner kiln systems. The overview is mainly based on a review article by Kwech [28]. However, some more recently published designs, and a few others, have been added.

Table A.1: Precalciner kiln systems (in alphabetical order of the manufacturer).

Manufacturer	**Process name**	**System**	**Reference**
BKMI	Pre-Axial	AS-ILC	[28]
Buss	Convex Calcination	AT-ILC	[23]
Ciments Francaise	CF/FCB Low NOx Calciner	AS-SLC-S	[29, 30]
F.L.Smidth	ILC	AS-ILC	[28]
F.L.Smidth	SLC	AS-SLC	[28]
F.L.Smidth	SLC-S	AS-SLC-S	[28]
F.L.Smidth	SLC-Sx	AS-SLC-S	[31]
F.L.Smidth	SLC-D	AS-SLC-S	[31]
F.L.Smidth-Fuller	ILC-LowNO_x-Calciner	AS-ILC	[32]
Fuller	CO-SF	AS-ILC	[28]
IHI	Suspension Flash Calciner (SF)	AS-ILC	[28]
IHI	NSF	AS-ILC	[28]
IHI	C-FF	AS-ILC	[28]
Kawasaki	KSV	AS-ILC	[28]
Kawasaki	KS-5	AS-ILC	[28]
KHD Humboldt-Wedag	Pyroclon S	AT-ILC	[28]
KHD Humboldt-Wedag	Pyroclon R	AS-ILC	[28]
KHD Humboldt-Wedag	Pyroclon RP	AS-SLC-S	[28]
KHD Humboldt-Wedag	Pyroclon RT	AS-ILC	[28]
KHD Humboldt-Wedag	Pyrorapid short kiln	AS-ILC	[28]
KHD Humboldt-Wedag	Pyroclon LowNOx calciner	AS-ILC	[33, 34, 35]
Kobe Steel	DD	AS-ILC	[28]
Krupp-Polysius	Prepol AS	AS-ILC	[28]
Krupp-Polysius	Prepol AS-LC	AS-ILC	[28]
Krupp-Polysius	Prepol Air Through (AT)	AS-ILC	[28]
Krupp-Polysius	Prepol AS-MSC	AS-ILC	[36]
Lurgi	ZWS	AS-ILC	[28]
Mitsubishi	N-MFC	AS-ILC	[28]
Mitsubishi	GG	AS-SLC-S	[23]
Onoda	RSP	AS-SLC-S	[28]
Orenstein & Koppel	Miag-Bühler	AS-ILC	[28]
Sumitomo	SCS	AS-SLC	[28]
Technip CLE	MINOX	AS-SLC-S	[37]
Ube Industries	UNSP	AS-ILC	[28]
Voest-Alpine, SKET/ZAB	Pasec	AS-SLC	[28]

Appendix B

Brief description of MEBCEM

Table B.1 gives an overview of the m-files constituting MEBCEM, while Figure B.1 summarizes the relations between the various routines, functions, inputs and outputs. The detailed program structure and the source code of MEBCEM is not given here, but can be found elsewhere [13, 14, 15].

Required inputs to the program include:

- Mass flow [t/h] of:
  - all fuels
  - raw meal entering the preheater, string 1 and 2
  - raw materials entering the raw meal mill
  - raw coal entering the coal mills
- Volumetric flow [Nm^3/h] of:
  - gas exiting coal mill 1 and 2 (when operating)
  - cooling air
- Mass fraction of CaCO3 in the raw meal [-]
- Degree of calcination of the precalcined meal [%]
- Heating value of all fuels [J/kg]
- Proximate analysis of all fuels [-]
- Static pressure before and after the tertiary air gate valve [mbar]
- Tertiary air gate valve position [%]

- Concentration of:
  - O2 at the kiln inlet, after ESP 3 and before ESP 4 [vol%, dry]
  - CO at the kiln inlet, after ESP 3 and before ESP 4 [vol%, dry]
  - NO_x at the kiln inlet, after ESP 3 and before ESP 4 [mg/Nm3 @ 10 % O2]
- Electric power for the operation of the raw meal mill [W]
- Temperature [°C] of:
  - excess cooling air
  - meal/gas from the lower cyclone stage, string 1 and 2
  - tertiary air
  - hot clinker
  - gas entering the coal mills
  - off-gas from the coal mills
  - gas entering conditioning tower 1 and 2
  - off-gas from conditioning tower 1 and 2
  - off-gas from ESP 4
  - gas entering the raw meal mill
  - off-gas from the raw meal mill
  - gas entering the main fan in the raw meal mill
- Time vector [h] (or [min])

The most important unknowns that are calculated, are:

- Mass flow [kg/s] of:
  - off-gas from the preheater, precalciner, tertiary air chamber, reburning chamber, rotary kiln, conditioning tower 1, conditioning tower 2, ESP 3, ESP 4, raw meal mill and ESP in the raw meal mill
  - primary, secondary and tertiary air
  - excess cooling air
  - gas entering coal mills, conditioning tower 1 and conditioning tower 2
  - gas bypassing the raw meal mill

  - false air in the preheater, rotary kiln, cooler, coal mills, conditioning tower 1, conditioning tower 2, ESP 3, ESP 4 and raw meal mill
  - conveying air for the transportation of secondary coal
  - N_2, CO_2, O_2 and H_2O exiting the rotary kiln
  - CO_2 from the calcination in the tertiary air chamber and in the reburning chamber
  - water supply to the conditioning towers
  - water transferred from solids to gas phase during the drying of coal
  - materials exiting the raw meal mill
  - meal exiting the tertiary air chamber, reburning chamber and precalciner
  - cold and hot clinker
  - ash produced in the the rotary kiln, tertiary air chamber and reburning chamber
  - circulating substances
  - dust flowing from the cooler to the kiln and from the kiln to the precalciner

- Temperature [°C] of:
  - meal exiting the reburning chamber and tertiary air chamber
  - secondary air
  - kiln gas
  - cooled clinker

- Mass fraction, wet volume fraction and dry volume fraction of N_2, CO_2, O_2 and H_2O in the off-gas from all reactors

- Fuel equivalence ratio and air equivalence ratio of:
  - rotary kiln
  - reburning chamber
  - tertiary air chamber
  - precalciner

- Thermal efficiency of:
  - cooler
  - preheater
  - kiln system

Table B.1: Modules (MATLAB scripts and functions) in MEBCEM.

Module	Description
MEB13.M	Main program
MB_CONST.M	Definition of constants for the pyroprocessing units
MB_PARA.M	Parameter settings for the mass balance of the pyroprocessing units
MEB_DATA.M	Data conversion
MB_CALCX.M	Calculation of main mass flows in the pyroprocessing units
MB_CALC2.M	Calculation of secondary air, rotary kiln gas and rotary kiln species
MB_SPEC#.M	Calculation of gas species in the reburning chamber (#=2), the tertiary-air chamber (#=3), the burnout chamber (#=4), the preheater (#=5)
MB_FRACM.M	Calculation of mass fractions of gas species in the pyroprocessing units
MB_FRACV.M	Calculation of volume fractions of gas species in the pyroprocessing units
EB_PARAM.M	Parameter settings for the energy balance of the pyroprocessing units
EB_PH.M	Calculation of energy balance of the preheater
EB_TERT.M	Calculation of energy balance of the tertiary air chamber
EB_BOUT2.M	Calculation of energy balance of the burnout chamber
EB_REB2.M	Calculation of energy balance of the reburning chamber
EB_R2.M	Calculation of energy balance of the rotary kiln
EB_C2.M	Calculation of energy balance of the cooler
EB_HB.M	Calculation of heat balance of the pyroprocessing units
MEB_MISC.M	Calculation of various efficiencies of the pyroprocessing units
MEB_EQUI.M	Calculation of equivalence ratios of the pyroprocessing units
MEB_EXT1.M	Main program for the mass and energy balance of the system downstream of the pyroprocessing units
MEB_CM12.M	Calculation of mass and energy balance of the coal mills
MEB_CND1.M	Calculation of mass and energy balance of the conditioning tower 1
MEB_ESP1.M	Calculation of mass and energy balance of ESP 4
MEB_CND2.M	Calculation of mass and energy balance of conditioning tower 2 and ESP 3
MEB_AFM.M	Calculation of mass and energy balance of the aerofall mill
MEB_AFM2.M	Calculation of molar flows, mass fractions and mole fractions of gas species in the aerofall mill
MEB_POLL.M	Calculation of pollutant properties
MEB_REP.M	Report routine
MEB_RES1.M	Routine displaying data on the screen
MEB_MENZ.M	Menu system
MEB_PREZ.M	Plotting routine
EB_HB2.M	Heat balance display
CPM.M	Function calculating the mean specific heat of a substance in a given temperature interval

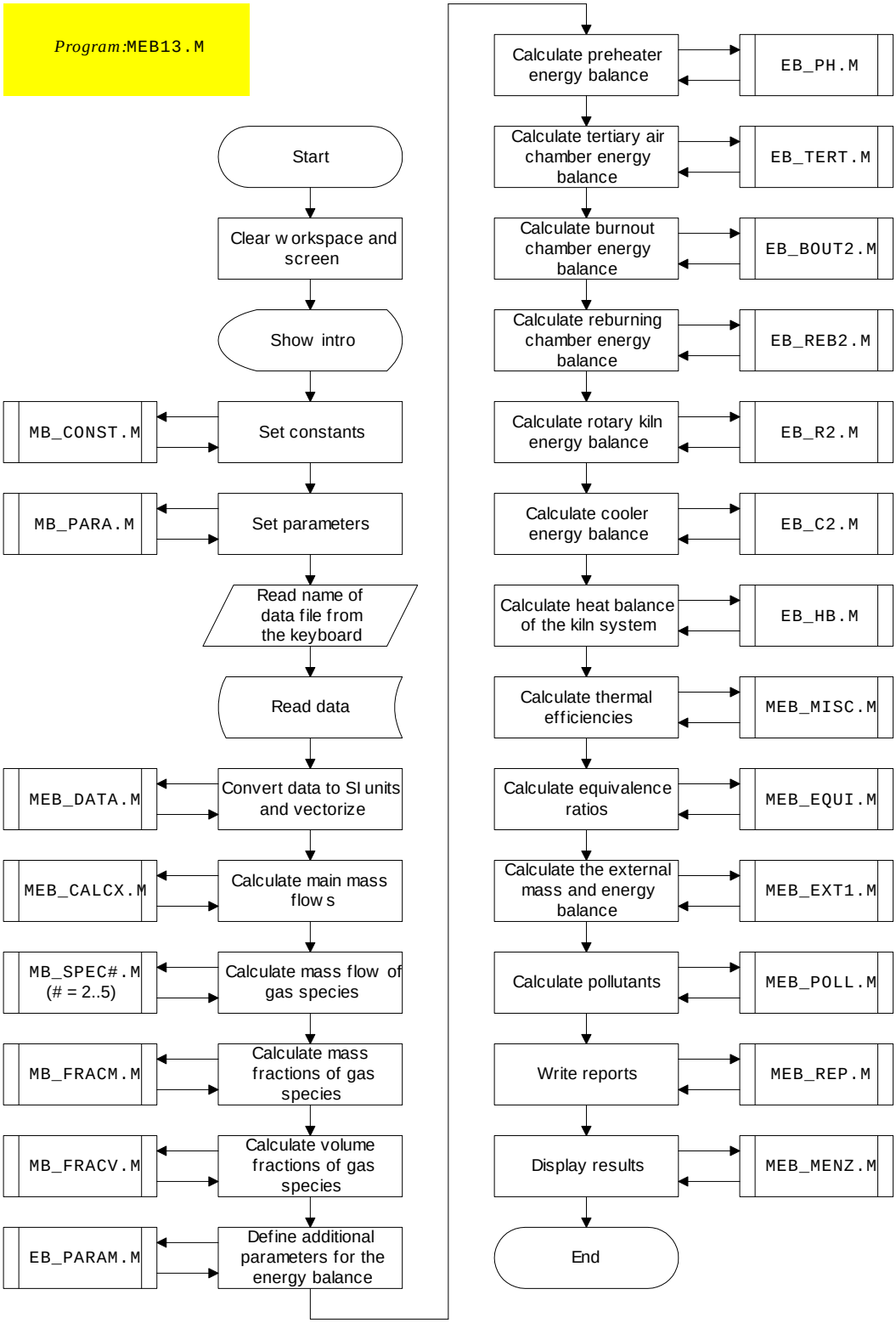

Figure B.1: Block diagram showing the program structure of MEBCEM.

Appendix C

Brief description of SEACEM

Table C.1 gives an overview of the m-files constituting SEACEM, while Figure C.1 and C.2 summarize the relations between the various routines, functions, inputs and outputs. The detailed program structure and the source code of SEACEM is not given here, but can be found elsewhere [16].

Required inputs to the program include:

- names of all species (N_2, CO_2, C_2H_4, H_2O, SO_2, CaS(s), O_2, SO_3, H_2, O, OH, $CaSO_4$(s), CaO(s), $CaCO_3$(s) and CO by default)
- the atoms matrix (rows = elements; columns = species)
- initital molar composition
- molecular weight of all species
- $c_p^0(T)$ coeffecients (in $a + bT + c/T^2$) for species not calculated by using tabulated enthalpy and entropy values, and $c_p^0(T)$ coeffecients (in $a + bT$) for inert solids
- standard entropy for all the species
- mass flow of inert solids
- indexes indicating whether the species are gases or solids
- standard enthalpy of formation for all the species
- operating pressure
- phase index; i.e. an index indicating whether the species are gas (1) or solid (2, 3, ...) species
- initial temperature of gas and solids

Program: SC.M

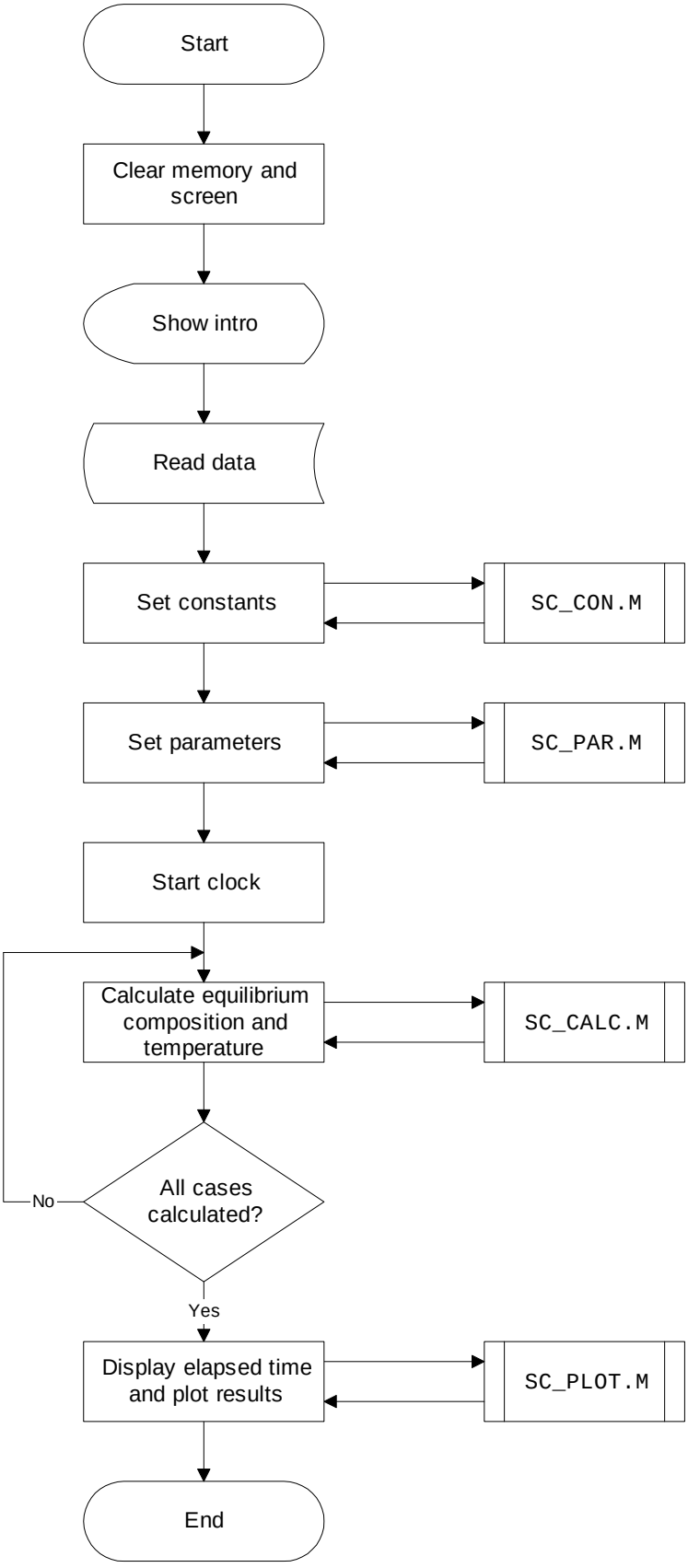

Figure C.1: Block diagram showing the program structure of SEACEM.

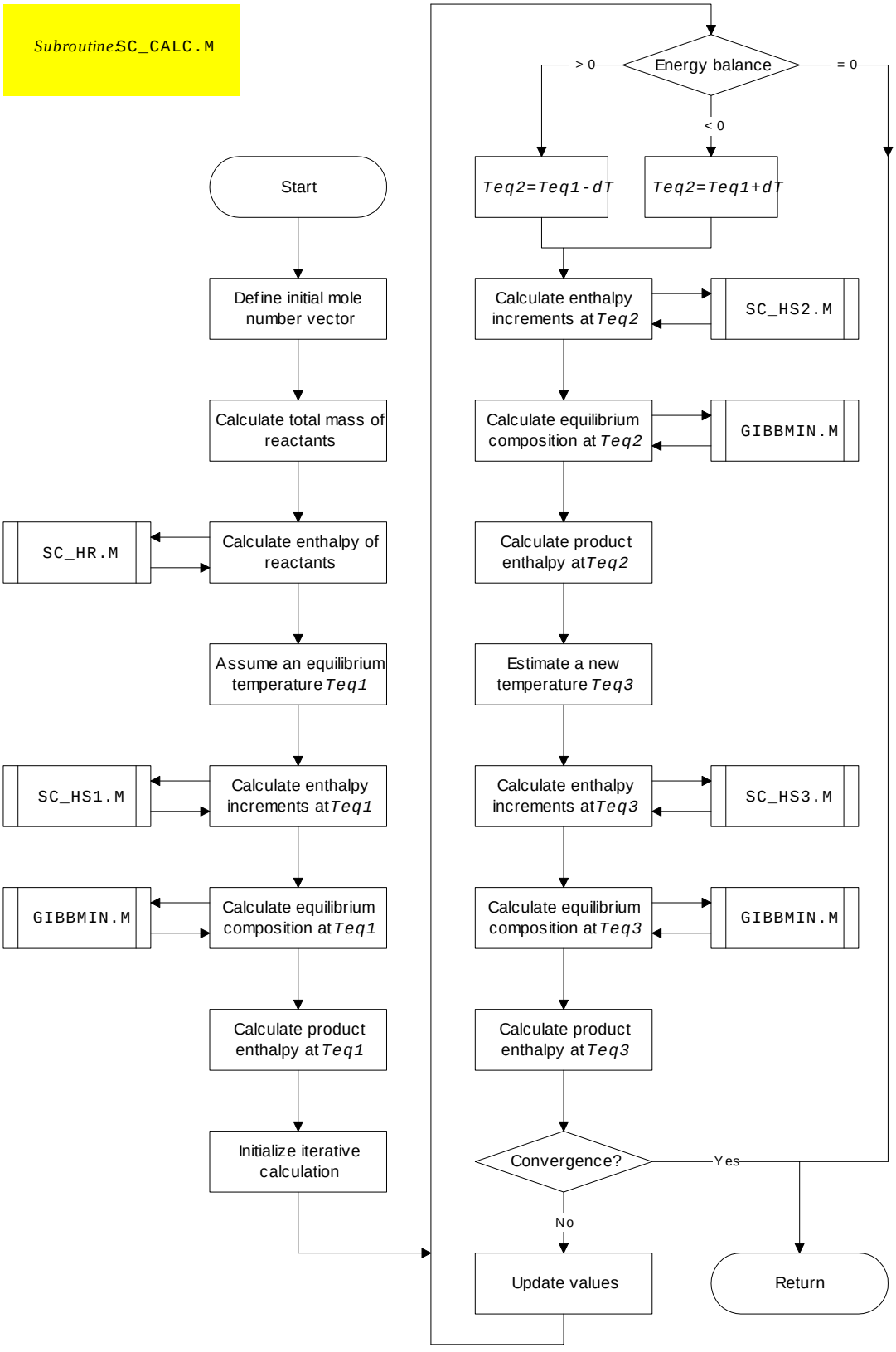

Figure C.2: Block diagram showing the structure of the main calculation routine in SEACEM.

Table C.1: Modules (MATLAB scripts and functions) in SEACEM.

Module	Description
SC.M	Main program; calls SC_CON.M, SC_PAR.M, SC_CALC.M and SC_PLOT.M
SC_CON.M	Definition of constants
SC_PAR.M	Parameter settings
SC_CALC.M	Main calculation module; calls SC_HR.M, SC_HS1.M, GIBBMIN.M, SC_HS2.M and SC_HS3.M
SC_HR.M	Calculation of reactant enthalpy
SC_HS#.M	Calculation of product enthalpy at the temperature Teq# (#=1,2,3); calls HS0.M and the MATLAB® intrinsic function INTERP1.M
SC_PLOT.M	Plotting routine
GIBBMIN.M	Function calculating the equilibrium composition for a given temperature (by means of Gibbs energy minimization)
HS0.M	Function calculating enthalpy increments and entropy of chemical species

- initial mole number vector of the component which is varied (C_2H_4 by default); this vector is entered from the keyboard during running of the program
- enthalpy and entropy increment data for species not calculated by means of $c_p^0(T)$ polynomials; these data, which are tabulated in JANAF format, are saved in a MATLAB® data file[1].

[1] Default file name is SVOVSIRK.MAT.

Appendix D

Particle trackings

Results from three of the cases calculated are given in Figure D.1–D.3. Sawdust at an inlet velocity of -1 m/s is readily entrained by the kiln gases. At an inlet velocity of -3 m/s most of the plastic screw caps also tend to be transported up into the calciner along with the kiln gas. Pieces of car tyres at an inlet velocity of -5 m/s, however, are too big/heavy to be entrained.

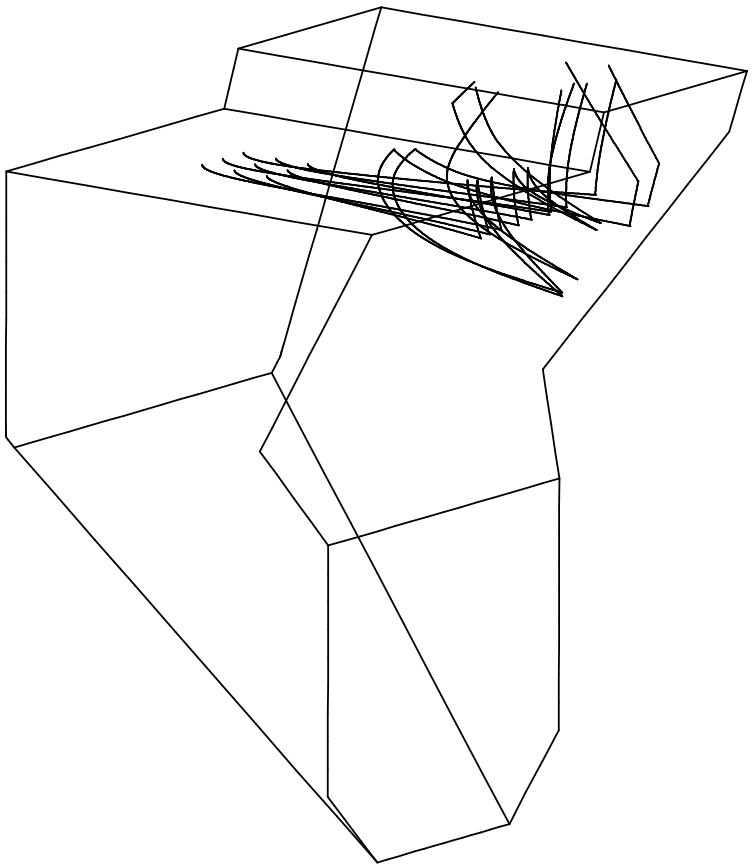

Figure D.1: Case 1b; sawdust at an inlet velocity of -1 m/s; all particles are entrained by the kiln gases.

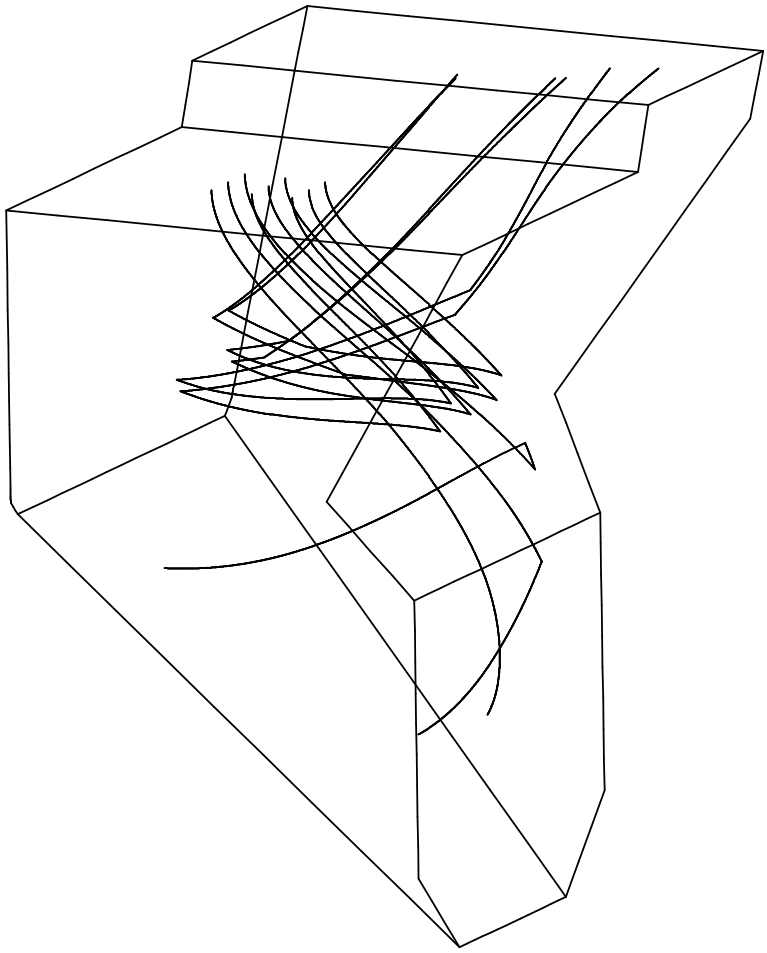

Figure D.2: Case 3c; plastic screw caps at an inlet velocity of -3 m/s; six out of nine particles are entrained by the kiln gases.

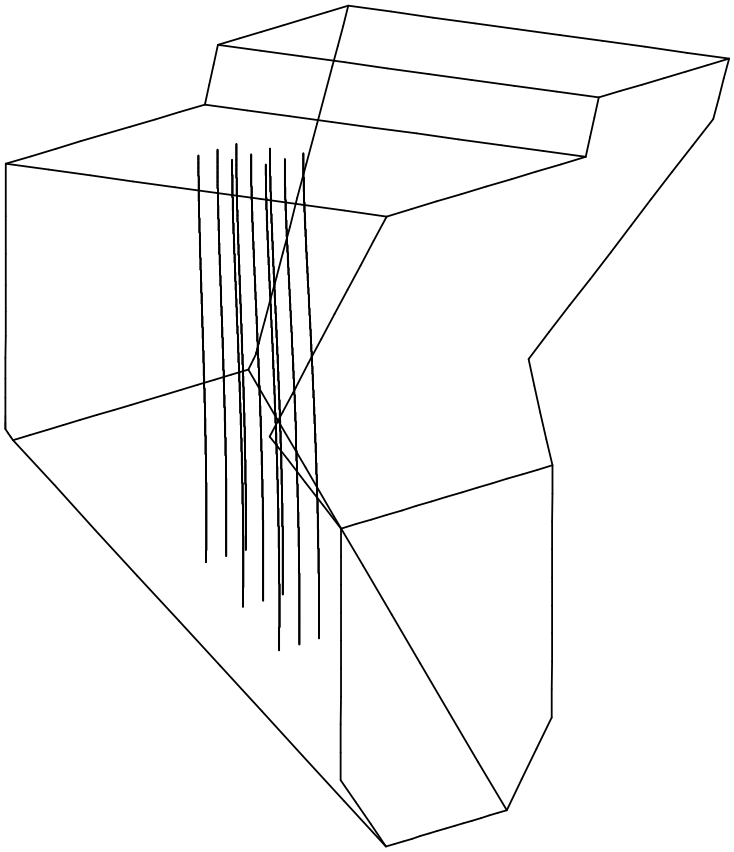

Figure D.3: Case 6d; shredded car tyres at an inlet velocity of -5 m/s; no particles are entrained by the kiln gases.

Appendix E

Solving the preheater mass balance equations

The equations 10.1–10.20 can be rearranged and written in a matrix form:

$$\mathbf{Ax} = \mathbf{b} \tag{E.1}$$

$$\mathbf{A} = [\mathbf{A}_1\mathbf{A}_2] \tag{E.2}$$

$$\mathbf{A}_1 = \begin{bmatrix}
1 & \eta_1 - 1 & 0 & 0 & 0 & 0 & 0 & 0 & 0 & 0 \\
0 & -1 & 1-\eta_2 & 0 & 1-\eta_2 & 0 & 0 & 0 & 0 & 0 \\
0 & 0 & -1 & 1-\eta_3 & 0 & 1-\eta_3 & 0 & 0 & 0 & 0 \\
0 & 0 & 0 & 1 & 0 & 0 & 0 & 0 & \eta_4 - 1 & 0 \\
1 & -1 & 0 & 0 & 1 & 0 & 0 & 0 & 0 & 0 \\
0 & 1 & -1 & 0 & -1 & 1 & 0 & 0 & 0 & 0 \\
0 & 0 & 1 & -1 & 0 & -1 & 1 & 0 & 0 & 0 \\
0 & 0 & 0 & 1 & 0 & 0 & 0 & 1 & -1 & 0 \\
0 & 0 & 0 & 0 & 0 & 0 & 1 & 0 & -1 & -1 \\
0 & 0 & 0 & 0 & 0 & 0 & 0 & 0 & 0 & 0 \\
0 & 0 & 0 & 0 & 0 & 0 & 0 & 0 & 0 & 0 \\
0 & 0 & 0 & 0 & 0 & 0 & 0 & 0 & 0 & 0 \\
0 & 0 & 0 & 0 & 0 & 0 & 0 & 0 & 0 & 0 \\
0 & 0 & 0 & 0 & 0 & 0 & 0 & 0 & 0 & 0 \\
0 & 0 & 0 & 0 & 0 & 0 & 0 & 0 & 0 & 0 \\
0 & 0 & 0 & 0 & 0 & 0 & 0 & 0 & 0 & 0 \\
0 & 0 & 0 & 0 & 0 & 0 & 0 & 0 & 0 & 0 \\
0 & 0 & 0 & 0 & 0 & 0 & 0 & 0 & 0 & 0 \\
0 & 0 & 0 & 0 & 0 & 0 & 0 & 1 - c_2c_2 & 0 & 0 \\
0 & 0 & 0 & 0 & 0 & 0 & 0 & 0 & 0 & c_2
\end{bmatrix} \tag{E.3}$$

$$\mathbf{A}_2 = \begin{bmatrix} 0 & 0 & 0 & 0 & 0 & 0 & 0 & 0 & 0 & 0 \\ 0 & 0 & 0 & 0 & 0 & 0 & 0 & 0 & 0 & 0 \\ 0 & 0 & 0 & 0 & 0 & 0 & 0 & 0 & 0 & 0 \\ 0 & 0 & 0 & 0 & 0 & 0 & 0 & 0 & 0 & 0 \\ 0 & 0 & 0 & 0 & 0 & 0 & 0 & 0 & 0 & 0 \\ 0 & 0 & 0 & 0 & 0 & 0 & 0 & 0 & 0 & 0 \\ 0 & 0 & 0 & 0 & 0 & 0 & 0 & 0 & 0 & 0 \\ 0 & 0 & 0 & 0 & 0 & 0 & 0 & 0 & 0 & 0 \\ 0 & 0 & 0 & 0 & 0 & 0 & 0 & 0 & 0 & 0 \\ 1 & \eta_1 - 1 & 0 & 0 & 0 & 0 & 0 & 0 & 0 & 0 \\ 0 & -1 & 1-\eta_2 & 0 & 1-\eta_2 & 0 & 0 & 0 & 0 & 0 \\ 0 & 0 & -1 & 1-\eta_3 & 0 & 1-\eta_3 & 0 & 0 & 0 & 0 \\ 0 & 0 & 0 & 1 & 0 & 0 & 0 & 0 & \eta_4 - 1 & 0 \\ 1 & -1 & 0 & 0 & 1 & 0 & 0 & 0 & 0 & 0 \\ 0 & 1 & -1 & 0 & -1 & 1 & 0 & 0 & 0 & 0 \\ 0 & 0 & 1 & -1 & 0 & -1 & 1 & 0 & 0 & 0 \\ 0 & 0 & 0 & 1 & 0 & 0 & 0 & 1 & -1 & 0 \\ 0 & 0 & 0 & 0 & 0 & 0 & 1 & 0 & -1 & 1 \\ 0 & 0 & 0 & 0 & 0 & 0 & 0 & 1-c_1 & 0 & 0 \\ 0 & 0 & 0 & 0 & 0 & 0 & 0 & 0 & 0 & -1 \end{bmatrix} \tag{E.4}$$

$$\mathbf{x} = \begin{bmatrix} A_{\mathrm{D1}} \\ A_{\mathrm{D2}} \\ A_{\mathrm{D3}} \\ A_{\mathrm{D4}} \\ A_1 \\ A_2 \\ A_3 \\ A_4 \\ A_3' \\ A_{\mathrm{calc}} \\ B_{\mathrm{D1}} \\ B_{\mathrm{D2}} \\ B_{\mathrm{D3}} \\ B_{\mathrm{D4}} \\ B_1 \\ B_2 \\ B_3 \\ B_4 \\ B_3' \\ B_{\mathrm{calc}} \end{bmatrix} \tag{E.5}$$

$$\mathbf{b} = \begin{bmatrix} (1-\eta_1)\,A_0 \\ 0 \\ 0 \\ 0 \\ A_0 \\ 0 \\ 0 \\ 0 \\ 0 \\ 0 \\ 0 \\ 0 \\ 0 \\ 0 \\ 0 \\ 0 \\ 0 \\ -B_{\mathrm{DK}} \\ 0 \\ 0 \end{bmatrix} \tag{E.6}$$

In Equations E.3 and E.4, the following definitions are used:

$$c_1 \triangleq 1 + \frac{1-\eta_{\mathrm{calc}}}{\frac{M_{\mathrm{CaCO_3}}}{M_{\mathrm{CO_2}} w_{\mathrm{CaCO_3}}} - 1} \tag{E.7}$$

$$c_2 \triangleq 1 - \frac{M_{\mathrm{CO_2}} w_{\mathrm{CaCO_3}}}{M_{\mathrm{CaCO_3}}} \tag{E.8}$$

When the matrix $\mathbf{A}$ and the right-hand-side vector $\mathbf{b}$ are specified, Equation E.1 is easily solved, i.e. the solution vector $\mathbf{x}$ is found, by means of MATLAB®.

Appendix F

Brief description of CIRCCEM

CIRCCEM uses a MEBCEM datafile[1], and a datafile with circulation data[2] as input data. The name of the MEBCEM datafile is user specified; whereas CIRCCEM automatically loads the correct circulation datafile on the basis of the name of the given MEBCEM datafile. CIRCCEM then calculates the mass flow of all circulating components. The output data are saved in a separate datafile[3]. Important outdata calculated are printed on screen and saved in reports[4].

Table F.1 gives an overview of the m-files constituting CIRCCEM, while Figure F.1 summarizes the relations between the various routines, functions, inputs and outputs. The detailed program structure and the source code of CIRCCEM is not given here, but can be found elsewhere [18].

[1] Such datafiles are named `rdata#.mat`, where `#` corresponds to the datafile ID.

[2] The circulation data files are named `cirin#.mat`.

[3] These datafiles are named `cd_$#.mat`, where `$` corresponds to the element symbol of the circulating component.

[4] The reports are named `rep_$#.txt`.

Table F.1: Modules (MATLAB scripts and functions) in CIRCCEM.

Module	Description
CIRC10.M	Main program
MB_TOWER.M	Calculation of mass flow of meal, dust and gas in the cyclone tower; calls the function TOWER2.M
TOWER2.M	Function calculating the mass flow of meal, dust and gas in a cyclone tower string
CIR_INT1.M	Data interpolation, calls the MATLAB® intrinsic function INTERP1.M
CIR_S.M	Calculation of sulphur flows; calling the subroutines CIR_EXT1.M, CIR_TOW.M and CIR_KILN.M
CIR_K.M	Calculation of potassium flows; calling the subroutines CIR_EXT1.M, CIR_TOW.M and CIR_KILN.M
CIR_NA.M	Calculation of sodium flows; calling the subroutines CIR_EXT1.M, CIR_TOW.M and CIR_KILN.M
CIR_CL.M	Calculation of chlorine flows; calling the subroutines CIR_EXT1.M, CIR_TOW.M and CIR_KILN.M
CIR_EXT1.M	Calculating circ. comp. into and out of the system as well as downstream of the preheater
CIR_TOW.M	Calculating circ. comp. in the meal in the cyclone tower
CIR_KILN.M	Calculating circ. comp. in the gas/dust in the preheater, precalciner and rotary kiln
CIR_RES1.M	Report routine

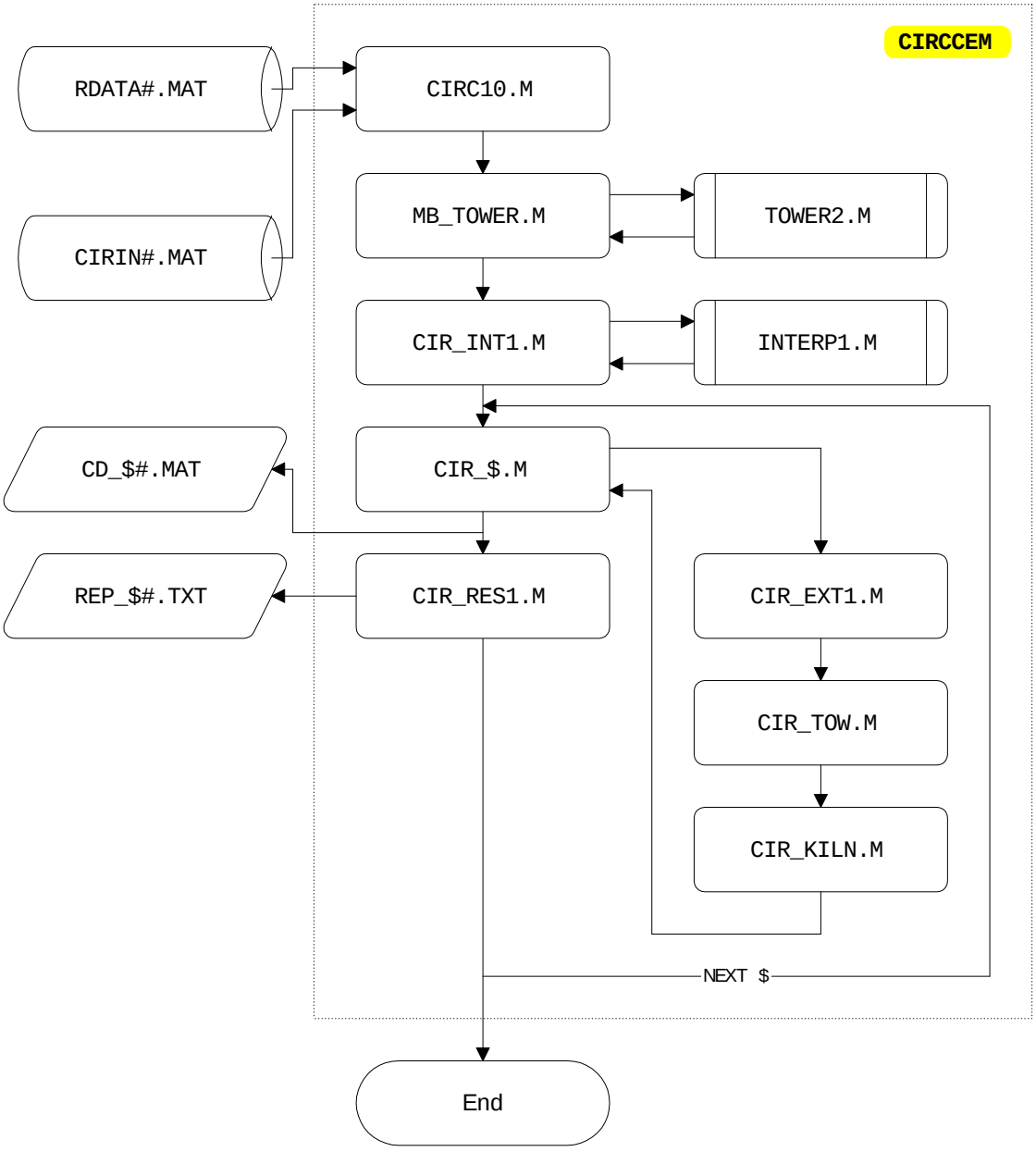

Figure F.1: Overview of CIRCCEM: scripts, functions, inputs and outputs.

Bibliography

[1] Weinberg, F.: "The first half-million years of combustion research and today's burning problems", *Symposium (International) on Combustion*, **15**, 1–17, The Combustion Institute, Pittsburgh, Pennsylvania, 1975

[2] Bowman, C.T.: "Control of combustion generated nitrogen oxide emissions: Technology driven by regulations", *Symposium (International) on Combustion*, **24**, 859–878, The Combustion Institute, Pittsburgh, Pennsylvania, 1992

[3] Fuglestvedt, J.S., Isaksen, I.S.A. and Wang, W.-C.: "Direct and indirect global warming potentials of source gases", Report 1994:1, Center for International Climate and Energy Research, Oslo, 1994

[4] Berntsen, T. and Isaksen, I.: "NO_x emissions from aircraft - Effects of lightning and convection on changes in tropospheric ozone", Working Paper 1998:5, Center for International Climate and Energy Research, Oslo, 1998

[5] Statistics Norway, http://www.ssb.no

[6] Billhardt, W., Kuhlmann, K., Ruhland, W., Schneider, M. and Xeller, H.: "Current state of NO_x abatement in the cement industry", *Zement-Kalk-Gips*, **49**, No. 10, 545–560, 1996

[7] "Europäische Mitverbrennungsrichtlinie" (in German), *VDZ-Mitteilungen*, No. 106, 7, May 1998

[8] "NO_x emissions from cement manufacture and evaluation of various possibilities for NO_x reduction in the cement industry", Contract no. EV5V-CT94-551, Report, EU Environment Research Programme, 1998

[9] Tokheim, L.A., Bjerketvedt, D., Husum, I. and Høidalen, Ø.: "NO_x reduction in a precalciner cement kiln using plastic as reburning fuel", *Zement-Kalk-Gips*, **51**, No. 1, 12–23, 1998

[10] Svinning, K., Tokheim, L.A. and Bjerketvedt, D.: "Statistical analysis of the correlation between NO_x emissions and production conditions in a cement kiln applying staged combustion", *World Cement*, **15**, No. 1, 68–75, 1998

[11] Tokheim, L.A. and Bjerketvedt, D.: "NO_x reduction by staged combustion in a precalciner cement kiln using alternative fuels", Work-in-progress poster no. 1G18, *Symposium (International) on Combustion*, **27**, The Combustion Institute, USA, 1998

[12] Tokheim, L.A. and Bjerketvedt, D.: "Experimental determination of entrainment velocity and drag coefficient of chopped car tyres, refuse derived fuel and shredded plastic", Tel-Tek report nr. 220025-1, Porsgrunn, 1997

[13] Tokheim, L.A. and Bjerketvedt, D.: "MEBCEM 1.1 - A Matlab® program for the calculation of mass and energy balances in a precalciner cement kiln system", Tel-Tek report nr. 220025-5, Porsgrunn, 1997

[14] Tokheim, L.A. and Bjerketvedt, D.: "MEBCEM 1.2 - A Matlab® program for the calculation of mass and energy balances in a precalciner cement kiln system - extended version", Tel-Tek report nr. 220288-1, Porsgrunn, 1998

[15] Tokheim, L.A. and Bjerketvedt, D.: "MEBCEM 1.3 - A Matlab® program for the calculation of mass and energy balances in a precalciner cement kiln system - new version", Tel-Tek report nr. 220288-2, Porsgrunn, 1998

[16] Tokheim, L.A. and Bjerketvedt, D.: "SEACEM 1.0 - A Matlab® program for performing sulphur equilibrium analyses of a cement kiln unit", Tel-Tek report no. 220025-4, Porsgrunn, 1997

[17] Tokheim, L.A. and Bjerketvedt, D.: "Betydningen av interne sirkulasjonssløyfer ved anvendelse av reburning i forkalsinatoren i Ovn 6 ved NORCEM i Brevik" (in Norwegian), Tel-Tek report no. 220025-6, Porsgrunn, 1997

[18] Tokheim, L.A. and Bjerketvedt, D.: "CIRCCEM – A Matlab® program for the calculation of internal material cycles in a precalciner cement kiln system", Tel-Tek report nr. 220288-3, Porsgrunn, 1998

[19] Tokheim, L.A. and Bjerketvedt, D.: "Fullskalaforsøk på ovn 6, Norcem, Brevik, 16.–20. mars 1998" (in Norwegian), Tel-Tek report nr. 220288-4, Porsgrunn, 1998

[20] "Integrated pollution prevention and control (IPPC) — Reference document on best available techniques in the cement and lime manufacturing industries. Draft", European Commission, Directorate-General JRC, Joint Research Centre, Institute for Prospective Technological Studies, Sevilla, June, 1999

[21] Neuffer, W.J.: "Alternative control techniques document - NOx emissions from cement manufacturing", EPA report no. EPA-453/R-94-004, U.S. Environmental Protection Agency, 1994

[22] Labahn, O and Kohlhaas, B.: "Cement engineer's handbook", Bauverlag GmbH, 1983

[23] Duda, W.H.: "Cement data book Volume 1, 3rd edition", Bauverlag GmbH, 1985

[24] Peray, K.E. and Waddell, J.J.: "The rotary cement kiln", Chemical Publishing Co., Inc., New York, 1972

[25] Taylor, H.F.W.: "Cement Chemistry", Academic Press, 1990

[26] Rosemann, H.: "Theoretische und betriebliche Untersuchungen zum Brennstoffenergieverbrauch von Zementdrehofenanlagen mit Vorcalcinierung" (in German), *Schriftenreihe der Zementindustrie*, **48**, Beton-Verlag, Düsseldorf, 1987

[27] Hashimoto, I. and Watanabe, T.: Clinker burning in the fluidized bed - an innovative technology, *Zement-Kalk-Gips*, **52**, No. 1, 1–19, 1999

[28] Kwech, L.: "Precalcining in the cement industry - the state of the art", *Zement-Kalk-Gips*, **39**, No. 9, 251–264, 1986

[29] Jorget, S.: "The new CF/CFB low-NOx precalciner", *World Cement*, **9**, No. 11, 34–36, 1992

[30] Jorget, S.: "The new CF/CFB low-NOx precalciner - a decisive advance in environment protection", *Zement-Kalk-Gips*, **46**, No. 4, 193–196, 1993

[31] Hundebøl, S. and Rosholm, P.: "High efficiency calciner", *World Cement*, **15**, No. 10, 83–88, 1998

[32] Thomsen, K., Jensen, L.S. and Schomburg, F.: "FLS-Fuller ILC-lowNOx calciner commisioning and operation at Lone Star St. Cruz in California", *Zement-Kalk-Gips*, **51**, No. 10, 545–560, 1998

[33] Deussner, M.: "New 5000 t/d kiln plant with short rotary kiln and lowNOx calciner at Hualien, Taiwan", *Ciments, Bétons, Plâtres, Chaux*, **806**, No. 1, 52–57, 1994

[34] Deussner, M.: "The 5000 t/d PYRORAPID® short rotary kiln plant at the Hualien cement works in Taiwan", *Zement-Kalk-Gips*, **48**, No. 11, 567–575, 1995

[35] Deussner, M.: "Clinker burning with reduced NOx emission", *World Cement*, **12**, No. 12, 52–58, 1995

[36] Bertschinger, P.: "Swiss plant succesfully reduces NOx emissions", *World Cement*, **13**, No. 8, 16–20, 1996

[37] Dusome, D.: "Staged combustion for NOx control at the Calaveras Tehachapi plant", *World Cement*, **12**, No. 2, 2–8, 1995

[38] Alsop, P.A. and Post, J.W.: "Cement plant operations handbook for dry process plants", Tradeship Publications Ltd., 1995

[39] Nielsen, P.B. and Jepsen, O.L.: "An overview of SO_x and NO_x in various pyro-processing systems", *1990 IEEE Cement Ind. Tech. Conf.*, 32, 255-276, 1990

[40] Zeldovich, J.: "The oxidation of nitrogen in combustion and explosions", *Acta Physiochimica U.R.S.S.*, **XXI**, No. 4, 577–628, 1946

[41] Flagan, R.C. and Seinfeld, J.H.: "Fundamentals of air pollution engineering", Prentice-Hall, Inc., 1988

[42] Fenimore, C.P.: "Formation of nitric oxide in premixed hydrocarbon flames", *Symposium (International) on Combustion*, **13**, 373–380, The Combustion Institute, Pittsburgh, Pennsylvania, 1971

[43] Turns, S.R.: "An introduction to combustion: concepts and applications", McGraw-Hill, 1996

[44] Smart, J.P., Mullinger, P.J. and Jenkins, B.G.: "Combustion, heat transfer and NO_x", *World Cement*, **15**, No. 12, 14–25, 1998

[45] Gardeik, H.O., Rosemann, H., Sprung, S. and Rechenberg, W.: "Verhalten der Stickstoffoxide in Drehofenanlagen der Zementindustrie" (in German), *Zement-Kalk-Gips*, **37**, No. 10, 499–507, 1984

[46] Gardeik, H.O., Rosemann, H. and Scheuer, A.: "Bildung und Abbau von NO in Zementofenanlagen — Teil I: Messungen an Industrieanlagen" (in German), *Zement-Kalk-Gips*, **37**, No. 10, 508–512, 1984

[47] Scheuer, A. and Gardeik, H.O.: "Bildung und Abbau von NO in Zementofenanlagen — Teil II: Modellrechnungen und Vergleich mit Messungen" (in German), *Zement-Kalk-Gips*, **38**, No. 2, 57–66, 1985

[48] Scheuer, A.: "Theoretische und betriebliche Untersuchungen zur Bildung und zum Abbau von Stickstoffmonoxid in Zementdrehofenanlagen" (in German), Schriftenreihe der Zementindustrie, **49**, Beton-Verlag, Düsseldorf, 1987

[49] Gartner, E.M. and Wilk, C.M.: "The influence of raw materials on nitrogeneous emissions from cement kilns", *Zement-Kalk-Gips*, **40**, No. 2, 95–100, 1987

[50] Jøns, E. and Rabia, O.: "Laboratory simulation of preheater emissions", *World Cement*, **16**, No. 5, 95–99, 1999

[51] Xeller, H.: "New developments in NO_x abatement in the cement industry - Part 2", *Zement-Kalk-Gips*, **51**, No. 4, 208–218, 1998

[52] Xeller, H.: "NOx-Minderung durch Einsatz eines Stufenbrenners mit Rauchgasrückführung vom Vorwärmer" (in German), *Zement-Kalk-Gips*, **40**, No. 2, 57–63, 1987

[53] Xeller, H.: "Reducing NOx formation using a step burner with exit gas recycling from preheater", *World Cement*, **5**, No. 3, 84–92, 1988

[54] Jacques, S. and Gillouin, G.: "The Rotaflam® kiln burner", *World Cement*, **7**, No. 6, 266–267, 1990

[55] Breitenbaumer, C.: "Operating results and NO_x emissions with ROTAFLAM burner at the Retznei cement works", *Zement-Kalk-Gips*, **45**, No. 7, 187–190, 1992

[56] Kupper, D. and Brentrup, L.: "SNCR technology for NOx reduction in the cement industry", *World Cement*, **9**, No. 3, 4–8, 1992

[57] Steuch, H.E., Hille, J., Sun, W.H., Bisnett, M.J. and Kirk, D.W.: "NO_x-Minderung mit dem NO_xOUT-Verfahren an einer Ofenanlage nach dem Trockenverfahren", *Zement-Kalk-Gips*, **49**, No. 1, 1–11, 1996

[58] Stjärnberg, A., Process Engineer at Cementa AB, Slite, Sweden, Personal Communication

[59] von Harpe, T.: "Modified NOxOUT and NOx control", *World Cement*, **15**, No. 12, 28–33, 1998

[60] Wendt, J.O.L., Sternling, C.V. and Matovich, M.A.: "Reduction of sulfur and nitrogen oxides by secondary fuel injection", *Symposium (International) on Combustion*, **14**, 897–904, The Combustion Institute, Pittsburgh, Pennsylvania, 1973

[61] Chen, S.L., McCarthy, J.M., Clark, W.D., Heap, M.P., Seeker, W.R. and Pershing, D.W.: "Bench and pilot scale process evaluation of reburning for in-furnace NO_x reduction", *Symposium (International) on Combustion*, **21**, 1159–1166, The Combustion Institute, Pittsburgh, Pennsylvania, 1988

[62] Smoot, L.D., Hill, S.C. and Xu, H.: "NO_x control through reburning", *Progress in Energy and Combustion Science*, **24**, 385–408, 1998

[63] Song, Y.H, Beér, J.M. and Sarofim, A.F.: "Reduction of nitric oxide by coal char at temperatures of 1250–1750 K", *Combustion Science and Technology*, **25**, 237–240, 1981

[64] Chan, L.K., Sarofim, A.F. and Beér, J.M.: "Kinetics of the NO-carbon reaction at fluidized bed combustor conditions", *Combustion and Flame*, **52**, 37–45, 1983

[65] Furusawa, T., Tsunoda, M., Tsujimura, M. and Adschiri, T.: "Nitric oxide reduction by char and carbon monoxide — Fundamental kinetics of nitric oxide reduction in fluidized-bed combustion of coal", *Fuel*, **64**, 1306–1309, 1985

[66] Johnsson, J.E.: "Formation and reduction of nitrogen oxides in fluidized-bed combustion", *Fuel*, **73**, 1398–1415, 1994

[67] Aarna, I. and Suuberg, E.M.: "A review of the kinetics of the nitric oxide–carbon reaction", *Fuel*, **76**, No. 6, 475–491, 1997

[68] Ono, M., Katsuki, T. and Akita, M. : "Katalytische Reduktion von Stickstoffmonoxid mit Kohlenmonoxid über Zementrohmel" (in German), *Zement-Kalk-Gips*, **31**, No. 5, 242–244, 1978

[69] Tsujimura, M, Furusawa, T. and Kunii, D. : "Catalytic reduction of nitric oxide by carbon monoxide over calcined limestone", *Journal of Chemical Engineering of Japan*, **16**, No. 2, 132-136, 1983

[70] Tsujimura, M, Furusawa, T. and Kunii, D. : "Catalytic reduction of nitric oxide by hydrogen over calcined limestone", *Journal of Chemical Engineering of Japan*, **16**, No. 6, 524–526, 1983

[71] Furusawa, T., Koyama, M. and Tsujimura, M.: "Nitric oxide reduction by carbon monoxide over calcined limestone enhanced by simultaneous sulphur retention", *Fuel*, **64**, 413–415, 1985

[72] Dam-Johansen, K., Hansen, P.F.B. and Rasmussen, S.: "Catalytic reduction of nitric oxide by carbon monoxide over calcined limestone: reversible deactivation in the presence of carbon dioxide", *Applied Catalysis B: Environmental*, **5**, 283–304, 1995

[73] Scheuer, A.: "NOx-Minderung in Drehofenanlagen der Zementindustrie" (in German), *Zement-Kalk-Gips*, **39**, No. 10, 552–554, 1986

[74] Rother, W. and Kupper, D.: "Brennstoffstufung - ein wirksames Mittel zur NO_x-Emissions-minderung" (in German), *Zement-Kalk-Gips*, **42**, 9, 444–447, 1989

[75] Høidalen, Ø.: "Modernization and increase of capacity of rotary kiln 6 in the Dalen plant of Norcem A/S", *Zement-Kalk-Gips*, **43**, No. 3, 132–138, 1990

[76] Syverud, T., Thomassen, A. and Høidalen, Ø.: "Reducing NO_x at the Brevik cement works in Norway - Trials with stepped fuel supply to the calciner", *Zement-Kalk-Gips*, **47**, No. 3, 92–93, 1994

[77] Syverud, T., A. Thomassen and T. Gautestad: "Utilization of chipped car tyres for reducing NO_x emissions in a precalciner kiln", *World Cement*, **11**, No. 11, 39–43, 1994

[78] Hansen, E.R.: "Tire power is fire power", *Rock Products*, No. 4, 29-31 1992

[79] de Val, D.: "Återvinning av däck i USA" (in Swedish), Report no. 9502, Sveriges tekniske attachéer, Stockholm, 1995

[80] Gerger, W. and Liebl, P.: "Thermische Verwertung von Sekundärbrennstoffen bei den Gmunder Zementwerken" (in German), *Zement-Kalk-Gips*, **44**, No. 9, 457–462, 1991

[81] Brooks, C.L., Blankenship, J.E. and Daugherty, K.E.: "Co-firing of RDF in cement kilns", *International Cement Review*, No. 9, 54–57, 1992

[82] Lockwood, F.C. and Ou, J.J.: "Review: burning of refuse-derived fuel in a rotary cement kiln"; *Proc. Instn. Mech. Engnrs.*, **207**, 65–70, 1993

[83] Caluori, A., Mark, F.E., Moser, M. and Prisse, A.: "An alternative fuel for cement production — source separated plastics waste", Technical paper, Association of Plastics Manufacturers in Europe, Brussels, 1997

[84] Vocht-Mields, R.: "Profits on paper", *International Cement Review*, No. 11, 30, 1991

[85] Mantus, E.K.: "All fired up - Burning hazardous waste in cement kilns", Report, Environmental Toxicology International Inc., USA, 1992

[86] Karstensen, K.H.: "Forbrenning av spesialavfall i dedikerte anlegg og sementovner" (in Norwegian), Report no. STF27 A94044, SINTEF Industriell kjemi, September 1994

[87] Miller, C.A., Touati, A.D., Becker, J. and Wendt, J.O.L.: "NO_x abatement by fuel-lean reburning: Laboratory combustor and pilot-scale package boiler results", *Symposium (International) on Combustion*, **27**, 3189–3195, The Combustion Institute, Pittsburgh, Pennsylvania, 1998

[88] Newhall Pont, J., Evans, A.B., England, G.C., Lyon, R.K. and Seeker, W.R.: "Evaluation of the CombiNO_x process at pilot scale", *Environmental Progress*, **12**, No. 2, 140-145, 1993

[89] Zamansky, V.M., Maly, P.M., Seeker, W.R. and Folsom, B.A.: "Biomass fuels in reburning technologies", Work-in-progress poster no. 5F25, *Symposium (International) on Combustion*, **27**, The Combustion Institute, USA, 1998

[90] Zamansky, V.M., Maly, P.M., Seeker, W.R. and Folsom, B.A.: "Biomass fuels in reburning technologies", 10th European Conference and Technology Exhibition - Biomass for Energy and Industry, 1537–1540, 1998

[91] Zamansky, V.M., Ho, L., Maly, P.M. and Seeker, W.R.: "Reburning promoted by nitrogen- and sodium-containing compounds", *Symposium (International) on Combustion*, **26**, 2075–2082, The Combustion Institute, USA, 1996

[92] Zamansky, V.M., Maly, Ho, L., Lissianski, V.V., Rusli, D. and Gardiner Jr., C.G.: "Promotion of selective non-catalytic reduction of NO by sodium carbonate", *Symposium (International) on Combustion*, **27**, 1443–1449, The Combustion Institute, USA, 1998

[93] Maly, P.M., Zamansky, V.M., Ho, L. and Payne, R.: "Alternative fuel reburning", *Fuel*, **78**, No. 3, 327–334, 1999

[94] Heap, M.P., Chen, S.L., Kramlich, J.C., McCarthy, J.M. and Pershing, D.W.: "An advanced selective reduction process for NO_x control", *Nature*, **335**, No. 10, 620-3622, 1988

[95] Gardeik, H.O. and Rosemann, H.: "Brennstoffenergiebedarf und Brennstoffenergieaufteilung beim Vorcalcinierverfahren" (in German), *Zement-Kalk-Gips*, **34**, No. 9, 435–444, 1981

[96] Gardeik, H.O.: "Aufwand an Brennstoffenergie beim Brennen mit Vorcalcinierung" (in German), *Zement-Kalk-Gips*, **34**, 12, 611–617, 1981

[97] Farag, L.M.: "Thermal evaluation of cement dry process with complete exit gases removal through bypass", *Zement-Kalk-Gips*, **43**, No. 11, 542–549, 1990

[98] Jeschar, R., Jennes, R., Kremer, H. and Kellerhof, T.: "Optimierung der Verbrennung im Calcinator einer Zementdrehofenanlage", *Zement-Kalk-Gips*, **49**, No. 6, 304–317, 1996

[99] Gardeik, H.O. and Jeschar, R.: "Vereinfachte matematische Modelle zur Berechnung der Wärmeübertragung in innenbeheizten, adiabaten Drehrohren (Konvektionsmodelle). Teil 1: Idealisiertes Drehrohr mit unendlich groβem Wärmeleitskoeffizienten der Wand" (in German), *Zement-Kalk-Gips*, **32**, No. 5, 201–210, 1979

[100] Gardeik, H.O. and Jeschar, R.: "Vereinfachte matematische Modelle zur Berechnung der Wärmeübertragung in innenbeheizten, adiabaten Drehrohren (Konvektionsmodelle). Teil 2: Drehrohr mit endlichem Wert des Wärmeleitskoeffizienten der Wand" (in German), *Zement-Kalk-Gips*, **32**, No. 9, 434–441, 1979

[101] Frisch, V., Jeschar, R. and Gardeik, H.O.: "Vorcalcinierung mit und ohne Tertiärluftleitung" (in German), *Zement-Kalk-Gips*, **35**, No. 2, 58–65, 1982

[102] Frisch, V. and Jeschar, R.: "Möglichkeiten zur Optimierung des Brennprozesses in Zementdrehöfen" (in German), *Zement-Kalk-Gips*, **36**, No. 10, 549–560, 1983

[103] Ghoshdastidar, P.S. and Unni, V.K.A.: "Heat transfer in the non-reacting zone of a cement rotary kiln", *Journal of Engineering for Industry*, **118**, No. 2, 169–172, 1996

[104] Gardeik, H.O., Rosemann, H. and Steinbach, V.: "Thermische Beurteiling von Klinkerkühlern — Empfehlungen des VDZ-Arbeitskreises Klinkerkühler" (in German), *Zement-Kalk-Gips*, **40**, No. 5, 230–237, 1987

[105] Steinbach, V.: "Ein matematisches Modell eines Rohrkühlers" (in German), *Zement-Kalk-Gips*, **40**, No. 9, 458–462, 1987

[106] Sælid, S.: "Modelling, estimation and control of a rotary cement kiln", Dr.ing. thesis, Report no. 76 157 W, The Norwegian Institute of Technology, 1976

[107] Mordt, H.E.: "Control of kilns for the production of expanded clay aggregates", Dr.ing. thesis, The Norwegian Institute of Technology, 1990

[108] Huttunen, M. and Kjäldman, L.: "Computational analysis of gas flow and of trajectories of car tire particles in the shaft of a cement kiln", Report no. ENE21/2/96, VTT Energia, 1996

[109] Kolyfetis, E. and Markatos, N.C.: "Aerodynamics and coal — Flame modelling in the burning zone of cement rotary kilns, Part 1", *Zement-Kalk-Gips*, **49**, No. 1, 24–35, 1996

[110] Kolyfetis, E. and Markatos, N.C.: "Aerodynamics and coal — Flame modelling in the burning zone of cement rotary kilns, Part 2", *Zement-Kalk-Gips*, **49**, No. 6, 326–334, 1996

[111] Eike, J.: "Forbrenning av alternative brensler i sementovn" (in Norwegian), M.Sc. thesis, Telemark College, 1997

[112] Mastorakos, E., Massias, A., Tsakiroglou, C.D., Goussis, D.A., Burganos, V.N. and Payatakes, A.C.: "CFD predictions for cement kilns including flame modelling, heat transfer and clinker chemistry", *Applied Mathematical Modelling*, **23**, 55–76, 1999

[113] Goes, C.: "Über das Verhalten der Alkalien beim Zementbrennen" (in German), Schriftenreihe der Zementindustrie, **24**, Verein Deutscher Zementwerke, Düsseldorf, 1960

[114] Sprung, S.: "Das Verhalten des Schwefels beim Brennen von Zementklinker" (in German), Schriftenreihe der Zementindustrie, **31**, Beton-Vorlag, Düsseldorf, 1964

[115] Ritzmann, H: "Kreisläufe in Drehofensystemen" (in German), *Zement-Kalk-Gips*, **24**, No. 8, 338–343, 1971

[116] Hatano, H: "Über das verhalten des Schwefels im Wärmetauscherofen" (in German), *Zement-Kalk-Gips*, **25**, No. 1, 18–19, 1972

[117] Goldmann, W., Kreft, W. and Schütte, R.: "Cyclic phenomena of sulfur in cement kilns", *World Cement Technology*, No. 12, 424–430, 1981

[118] Rosemann, H. and Gardeik, H.O.: "Einflüsse auf die Energieumsetzung in Calcinatoren bei der Vorcalcination von Zementrohmehl" (in German), *Zement-Kalk-Gips*, **36**, No. 9, 506–511, 1983

[119] Kreft, W: "Alkali- und Schwefelverdampung in Zementöfen in Gegenwart hoher Chloreinnahmen" (in German), *Zement-Kalk-Gips*, **38**, No. 8, 418–422, 1985

[120] Kreft, W: "Die Unterbrechung von Stoffkreisläufen mit Berücksichtigung der integrierten Weiterverwertung im Zementwerk" (in German), *Zement-Kalk-Gips*, **40**, No. 9, 447–450, 1987

[121] Kupper, D., Kreft, W. and Menzel, K.: "The effect of salt compounds from cyclic processes upon the combustion of solid phases in raw meal calciners", *Zement-Kalk-Gips*, **39**, No. 5, 149–152, 1986

[122] Schütte, R.: "Möglichkeiten der Entstehung und Minderung von SO2-Emissionen in Zementwerken" (in German), *Zement-Kalk-Gips*, **42**, No. 3, 128–133, 1989

[123] Schütte, R. and Kupper, D.: "The importance of recircualtion considerations in relation to product quality and environmental compatibility in cement production", *Zement-Kalk-Gips*, **44**, No. 2, 27–29, 1991

[124] Kupper, D, Rother, W. and Unland, G.: "Trends in desulphurisation and denitration techniques in the cement industry", *World Cement*, **8**, No. 3, 94–103, 1991

[125] Schulz, W., Kremer, H. and Rodenhäuser, F.: "Inhibitor effect of vaporized salts on pulverized coal firing in precalcining installation", *Zement-Kalk-Gips*, **39**, No. 4, 107–108, 1986

[126] Schmidt, K.D., Gardeik, H.O. and Ruhrland, W.: "Process engineering influences on SO_2 emissions from rotary kiln plants - Results of long-term investigations", *Zement Kalk-Gips*, **39**, No. 4, 110–116, 1986

[127] Faraq, L.M. and Kamel, H.M.: "Effect of high intakes of chlorine, sulfur and alkalies on cement kiln operation", *Zement-Kalk-Gips*, **47**, No. 10, 586–590, 1994

[128] Dam-Johansen, K., Johnsson, J.E., Glarborg, P., Frandsen, F., Jensen, A. and Østberg, M.: "Combustion Chemistry - Activities in the CHEC research programme", Rep.No. 9616, Technical University of Denmark, 1996

[129] Kramlich, J.C., Malte, P.C. and Grosshandler, W.L.: "The reaction of fuel-sulfur in hydrocarbon combustion", *Symposium (International) on Combustion*, **18**, 151–161, The Combustion Institute, Pittsburgh, Pennsylvania, 1981

[130] Chatterjee, A.K.: "Role of volatiles in cement manufacture and in the use of cement", in: Ghosh, S.N. (ed.): "Advances in cement technology — Critical reviews and case studies on manufacturing, quality control, optimazation and use", Pergamon Press, 1983

[131] Lowes, T.M. and L.P. Evans: "The effect of burner design and operating parameters on flame shape, heat transfer, NO_x and SO_3 cycles", *Zement-Kalk-Gips*, **46**, No. 12, 761–768, 1993

[132] Bonn, W. and Lang, T.: "Brennverfahren" (in German), *Zement-Kalk-Gips*, **39**, No. 3, 105–114, 1986

[133] Arora, V.K., Sethi, Y.P. and Pandey, G.C.: "Coating and build-up problems in the cement industry", *World Cement*, **13**, No. 12, 64–68, 1996

[134] Enestam, S.: "Modelling the alkali and sulphur chemistry in the cement kiln - the influence of using car tyres as additional fuel", Report 98-6, Åbo Akademi, Faculty of Chemical Engineering, Combustion Chemistry Research Group, Åbo, 1998

[135] Wikstedt, S: "Alternative bränslen för cementindustrin - Delprojekt 5: Alkali- och svavelkretslopp. Resultatrapport över jämnviktsberäkningar gjorda med ChemSage" (in Swedish), Report, Åbo University, 1996

[136] Backman, R: "Alternative bränslen för cementindustrin - Delprojekt 5: Alkali- och svavelkretslopp. Slutrapport över delprojektet" (in Swedish), Report, Åbo University, 1996

[137] "Miljørapport 1997" (in Norwegian), Norcem AS, Brevik, 1998

[138] Conroy, J.: "LowNOx pyro-systems design and operation", *IEEE Transactions of industry applications*, **29**, 867–875, 1993

[139] Kunii, D. and Levenspiel, O.: "Fluidization engineering, Second edition", Butterworth-Heinemann, 1991

[140] Hundebøl, S. and Kumar, S.: "Retention time of particles in calciners of the cement industry", *Zement-Kalk-Gips*, **40**, No. 8, 422–425, 1987

[141] Perry, R.H. and Green, D.: "Perry's Chemical Engineers' Handbook, Sixth Edition", McGraw-Hill, 1984

[142] Beér, J.M.: "Minimizing NO_x emissions from stationary combustion; reaction engineering methodology", *Chemical Engineering Science*, **49**, No. 24A, 4067–4083, 1994

[143] Chagger, H.K, Goddard, P.R., Murcoch, P. and Williams, A.: "Effect of SO_2 on the reduction of NO_x by reburning with methane", *Fuel*, **70**, 1137–1142, 1991

[144] Smith, J.M. and van Ness, H.C.: "Introduction to chemical engineering thermodynamics, fourth edition", McGraw-Hill, 1987

[145] Moran, M.J. and Shapiro, H.N.: "Fundamentals of engineering thermodynamics, Second edition", John Wiley & Sons, 1993

[146] Barin, I.: "Thermochemical data of pure substances, third edition", VCH, Germany, 1995

[147] Chase, M.W., Jr., Davies, C.A., Downey, J.R., Jr., Frurip, D.J., McDonald, R.A.and Syverud, A.N.: "JANAF thermochemical tables, third edition", *Journal of physical and chemical reference data*, **14**, 1985

[148] Haug-Warberg, T.: "Calculation of thermodynamic equilibria", Dr.ing. thesis, Norwegian Institute of Technology, Trondheim, 1988

[149] Hayhurst, A.N. and Tucker, R.F.: "The reductive regeneration of sulphated limestone for flue-gas desulphurisation: Thermodynamic considerations of converting calcium sulphate to calcium oxide", *Journal of the Institute of Energy*, **64**, 212–229, 1991

[150] Reynolds, W.C.: "The element potential method for chemical equilibrium analysis: Implementation of the interactive program STANJAN – Version 3", Department of Mechanical Engineering, Stanford University, January, 1986

[151] Lea, F.M.: "The chemistry of cement and concrete, Third edition", Edward Arnold (Publishers) Ltd., London, 1970

[152] Atal, A. and Levendis, Y.A.: "Comparison of the combustion behaviour of pulverized waste tyres and coal", *Fuel*, **74**, No. 11, 1570–1581, 1995

[153] Patankar, S.V.: "Numerical heat transfer and fluid flow", Hemisphere Publishing Corporation, 1980

[154] "Fluent User's Guide, Release 4.4", Fluent Inc., 1996

[155] Xeller, H.: "New developments in NO_x abatement in the cement industry - Part 1", *Zement-Kalk-Gips*, **51**, No. 3, 144–150, 1998

[156] Mortensen, A.H., Hintsteiner, E.A. and Rosholm, P.: "Converting two kiln lines to 100 % high sulphur petroleum coke firing — Procedures for implementing a cost-saving scheme, Part 1", *Zement-Kalk-Gips*, **51**, No. 2, 84–93, 1998

[157] Mortensen, A.H., Hintsteiner, E.A. and Rosholm, P.: "Converting two kiln lines to 100 % high sulphur petroleum coke firing — Procedures for implementing a cost-saving scheme, Part 2", *Zement-Kalk-Gips*, **51**, No. 2, 184–196, 1998

[158] Karlsson, M., Zevenhoven, R. and Hupa, M.: "Alternative bränslen för cementindustrin - Delprojekt 1: Undersökning av förbränning av gummiflis i laboratorieugn. Slutrapport til Finncement AB" (in Swedish), Report, Åbo University, 1995

[159] Karlsson, M., Zevenhoven, R. and Hupa, M.: "Laboratory characterisation of waste tyre particles for combustion in a cement kiln", *Finnish-Swedish Flame Days*, Finland, 1996

[160] Conesa, J.A., Font, R., Fullana, A. and Caballero, J.A.: "Kinetic model for the combustion of tyre wastes", *Fuel*, **77**, No. 13, 1469–1475, 1998

[161] Williams, P.T. and Besler, S.: "Pyrolysis-thermogravimetric analysis of tyres and tyre components", *Fuel*, **74**, No. 9, 1277–1283, 1995

[162] Schmidthals, H. and Rose, D.: "Investigations into the thermal utilization of secondary fuels in lump form in the cement burning process. Part 1: Pilot trials in a Swiss cement works, *Zement-Kalk-Gips*, **52**, No. 2, 88–97, 1999